

Reassessment of precipitation return levels in Iceland

Andréa-Giorgio R. Massad, Guðrún Nína Petersen, Tinna
Þórarinsdóttir, Matthew James Roberts

Reassessment of precipitation return levels in Iceland

Andréa-Giorgio R. Massad, Guðrún Nína Petersen, Tinna Þórarinsdóttir, Matthew James Roberts

Skýrsla nr. VÍ 2020-008	Dags. Október 2020	ISSN 1670-8261	Opin <input checked="" type="checkbox"/> Lokuð <input type="checkbox"/> Skilmálar:
Heiti skýrslu / Aðal- og undirtitill: Reassessment of precipitation return levels in Iceland		Upplag: 14 Fjöldi síðna: 138	
		Framkvæmdastjóri sviðs: Jórunn Harðardóttir	
Höfundar: Andréa-Giorgio R. Massad, Guðrún Nína Petersen, Tinna Þórarinsdóttir og Matthew James Roberts		Verkefnisstjóri: Guðrún Nína Petersen	
		Verknúmer: 4711-0-0006	
Gerð skýrslu/verkstig:		Málsnúmer: 2020-0198	
Unnið fyrir: Ofanflóðasjóð			
Samvinnuaðilar:			
Útdráttur: Aftakaúrkoma veldur oft vatnsflóðum á Íslandi og á undanförunum árum hafa orðið nokkur skyndi-flóð vegna úrhellisrigningar í brattlendi við byggð. Tilgangur þessarar skýrslu er tvískiptur: að kynna uppført mat á endurkomutíma úrkomu og að endurgera 1M5 kort sem sýnir 24 stunda úrkomu fyrir atburð með 5 ára endurkomutíma. Úrkomumælingar frá 43 veðurstöðvum eru notaðar sem og útreiknuð úrkoma í þéttriðnu neti yfir landinu, byggð á gögnum úr íslensku endurgreiningunni (ICRA). Val á aftakagreiningu er skoðað vandlega og niðurstaðan að nýta þröskulsaðferðina (e. Peak-over-threshold) þar sem gagnamengin tvö eru líkari með þeirri aðferð en með hámark innan tímabilsaðferðarinnar (e. Block Maxima). Ferlar sem sýna samtímis ákefð, tímallengd og tíðni (e. Intensity-duration-frequency curves) eru birtir fyrir hverja stöð, byggðir á úrkomumælingum og útreiknaðri úrkomu. Afurðir verkefnisins eru tvö 1M5 kort, í fyrsta lagi kort byggt á daggildum úrkomu (frá miðnætti til miðnætti) tilsvarendi eldri útgáfu og í öðru lagi byggt á 24 stunda úrkomu, fyrir fljótandi tímabil. Bæði kortin innihalda fleiri smáatriði en eldri útgáfa þar sem innlagsgögn eru í mun þéttriðnara neti. Hærrí endurkomugildi eru á Snæfellsnesi og Tröllaskaga, sem og í Bláfjöllum og á Aust- og Vestfjörðum. Nýja 1M5 kortið má nýta í ýmsa vinnu, s.s. við gerð hættumats vegna aftakaúrkomu og við hönnun á frárennsli og flóðvörnum.			
Lykilorð: úrkoma, endurkomutími, aftakagreining, þröskulsaðferðin, 1M5 kort, IDF ferlar precipitation, rainfall, extreme value analysis, return periods, 1M5 map, IDF curves		Undirskrift framkvæmdastjóra sviðs:	
		Undirskrift verkefnisstjóra:	
		Yfirfarið af: SG, TóJ, TJ, EBJ	

Contents

GLOSSARY	8
ABSTRACT	9
ENDURKOMUTÍMI ÚRKOMU – SAMANTEKT	10
1 INTRODUCTION	15
1.1 Aim	18
2 THE 1M5 MODEL, WEATHER PREDICTION AND PRECIPITATION OBSERVATIONS	19
3 METHODOLOGY.....	20
3.1 Block Maxima.....	21
3.2 Peak-over-Threshold.....	22
3.3 Estimation of the distribution parameters.....	22
4 DATA	23
4.1 Precipitation measurements.....	23
4.2 Reanalysis.....	27
4.3 Extraction of the ICRA timeseries	28
5 RESULTS	29
5.1 Comparison of precipitation intensity between ICRA and selected rain gauge stations..	29
5.2 Model implementation and selection.....	38
5.3 IDF curves	44
5.4 Revised 1M5 map	45
6 DISCUSSION	49
6.1 Differences in return levels between observed and simulated precipitation	49
6.2 Sensitivity of the EVA methods.....	52
6.3 Comparison between 1M5 maps.....	54
7 CONCLUSIONS.....	61
ACKNOWLEDGEMENT	63
REFERENCES.....	63
APPENDICES.....	65

Figures

Figure 1. Map of Iceland with all automatic gauging stations measuring precipitation as of January 2020.	17
Figure 2. The 1M5 map currently in use in Iceland.	18
Figure 3. A schematic of a probability distribution representing precipitation.....	20
Figure 4. Location of selected IMO automatic weather stations measuring precipitation in Iceland.	26
Figure 5. Daily observed precipitation as measured at all stations ranked decreasingly.	27
Figure 6. Four methods to derive a precipitation value from a given location based on values from a regular gridded dataset.	28
Figure 7. Scatterplots and Q–Q plots comparing daily precipitation from the ICRA dataset and observations with different extraction methods for station Eskifjörður.	30
Figure 8. Stations ranked according to their average CC for the 20 highest rainfall daily events.	33
Figure 9. Ranked values of the 50 highest 24-hour accumulated precipitation events plotted against ranked values of the 50 highest daily precipitation events.	34
Figure 10. Histograms showing 3-hour accumulated observed and simulated precipitation over 72 hours for the three largest precipitation events at Laufbali.	35
Figure 11. Heat maps showing daily precipitation from the ICRA dataset around the four nearest grid-points to station Neskaupstaður over a 3-day period.	36
Figure 12. Stacked heat map for station Seyðisfjörður for the 10 largest daily precipitation events from the ICRA simulation.	37
Figure 13. Daily simulated precipitation at station Eskifjörður for the period 2009–2015.	38
Figure 14. Declustering of the first 1,000 days of data for a randomly selected grid-point using a minimum time window of five days.	39
Figure 15. Scatterplots comparing return levels of precipitation based on simulations and observations.	41
Figure 16. Closeness coefficient between observations and simulations for daily precipitation with a 10-year return period at the 43 gauging stations selected for the study.	43
Figure 17. IDF curves for station Kvísker from the entire ICRA dataset.	44
Figure 18a. 1M5 map based on daily precipitation from the entire ICRA dataset using the Peak-over-Threshold method with MLE.	47
Figure 18b. 1M5 map based on daily precipitation from the entire ICRA dataset using the Peak-over-Threshold method with MLE, modified using a maximum-value filter among the nine nearest grid-points.	47
Figure 19. IDF curves for stations Höfn í Hornafirði and Neskaupstaður comparing results based on observations to results based on ICRA simulations obtained for the same time period.	51
Figure 20. 10-year return period normalised IDF curves stacked for all stations and calculated from observed data and ICRA results.	53

Figure 21. Geographic differences between the 1M5 map developed in this study and the 1M5 map from Eliasson et al., both based on daily precipitation.....	56
Figure 22. Distribution of annual rainfall in Iceland for the period 1981–2010.	56
Figure 23. New 1M5 values plotted against 1M5 values from Eliasson for all 43 stations.....	57
Figure 24a. 1M5 map based on 24-hour accumulated precipitation, obtained from the entire ICRA dataset using the Peak-over-Threshold method with MLE.	59
Figure 24b. 1M5 map based on 24-hour accumulated precipitation, obtained from the entire ICRA dataset using the Peak-over-Threshold method with MLE, modified using a maximum-value filter among the nine nearest grid-points.	60

Tables

Table 1. Station list along with the date of their first recording, the number of missing daily values since they started recording and the highest recorded values.	24
Table 2. Evaluation of the four interpolation methods for scatter and Q–Q plots.	31
Table 3. The values and dates of the 20 highest daily values of precipitation in Neskaupstaður	32
Table 4. Return levels for station Eskifjörður for different return periods using daily ICRA values.....	40
Table 5. RMSE between return levels based on observations and ICRA at each station for all methods, time durations and return periods.	42
Table 6. Return levels based on the entire ICRA dataset for station Seyðisfjörður.....	45
Table 7. 1M5 values for each control station as obtained by the Peak-over-Threshold with MLE from ICRA and observations.....	49
Table 8. 1M5 values at each control station as obtained by Eliasson using the Block Maxima method, Peak-over-Threshold and Block Maxima methods with MLE based on daily precipitation from the entire ICRA dataset.	54
Table 9. 1M5 values for each control station, as obtained by the Peak-over-Threshold with MLE applied on daily and 24-hour accumulated precipitation from the ICRA.	58

Glossary

1M5 – Daily or 24-hour precipitation return level with a 5-year return period

AMS – Annual Maxima Series

CC – Closeness Coefficient

CDO – Climate Data Operator

EVA – Extreme Value Analysis

GP – Generalized Pareto

ICRA – Icelandic Reanalysis

IDF – Intensity-Duration-Frequency

IMO – Icelandic Meteorological Office

ME – Mean Error

MLE – Maximum Likelihood Estimation

RMSE – Root Mean Squared Error

Abstract

In Iceland, extreme precipitation can often lead to flooding. In coastal regions, short-lived torrents can develop on steep slopes close to inhabited areas. The purpose of this report is twofold: to present an updated assessment of precipitation return periods, and to apply the results to a new 1M5 map of 24-hour precipitation thresholds for a 5-year event. Both observed precipitation at 43 stations around Iceland and gridded precipitation values from retrospective meteorological forecasts (ICRA) are used in the analysis. The choice of an appropriate Extreme Value Analysis method is studied thoroughly, leading to the selection of the Peak-over-Threshold method as it shows more similarities when applied to both sets of data. Intensity–duration–frequency (IDF) graphs are presented for each station, based on simulated precipitation values and station observations. The project results in two 1M5 maps: one based on daily values from midnight to midnight in line with the earlier 1M5 map, and the other based on accumulated precipitation over running 24-hour windows. Both maps include important details that the earlier version could not encompass. Higher return levels are found on the Snæfellsness and Tröllaskagi peninsulas, the Bláfjöll mountainous region, as well as in the East- and Westfjords. Those new results have several potential uses, including thresholds for extreme precipitation in risk assessment studies and design parameters for drainage structures and flood defences.

Samantekt. Endurkomutími úrkomu

Vatnsflóð sem verða vegna mikilla rigninga geta valdið töluverðum skemmdum á innviðum sem og raskað atvinnulífi og umferð. Þegar slík úrkoma fellur að vetri eða vori samfara asahláku geta orðið skyndiflóð. Tíðni og stærð slíkra flóða er háð því hve mikilli úrkomu vatnasviðið og árfarvegurinn geta tekið við, en í mikilli úrkomu geta ár flætt yfir bakka sína. Í bröttu landslagi getur mikil úrkoma einnig valdið því að vatn flæði niður hlíðar og þannig valdið skyndiflóðum.

Á undanförnum árum hafa nokkur skyndiflóð orðið vegna úrhellisrigningar í brattlendi í nánd við byggð. Nefna má skyndiflóðin á Siglufirði í ágúst 2015 en þar urðu miklar skemmdir. Dæmi um vatnsflóð vegna mikillar rigningar yfir lengri tími eru flóðin á Suðausturlandi í september 2017, en þá skemmdust vegir, fráveitukerfi og ræktað land og tryggingarkröfur námu 168 milljónum króna (Náttúruhamfaratrygging Íslands, 2019).

Við kortlagningu á úrkomu, og breytileika hennar í tíma og rúmi, er mat á aftakaúrkomu mjög mikilvægur þáttur. Að auki er slíkt mat undirstaða flóðaviðvarana og hönnunar ýmissa mannvirkja, s.s. fráveitukerfa, sem notast við hönnunarflóð sem mælikvarða á hámarksafkastagetu kerfa. Á Íslandi hafa flestir nýtt sér gögn um fimm ára endurkomugildi hámarkssólarhringsúrkomu á kortaformi, svonefnt IM5 kort. Sú vinna var unnin af Jónasi Elíassyni (2000) og Jónasi Elíassyni ofl. (2009) en byggir á eldri vinnu hjá NERC (1975) um samhengi úrkomumagns í úrkomuatburðum og endurkomutíma. IM5 kortið er meðal annars mikið notað við hönnun vega og fráveitukerfa (Hlodversdóttir ofl., 2015).

Frá aldarmótum hefur notkun sjálfvirkra úrkomumæla aukist jafnt og þétt á Íslandi. Slíkir mælar eru nú vítt og breitt um landið og skrá mælingar á 10 mínútna fresti. Þessar mælingar gefa því góðan grunn fyrir prófanir og uppfærslu á upprunalega IM5 kortinu. Að auki hafa orðið miklar framfarir í veðurlíkanagerð og hermt úrkomumunstur í flóknu landslagi batnað til muna (Clark ofl., 2016). Því er þarft að endurmeta útbreiðslu aftakaúrkomu, með tilliti til hönnunar mannvirkja sem og svo hægt sé að skilgreina úrkomumörk sem kunna að valda vatnsflóðum.

Við greiningu á aftakaúrkomu er nauðsynlegt að taka tillit til óvissu. Í mælingum er mælióvissa og í veðurútreikningum er óvissa vegna þeirra nálgana sem þarf að gera við líkanagerð. Mikilvægt er að hönnunaraðilar séu meðvitaðir um þessar takmarkanir þegar aftakaafrennsli er metið. Hér eru listaðir tíu veðurfræði-, vatnafræði- og vatnaverkefrafæðilegir þættir sem þarf að hafa í huga.

1. Með auknum vindhraða mælist úrkoma verr, almennt er úrkoma vanmæld.
2. Uppsafnað úrkomumagn er mismunandi eftir vali á tímabili, þó jafnlöng séu. Það er, uppsöfnuð 24 stunda úrkoma fyrir fast tímabil frá miðnætti til miðnættis, eða 09 til 09, er alltaf minni en eða jafnmikil þeirri úrkomu sem er safnað yfir fljótandi 24 stunda tímabil.
3. Áhrif staðháttanna á úrkomumunstur og ákefð þýðir að úrkomumælingar á veðurstöðvum eru oft ekki dæmigerðar fyrir vatnasvið.
4. Vatnsflóð vegna úrkomu á tilteknu vatnasviði kunna að vera algengari en aftakaúrkoma á mælistöð gefur til kynna, þar sem flóðvatn kemur oft af stóru svæði en mælingin er á einum ákveðnum stað, til dæmis á láglandi í þröngum fjörðum.

5. Flóðaskemmdir á einum stað geta orðið vegna mikils afrennslis af mörgum hlutvatnasviðum. Af því leiðir að mat á afrennslu byggð á gögnum frá einu vatnasviði, hlutvatnasviði eða veðurstöð getur vanmetið endurkomutíma og endurkomugildi vatnsflóða vegna úrkomu.
6. Stærð flóða vegna aftakaúrkomu er háð úrkomumagni, snjóbráðnun og lofthita dögum og jafnvel vikum fyrir atburðinn, þar sem þessir þættir hafa áhrif á hvort og hve miklu vatni jarðvegur getur tekið við.
7. Lárétt reikninet veðurlíkana jafnar út hæðir og dali í landslagi sem veldur meðal annars vanmati á úrkomumögnun við fjöll.
8. Veðurútreikningar geta ekki líkt eftir staðbundinni aftakaúrkomu á styttri tímakvarða en tímaupplausn líkansins.
9. Meta þarf hættu á skyndiflóðum, miðað við hvert vatnasvið fyrir sig, út frá endurkomutíma uppsafnaðrar úrkomu fyrir föst tímabil, venjulega 24 stundir.
10. Endurkomutíma úrkomu þarf að færa yfir í sérhæfðar verkfræðilegar leiðbeiningar fyrir mismunandi tegundir mannvirkja eða starfsemi.

Þessi skýrsla tekur á þáttum 1, 2, 3, 4 og 7 af ofangreindum lista en tæpt er á þætti 9. Aðra þætti þarf að kanna út frá vatnasviðum og hönnun fráveitukerfa og flóðvarna.

Þess ber einnig að geta að gert er ráð fyrir að úrkoma á Íslandi aukist vegna loftslagsbreytinga um 1,5% við hverja 1°C hækkun í lofthita (Björnsson ofl., 2018). Mælingar sýna að á síðastliðnum áratugum hefur ársúrcoma aukist, einkum sumarúrcoma á vestanverðu landinu. Engar rannsóknir hafa farið fram á því hvaða breytinga má vænta í aftakaúrkomu vegna loftslagsbreytinga.

Tilgangur þessarar skýrslu er í fyrsta lagi að uppfæra mat á endurkomutíma úrkomu og í öðru lagi að teikna nýtt IM5 kort. Jafnframt eru birtir svokallaðir IDF ferlar sem sýna samtímis ákefð, tímalengd og tíðni (e. Intensity-Duration-Frequency) fyrir hverja veðurstöð, byggðir á úrkomumælingum og útreiknaðri úrkomu.

Verkefnið var styrkt af Ofanflóðasjóði og er hluti af VATNAVÁ verkefnum Veðurstofu Íslands (VÍ) sem snúa að hættumati vegna vatnsflóða á Íslandi.

Í verkefninu er útreiknuð úrkoma úr íslensku endurgreiningunni (ICRA, Nawri ofl., 2017) notuð til að meta endurkomutíma úrkomu í þéttriðnu neti yfir landinu. Útreikningarnir eru í 2,5 x 2,5 km neti á 1 klukkustundar fresti fyrir tímabilið september 1979 til desember 2016. Einnig eru notaðar sjálfvirkar úrkomumælingar frá 49 stöðvum sem allar hafa mælt samfellt í yfir 10 ár. Í báðum tilvikum er um daggildi að ræða, þ.e. uppsafnaða úrkomu frá miðnætti til miðnættis. Í næmniathugunum eru mælingar frá 12 stöðvum, svokölluðum kjarnastöðvum, skoðaðar sérstaklega og bornar saman við útreiknaða úrkomu á sömu stöðum. Kjarnastöðvarnar voru valdar vegna staðsetningar í þröngum fjörðum og nálægt bröttum fjöllum (Eskifjörður, Neskaupstaður, Flateyri og Ísafjörður), þekktra vatnsflóða á svæðinu (Siglufjörður, Ólafsfjörður og Seyðisfjörður), mikillar ársúrkomu (Kvísker og Laufbali) og vegna langra og góðra úrkomuraða (Reykjavík og Höfn í Hornafirði).

Við samanburð á ICRA útreiknaðri úrkomu og mælingum er valið að nýta gildin í þeim fjórum reiknipunktum sem eru næst hverri veðurstöð og reikna vegið meðaltal.

Tvær útgildagreininar voru skoðaðar, hámark innan tímabils aðferðin (e. Block Maxima) og þröskuldaaðferðin (e. Peak-over-threshold). Fyrri aðferðin notar hámarksgildi innan tímabils,

yfirleitt árs, og metur stika GEV tíðnidreifingarrinnar (e. General Extreme Value distribution) en sú seinni stika GP tíðnidreifingarrinnar (e. General Pareto distribution). Einnig finnast fleiri aðferðir til að aðlaga útgildadreifingu að gögnunum, tvær sem eru skoðaðar í þessari skýrslu eru hámarkssennileikamat (e. Maximum Likelihood Estimate) og L-moments aðferðin. Eftir næmnisathuganir, sem beitt er á bæði úrkomumælingar og útreikninga er niðurstaðan sú að endurkomutímaútreikningar eru byggðir á þröskuldsaðferðinni og hámarkssennileikamati.

Gerður er samanburður á mældri og útreiknaðri úrkomu fyrir 20 stærstu úrkomuatburðina á hverri stöð. Þær stöðvar þar sem mismunurinn er ásættanlegur eru notaðar áfram, eða 43 stöðvar.

Á hverri stöð eru valdir þrjár stærstu mældu úrkomuatburðirnir og ICRA úrkoma borin saman við þá mældu. Niðurstöðurnar sýna að í mörgum atvikum er útreiknuð úrkoma hliðruð í tíma miðað við melda en oft samt sem áður sambærileg þegar skoðuð er uppsöfnun yfir þrjá daga. Enn fremur kemur í ljós að á klukkustundar tímakvarða er úrkoma endurgreiningarrinnar óáreiðanleg. Athugun á úrkomuútbreiðslu sýnir að þegar útreiknuð úrkoma er vanmetin má oft finna gildi sem eru tilsvareandi þeim mældu í 5-10 km fjarlægð. Það sýnir mikilvægi þess að skoða gildi í meira en einum punkti þegar útreiknuð úrkomugögn eru nýtt, til dæmis við hönnun innviða.

Við útreikninga á endurkomutíma úrkomu er notuð þröskuldsaðferðin með sennileikamati á útgildadreifingunni. Mikilvægt er að vanda val á þröskuldi og að útgildin yfir háum þröskuldi séu óháð. Þegar um margar tímaröðir er að ræða er ómögulegt að velja sérstaklega þröskuld fyrir hverja og eina tímaröð. Hér er annars vegar um 43 tímaröðir að ræða fyrir bæði mælingar og endurgreiningu og hins vegar 66.181 tímaröð úr ICRA endurgreiningunni, þ.e. fyrir sérhvern reiknipunkt yfir landi. Niðurstaðan er að nýta 0,9 hlutfallsmarkið sem staðarháðan þröskuld, þ.e. fyrir hverja tímaröð eru 10% af atburðum yfir þröskuldinum. Til að uppfylla skilyrði um að útgildin séu óháð er sett takmörkun á því hve nálægt í tíma gildi geta verið til að teljast óháð. Þar sem úrkomuatburðir á Íslandi tengjast veðrakerfum er eðlilegt að hágildi sem eru innan lægðakvarða séu háð. Því er valið að krefjast fimm daga tímabils á milli útgilda. Sama tímabil var notað í skýrslu Guðrúnar Nínu Petersen (2015) fyrir aftakavind á Íslandi.

Stíkar útgildadreifingar, skölunar- og lögunarstíkar, eru fundnir fyrir allar 43 veðurstöðvarnar, bæði frá mælingum og útreikningum, fyrir tímabil mælinga á hverjum stað. Í framhaldi eru sömu stíkar fundnir fyrir alla landpunkta og allt tímabil ICRA endurgreiningarrinnar.

Útbúnir eru IDF ferlar fyrir veðurstöðvarnar sem sýna endurkomugildi úrkomuákefðar fyrir nokkra endurkomutíma, 2, 5, 10, 25, 50 og 100 ár, og fyrir uppsafnaða úrkomu yfir 3, 6, 12, 24 og 48 klukkustundir. IDF ferlar eru ekki reiknaðir fyrir styttri tíma en 3 klukkustundir þar sem endurgreiningin þykir ekki áreiðanleg fyrir styttri tímaglugga. Í sumum tilfellum er mjög gott samræmi á milli niðurstaða byggðum á mælingum og ICRA fyrir sama tímabil, t.d. fyrir Höfn í Hornafirði en á öðrum stöðvum vanmetur ICRA endurkomugildin miðað við mælingar, s.s. á Neskaupstað. Rétt er að taka fram að ICRA nær mjög illa að herma melda úrkomu á Neskaupstað, mun verr en á flestum öðrum veðurstöðvum, og því koma þessar niðurstöður ekki á óvart. IDF ferlar byggðir á öllu ICRA tímabilinu fyrir allar 43 veðurstöðvarnar eru í viðauka skýrslunnar.

IDF ferlarnir eru bornir saman við tilsvareandi ferla byggðir á vinnu Jónasar Eliassonar ofl. (2009) og á svokallaðri Wussow jöfnu (Páll Bergþórsson, 1968). Báðar aðferðir nýta endurkomugildi hámarksdagsúrkomu til að áætla úrkomu á styttri tímakvarða. Einnig eru IDF-ferlar

byggðir á hámark innan tímabils aðferðinni reiknaðir. Þegar skoðuð eru miðgildi auk útgilda fyrir allar stöðvar, fyrir 10 ára endurkomutíma, kemur í ljós að Jónasar Eliássonar og Wussow aðferðirnar gefa svipuð og hærri endurkomugildi fyrir styttri tímabil uppsafnaðrar úrkomu en þröskuldsaðferðin og hámark innan tímabils, sem gefa báðar svipaðar niðurstöður. Fyrir 24 og 48 klukkustunda uppsafnaða úrkomu gefa seinni tvær aðferðirnar hærri gildi.

Endurskoðað IM5 kort er útbúið og borið saman við núverandi kort. Í grófum dráttum gefur nýja IM5 kortið svipaða niðurstöðu og núverandi kort, en staðbundið getur verið mikill munur. Ljóst er af samanburðinum að aukin lárétt upplausn hefur mikið að segja, munstur endurkomugilda eru betur tengd landslagi, einkum þar sem landslag er flókið. Mun hærri endurkomugildi er til dæmis að finna í Blá fjöllum, á Snæfellsnesi, Vestfjörðum, Tröllaskaga og Austfjörðum. Jafnframt má sjá að lárétt upplausn útreikninga, 2,5 x 2,5 km, er ekki nóg til að lýsa landslagi í til dæmis mjög þröngum fjörðum og vegna útjöfnunar landslags er úrkomuákefð í nálægð brattrar hlíða vanmetin. Því er til viðbótar bætt við IM5 korti þar sem í hverjum punkti er sýnt hæsta gildi næstu níu reiknipunkta. Þörf er á að kanna betur með greiningu og niðurkvörðun úrkomu hvernig megi nálgast þetta viðfangsefni betur.

Að lokum er útbúið endurbætt IM5 kort sem byggir á sólarhringsúrkomu, þ.e. fyrir fljótandi 24 stunda tímabil. Miðgildi IM5 kortsins fyrir allt landið er 14% hærra en fyrir daggildi úrkomu, frá miðnætti til miðnættis. Þetta kort, og tilsvareandi korti sem sýnir hæsta gildi næstu níu reiknipunkta, er talið nýtast betur við hönnun mannvirkja hvað varðar úrkomu og afrennsli en kortið sem byggir á daggildum.

Hvað varðar loftslagsbreytingar á Íslandi ríkir enn mikil óvissa varðandi breytingar í úrkomu. Vísbendingar eru um að úrkoma muni aukast, einkum síðsumars og að hausti (Halldór Björnsson ofl., 2018). Ekki reyndist rými innan þessa verkefnis til að meta áhrif þessa á endurkomutíma úrkomu. Það er þarft verk að byggja slíka vinnu ofan á niðurstöður þessarar skýrslu og gefa þannig verðmætar upplýsingar sem myndu nýtast vel við hönnun mannvirkja til lengri tíma, sem og að draga úr áhrifum aftakaúrkomu á mikilvæga innviði.

Mikil vinna er lögð í val á aðferðum í öllum skrefum vinnunar, rætt við aðra sérfræðinga á sviðinu sem og notendur. Við teljum að nýja IM5 kortið eigi eftir að nýtast vel við gerð flóðaviðvarana og hönnun mannvirkja sem og að vinnan eigi eftir að nýtast sem grundvöllur fyrir áframhaldandi rannsóknir og úrvinnslu á sviði aftakaúrkomu og -flóða.

Aðferðir hafa verið vandlega valdar í öllum skrefum verkefnisins og rætt við aðra sérfræðinga á sviðinu sem og notendur. Talið er að nýju IM5 kortin eigi eftir að nýtast vel við gerð flóðaviðvarana og hönnun mannvirkja. Enn fremur mun vinnan nýtast sem grundvöllur fyrir áframhaldandi rannsóknir og úrvinnslu á sviði aftakaúrkomu og -flóða.

1 Introduction

In areas throughout Iceland, periods of heavy precipitation cause localised damage and disruption to travel and economic activities. Often, such precipitation occurs during the winter-time, resulting in rapid melting of snow and, in some cases, flash flooding. The occurrence of a flood depends on whether the receiving catchment and river path can accommodate the precipitation. For established watercourses, heavy precipitation can result in a river overtopping its banks. In steep terrain, the same process could result in a torrent of overland flow, leading to flash flooding.

In Iceland, most inhabited areas are in coastal settings close to mountainous terrain and the majority of the rain gauges are located in the vicinity of populated regions (Figure 1). Recent flooding in Iceland includes short-lived rainwater torrents, which have developed on steep slopes close to settled areas, including a damaging flash flood in the coastal town of Siglufjörður in August 2015. There are also numerous examples of river floods due to prolonged, intense precipitation. For example, in September 2017, widespread flooding due to precipitation occurred in southeast Iceland; the floods caused damage to roads, culverts, and agricultural land. Insurance claims due to the flooding amounted to 168 million ISK (Natural catastrophe Insurance of Iceland, personal communication, November 2018).

Estimates of precipitation extremes are an important measure for assessing the spatial and temporal variability of precipitation; they are also used as the basis for flood warnings and in the design of the built environment, including culverts and other forms of artificial drainage. So-called ‘design flood’ estimates are used as a guideline for the maximum capacity of drainage constructions. In Iceland, the main dataset for precipitation extremes comes from the research of Jónas Eliasson (Eliasson, 2000; Eliasson *et al.*, 2009), who created a national map – known as 1M5 – of daily precipitation thresholds based on a 5-year return period (Figure 2). The 1M5 method is derived from earlier, pioneering work by NERC (1975), which related precipitation depth from a storm of given duration to a return period. The 1M5 map is used widely in Iceland as an engineering resource in the design of highway infrastructure and sewer systems (Hlodversdottir *et al.*, 2015).

Climate-change predictions for Iceland suggest that precipitation amounts will increase in line with a warming climate at a rate of at least 1.5% for a 1°C increase in temperature (Björnsson *et al.*, 2018). The same study documents a slight increase in annual precipitation in recent decades in most areas of Iceland, including summer precipitation in the west of the country. To date, no attempt has been made to investigate trends in extreme precipitation for Iceland. As signs of rapid climate-change become apparent, Iceland is also experiencing sustained levels of year-round tourism, with around two million foreign visitors annually between 2016 and 2019 (Icelandic Tourist Board, 2020). The influence of high tourism and continued economic development puts increasing dependence on various forms of infrastructure, including highways, bridges, and culverts. This dependency necessitates a new analysis of precipitation extremes and a reassessment of precipitation return periods. The modern-day availability of high temporal frequency precipitation measurements, i.e. down to 10 minutes, at various locations around the country enables testing and refinement of the original 1M5 model. Moreover, there have been major advances in the development of numerical weather prediction (NWP) models, resulting in more realistic precipitation patterns in complex terrain (see e.g. Clark *et al.*, 2016). Taken

together, there is a need to reassess the spatial variability of precipitation extremes, both for design purposes and for the identification of precipitation thresholds that could result in hazardous levels of runoff.

From a broader perspective, the analysis of extreme measured or simulated precipitation must consider uncertainties in measurement accuracy and unavoidable simplifications in meteorological models. These influences are pertinent for hydrologists and civil engineers when considering extreme runoff at a catchment scale. The following ten factors encompass meteorological and hydrological uncertainties, as well as some hydrological engineering aspects.

1. Wind-caused undercatch of rainfall by rain gauges.
2. Differences in accumulated precipitation over fixed intervals; for instance, 24-hour periods from midnight to midnight (referred to here as daily values), or from 09:00 to 09:00 the following day, in comparison to precipitation accumulated over a constantly sliding 24-hour window (see Dunkerley, 2020).
3. Local variations in the distribution and intensity of precipitation mean that station measurements are typically not representative of the whole catchment.
4. Rainfall-driven flooding in a catchment may be more frequent than extreme precipitation at a single meteorological station. This is because the routing of floodwater is often integrated over a large part of the catchment, whereas precipitation measurements are typically at a single, logistically accessible location (for instance, a lowland location in a mountainous fjord).
5. Flood damage at a specific location could be the result of extreme runoff from several sub-catchments, hence runoff estimates derived from a single catchment or a meteorological station could underrepresent the return periods and return levels of rainfall-driven floods.
6. Severe floods due to extreme precipitation may vary substantially depending on levels of precipitation, snowmelt and air temperature in the preceding days and weeks. These factors influence whether the ground is permeable to rainfall, fully saturated or frozen. In turn, this determines how rapidly surface runoff can develop.
7. The spatial resolution of meteorological simulations smooths-out the orography of the terrain, leading to substantial underestimates of orographic precipitation near to steep mountains.
8. Meteorological simulations do not represent localised precipitation extremes on timescales shorter than the model's temporal resolution.
9. Extreme runoff on short timescales, appropriate to the catchment in question, need to be estimated based on return periods for accumulated precipitation over a fixed timescale, which is typically 24 hours.
10. Precipitation return periods need to be translated into engineering recommendations suitable to the type of infrastructure and activity in question.

From the above list, this report addresses points 1, 2, 3, 4 and 7. Point 9 is considered but not addressed completely. The remaining points (5, 6, 8 and 10) need to be considered via catchment-scale investigations of flood impact and frequency, and the probabilistic design of drainage structures and flood defences.

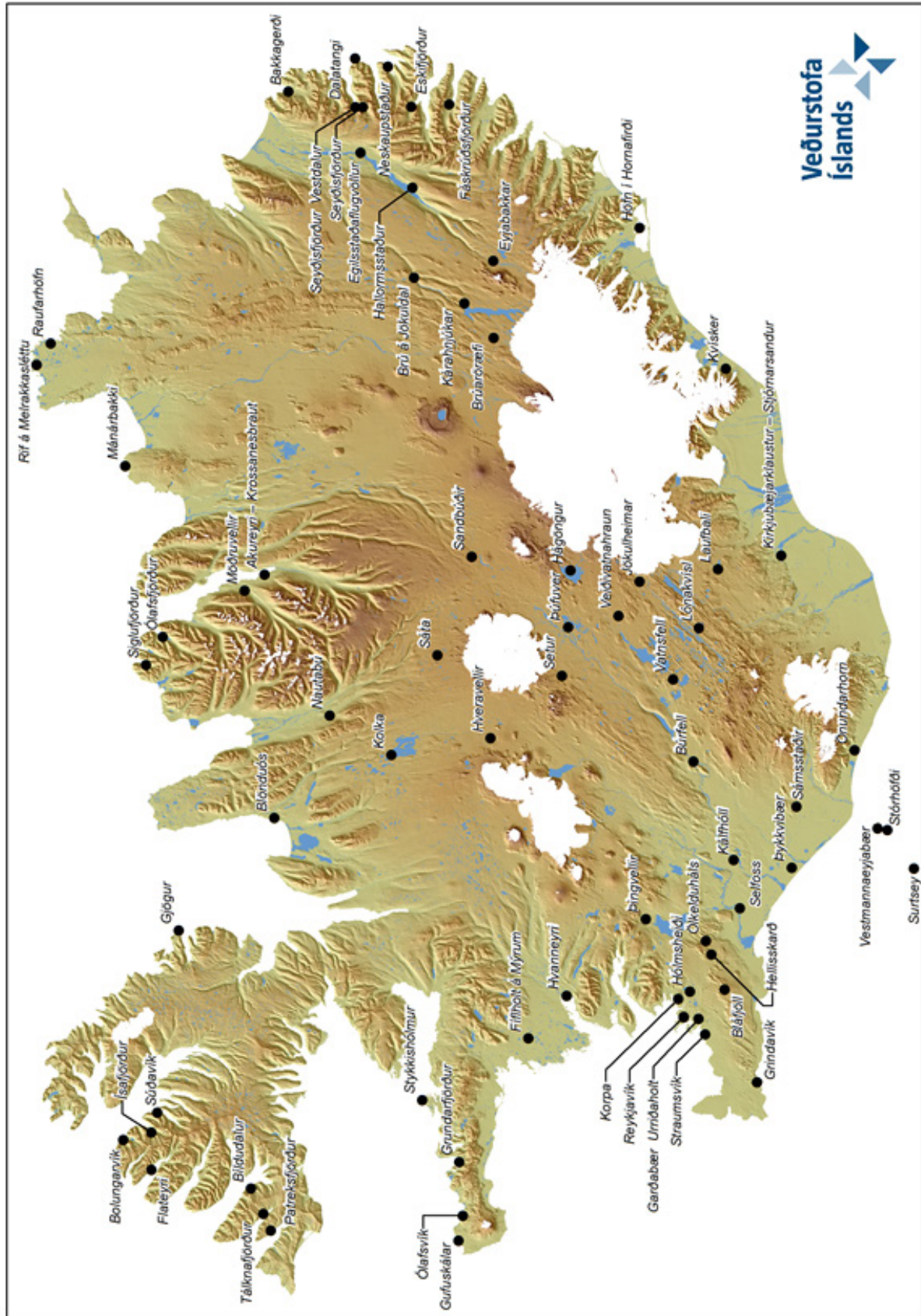


Figure 1. Map of Iceland with all automatic gauging stations measuring precipitation as of January 2020. Brown shadings reflect the complexity of the topography.

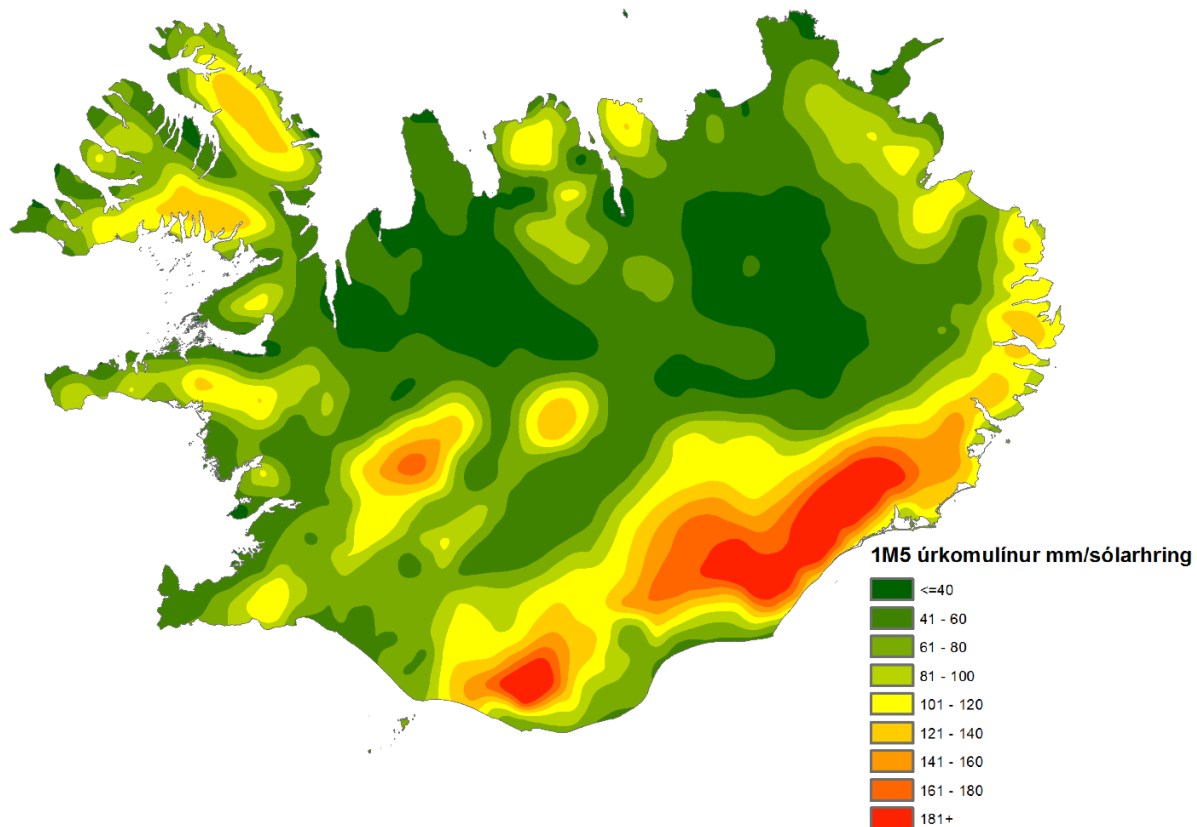


Figure 2. The 1M5 map currently in use in Iceland (Eliasson et al., 2009), showing the 5-year return value in millimetres of daily precipitation.

1.1 Aim

The purpose of this report is twofold: to present an updated assessment of precipitation return periods, and to apply the results to a new 1M5 map of 24-hour precipitation thresholds for a 5-year event. Both observed precipitation and gridded precipitation values from retrospective meteorological forecasts, termed reanalysis, are used in the analysis. The results are presented graphically and in map form. Intensity–duration–frequency (IDF) graphs are used to represent the relationship between the precipitation intensity, duration, and frequency. This type of data presentation allows users to visualise and compare return period thresholds from different locations. The results are also presented in map form, both within this report and via a forthcoming website intended for environmental and civil engineers. Note that the website is scheduled for release in 2022; those requiring a digital copy of the revised 1M5 maps should contact IMO via <https://www.vedur.is/>. The research was funded by Ofanflóðasjóður – Iceland’s National Snow Avalanche and Landslide Fund under the VATNAVÁ (flood hazards) programme at the Icelandic Meteorological Office (IMO).

2 The 1M5 model, weather prediction and precipitation observations

The current version of the 1M5 map presented in Figure 2 (Eliasson, 2000; Eliasson *et al.*, 2009) is based on data from NWP simulations using the PSU/NCAR Mesoscale Model MM5 (Grell *et al.*, 1994). The calculations were performed on an 8×8 km horizontal grid for the period 1961–2006 with meteorological outputs every 6 hours using daily precipitation values. An Extreme Value Analysis (EVA) was made for each grid-point using the Block Maxima method. Because the 1M5 map is based on an NWP output, it covers the whole of Iceland with 1,650 values. In contrast, a map based solely on observed precipitation would have comprised around 100 points, unevenly distributed over the country. The 1M5 map and derived results have proved to be important tools in the design of bridges, culverts and other forms of infrastructure for handling surface runoff. For further methodological details about the current 1M5 map, see Eliasson *et al.* (2009).

Since the publication of the original 1M5 map in 2000, the horizontal resolution of limited area NWP models has increased markedly. Given the complex orography of Iceland, high horizontal resolution is needed to describe the terrain. This is especially true of the East- and the Westfjord regions as well as Tröllaskagi in the north.

The operational NWP system of IMO is the non-hydrostatic HARMONIE–AROME model, with a horizontal resolution of 2.5 km and 65 vertical levels (Bengtsson *et al.*, 2017). The fine-scale gridding gives 66,181 terrestrial points over Iceland – 40 times greater than those in the current 1M5 calculations. The description of the terrain is therefore much improved. However, it should be noted that even at this resolution the narrowest fjords and dales are not properly resolved. For the most part, the model simulates frontal precipitation well, although convective precipitation is still challenging (Pálmason *et al.*, 2016). Because Iceland is in the middle of the North Atlantic storm track, the most extreme precipitation events occur during the passage of weather fronts associated with low-pressure systems. Thus, the model’s underestimation of shallow convection should not significantly affect periods of heavy precipitation. However, the model does not fully resolve small-scale precipitation events, which may arise in air flow over complex orography, resulting in locally higher precipitation intensity than the average over the 2.5×2.5 km grid of IMO’s current operational NWP system. The HARMONIE–AROME model has been used to reanalyse atmospheric conditions in Iceland at hourly time-steps between September 1979 and December 2016, resulting in the Icelandic Reanalysis (ICRA) dataset (Nawri *et al.*, 2017). From the range of simulated variables, gridded values of precipitation can be extracted and used for an expanded analysis of extreme precipitation.

Automatic rain gauges have been in use in Iceland for over two decades, allowing high-resolution measurements down to 10-minute intervals. The present-day network operated by IMO comprises 71 automatic gauges measuring precipitation at a 10 minute interval located throughout the country (Figure 1) as well as manned gauges that record the precipitation once or twice a day. Despite the network’s national coverage, it is often impossible to apply an individual timeseries to a region. In any setting, precipitation patterns can vary tremendously, in regard to intensity as well as spatial coverage, thus creating a major challenge in the collection and use of such measurements (Kidd *et al.*, 2017). The main issue is that precipitation measurements may not represent a larger area. Furthermore, rain gauges underestimate precipitation receipts in windy conditions (Førland *et al.*, 1996; Crochet, 2007). In fact, Pollock *et al.*

(2018) estimated that at exposed upland sites in the UK, the underestimation of rain can be as much as 23% on average due to wind only. In addition, observing solid precipitation and especially precipitation rate are even more difficult to measure. The result of often complicated spatial pattern of precipitation, and undercatch being dependent on wind speed and temperature, is that there are larger uncertainties in precipitation observations than other conventional meteorological measurements. Thus, measurement sites must be chosen carefully and timeseries interpreted with caution with the surrounding terrain considered. In general, interpolation of observations should be avoided due to the natural heterogeneity of precipitation at temporal and spatial scales (Kidd *et al.*, 2017). This general variability is enhanced in complex terrain.

3 Methodology

The gridded ICRA precipitation dataset is compared to observations from selected rain-gauges. Several techniques for retrieving representative grid-point data relative to a given station are described later in this section. Comparisons between observed and modelled precipitation give an estimate of the uncertainty and the potential difference between observations and ICRA data. From this comparison, an EVA method is selected for the ICRA data. Lastly, return period maps are produced using the ICRA dataset.

EVA is a statistical discipline used to predict the occurrence of rare events by assessing their frequency from the most extreme values of a dataset, either observed or simulated. These extreme values are found in the tails of a probability distribution, in the case of precipitation in the right tail, see Figure 3. EVA allows the calculation of return levels associated with periods that can be much longer than the length of the timeseries available for the analysis. Ever since its introduction in the 1920s (Fisher and Tippett, 1928), EVA has been used in a large domain of disciplines such as meteorology, hydrology, human sciences as well as finance (e.g. Embrechts *et al.*, 1997; Watts *et al.*, 2007). Basic concepts will be presented here through two methods for finding the return levels: the Block Maxima approach and the Peak-over-Threshold approach. The theory presented in this chapter is far from exhaustive and it is derived from Coles (2001), where extensive details can be found.

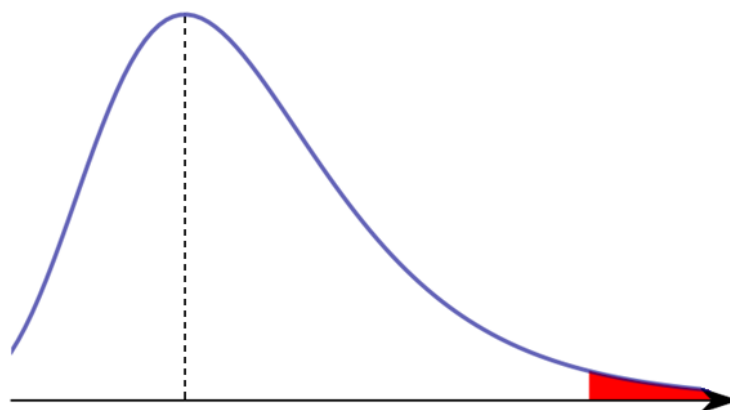


Figure 3. A schematic of a probability distribution (blue line) representing precipitation. The extreme values are located on the right tail of the distribution (red shading). The vertical dashed line shows the maximum precipitation frequency.

3.1 Block Maxima

In EVA, the Block Maxima approach consists of dividing the timeseries into non-overlapping periods of equal size and retaining only the maximum values within each period. When dealing with meteorological and hydrological data, it is common to use the maximum hourly or daily measurements values from each year. A new timeseries that includes only the maxima is thus generated and referred to as an Annual Maxima Series (AMS). Under extreme value conditions, the AMS follows a General Extreme Value (GEV) family of distribution of the form:

$$G(z) = \exp \left\{ \left[1 + \xi \left(\frac{z - \mu}{\sigma} \right) \right]^{-1/\xi} \right\}$$

where z is the extreme value and μ , σ and ξ are the three parameters of the GEV model $G(z)$, defining location, scale and shape parameters, respectively. This three-parameter distribution unites the three possible extreme value distributions, namely type I (Gumbel), type II (Fréchet), and type III (Weibull). The choice of distribution type depends on the extreme value characteristics of the parent dataset. This can be established by the shape factor ξ . The shape factor determines which GEV distribution is applicable, based on the following conditions:

$$\text{Type I } (\xi = 0, \text{ Gumbel}): G(z) = \exp \left\{ -\exp \left[-\left(\frac{z - \mu}{\sigma} \right) \right] \right\}, \quad z \in \mathbf{R}$$

$$\text{Type II } (\xi > 0, \text{ Fréchet}): G(z) = \begin{cases} 0, & z \leq \mu \\ \exp \left\{ \left[-\left(\frac{z - \mu}{\sigma} \right) \right]^{-1/\xi} \right\}, & z > \mu \end{cases}$$

$$\text{Type III } (\xi < 0, \text{ Weibull}): G(z) = \begin{cases} \exp \left\{ -\left[-\left(\frac{z - \mu}{\sigma} \right) \right]^{-1/\xi} \right\}, & z \leq \mu \\ 1, & z > \mu \end{cases}$$

Once the GEV distribution has been fitted to the AMS, the return level r associated with the return period $1/p$ can be estimated with the formula:

$$r = \begin{cases} \mu - \left[1 - \frac{\sigma}{\xi} \{-\log(1 - p)\}^{-\xi} \right], & \xi \neq 0 \\ \mu - \sigma \log\{-\log(1 - p)\}, & \xi = 0 \end{cases}$$

Furthermore, r is defined as the value expected to be exceeded on average once every $1/p$ year.

The Block Maxima approach is a simple method to implement as the data pre-processing requires only the creation of AMS by taking the yearly maxima at the time frequency considered. However, the main weakness is the omission of many possibly significant events because they do not represent an annual maximum value, even though they could be larger than maxima from other years. Also, there is a small potential for including dependent events if the yearly maximum spans a change of year.

3.2 Peak-over-Threshold

Another approach in EVA is known as the Peak-over-Threshold method. In that case, all independent values from a timeseries that exceed a defined threshold, are extracted and fitted to a family of distributions known as the Generalized Pareto (GP) family. The GP family of distributions has the following form:

$$H(x) = 1 - \left[1 + \xi \left(\frac{x - u}{\sigma} \right) \right]^{-1/\xi}$$

where x is the threshold excess, u is the threshold, σ the scale parameter and ξ the shape parameter. Note that ξ is equal to the shape parameter of the corresponding GEV distribution. Return level r is defined as the value that is exceeded once every m observations and can be calculated as follows:

$$r = \begin{cases} u + \frac{\sigma}{\xi} [(m\zeta_u)^\xi - 1], & \xi \neq 0 \\ u + \sigma \log(m\zeta_u), & \xi = 0 \end{cases}$$

where $m = N \cdot n_y$ with N being the return period, n_y , the total number of values in the timeseries and ζ_u the probability that the value is larger than u .

Most of the main issues encountered by the Block Maxima model from a physical point of view are solved by the Peak-over-Threshold method as the extreme values extracted from the timeseries are not limited by their year of occurrence. However, the user must instead ensure independency of values and define a suitable threshold. In general, values in meteorological timeseries are dependent but, by declustering the data with a suitable minimum time window, the remaining values can be assumed approximately independent. For Icelandic conditions, a time window of five days as the minimum time separating two values in a timeseries was selected. It is a realistic interval due to extreme precipitation being associated with weather systems, and thus a synoptic timescale is appropriate to ensure independent events. Furthermore, the same interval has been used for extreme analysis of winds in Iceland (Petersen, 2015). The biggest challenge when setting up the Peak-over-Threshold model is to select a threshold that is large enough not to violate the basis of the GP distribution, but low enough so that enough data are extracted from the original timeseries. Several methods exist to determine the ideal threshold for a timeseries, often done manually (e.g. Coles, 2001). This is not possible when dealing with a large set of timeseries. One way of generalising thresholds for large datasets is to use a percentile, for example the 90th percentile (DuMouchel, 1983), or the square root of n , where n is the number of data (Ferreira *et al.*, 2003). Threshold selection has been the subject of wide research, and an overview of the different options is given by Scarrott and MacDonald (2012).

3.3 Estimation of the distribution parameters

Several methods exist to estimate the parameters of the GEV and GP distributions, with the Maximum Likelihood Estimation (MLE) being the one most widely used. The maximum likelihood estimators are obtained by maximising the likelihood function (Fisher, 1922; Hosking, 1985). Another method makes use of the L-moments that are defined as linear combinations of expected values of order statistics. The L-moments method has been shown to give less weight to outliers in the data and can sometimes lead to more efficient parameters estimates than the MLE (Hosking, 1985). Many other methods have been introduced and

compared (Makkonen and Tikanmaki, 2019), but only those two have been used in this study, mainly to test the sensitivity of the results.

3.4 Software used for computation

In this project, the calculation of return levels was done using the R programming language (R Core Team, 2014) with a package called *extRemes* (Gilleland and Katz, 2016). The package provides many functions and visual tools for EVA. The main functions used in this project covered the fitting of GEV and GP distributions using MLE or L-moments methods, in addition to a declustering function and a return level computation. Most of the pre-processing of the data was done using the Python programming language (Python Software Foundation, <https://www.python.org>), e.g. the extraction of the AMS for the Block Maxima approach. The Climate Data Operator (CDO, Schulzswida, 2019) was also used to apply simple operations directly to NetCDF data files.

4 Data

4.1 Precipitation measurements

In 1995, the first automatic digitised rain gauges were established in Iceland, recording precipitation on an hourly basis. Today, IMO operates more than 70 automatic stations around the country, most of them with a measurement frequency of 10 minutes. In this study, only gauges that had been recording for more than 10 years and that counted less than 1,000 missing days of data over that period were selected, with three exception (due to long series), resulting in 49 stations. Among those stations, 12 were hand-picked as control stations and will subsequently be used to test results from the ICRA reanalysis. Those stations were selected due to their location in narrow fjords or close to complex orography (Eskifjörður and Neskaupstaður in the east; Flateyri, Ísafjörður and Súðavík in the north-west), their exposure to frequent flash-flooding events (Siglufjörður and Ólafsfjörður in the north, Seyðisfjörður in the east), their annual rain intensity (Kvísker and Laufbali in the south-west) or the quality and long timespan of their recording (Reykjavík and Höfn í Hornafirði, see Figure 4 for locations).

Table 1 lists all 49 stations along with the date of their first recording of precipitation, total number of missing daily values and maximum recorded daily precipitation (from midnight to midnight). The 12 control stations are listed alphabetically in the first rows of the table and are written in bold characters for emphasis. Other stations then follow in the table and are listed according to their geographic location. Note that even though Siglufjörður, Þykkvibær and Hágöngur do not fulfil all criteria, their timeseries extend over more than a decade and the stations were therefore kept in this study.

Table 1. Station list along with the date of their first recording, the number of missing daily values since they started recording and the highest recorded values in mm day^{-1} . The first 12 stations (bold) are the control stations.

Station	Abbreviation	First day of recording	Number of missing daily values days	Maximum daily value mm day^{-1}
Eskifjörður	ESK	1998-10-24	103	188
Flateyri	FLA	1997-10-21	29	80
Höfn í Hornafirði	HOFN	2008-01-01	167	80
Ísafjörður	ISA	1998-09-25	0	56
Kvísker	KVI	2009-01-01	488	185
Laufbali	LAUF	2004-06-01	780	134
Neskaupstaður	NESK	1997-10-27	0	198
Ólafsfjörður	OLAFS	1997-10-30	372	132
Reykjavík	RVK	1997-01-01	2	56
Seyðisfjörður	SEYÐ	1995-11-10	69	160
Siglufjörður	SIGL	1995-11-09	1,064	138
Súðavík	SVK	1999-09-29	42	36
Grindavík	GVK	2009-01-01	0	49
Korpa	KOR	2000-01-01	268	73
Hellisskarð	HELL	2001-01-18	343	141
Ölkelduháls	OLK	2001-01-18	141	157
Þingvellir	ÞVL	1998-03-01	277	77
Hvanneyri	HVA	1999-01-01	47	93
Fíflholt	FIF	2006-03-01	125	50
Gufuskálar	GUF	2005-01-01	175	61
Ólafsvík	OVK	2000-04-05	291	178
Grundarfjörður	GRU	2005-01-01	0	167
Stykkishólmur	STYK	2005-06-11	27	42
Patreksfjörður	PATR	1996-04-27	295	75
Tálknafjörður	TALK	2009-01-01	181	60
Bíldudalur	BILD	1998-09-26	12	80
Bolungarvík	BOL	2005-01-01	7	50
Nautabú	NAU	2005-02-05	65	39

Blönduós	BLO	2005-01-01	5	33
Möðruvellir	MOD	2005-11-01	58	82
Akureyri	AKU	2005-12-01	120	51
Hallormsstaður	HALL	1999-10-01	304	97
Dalatangi	DALA	2006-10-01	473	111
Egilsstaðaflugvöllur	EGIL	1998-11-01	87	64
Raufarhöfn	RAUF	2005-05-26	0	53
Brúaröræfi	BRUA	2007-01-01	358	64
Karahnjúkar	KARA	2003-09-01	3	35
Brú á Jökuldal	BRU	1998-11-17	64	46
Eyjabakkar	EYJA	2003-09-01	87	79
Þykkvibær	ÞYKK	1996-09-24	1,130	57
Sámsstaðir	SAMS	2000-07-01	392	100
Kirkjubæjarklaustur	KLAU	2006-09-01	7	83
Kálfhóll	KALF	2005-01-01	119	70
Búrfell	BURF	2003-09-01	48	59
Vatnsfell	VATN	2004-12-01	219	53
Veiðivatnahraun	VEID	2003-09-01	451	56
Hágöngur	HAG	2004-08-26	1,197	48
Hveravellir	HVE	2002-06-27	114	73
Sandbúðir	SBÐ	2003-09-01	403	56

As seen in Figure 4, the IMO rain gauge network is generally well-spread around the country. However, there is only one station in NE-Iceland between Akureyri and Egilsstaðir and only a few stations in the northern highland. Dividing the country into five sectors, 15 stations can be found in the north-eastern quadrant (most of them in the Eastfjords and the north-eastern highland), four in the southeast, 12 in the southwest, 13 in the northwest and five in the central highlands.



Figure 4. Location of selected IMO automatic weather stations measuring precipitation in Iceland in 2019. The control stations are marked by red dots, other stations by blue dots. Quadrants (NW, SW, SE, NE) and highland regions (HL) are also represented.

As can be seen in Table 1, of the stations listed, Neskaupstaður holds the record for the highest daily value of precipitation with 198 mm day^{-1} , recorded in October 1997. Figure 5 presents daily observed precipitation at all stations where values exceeded 10 mm day^{-1} , ranked decreasingly, showing that there are 109 occurrences exceeding 100 mm day^{-1} , but only nine occurrences of more than 150 mm day^{-1} . Among those 109 occurrences, are the events that induced floods in Neskaupstaður on 27 November 2002 (146 mm day^{-1}) and 28 December 2015 (102 mm day^{-1}), as well as in Siglufjörður on 28 August 2015 (101 mm day^{-1}).

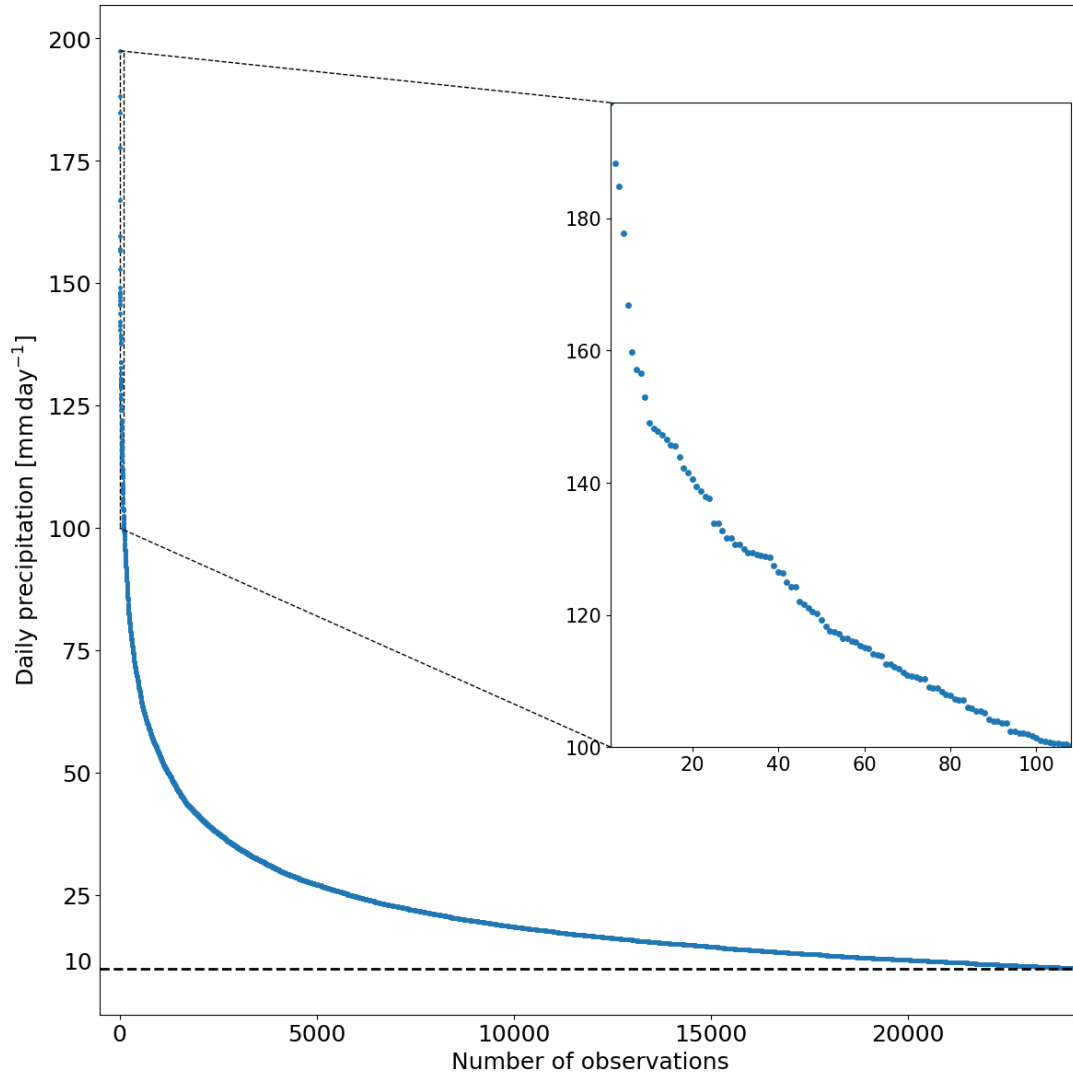


Figure 5. Daily observed precipitation as measured at all stations ranked decreasingly with a cut-off value of 10 mm day^{-1} . The inset graph shows values above 100 mm day^{-1} .

4.2 Reanalysis

Hourly simulated precipitation are retrieved from the ICRA dataset based on the non-hydrostatic NWP HARMONIE–AROME mesoscale model with horizontal resolution of 2.5 km. ICRA starts on 1 September 1979 and currently ends on 31 August 2017, providing data for 38 entire years. Precipitation rate is not a direct output of the model but a sum of different type of precipitation rates: the rainfall rate, the rate of fall of graupel and the snowfall rate.

Nawri *et al.* (2017) provides extensive background regarding the model set-up and quality of the simulation. Model biases of precipitation are shown to be mostly negative along the south coast and less negative or slightly positive over the northern part of the country. Regions of complex orography such as the Westfjords have both positive and negative biases in winter but a close match with measured values in summer. Due to the larger precipitation events being associated with weather fronts, the model's underestimation of convective precipitation has little effect on general precipitation biases.

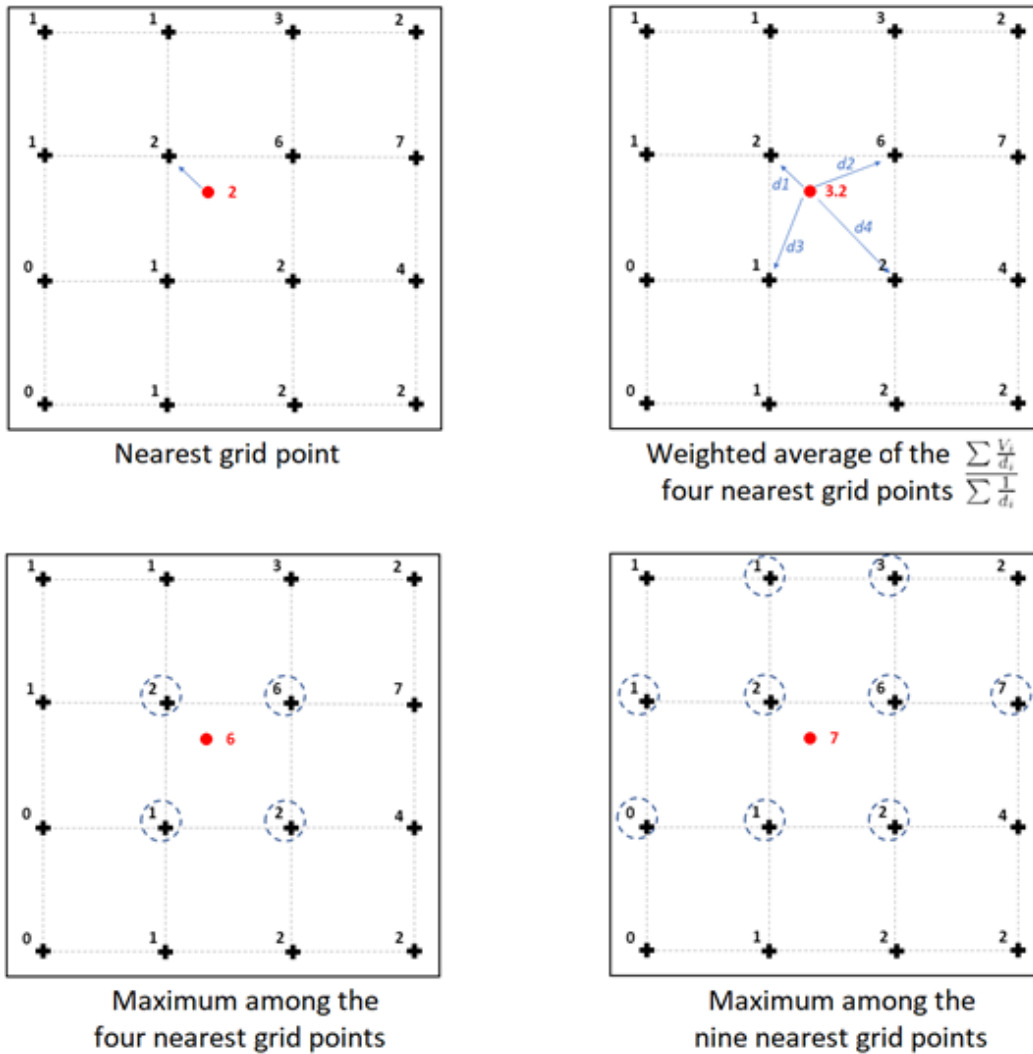


Figure 6. Four methods to derive a precipitation value from a given location (red dot) based on values from a regular gridded dataset (black crosses). Values are indicative and not based on actual data.

4.3 Extraction of the ICRA timeseries

In order to validate the use of the ICRA dataset, results from the reanalysis have been compared to measurements at the 12 control stations. Four options were investigated to retrieve the data at the location of the control stations, as shown in Figure 6. The simplest method picks the value of the nearest grid-point to the location of the station. The other methods use the weighted-average among the four nearest grid-points or select the maximum value among the four or nine nearest grid-points.

5 Results

5.1 Comparison of precipitation intensity between ICRA and selected rain gauge stations

In this section, the focus is on the results for the rain gauge stations. As stated in Section 4.1, 12 control stations were selected to investigate the strengths and limitations of the reanalysis before applying the tests and methods to the entire set of rain gauges.

5.1.1 Interpolation of ICRA results at station locations

In Section 4.3, four interpolating techniques were introduced for retrieving values at station locations from a gridded dataset. By applying them all to the control station data, the daily simulated values can be compared to daily observations in order to select the method that gives the best fit. Figure 7 presents results from those interpolations in the form of scatterplots and quantile-quantile plots (Q–Q plots) for Eskifjörður, comparing the results of daily measurements and daily ICRA data over a 10-year period. Only summer months between May and October were used in order to discard most of the snowfall, which is often under-caught by the gauges. In Q–Q plots, each quantile of the observed timeseries is plotted against the corresponding quantile from the ICRA timeseries, to see if both datasets share a common distribution. In this case it can be seen in both scatterplots and Q–Q plots that the observations are usually higher than the simulated values. Those differences increase for values above 40 mm day^{-1} , as seen clearly in the Q–Q plots. In order to further quantify those differences, two indices are considered: the root-mean-square error (RMSE) and the mean error (ME), shown above the plots in Figure 7. In this case, there is little difference between the nearest grid-point method and the weighted average of the four nearest grid-points. However, when all 12 stations are considered, the weighted average has the smallest RMSE (Table 2). Moreover, it should be noted that the results do not differ greatly when considering intervals shorter or longer than a day. Results are also similar when selecting only values above 10 mm day^{-1} and only values above the 90th percentile (not shown). A decision was made to use the weighted average method and entire timeseries were then extracted at the station locations.

Eskifjörður

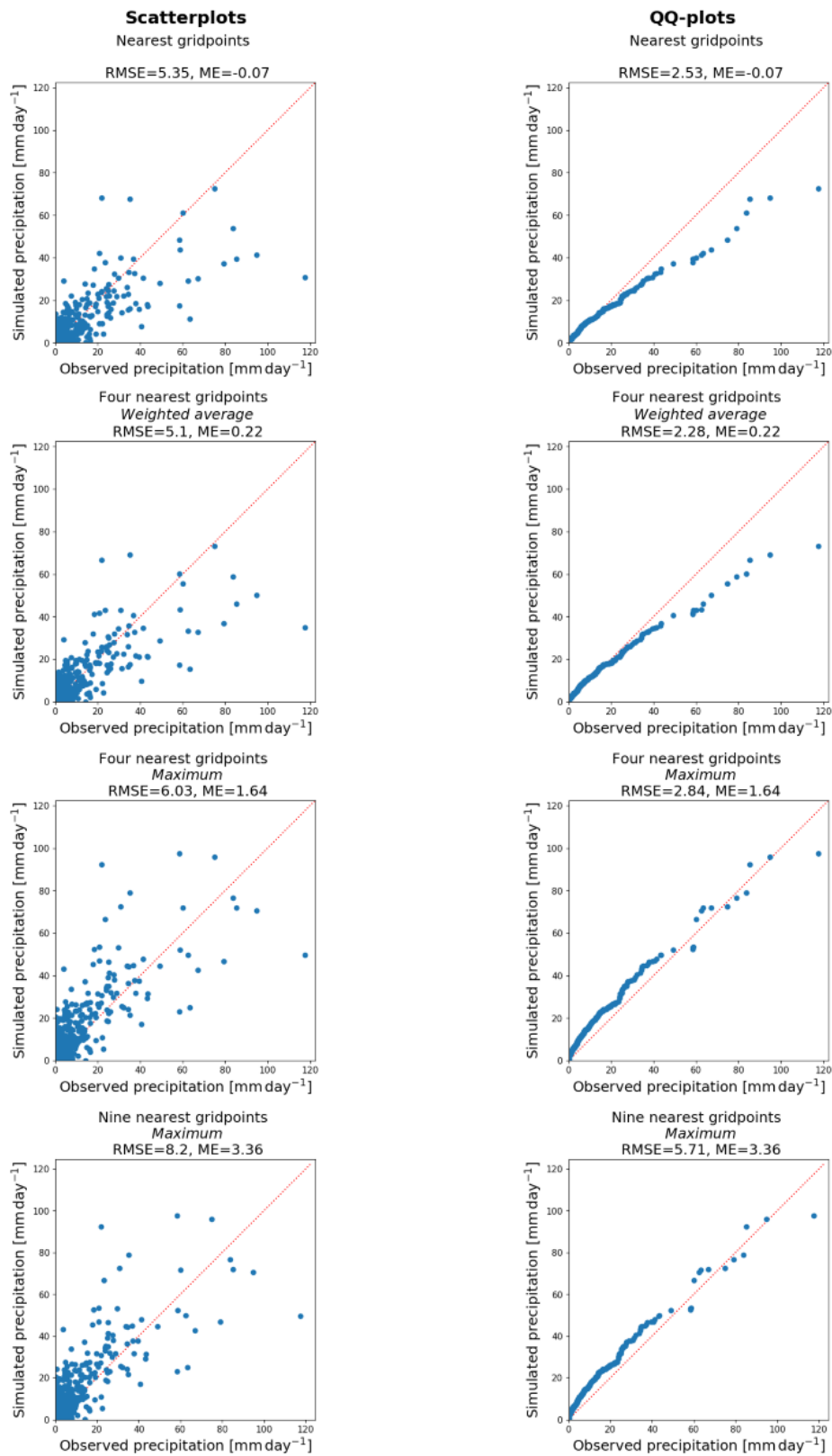


Figure 7. Scatterplots (left panels) and $Q-Q$ plots (right panels) comparing daily precipitation (mm day^{-1}) from the ICRA dataset and observations with different extraction methods for station Eskifjörður. Only data from May to October between 2007 and 2016 were used. RMSE and ME are given for each method in mm day^{-1} .

Table 2. Evaluation of the four interpolation methods for scatter and Q–Q plots. For each interpolation method, the number of stations where the method showed better RMSE values is counted for the 12 control stations.

Scatterplots	Nearest grid-point	3
	Weighted average among four nearest grid-points	8
	Maximum among four nearest grid-points	1
	Maximum among nine nearest grid-points	0
Q–Q plots	Nearest grid-point	5
	Weighted average among four nearest grid-points	6
	Maximum among four nearest grid-points	1
	Maximum among nine nearest grid-points	0

5.1.2 Station statistics

For each station, the 20 highest daily measurements of precipitation have been ranked. Those values are compared to the simulated daily values for the same days and a closeness coefficient used to determine how well the values from the ICRA dataset match the measurements. The closeness coefficient, CC , is calculated as follow:

$$CC = \frac{\min (ICRA, obs)}{\max (ICRA, obs)} \times 100\%$$

CC quantifies simply how close the simulated value is to the observed one, independently of whether the value is higher or lower than the observation. In that sense, CC should be used as a percentage match between two values of a same event. An example is given for station Neskaupstaður in Table 3. For some events, ICRA results are close to the observed value, e.g. on 19 May 2011 while in other cases it seems to have almost missed the event. This is apparent for the most extreme event on 13 May 2017 when the simulated daily value is only one third of the observed amount. However, it should be noted that Neskaupstaður is a challenging location to both simulate and measure precipitation, as the station is in a narrow fjord with steep mountains and a variable spatial distribution of precipitation is therefore likely. Note that the CC is always between 0 and 100% and therefore does not distinguish between overprediction or underprediction of the ICRA compared with the observations.

Table 3. The values and dates of the 20 highest daily values of precipitation (mm day^{-1}) in Neskaupstaður, ranked in descending order according to measurements. Corresponding values from the ICRA dataset are shown, as well as the closeness coefficient (%).

Rank	Daily precipitation mm day^{-1}		Closeness coefficient %	Date
	Observations	ICRA		
1	198	66	34	13-05-2017
2	149	107	72	19-10-2004
3	148	130	88	23-09-2007
4	147	91	62	09-02-2017
5	146	26	18	27-11-2002
6	146	73	50	07-10-2008
7	142	49	34	01-06-2017
8	139	92	71	23-06-2017
9	127	50	39	28-12-2005
10	115	120	96	19-05-2011
11	114	94	82	26-12-2010
12	111	65	59	30-09-2005
13	106	57	54	13-11-2015
14	102	77	76	14-05-2017
15	97	84	87	27-05-2013
16	96	73	77	15-09-1999
17	96	66	69	30-06-2004
18	96	75	79	09-01-2017
19	95	39	41	06-11-2014
20	94	67	70	07-11-1998

Figure 8 illustrates the average CC of the 20 highest precipitation events for each station, ranked in descending order. The range varies greatly, from an average CC of almost 80% (Laufbali) down to 20% (Hallormsstaður). Neskaupstaður aligns close to the middle of the ranked stations with an average CC of 62.9%. For the remainder of the study, stations with an average lower than 50% are discarded, leaving 43 stations for further research. Unrepresentable observations are the most likely reason for CC fits below 50. For example, the rain gauge in Hallormsstaður is located in a forest so the measurements are probably affected by tree-cover, resulting in an undercatch of precipitation. Eyjabakkar, Sandbúðir, Brú and Brúaraöræfi are all located in the highland in remote locations where the weather conditions are often challenging, and solid

precipitation is possible throughout the year. In the case of Laufbali, the *CC* is surprisingly high for a highland station. The average *CC* of the 20 highest precipitation events of all stations above 50% is 64.9%.

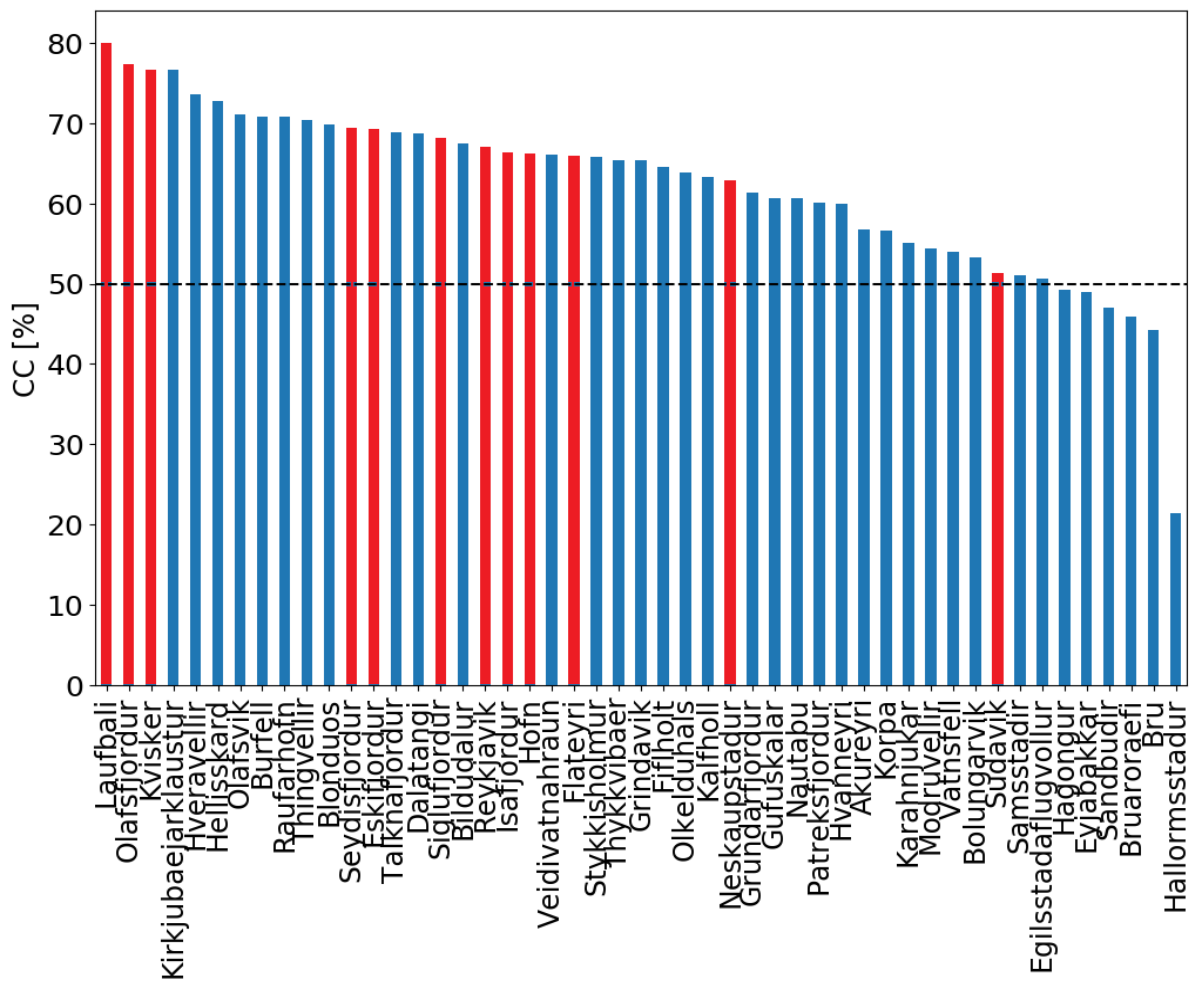


Figure 8. Stations ranked according to their average *CC* (%) for the 20 highest rainfall daily events. The control stations are represented by the red bars. The horizontal dashed line indicates a *CC* of 50%.

In order to test for the difference between daily precipitation from midnight to midnight and precipitation accumulated over a rolling 24-hour window, the 50 highest daily accumulated precipitation events were selected and compared to the 50 highest 24-hour accumulated precipitation events at each control station. Timeseries for simulated precipitation were narrowed to match timeseries of observed precipitation. Only values separated by at least five days were kept in order to consider only independent events. Figure 9 shows the results normalised for all control stations, using both the observation and the ICRA datasets over the same period. As expected, precipitation accumulated over 24 hours always leads to higher values than from midnight to midnight. This is reflected by the values of the RMSE averaged over the 12 control stations: 14% for the observations and 13% for the reanalysis. A decision was made to focus on daily values so that the revised results were comparable to the 1M5 map from Eliasson *et al.* (2009). Furthermore, 1M5 values based on 24-hour accumulated precipitation are also presented at the end of the report.

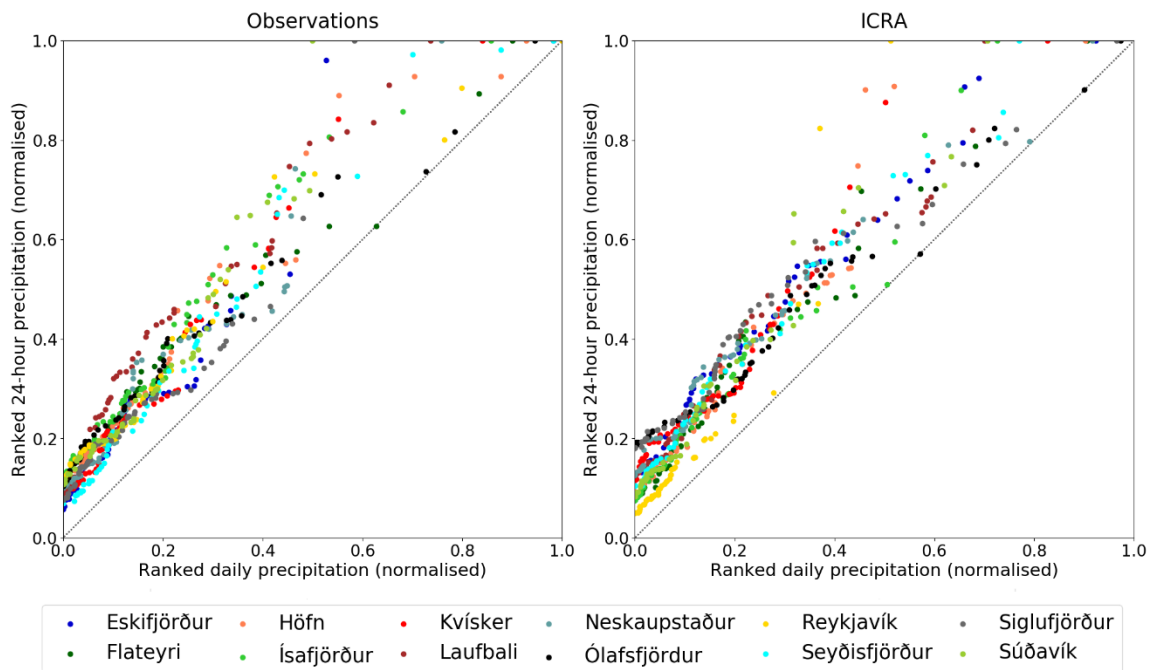


Figure 9. Ranked values of the 50 highest 24-hour accumulated precipitation events plotted against ranked values of the 50 highest daily precipitation events. Results were normalised for the observation (left) and ICRA (right) datasets based on available, overlapping timeseries for the station in question. The colours show the 12 control stations.

5.1.3 Histograms

For each control station, histograms of observed and simulated precipitation accumulated over three hours, have been created for the three largest daily precipitation events. The histograms cover a time span of 72 hours, thus including one day before and one day after the event.

These histograms are helpful to understand how the model represents extreme precipitation. It is worth noticing that even if the model does not reproduce exactly the hourly development of the extreme precipitation event, the accumulated precipitation values over the 72 hours are often close to the actual measurements. Histograms comparing hourly accumulated observations and simulations were also produced, but they are not presented here as they lead to the clear conclusion that the model is unreliable for time duration shorter than three hours. Figure 10 shows an example for the station Laufbali, illustrating the good fit between observations and simulations over the 72-hour timespan, even when 3-hour accumulated precipitation is not correctly reproduced by the model. Histograms for the other control stations can be found in Appendix I. It should be noted that the precipitation measurements depicted in the histograms have not been corrected for undercatch so that some overprediction by the modelled results should be expected.

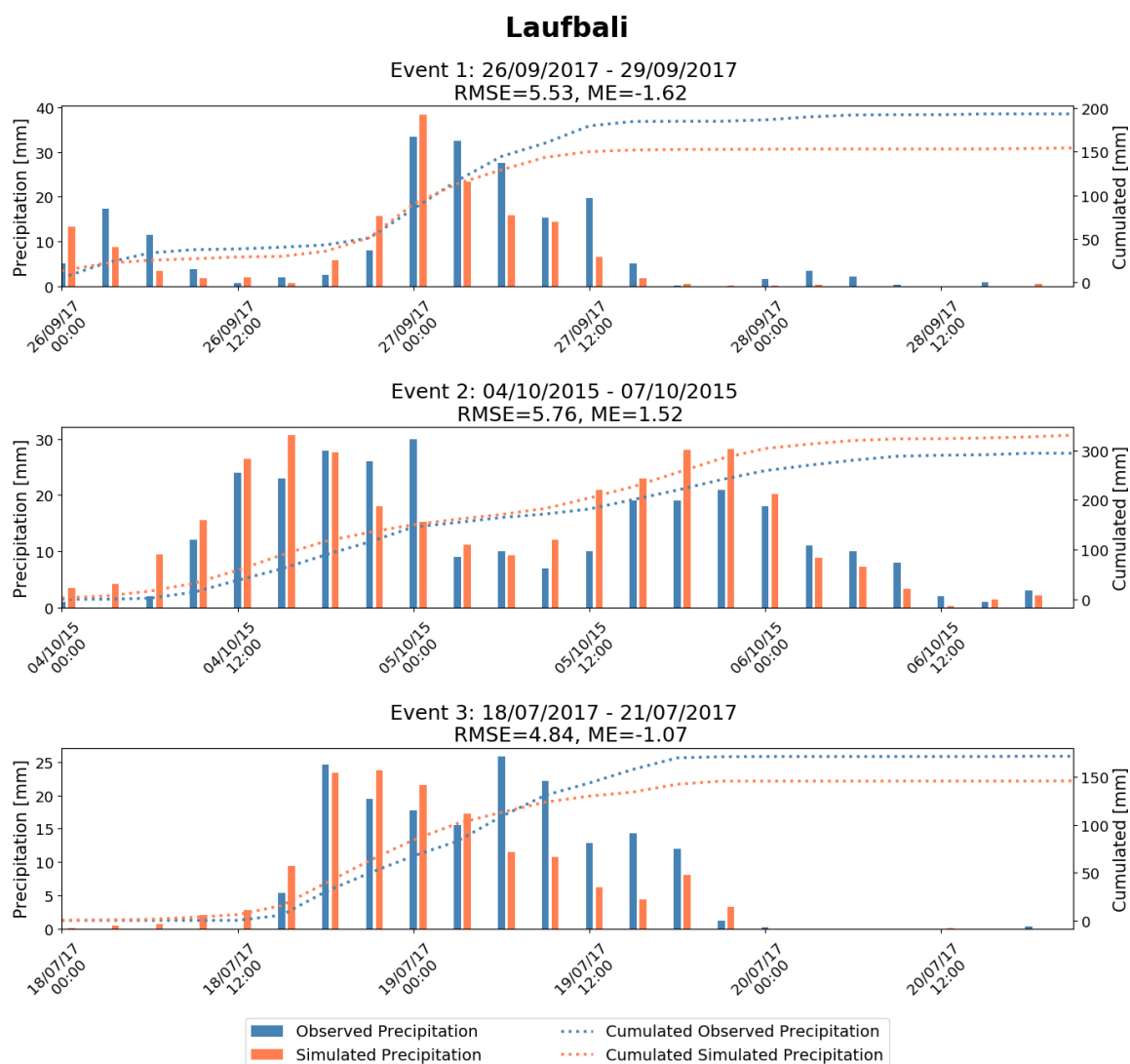


Figure 10. Histograms showing 3-hour accumulated observed (blue) and simulated (orange) precipitation (mm) over 72 hours for the three largest precipitation events at Laufbali. Dashed lines show the corresponding accumulation over 72 hours.

5.1.4 Heat maps

Heat maps were also produced for each of the 12 control stations for the three largest precipitation events over a 3-day span (from one day before the event until one day after). The heat maps in this report are a gridded representation of precipitation distribution, allowing spatial variability and magnitude to be displayed in colour. An example is given in Figure 11 for Neskaupstaður, for the other control stations see Appendix II. Those heat maps help to visualise if values closer to the observed ones are to be found outside the four nearest grid-points used for the interpolation of the reanalysis. For the second day (which is the day with the highest observed precipitation), the reanalysis underestimates the precipitation with 107 mm day^{-1} simulated against 149 mm day^{-1} measured (bar diagram on the right). However, only a few grid-points to the southwest of the station, a value very close to the observations can be found (147 mm day^{-1}), showing that the model is able to simulate values close to the ones observed, but with a small spatial shift (in this case between 5 and 10 km).

Neskaupstaður

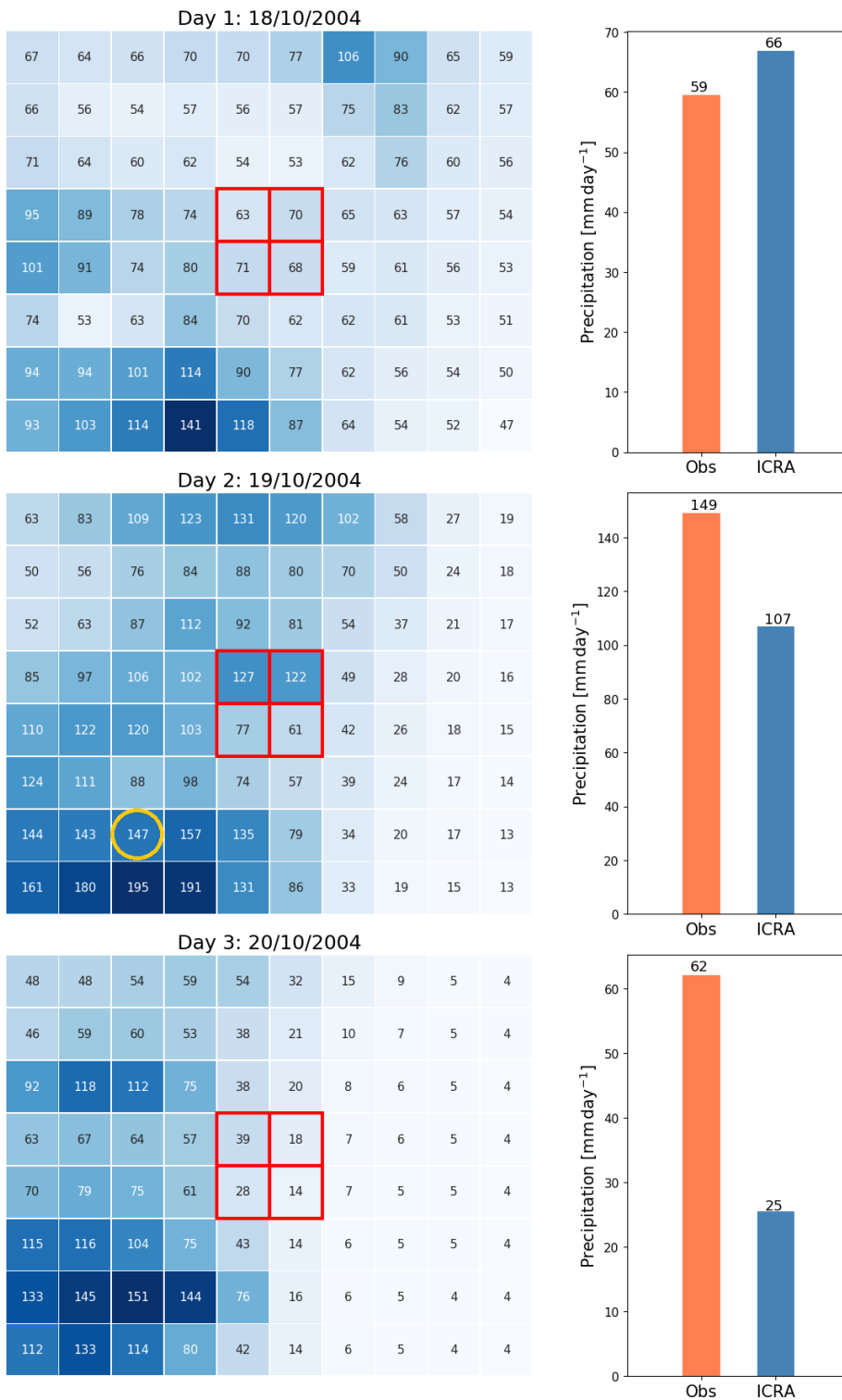


Figure 11. Heat maps showing daily precipitation from the ICRA dataset around the four nearest grid-points (red squares) to station Neskaupstaður over a 3-day period, with corresponding bar diagrams indicating the observed value at the station (orange) and the simulated value (blue). The station is located within the four nearest grid-points. The yellow circle shows the grid-point with the closest value to the measured precipitation on day two.

Seyðisfjörður

Observed accumulated rainfall: 1131 mm

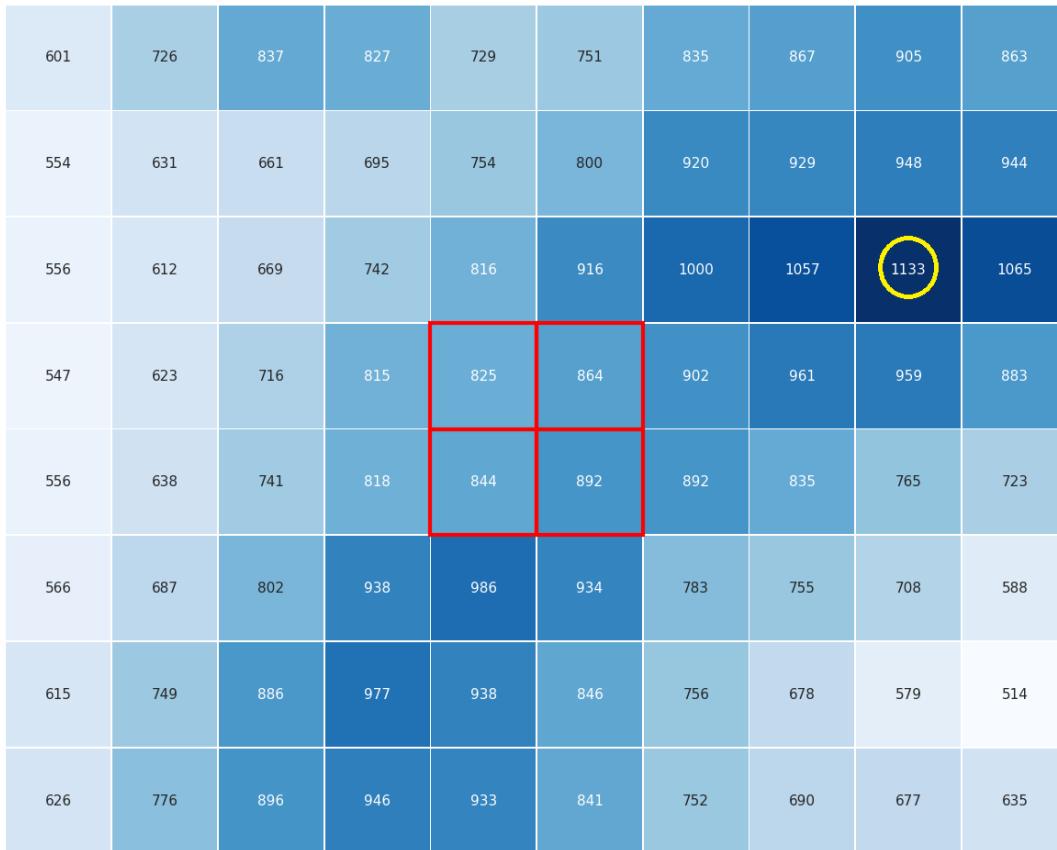


Figure 12. Stacked heat map for station Seyðisfjörður for the 10 largest daily precipitation events (mm) from the ICRA simulation. The red cells show the four nearest grid-points to the location of the gauging station; the corresponding station measurement is indicated above the heatmap. The yellow circle shows the grid-point with the closest value to the measured precipitation.

This is further apparent in Figure 12, where the 10 highest daily events have been stacked for station Seyðisfjörður. At the location of the gauge, the ICRA results underestimate the accumulated precipitation by around 250 mm (which is not a bad result considering the number of events stacked). Moreover, only 5 to 10 km to the northeast, a value of 1,133 mm has been simulated which is extremely close to the one measured by the gauge (1,131 mm).

These examples illustrate the usefulness of the ICRA results for identifying the highest daily precipitation events, even though a small spatial shift is noticeable as may be expected due to the smoothing of the terrain to create the orography used in the ICRA downscaling. Consequently, the ICRA results should be interpreted in relation to neighbouring grid-points to produce the 1M5 map presented later in this report (Section 5.4), as described below. However, station measurements are still required for verification purposes and statistical analysis, such as the production of IDF curves (Section 5.3). Additionally, note that the stations in Figure 11 and 12 are in fjords and the high precipitation values are therefore influenced by local terrain.

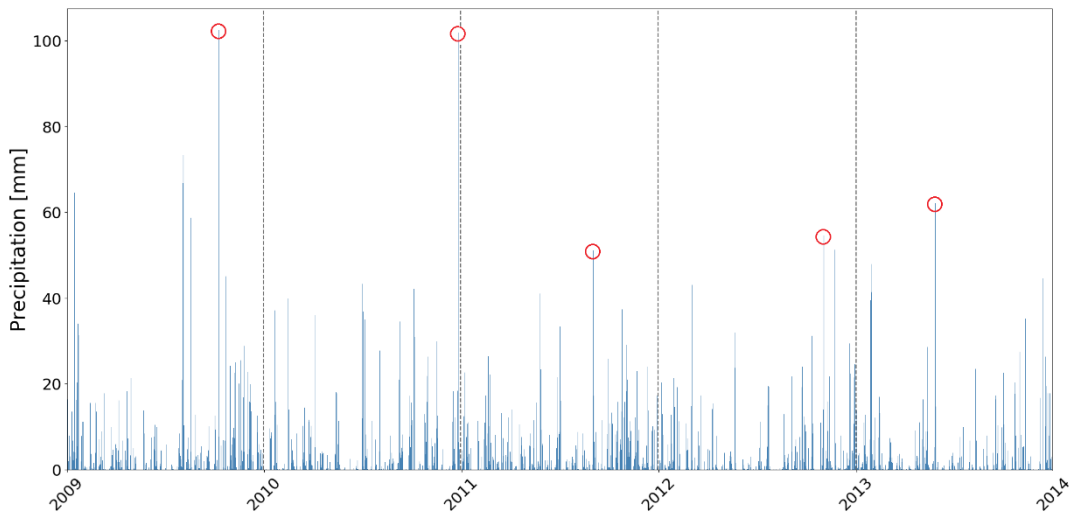


Figure 13. Daily simulated precipitation (blue bars, mm) at station *Eskifjörður* for the period 2009–2015. The values kept for the AMS are marked with red circles. The dashed lines show the start of each calendar year.

5.2 Model implementation and selection

As stated earlier, the aim of this research is to reassess and update return levels of extreme precipitation in Iceland using recent precipitation measurements at automatic weather stations and high-resolution precipitation downscaling with the HARMONIE–AROME model. Two methods were introduced in Section 3 and will here be tested to determine the methodology of calculating new return levels for the production of IDF curves and a new 1M5 map.

5.2.1 Block Maxima

Implementing Block Maxima was done in the following several steps. From ICRA, hourly precipitation was extracted at each control station by interpolating the data to the station location using the weighted average among the four nearest grid-points. The precipitation was then summed over different time durations (3, 6, 12, 24 or 48 hours) for comparison with accumulated observations. For each duration, yearly maximum values were kept to produce the different AMS. An example of data kept for an AMS is shown in Figure 13. The GEV was then fitted for each AMS using both MLE and L-moments methods to find the shape, location and scale parameters. Finally, return levels were calculated for 2, 5, 10, 25, 50 and 100 years.

5.2.2 Peak-over-Threshold

Implementing this model demands more pre-processing of the data than for the Block Maxima method. After obtaining complete timeseries for all time durations in a similar way as for the Block Maxima, a threshold needs to be selected. As mentioned already, it is impossible to manually choose the threshold for each of the 66,181 timeseries. Instead, in this study, at each grid-point, the 90th percentile was selected as the threshold. A few other thresholds were tested, e.g. the 95th percentile, but the differences in results were relatively small. To ensure independent data points, the data were then declustered using a minimum time window of five days. An

example of declustering applied to daily accumulated values is shown in Figure 14 for a randomly selected grid-point. Here, the 90th percentile threshold corresponds to a value of 11.1 mm. If no declustering is performed the above-threshold timeseries would contain 1,017 daily values. However, after implementing a minimum time window of five days, the number of values drops to 639, emphasising that precipitation events often last for a few days. In Figure 14, only the first 1,000 days of the timeseries are displayed, for visualisation reasons only, and it shows that values above the threshold that are not separated by at least five days are discarded by assigning them to the threshold value, meaning that they are not used for the fitting. The GP distribution is then fitted to the declustered data using either MLE or L-moments methods and return levels for 2, 5, 10, 25, 50 and 100 years are calculated.

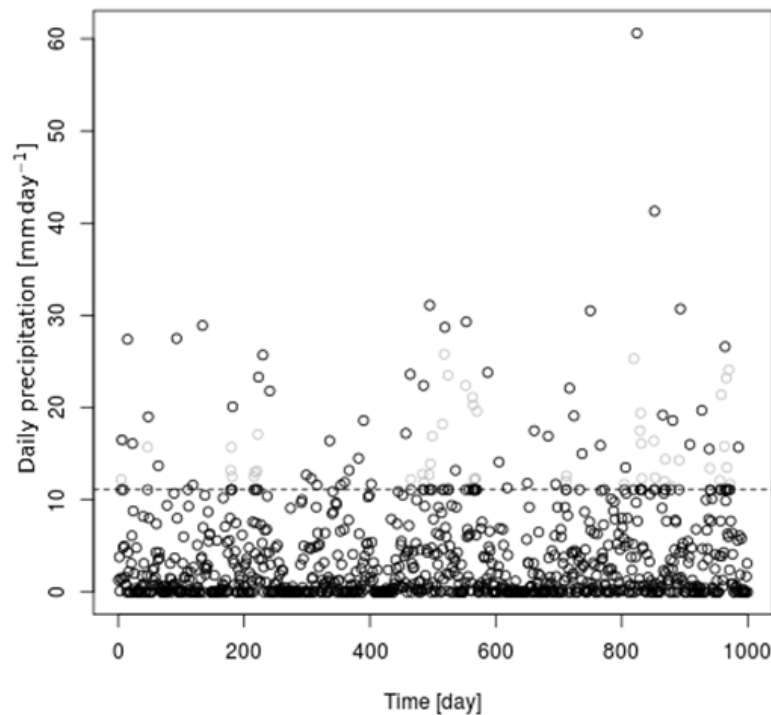


Figure 14. Declustering of the first 1,000 days of data for a randomly selected grid-point (150, 150) using a minimum time window of five days. The 90th percentile threshold is represented by the dashed line and data within the time window are coloured in grey, moved to the threshold line and not used for the GP fitting. The figure is plotted with the extRemes package.

5.2.3 Method selection

Table 4 shows the return levels for daily accumulated precipitation in Eskifjörður, applying both Block Maxima and Peak-over-Threshold methods with MLE and L-moments. The results are very much within the same range using either model for return periods up to 10 years. For both models, the L-moment method of estimating the parameters gives the higher values. For return periods above 25 years, results between methods fluctuate more and the Peak-over-Threshold method always gives higher values.

Table 4. Return levels (mm day^{-1}) for station Eskifjörður for different return periods using daily ICRA values. Values are given for both models using MLE and L-moments methods.

Return period	Return level for daily precipitation mm day^{-1}			
	Block Maxima		Peak-over-Threshold	
	<i>MLE</i>	<i>L-moments</i>	<i>MLE</i>	<i>L-moments</i>
2 years	78	78	78	80
5 years	95	96	97	100
10 years	104	105	111	116
25 years	113	115	126	132
50 years	119	122	146	155
100 years	124	127	162	174

This trend is confirmed for the other control stations: for return periods of up to 25 years, results with both methods are similar. Block Maxima and Peak-over-Threshold are both valid models with distinct and different strengths and weaknesses. Thus, for the rest of the study the method that gives the closest results between observations and ICRA is used. As discussed earlier, timeseries for simulated precipitation were narrowed to match timeseries of observed precipitation as measured at the 43 selected stations. Days where no measurements were made were discarded from the reanalysis data for the comparison to be made between two timeseries of the same length.

Figure 15 presents scatterplots for each method plotting return levels based on observations against simulations for all control stations, time durations (3, 6, 12, 24 or 48 hours) and return periods (2, 5, 10, 25, 50 and 100 years). RMSE and ME averaged over the data are also shown. The Peak-over-Threshold method gives less differences between ICRA and observations at the control stations with RMSE between 1.5 and 2 mm h^{-1} while RMSE values for Block Maxima method are around 2.5 mm h^{-1} . ME values are also closer to 0 mm h^{-1} for the Peak-over-Threshold methods.

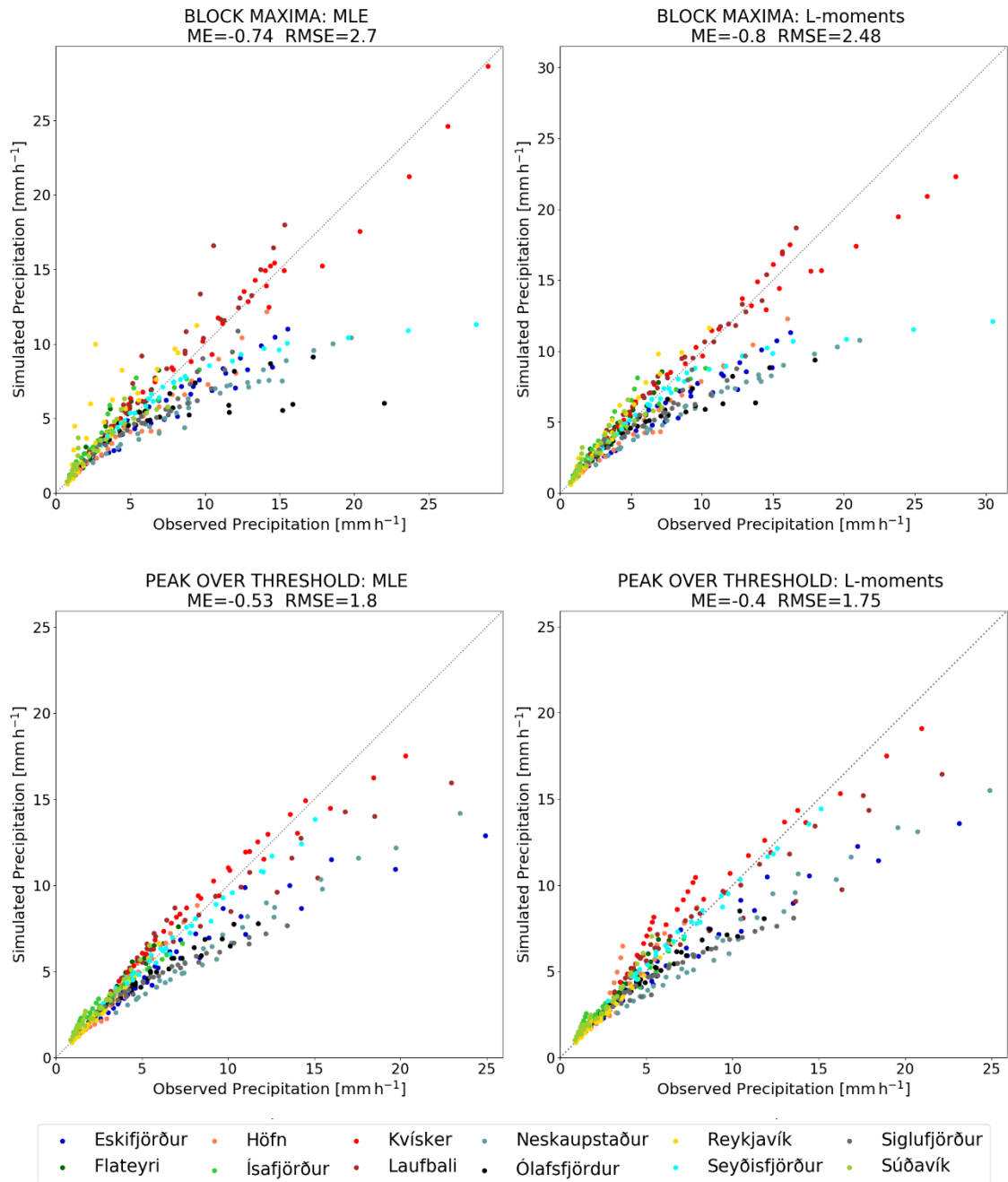


Figure 15. Scatterplots comparing return levels of precipitation (mm h^{-1}) based on simulations and observations. The panels show results for different methods and the colours show the different stations, with each point representing a time duration (3, 6, 12, 24 or 48 hours) and return period (2, 5, 10, 25, 50 or 100 years), totalling 30 points. Note that ME and RMSE values are shown for each method.

Those results are confirmed in Table 5, where RMSE is used to quantify the goodness of fit at each control station. Lower RMSE values are calculated for the Peak-over-Threshold methods with the lowest values obtained for five stations (out of the 12 control stations) with MLE and also for five stations using L-moments. The Peak-over-Threshold method is therefore chosen rather than the Block Maxima method.

Table 5. RMSE ($mm h^{-1}$) between return levels based on observations and ICRA at each station for all methods, time durations and return periods. Minimum values for each station are shown in bold.

Station	RMSE $mm h^{-1}$			
	Block Maxima		Peak-over-Threshold	
	<i>MLE</i>	<i>L-moments</i>	<i>MLE</i>	<i>L-moments</i>
Eskifjörður	2.72	2.78	2.93	2.68
Flateyri	0.53	0.55	0.41	0.52
Höfn	2.45	1.62	0.23	0.63
Ísafjörður	1.07	1.07	0.50	0.53
Kvísker	4.35	1.35	1.00	1.86
Laufbali	1.39	1.12	1.87	1.95
Neskaupstaður	4.64	4.60	3.88	3.81
Ólafsfjörður	2.01	2.63	1.40	1.25
Reykjavík	1.96	1.01	0.33	0.27
Seyðisfjörður	4.39	4.73	0.65	0.48
Siglufjörður	1.65	1.90	2.38	2.18
Súðavík	0.82	0.75	0.50	0.56

Given that it is difficult to conclude on a choice between the two estimation methods from the control stations, *CC* was calculated for all 43 stations with MLE and L-moments for the 10-year return period on daily observed and simulated precipitation. Results are shown on a map in Figure 16. The 10-year return period was selected as it is expected to give reliable values considering the datasets available (observed timeseries of up to 20 years are only available at a handful of stations). Using MLE gives slightly better results, with a mean *CC* on all stations of 91.3% against 90.7% with L-moments. Moreover, MLE gives *CC* superior to 90% in 29 stations against 26 stations with L-moments. The Peak-over-Threshold method with MLE is therefore used in the rest of the study to reassess return periods of extreme precipitation.

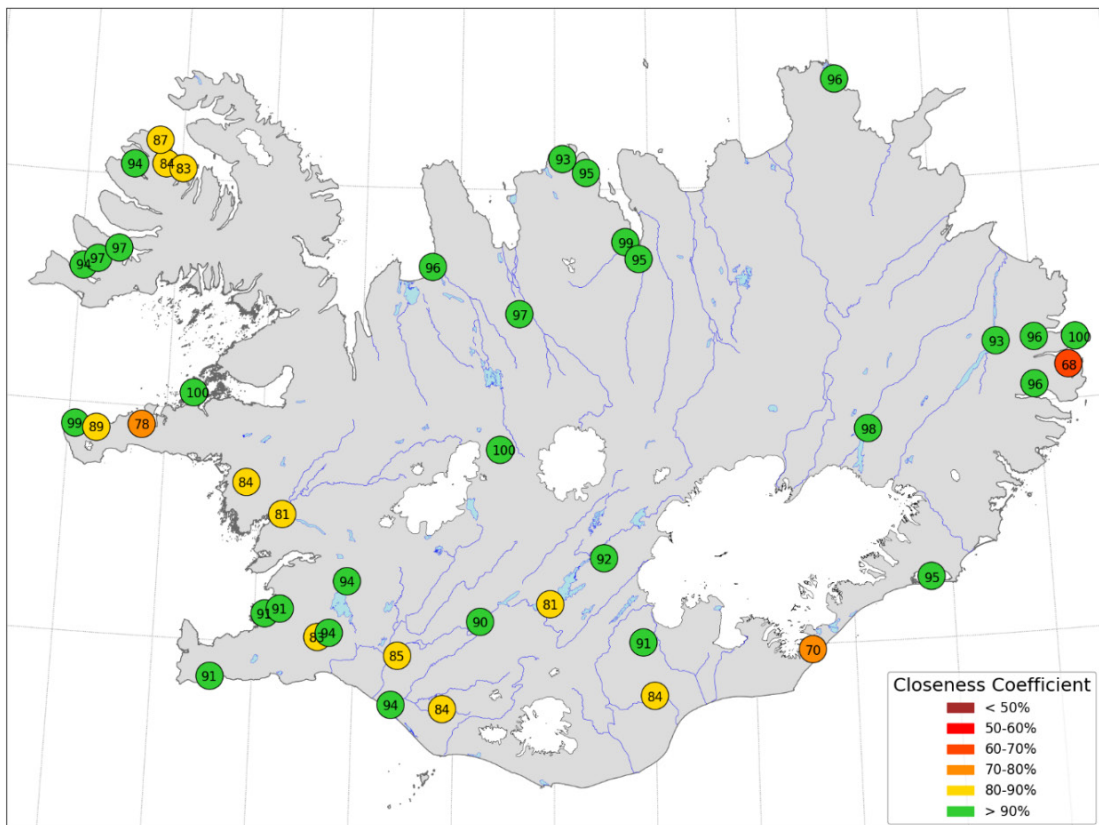
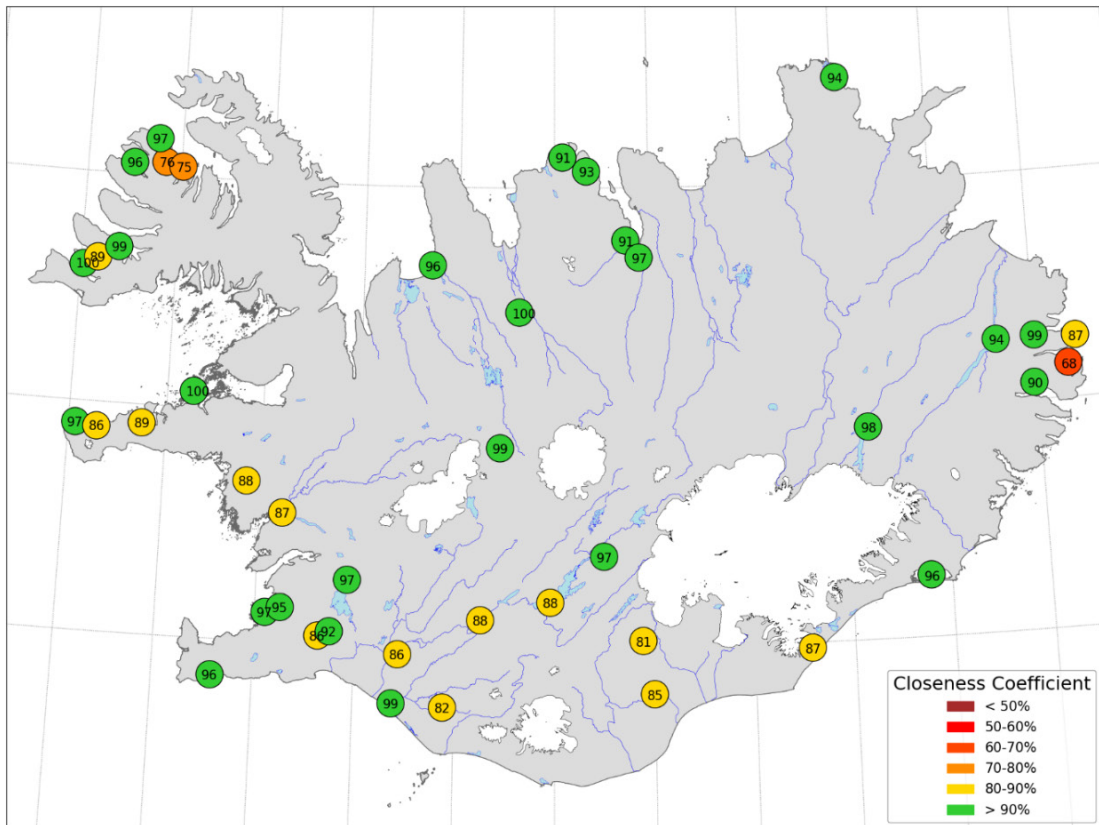


Figure 16. Closeness coefficient (%) between observations and simulations for daily precipitation with a 10-year return period at the 43 gauging stations selected for the study. Results are presented for Peak-over-Threshold method with MLE (top) and L-moments (bottom).

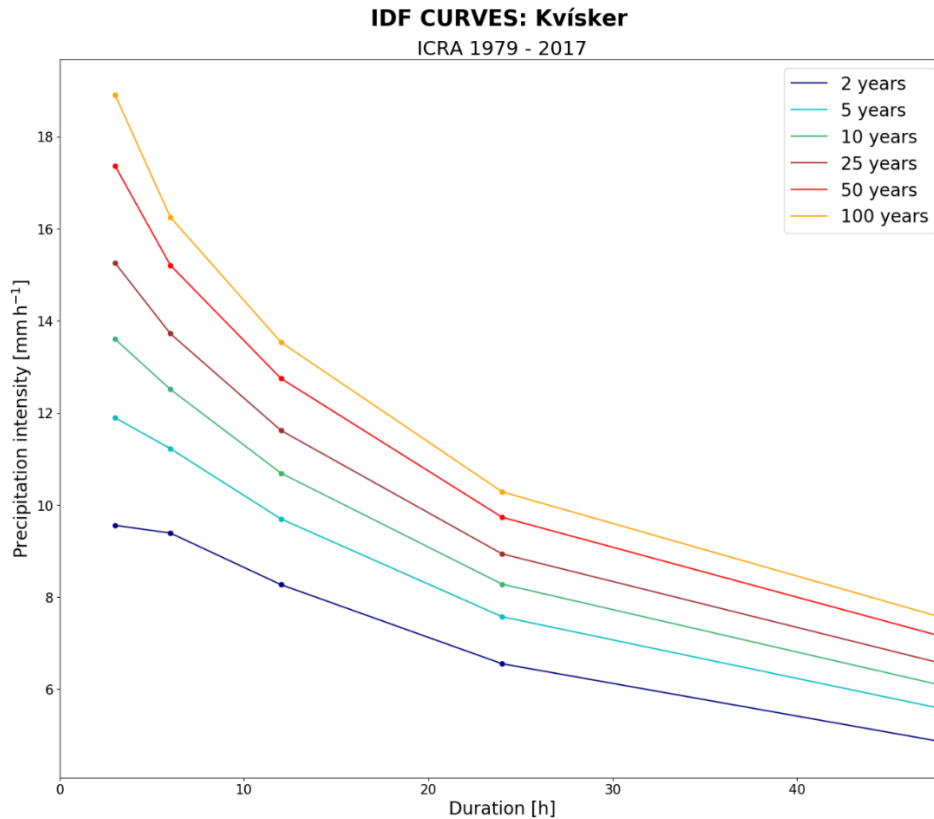


Figure 17. IDF curves for station Kvísker from the entire ICRA dataset. Solid points give return levels for 3-, 6-, 12-, 24-, 48-hour duration with a 2-, 5-, 10-, 25-, 50- and 100-year return period. Each coloured line corresponds to a different return period, as stated by the legend.

5.3 IDF curves

IDF curves have been created for each gauging station using the Peak-over-Threshold approach with MLE applied to the entire reanalysis timeseries. Return levels for the periods 2, 5, 10, 25, 50 and 100 years were calculated for 3-, 6-, 12-, 24- and 48-hours accumulated precipitation. As noted in Section 5.1.3, values for time frequencies smaller than 3 hours were not calculated, as the ICRA does not reliably match the observations for resolution of less than 3 hours. The results were calculated using fixed clock-time intervals.

An example is given in Figure 17 for Kvísker and IDF curves for each of the selected station can be found in Appendix III. Contrary to the 1M5 values, given in mm day^{-1} , precipitation intensity in IDF curves are to be read in mm h^{-1} on the y-axis. From the figure, daily precipitation with a 5-year return period at Kvísker is 7.6 mm h^{-1} or 182 mm day^{-1} . It should be noted that the precipitation intensity at Kvísker is high compared to other stations as it is located in the wettest lowland region of Iceland.

Appendix III contains individual station tables showing the return values for the same return periods and durations as in Figure 17. An example is given in Table 6 for station Seyðisfjörður.

As expected, the amount of precipitation over a given interval increases with the duration of the event. However, for some stations such as Seyðisfjörður, Ólafsfjörður or Siglufjörður, when converted to mm h^{-1} and shown as IDF curves, precipitation intensities sometimes increase with the duration, creating a bump in the usually decreasing IDF curves. Those values are attributed to the fact that the Peak-over-Threshold method was applied independently on timeseries for each duration.

Table 6. Return levels based on the entire ICRA dataset for station Seyðisfjörður. Values are given for 3-, 6-, 12-, 24-, 48-hour duration with a 2-, 5-, 10-, 25-, 50- and 100-year return period.

	2 years	5 years	10 years	25 years	50 years	100 years
3 hours	14	19	23	28	35	41
6 hours	29	38	45	52	62	71
12 hours	56	72	85	99	118	133
24 hours	96	117	133	149	170	186
48 hours	147	177	200	223	253	276

5.4 Revised 1M5 map

A new 1M5 map has been obtained with the Peak-over-Threshold method with MLE and is presented in Figure 18a. Timeseries were extracted for each land grid-point of the ICRA dataset and daily precipitation values with a 5-year return period were calculated for each grid-point independently. Contour lines were then selected to match the current 1M5 map by Eliasson for further comparison purposes, with dark green colour for lowest values and bright red for highest values.

Because of the model's 2.5 km horizontal resolution, the grid-points do not match the coastlines perfectly and many fjords in the West- and Eastfjords regions are too narrow to be resolved properly. As a result, in some places the isolines give values offshore, and these were left deliberately to emphasise the model's spatial resolution.

On the new map, higher values are found over icecaps (most notably on Vatnajökull, Mýrdalsjökull and Langjökull). The highest 1M5 value is 435 mm day^{-1} and it was calculated for a grid-point on the southern part of the Vatnajökull icecap. Except for Snæfellsjökull and Drangajökull, higher values are to be found on the southern sides of the icecaps. Lower values were calculated in drier lowland areas with a minimum 1M5 value of 25 mm day^{-1} . The northern lowlands are generally drier with a large dark green area on the map corresponding to 1M5 values lower than 40 mm day^{-1} . Lowlands in the southern half of the country typically have values ranging between 40 and 60 mm day^{-1} and a few places under 40 mm day^{-1} . Regions of complex orography such as the East- and Westfjords are associated with higher 5-year return levels than the lowlands, with values ranging from 80 to 180 mm day^{-1} in the East and values between 60 and 140 mm day^{-1} in the Westfjords. Locally, higher values are also reached in other mountainous regions such as Bláfjöll, Tröllaskagi or Flateyjarskagi. The median 1M5 value throughout Iceland is 63 mm day^{-1} .

However, a problem with this new map is the tendency for artificially lower extreme values near the coast in steep mountainous terrain, for instance in the Eastfjords and Tröllaskagi. In those regions, 1M5 values near the coast are reduced by tens of percent compared with higher values in the mountains just a few kilometres farther inland. This artificial gradient in the 1M5 values is caused by the smoothing of the terrain on the 2.5×2.5 km computational grid, whereas in reality the terrain may be steep and rising to more-or-less full relief near the coast. Consequently, each grid-point of the 1M5 map was post-processed by selecting the maximum return level from the nearest nine grid-points, resulting in a square-shaped filter (Figure 18b). This shifts high 1M5 values simulated in mountainous terrain up to 2.5 km horizontally. This arbitrary post-processing has the drawback that it will extend too high 1M5 values into precipitation shadows on the lee side of mountains, but this is a less serious bias than an underestimate in the extreme precipitation on the windward side, where many settled areas are located.

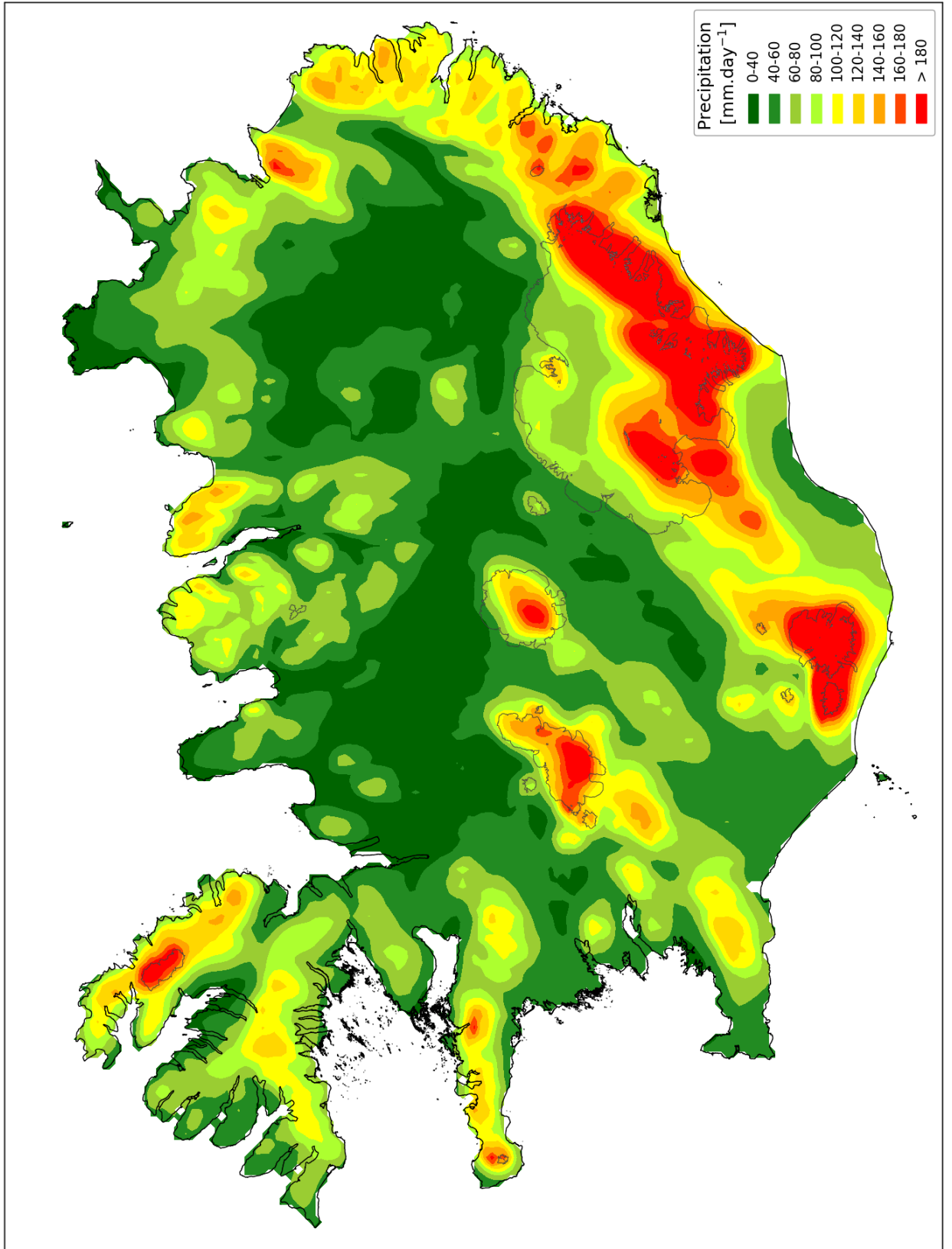


Figure 18a. The new 1M5 map based on daily precipitation from the entire ICRA dataset using the Peak-over-Threshold method with MLE.

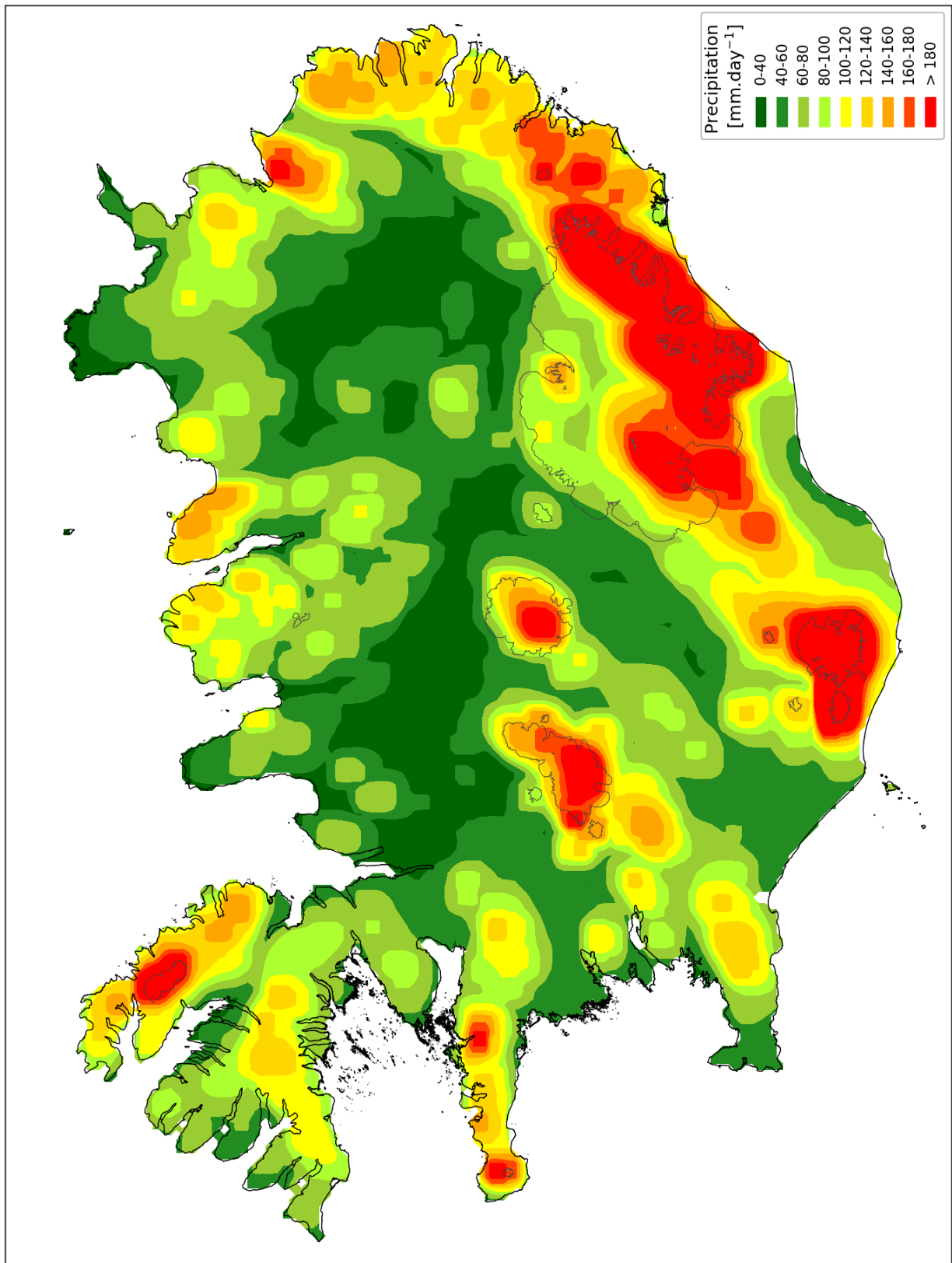


Figure 18b. The new IM5 map based on daily precipitation from the entire ICRA dataset using the Peak-over-Threshold method with MLE, modified using a maximum-value filter among the nine nearest grid-points. Note that the square-shaped imprinting on the map is an artefact of the filtering procedure.

6 Discussion

6.1 Differences in return levels between observed and simulated precipitation

Table 7 shows 1M5 values for the control stations using the Peak-over-Threshold method with MLE on both the ICRA results and observations. For comparison purposes, the timeseries are identical for each station and days with no observations were also discarded in the reanalysis. Overall, results are within the same range, with *CC* ranging from 71% for station Neskaupstaður to 100% for Reykjavík. The return levels differ more for stations located in complex terrain such as Neskaupstaður, Ísafjörður, Súðavík and, to a lesser extent, Eskifjörður, as well as for stations located in wet areas (Kvísker and Laufbali) where ICRA results give higher values. For the remaining stations, Flateyri, Höfn í Hornafirði, Seyðisfjörður, Reykjavík as well as for the Tröllaskagi stations (Siglufjörður and Ólafsfjörður), the differences are smaller and *CC* are above 90%.

Table 7. 1M5 values (mm day^{-1}) for each control station as obtained by the Peak-over-Threshold with MLE from ICRA and observations.

Station	1M5 values over-Threshold with MLE day^{-1}		Peak- mm	CC %
	ICRA	Observations		
Eskifjörður	97	108		89
Flateyri	58	56		97
Höfn í Hornafirði	60	61		98
Ísafjörður	56	43		77
Kvísker	164	138		84
Laufbali	132	109		83
Neskaupstaður	99	140		71
Ólafsfjörður	90	91		99
Reykjavík	36	36		100
Seyðisfjörður	119	111		93
Siglufjörður	98	103		95
Súðavík	41	33		80

Although comparisons of the 1M5 values for all control stations using the Peak-over-Threshold method with MLE on both ICRA data and observations are promising, the differences in some cases is quite large. This can also be seen when looking at the IDF curves for the control stations. Figure 19 shows IDF curves based on observed and simulated precipitation for two stations:

Höfn í Hornafirði and Neskaupstaður. The former station has the lowest RMSE when applying the Peak-over-Threshold with MLE on observations and ICRA data over various durations and return periods, while the latter has the worst fit out of the control stations (see Figure 15 and Table 5 for RMSE values). For Höfn í Hornafirði, IDF curves based on the ICRA results follow quite closely the curves calculated from the observations, even for return periods of 50 and 100 years. For Neskaupstaður, results from ICRA are further away from the results from the observations, as was expected from the large values of RMSE and CC (3.88 mm h^{-1} and 63%, respectively) than for the other control stations. Here, it is important to remember that ICRA systematically underestimates precipitation in Neskaupsstaður, giving return levels much lower than values derived directly from measurements. Those differences are more pronounced when looking at particular events. In Section 4.1, values of intense daily precipitation that led to notable floods were given as examples and they can now be associated with return periods. In Siglufjörður, 101 mm day^{-1} were measured in August 2015 corresponding to a 5-year return period based on observations and simulations (103 mm day^{-1} and 98 mm day^{-1} , respectively). However, the 146 mm day^{-1} measured in Neskaupstaður in November 2002 is an event that occurs every 5 to 10 years according to observation-based results, whereas it corresponds to a 100-year return period event in the ICRA dataset.

When assessing the quality of the ICRA precipitation, the observations are considered to be accurate; however, it should be noted that it is clearly an oversimplification. Firstly, precipitation measurements are point measurements of a highly nonhomogeneous field and secondly there are large measurement uncertainties related to wind speed and precipitation type. As seen in Figure 19, in some places, results based on ICRA data are comparable to those based on observations, but there are also places where that is not true. In some cases, the difference is due to the precipitation measurement not being representable. This is known to be the case in Hallormsstaður and some highland stations (see Section 5.1.2). In narrow fjords and valleys, the model may not be able to represent the precipitation pattern, or the rain gauge may measure a local point maximum that the simulation cannot represent at its 2.5 km horizontal resolution. In fact, it may be impossible to determine the difference without a field campaign with multiple rain gauges and, even in such a case, the results from one area may not be representative of another. Therefore, the differences between observations and ICRA data at stations in complex orography should not be interpreted as ICRA precipitation estimates being unreliable. The heat maps in Figures 11 and 12 show that there is a large spatial variability in precipitation in complex terrain in the ICRA dataset – as expected in reality. Applying such heat maps together with information on terrain may assist in finding the most suitable locations for rain gauges. Heat maps may also give indications of differences in precipitation patterns between neighbouring watersheds.

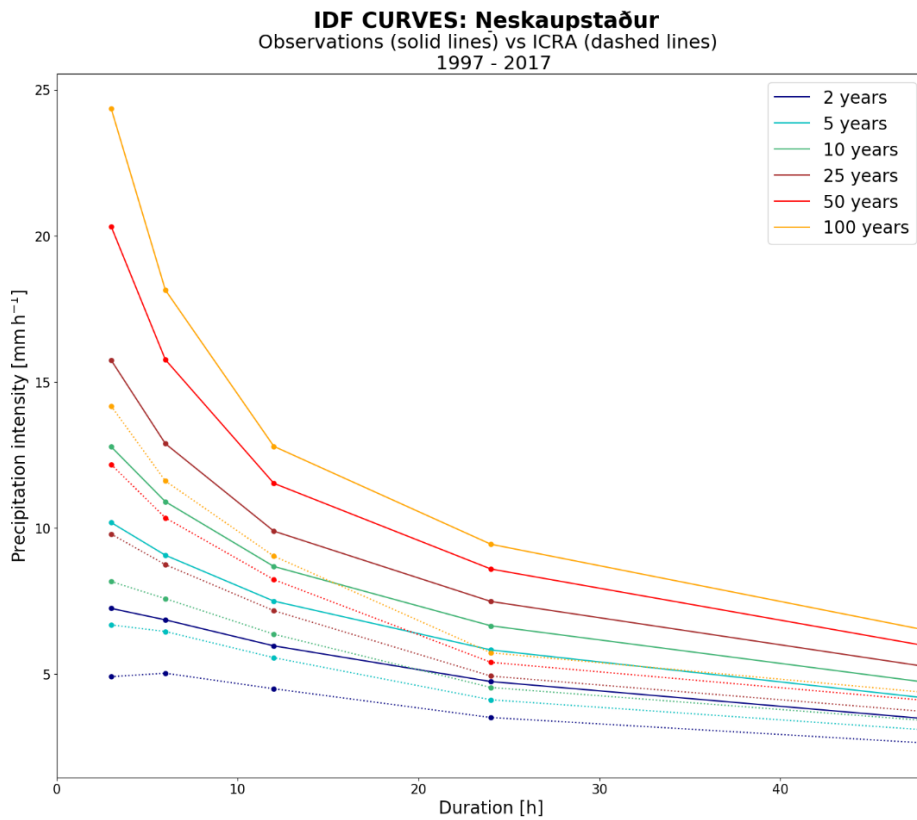
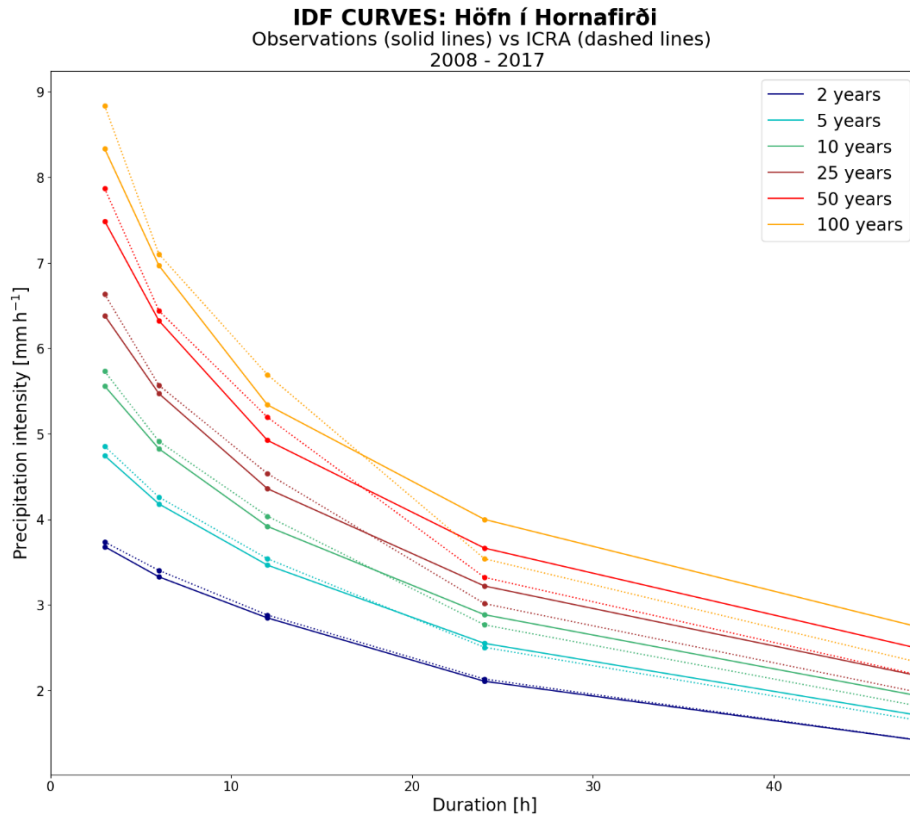


Figure 19. IDF curves for stations Höfn í Hornafirði (top) and Neskaupstaður (bottom) comparing results based on observations (solid lines) to results based on ICRA simulations (dashed lines) obtained for the same time period. Each coloured line corresponds to a different return period.

6.2 Sensitivity of the EVA methods

In order to analyse the sensitivity of the EVA methods, IDF curves, obtained from the Peak-over-Threshold with MLE, are compared to IDF curves that have been generated with Block Maxima, Eliasson and Wussow formulas. The latter two methods were previously used on Icelandic data and are detailed below. Results based on those four methods are shown on Figure 20, which shows 10-year return period IDF curves from all control stations stacked and normalised. Results are shown as they were calculated using observations (left panel) and simulations (right panel) for fixed clock-time intervals.

For the Block Maxima, the MLE method was selected for consistency with the estimators chosen for the Peak-over-Threshold. It should be noted that for both Block Maxima and Peak-over-Threshold methods, return levels were obtained independently for each time frequency and return period.

This is not the case for the Eliasson and Wussow formulas, where daily values are obtained and then values for all other durations derived from those return levels. In the case of Eliasson, IDF curves are generated using two parameters: the 1M5 values obtained from Block Maxima and a correction factor C_i . This factor is dependent on the geographical location and ranges between 0.19 and 0.25 but, for practical reasons, it was here set to 0.209, the country average (Eliasson, 2000). To test the formula, 1M5 values obtained by Block Maxima with MLE on observation and ICRA were used. The return level r associated to the duration t is given by the following formula:

$$r = \left\{ 1M5 \left[1 + C_i \left[-\log \left(\log \left(\exp \left(-\frac{1}{T} \right) \right) \right) - 1.5 \right] \right] \right\} \times \{ 0.02474 \sqrt{R_a(t)R_b(t)} \} \\ \times \left\{ \sqrt{\left[\frac{\log(R_a(t)) - \log(R_b(t))}{2} \right]^2 + 0.001} \right\} / t$$

where r is the return level in mm, $1M5$ is the daily precipitation for a 5-year return period in mm day⁻¹, T is the return period in years, t the duration in minutes and $R_a(t)$ and $R_b(t)$ are two functions defined as follow:

$$R_a(t) = 0.7642t^{0.58908}$$

$$R_b(t) = 6.4722t^{0.25232}$$

Another method that has also been tested on Icelandic data by Bergþórsson (1968) is Wussow's formula. Calculation of return levels in that case requires return levels for daily accumulated precipitation (r_{24}) at the return period considered. Computation of the return levels of lower time frequencies (t) is then made using the following formula:

$$r = \frac{r_{24}}{1440} \sqrt{t(2880 - t)}$$

In the figure, median values for each method are represented by solid lines and minimum-maximum intervals by shaded areas. Results show that values calculated by Peak-over-Threshold are lower than those calculated with the other methods for time periods under 24 hours but higher for periods of 24 and 48 hours. The Block Maxima and Peak-over-Threshold give values that are in a similar range while Eliasson and Wussow formulas give higher values for

shorter time frequencies. The results are similar when considering normalised precipitation intensities for 2-, 5-, 25-, 50- and 100-year return periods (not shown). Overall, the choice of EVA method leads to more variation for short durations (3 and 6 hours) than for longer ones.

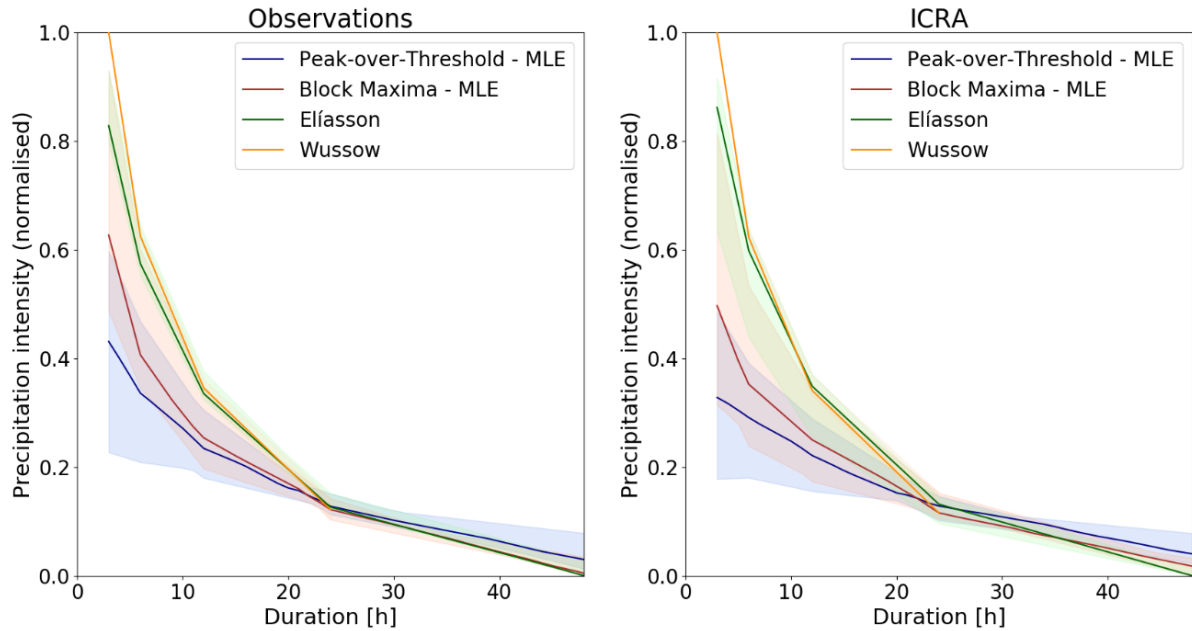


Figure 20. 10-year return period normalised IDF curves stacked for all stations and calculated from observed data (left) and ICRA results (right). Median values from all stations are shown with coloured solid lines, minimum-maximum ranges by shaded areas.

Table 8 shows daily precipitation return levels associated with a 5-year return period for all the control stations calculated by Eliasson, the Peak-over-Threshold with MLE and the Block Maxima with MLE. A table with values for all stations is shown in Appendix IV. Results after applying the square-shaped filter presented in Figure 18b are not shown. Here, values from Eliasson were directly extracted from the current 1M5 map. As stated previously, the Block Maxima method was used in the 2009 study to obtain Eliasson’s 1M5 values. Therefore, new results obtained by the Block Maxima method are comparable to the results by Eliasson, applying the same method but on a different set of data, with higher horizontal resolution, and covering another time period. It can be noted that 1M5 values calculated from Peak-over-Threshold and Block Maxima on the entire ICRA dataset are very similar. The most notable difference is 9 mm day^{-1} (corresponding to a 7% variation) for station Ólafsvík, located on the Snæfellsness peninsula (see Appendix IV). Thus, the differences between the new 1M5 values from the Peak-over-Threshold based on the reanalysis and the current 1M5 values are not as much a consequence of the choice of EVA as they are an expression of the model differences.

Table 8. 1M5 values (mm day^{-1}) at each control station as obtained by Eliasson *et al.* (2009) using the Block Maxima method, Peak-over-Threshold and Block Maxima methods with MLE based on daily precipitation from the entire ICRA dataset.

Station	1M5 values mm day^{-1}		
	Block Maxima (from Eliasson)	Peak-over-Threshold	Block Maxima
Eskifjörður	120	95	94
Flateyri	63	61	59
Höfn í Hornafirði	76	76	71
Ísafjörður	53	58	58
Kvísker	159	182	183
Laufbali	128	129	127
Neskaupstaður	105	104	103
Ólafsfjörður	79	95	89
Reykjavík	42	34	33
Seyðisfjörður	103	117	112
Siglufjörður	73	99	95
Súðavík	41	41	40

6.3 Comparison between 1M5 maps

6.3.1 1M5 maps based on daily precipitation

Earlier in this study, a decision was made to use daily precipitation values from midnight to midnight for direct comparison with the study from Eliasson *et al.* (2009). Differences between the new and current 1M5 maps are shown in Figure 21 where values from Eliasson were retrieved and interpolated to the resolution of the new map. This comparison was made using the unamended new 1M5 map presented on Figure 18a. The main features of the current (Figure 2) and the new 1M5 maps are similar and in agreement with the general precipitation pattern in Iceland (Figure 22); that is, high precipitation over mountainous terrain and in general higher values over the southern part of the country. This is expected as both datasets describe the large-scale terrain and one would expect that greatest variations in return levels to be found in the regions with the largest precipitation ranges. As seen in Figure 21, differences of $\pm 20 \text{ mm day}^{-1}$ cover the largest part of the country (pale orange and light blue colours), and more generally, the current 1M5 values are slightly higher than the new one (pale orange area). The differences between the two maps lie in the detail; most of the differences are related to an improved depiction of the topography. In general, the precipitation pattern is more detailed in the new map, both in relation

to higher and lower return levels, but there are also large spatial differences. This is especially visible in regions of steep, but not large, mountains, e.g. over the Snæfellsnes peninsula where the largest return level in the current 1M5 map is on the order 140–160 mm day⁻¹ but exceeding 180 mm day⁻¹ in the new map, sometimes leading to an offset of over 60 mm day⁻¹ (dark blue colour). These larger spatial differences over the more complex terrain are in accordance with meteorological expectations, as the new 1M5 is based on higher horizontal resolution simulations and should therefore be able to contain more details than the current one.

Those differences are further illustrated by the scatterplot in Figure 23 where new and current 1M5 values (from Table 8) are plotted against each other. Most stations that fall within the one standard deviation region (36 stations) have new 1M5 values slightly lower than those calculated by Elíasson. However, for six out of the seven stations outside this interval, the new 1M5 values are much higher. These are all stations close to or in complex topography: Ólafsvík and Grundarfjörður on the Snæfellsness peninsula, Ölkelduháls and Helliskarð in the Bláfjöll area, Siglufjörður in Tröllaskagi as well as Kvísker just south of the Vatnajökull icecap. The largest differences thus indicate an underestimation in the current version of the 1M5 map due to coarse terrain.

The new map is more physically detailed and accurate than the current 1M5 map, especially in the aforementioned regions of fjords where the terrain is particularly challenging. This was expected as the horizontal resolution of the model previously used was unable to resolve the topography in these regions. However, note that although the new map is more detailed, there are still unresolved fjords; for instance, the narrow fjords in the east, as can be reflected by the coastlines not matching the isolines.

6.3.2 1M5 map based on accumulated precipitation over running 24-hour windows

Differences between daily precipitation from midnight to midnight and precipitation accumulated over any 24-hour window were briefly investigated in Section 5.1.2. Results showed a 13% bias when comparing the 50 highest daily accumulated values to the 50 highest 24-hour accumulated precipitation events. In order to see the effects of this increase on a broader level, another 1M5 map is presented in Figure 24a; this time based on 24-hour accumulated values extracted from the entire ICRA dataset. For each timeseries, 24-hour accumulated values were calculated using a rolling sum and only daily maximum values were retained. Five-year return levels were then obtained after applying the Peak-over-Threshold method with MLE independently on all timeseries, again with a 5-day window chosen for declustering.

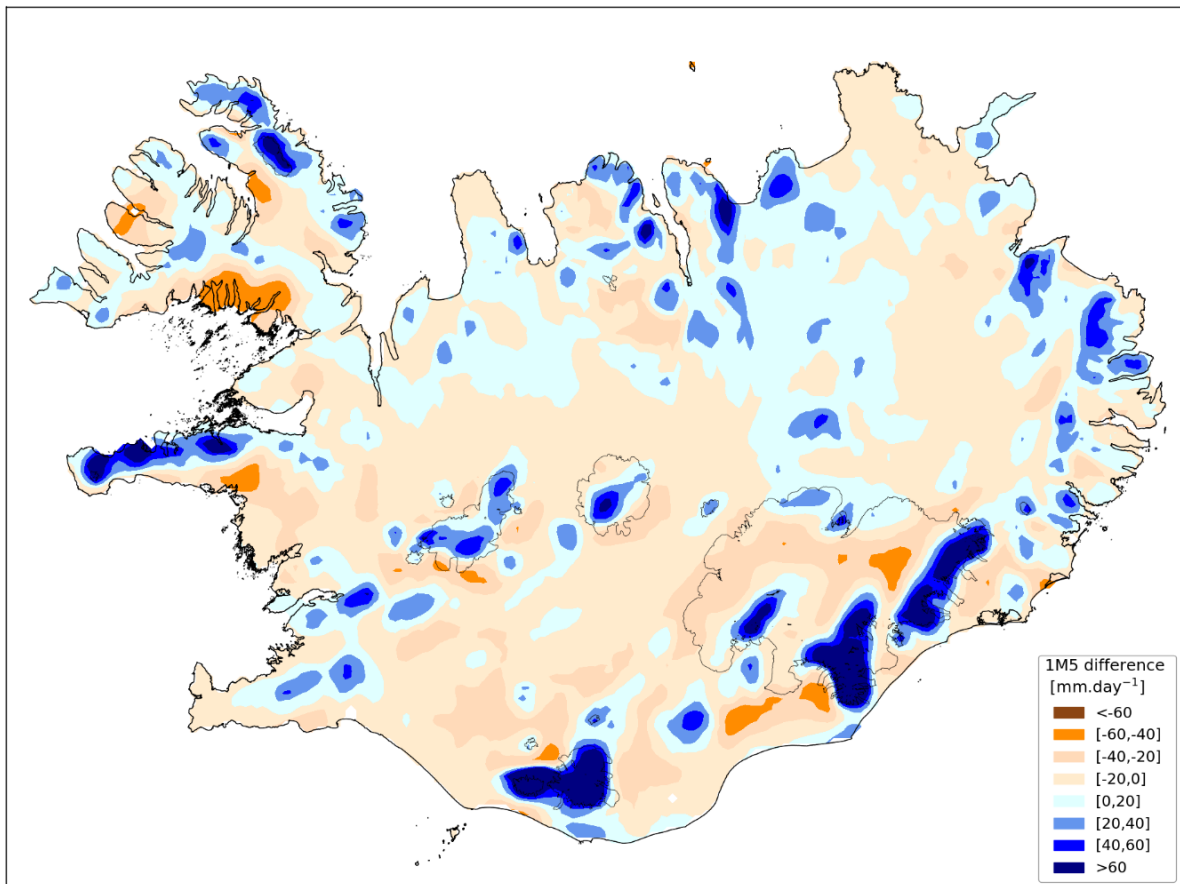


Figure 21. Geographic differences between the 1M5 map developed in this study and the 1M5 map from Eliasson et al. (2009), both based on daily precipitation. Blue-coloured shading signifies higher values in the new map.

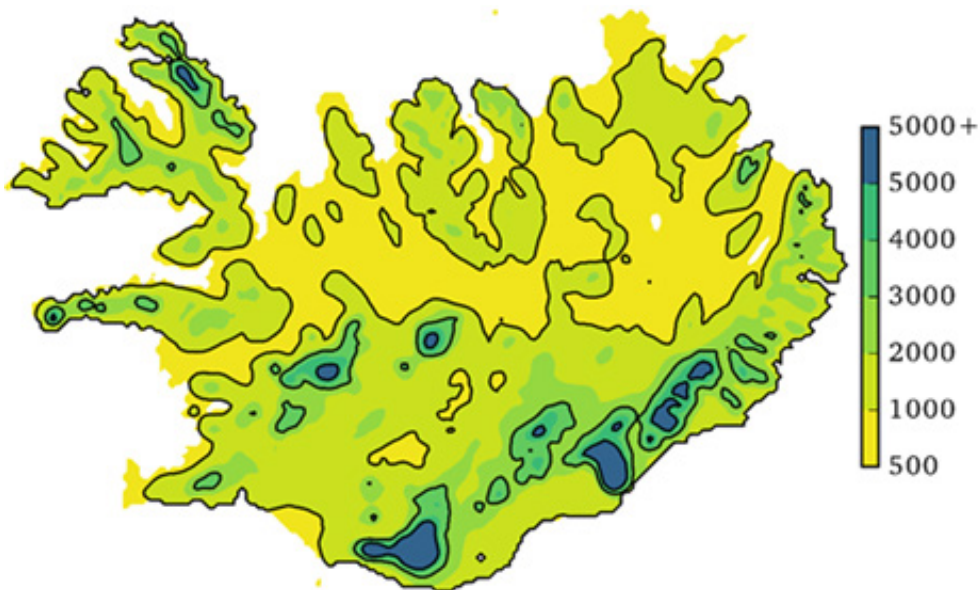


Figure 22. Distribution of annual rainfall (mm year^{-1}) in Iceland for the period 1981–2010. Solid lines show the 1000, 3000 and 5000 mm year^{-1} values. Results were based on the ICRA dataset (figure from Björnsson et al., 2018).

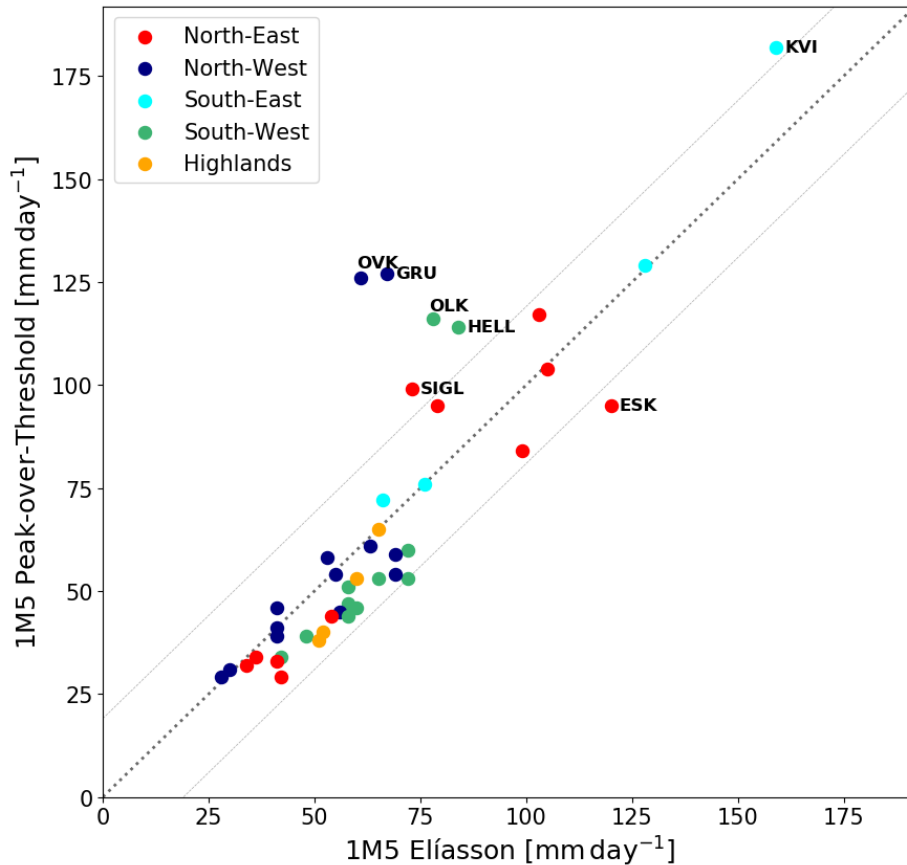


Figure 23. New 1M5 values plotted against 1M5 values from Eliasson et al. (2009) for all 43 stations. Colours correspond to the different regions of the country, see Figure 4. The broken line is the one-to-one line and the grey lines mark the one standard deviation region. The points outside of that region are marked specially. For station names, see Table 1.

Similar patterns are seen in Figure 24a in comparison to the 1M5 map based on daily values (Figure 18a). Higher values are found on the southern parts of the icecaps and in regions of complex orography. Again, the highest 1M5 value is obtained for a grid-point on the southern part of Vatnajökull, this time with a return-level of $470 \text{ mm } 24\text{-h}^{-1}$, corresponding to a 38 mm increase. The median value over Iceland is $72 \text{ mm } 24\text{-h}^{-1}$, which constitutes a 14% increase, in line with the results from Section 5.1.2. Overall, areas of large values, represented by colours in the yellow and red shades, are spatially more extensive than the original, revised map. Some regions with large values on the daily map now extend into the next colour interval; this is especially visible in the East- and Westfjords and in the Tröllaskagi peninsula, with values now reaching the $140\text{--}160 \text{ mm } 24\text{-h}^{-1}$ interval (dark orange on the map). Values ranging from 160 to $180 \text{ mm } 24\text{-h}^{-1}$ (light red on the map) are also observed in the Bláfjöll mountains and Flateyjarskagi.

These results are further illustrated in Table 9, where 1M5 values are given for each dataset and control station, along with the difference and percentage increase. Results for all 43 stations are shown in Appendix IV. For most stations, the increases range between 10 and 20%. The maximum difference among the control stations is found for station Ólafsfjörður, with a $35 \text{ mm } 24\text{-h}^{-1}$ difference, corresponding to a 37% increase. Looking more closely at the location of this

station on the map, there are changes from a bright green colour (80–100 mm interval) to a light orange (120–140 mm interval). This is inline with the amended map of daily values shown in Figure 18b, applying the square-shaped maximum filter to counteract the artificial gradient caused by the smoothing of the terrain.

Similarly, Figure 24b shows the 1M5 map based on 24-hour accumulated precipitation values after applying the maximum-value filter among the nine nearest grid-points. The locally high values from Figure 24a are now extended from the mountainous regions to larger areas, resulting in most of the regions of complex orography having values above 100 mm 24-h⁻¹ values (corresponding to the yellow, orange and red shading on the map).

Table 9. 1M5 values for each control station, as obtained by the Peak-over-Threshold with MLE applied on daily and 24-hour accumulated precipitation from the ICRA. Difference (mm) and increase (%) are given for each station.

Station	1M5 values			
	Daily precipitation <i>mm day⁻¹</i>	24-hour precipitation <i>mm 24-h⁻¹</i>	Difference <i>mm</i>	Increase <i>%</i>
Eskifjörður	95	103	8	8
Flateyri	61	70	9	15
Höfn í Hornafirði	76	87	11	14
Ísafjörður	58	67	9	16
Kvísker	182	205	23	13
Laufbali	129	153	24	19
Neskaupstaður	104	117	13	13
Ólafsfjörður	95	130	35	37
Reykjavík	34	42	8	24
Seyðisfjörður	117	134	17	15
Siglufjörður	99	108	9	9
Súðavík	41	48	7	17

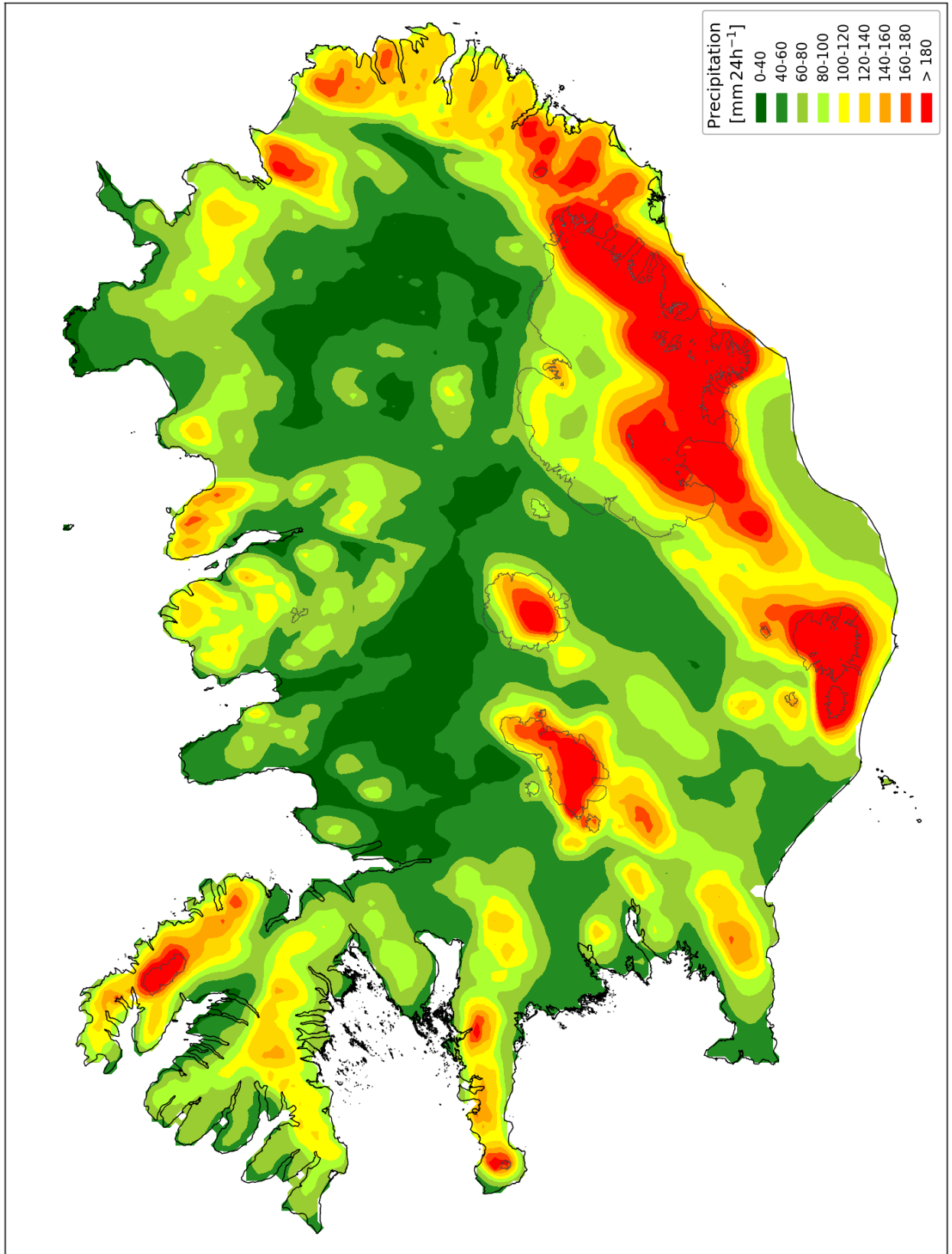


Figure 24a. IM5 map based on 24-hour accumulated precipitation, obtained from the entire ICRA dataset using the Peak-over-Threshold method with MLE.

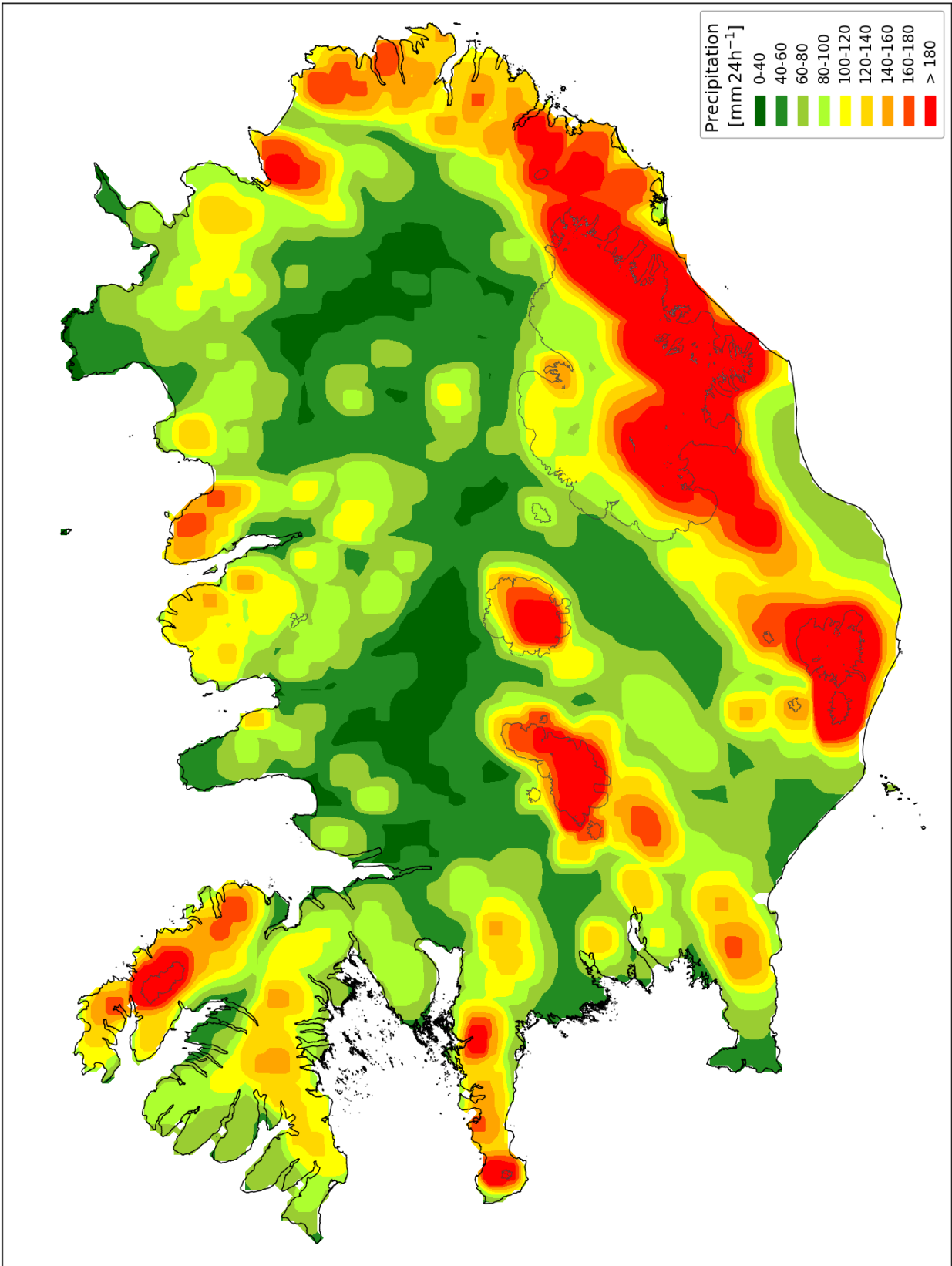


Figure 24b. IM5 map based on 24-hour accumulated precipitation, obtained from the entire ICRA dataset using the Peak-over-Threshold method with MLE modified using a maximum-value filter among the nine nearest grid-points. Note that the square-shaped imprinting on the map is an artefact of the filtering procedure.

7 Conclusions

An extreme value analysis of precipitation, resulting in return levels, IDF curves and two revised 1M5 maps, provides statistical benchmarks for the design of bridges, culverts and other infrastructure for handling large surface runoff. Since the publication by Eliasson *et al.* in 2009 of the current Icelandic 1M5 map, there have been several developments in numerical weather prediction, including the encapsulation of physical processes and the ability to resolve fine-scale results in time and space. Thus, it was evident that an updated assessment of extreme precipitation would further improve the current 1M5 map, especially in regions of complex orography. This is especially needed in the East- and Westfjords regions, as well as the Tröllaskagi peninsula where several flash floods have occurred in the past decade. In this project, the goals were to present an updated assessment of precipitation return levels and to convey the results as an improved 1M5 map. However, it should be emphasised that the aim of the project was not to simply repeat the work of Eliasson with higher resolution data, but to look at every step of the methodological analysis carefully. It should be noted that several aspects of extreme precipitation, which are not considered in the analysis presented here, need to be taken into account for practical decisions in the design of hydrological infrastructure. The most important of those are listed in the introduction (Section 1). In particular, engineers and local authorities should be aware of the possibility of underprediction of extreme precipitation due to localised downpours.

The study used precipitation measurements from 43 automatic meteorological stations that fulfilled various timeseries criteria for completeness and quality. Additionally, simulated precipitation from the Icelandic reanalysis dataset (ICRA), a gridded dataset over Iceland at 2.5 km horizontal resolution for the period 1979 to 2017, was used.

At the onset, it was decided to make the most of the observed precipitation timeseries from 43 stations around Iceland by comparing them to timeseries from the ICRA dataset, thereby investigating how to use the reanalysis in a reasonable and realistic way. For detailed comparison, 12 control stations were chosen. Several methods for interpolating the gridded data to the exact coordinates of the meteorological stations were examined before it was decided to use the weighted average among the four nearest grid points. Overall, for the most extreme events it was shown that the ICRA dataset is largely accurate (with an average *CC* of nearly 65% at all stations). At stations located in narrow valleys and fjords the differences between simulations and observations are larger, while closer matches are found for stations in the lowlands, away from mountains. A histogram-based comparison of the ICRA data with station measurements showed that the reanalysis does not adequately represent precipitation lasting less than three hours. Even though the ICRA has a small temporal shift in the hourly development of the most extreme events, precipitation accumulated over 72 hours was often close to the actual measurements. For stations located in complex terrain, a small spatial shift was observed on heat maps that is not believed to affect the accuracy of the new 1M5 map. This emphasises that comparisons should be made between gridded data and discrete observation points, when available. It should also be kept in mind that although the observed timeseries are taken as the truth, it is an oversimplification, as the spatial pattern of precipitation leads to great uncertainty compared to other meteorological measurements.

The choice of an appropriate EVA method was also studied thoroughly. In EVA, the task is to fit a model to the most extreme values of a timeseries. Thus, only a small part of the whole

dataset is used and how the subset is defined will affect the return level results. The Peak-over-Threshold method was selected rather than the Block Maxima previously used by Eliasson. This is not only because it is better suited for timeseries with high temporal resolution and large annual variability in local maxima, but also because when comparing return levels at the control stations between observations and simulations, there was higher similarity than with the Block Maxima method. The Peak-over-Threshold method was applied using MLE for the parameters estimations and 90th percentile as threshold to calculate the return levels associated to 2-, 5-, 10-, 25-, 50- and 100-year return periods and for time duration of 3, 6, 12, 24 and 48 hours. Values obtained with L-moments and for other thresholds were also discussed and did not lead to significant differences. Results were presented as IDF curves for each station based on the entire reanalysis and compared to IDF curves based on measurements. In some cases, this comparison showed similar results while the differences for other stations were more important, implying that a 2.5 km resolution is still too coarse to resolve properly some of the country's most complex terrain. When results at the control stations were normalised and compared to results from Block Maxima, Eliasson and Wussow's formulae, the Peak-over-Threshold and Block Maxima methods gave values in the same range and lower than Eliasson and Wussow's formulas for time frequencies shorter than 24 hours, but higher for time frequencies of 24 and 48 hours.

A new 1M5 map was presented after calculating daily precipitation thresholds based on a 5-year return period for each terrestrial grid-point of the ICRA. The new map shares many common features with the earlier one, based on results from the MM5 model for the period 1961–2006 at 8 km resolution. Both maps show an agreement with the general precipitation pattern in Iceland. The main differences lie in the detail, most of them related to a better description of the topography, which was expected using a dataset with more than three times higher horizontal resolution than the earlier map. Thus, the new 1M5 map includes important details that the earlier 1M5 could not encompass, especially in regions of complex orography. Much higher return values can be found on the new map in the Snæfellsness and Tröllaskagi peninsulas, the Bláfjöll mountainous region as well as in the East- and Westfjords. However, even at 2.5 km resolution some narrow fjords are not represented accurately. This problem was dealt with in a simplistic manner by a modified version of the 1M5 map produced by taking for each grid-point the maximum value among the nine nearest cells but this problem needs to be considered further with higher-resolution downscaling and improved analysis.

Another map, based on 24-hour accumulated precipitation was also introduced, with a median 1M5 value for the country 14% higher than the median value based on daily precipitation from midnight to midnight. Although there are many similarities in return levels between the maps, it is believed that the 24-hour map (Figure 24a) along with its amended version (Figure 24b) offer a more complete outline of possible precipitation extremes. It is therefore recommended that the 24-hour maps are used for the design of infrastructure subject to surface runoff.

In terms of predictions of climate change in Iceland, there are large uncertainties regarding precipitation. However, there are indications that precipitation may increase at a rate of at least 1.5% for every 1°C increase in temperature, with the most increase to occur during late summers and autumns. There are also indications of an increase in precipitation intensity (Björnsson *et al.*, 2018). Consequently, the research presented here should be expanded to include a potential climate factor. Such an expansion would add value to the current work, and it would be an important resource for the long-term design of the built environment, helping to minimise the impact of intense rainfall on critical infrastructure.

Acknowledgement

We thank Jónas Eliásson, Hersir Gíslason and Ólafur Rögnvaldson for providing us with the existing 1M5 map in digital format and for the necessary clarifications. Thanks to the reviewers Tómas Jóhannesson, Trausti Jónsson and Elín Björk Jónasdóttir for their helpful comments; especially Tómas for his enthusiasm towards the project and his valuable insights. We appreciate the discussion with those that attended the user meeting at the start of the project and helped us shape the outlines and outcomes of this work.

References

- Björnsson, H., Sigurðsson, B. D., Davíðsdóttir, B., Ólafsson, J., Ástþórsson, Ó. S., Ólafsdóttir, S., Baldursson, T. & Jónsson, T. (2018). Loftslagsbreytingar og áhrif þeirra á Íslandi – Skýrsla vísindanefndar um loftslagsbreytingar 2018. *Veðurstofa Íslands*.
- Bengtsson, L., Andrae, U., Aspelien, T., Batrak, Y., Calvo, J., de Rooy, W. & Køltzow, M.Ø. (2017). The HARMONIE-AROME model configuration in the ALADIN-HIRLAM NWP system. *Mon. Wea. Rev.*, **145**, 1919–1935.
- Bergþórsson, P. (1968). Hvað getur úrfelli orðið mikið á Íslandi? *Veðrið*, **13**, 52–58.
- Clark, P., Roberts, N., Lean, H., Ballard, S.P. & Charlton-Perez, C. (2016). Convection-permitting models: a step-change in rainfall forecasting. *Met. Apps*, **23**, 165–181. doi:10.1002/met.1538.
- Coles, S. (2001). An introduction to Statistical Modeling of Extreme Values. London; *Springer*.
- Crochet, P. (2007). A study of regional precipitation trends in Iceland using a high-quality gauge network and ERA-40. *Journal of Climate*, **20(18)**. doi: 10.1175/JCLI4255.1.
- DuMouchel, W.H. (1983). Estimating the stable index α in order to measure tail thickness: a critique. *The Annals of Statistics*, **11**, 1019–1031.
- Dunkerley, D. (2020). How us the intensity of rainfall events best characterised? A brief critical reviw and proposed new rainfall intensity index for application in the stufy of landsurface processes. *Water*, **12(4)**, 929.
- Grell, G.A., Dudhia, J. & Stauffer, D.R. (1994). A description of the fifth-generation Penn State/NCAR Mesoscale model (MM5). *NCAR technical note*, NCAR/TN-398+STR.
- Eliásson, J. (2000). Design values for precipitation and floods from M5 values; *Nordic Hydrology*, **31 (4/5)**, 357–372.
- Eliásson, J., Rögnvaldsson, Ó. & Jónsson, T. (2009). Extracting statistical parameters of extreme precipitation from a NWP model. *Hydrology & Earth System Sciences 13*, **11**, 2233–2240.
- Embrechts, P., Kluppelberg, S. & Mikosch, T. (1997). *Extremal Events in Finance and Insurance*. Springer Verlag.
- Ferreira, A., de Haan, L. & Peng, L. (2003). On optimising the estimation of highquantiles of a probability distribution. *Statistics*, **37**, 401–434.
- Fisher, R. A. (1922). On the mathematical foundations of theoretical statistics. *Phil. Trans. Roy. Soc., Ser. A*, **222**, 309–368.
- Natural Environment Resource Council (NERC). (1975). Flood Studies Report (FSR), Vol. II.

- Førland, E. J., Allerup, P., Dahlström, B., Elomaa, E., Jónsson, T., Madsen, H., Perälä, J., Rissanen, P., Vedin, H. & Vejen, F. (1996). Manual for operational correction of Nordic precipitation data. DNMI Rep. 24/96 Klima.
- Gilleland, E. & Katz, R.W. (2016). extRemes 2.0: An Extreme Value Analysis Package in R. *Journal of Statistical Software*, **72**, 1–39. doi: 10.18637/jss.v072.i08.
- Hlodversdottir, Á.Ó., Björnsson, B., Andradottir, H., Eliasson, J. & Crochet, P. (2015). Impacts of climate change on combined sewer systems in Reykjavik. *Water science and technology*, **71(10)**, 1471–1477. doi: 10.2166/wst.2015.119.
- Hosking, J.R.M. (1985). Maximum likelihood estimation of the parameters of the generalized extreme value distribution. *Applied Statistics*, **34**, 401–310.
- Icelandic Tourist Board. (2019). Numbers of foreign visitors. Accessed September 2020. <https://www.ferdamalastofa.is/en/research-and-statistics/numbers-of-foreign-visitors>
- Kidd, C., Becker, A., Huffman, G. H., Muller, C. L., Joe, P., Skofronick-Jackson, G. & Kirschbaum, D. (2017). So, How Much of the Earth’s Surface Is Covered by Rain Gauges? *Bull. Amer. Meteor. Soc.*, **98**, 69–78, <https://doi.org/10.1175/BAMS-D-14-00283.1>
- Makkonen, L. & Tikanmäki, M. (2019). An improved method of extreme value analysis. *Journal of Hydrology*. doi: 10.1016/j.hydroa.2018.100012.
- Nawri, N., Pálmason, B., Petersen, G. N., Björnsson, H. & Þorsteinsson, S. (2017). The ICRA atmospheric reanalysis project for Iceland. *Veðurstofa Íslands*. VÍ 2017-005.
- Rögnvaldsson, Ó., Jónsdóttir, J.F. & Ólafsson, H. (2010). Dynamical downscaling of precipitation in Iceland 1961–2006. *Hydrology Research*, **41**, 153–163. doi: <https://doi.org/10.2166/nh.2010.132>.
- Pálmason, B., Þorsteinsson, S., Nawri, N., Petersen, G.N. & Björnsson, H. (2016). HARMONIE activities at in IMO 2015. *ALADIN-HIRLAM Newsletter*, **6**, 73–75.
- Petersen, G.N. (2015). Greining á öfgaveðurhæð frá sjálfvirkum vindmælingum. *Veðurstofa Íslands*. VÍ 2015-004.
- Pollock, M.D., O’Donnell, G., Quinn, P., Dutton, M., Black, A., Wilkinson, M.E., Colli, M., Stagnaro, M., Lanza, L.G., Lewis, E., Kilsby, C.G. & O’Connell, P.E. (2018). Quantifying and mitigating wind-induced undercatch in rainfall measurements. *Water Resources Research*, **56**, issue 6. doi: 10.1029/2017WR022421.
- R Core Team. (2014). R: A language and environment for statistical computing. R Foundation for Statistical Computing, Vienna, Austria. URL <http://www.R-project.org/>
- Scarrott, C. & MacDonald, A. (2012). A review of extreme value threshold estimation and uncertainty quantification. *REVSTAT: Stat J*, **10(1)**, 33–60.
- Shulzweida, U. (2019). CDO User Guide (Version 1.9.8). doi: 10.5281/zenodo.3539275.

Appendices

Appendix I. Histograms.....	66
Appendix II. Heat maps.....	78
Appendix III. Intensity-Duration-Frequency curves and tables	91
Appendix IV. 1M5 values.....	137

Appendix I. Histograms

For each control station, histograms of observed and simulated 3-hour accumulated precipitation have been created for the three largest daily precipitation events. The histograms include the day prior to the event and the day after, covering a period of 72 hours. Cumulated precipitation over those 72 hours is also shown in the figures.

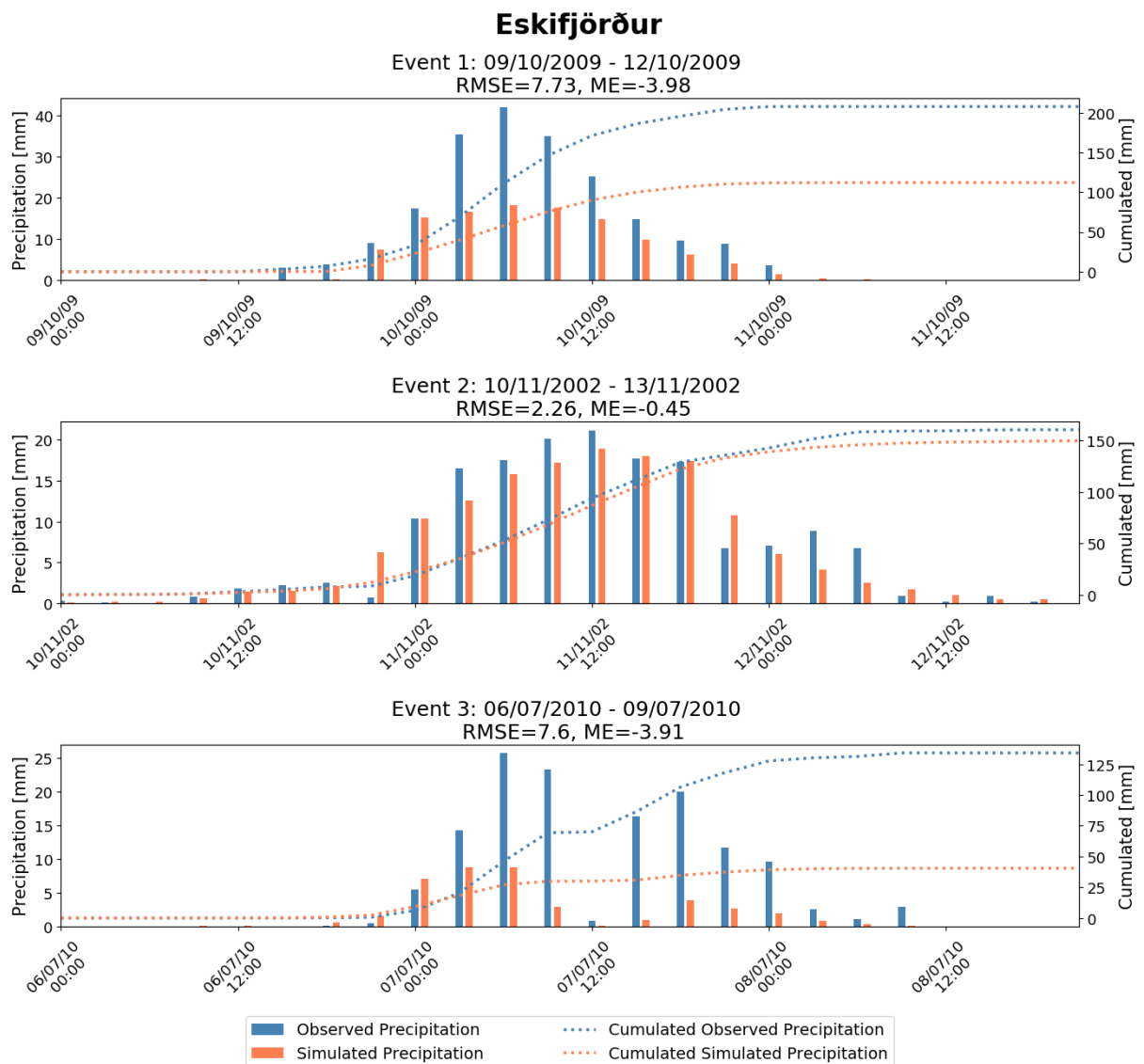


Figure I.1 – Histograms showing 3-hour accumulated observed (blue) and simulated (orange) precipitation (mm) over the course of 72 hours for the three largest precipitation events at Eskifjörður. Dashed lines show the corresponding accumulation over the 72-hours timespan.

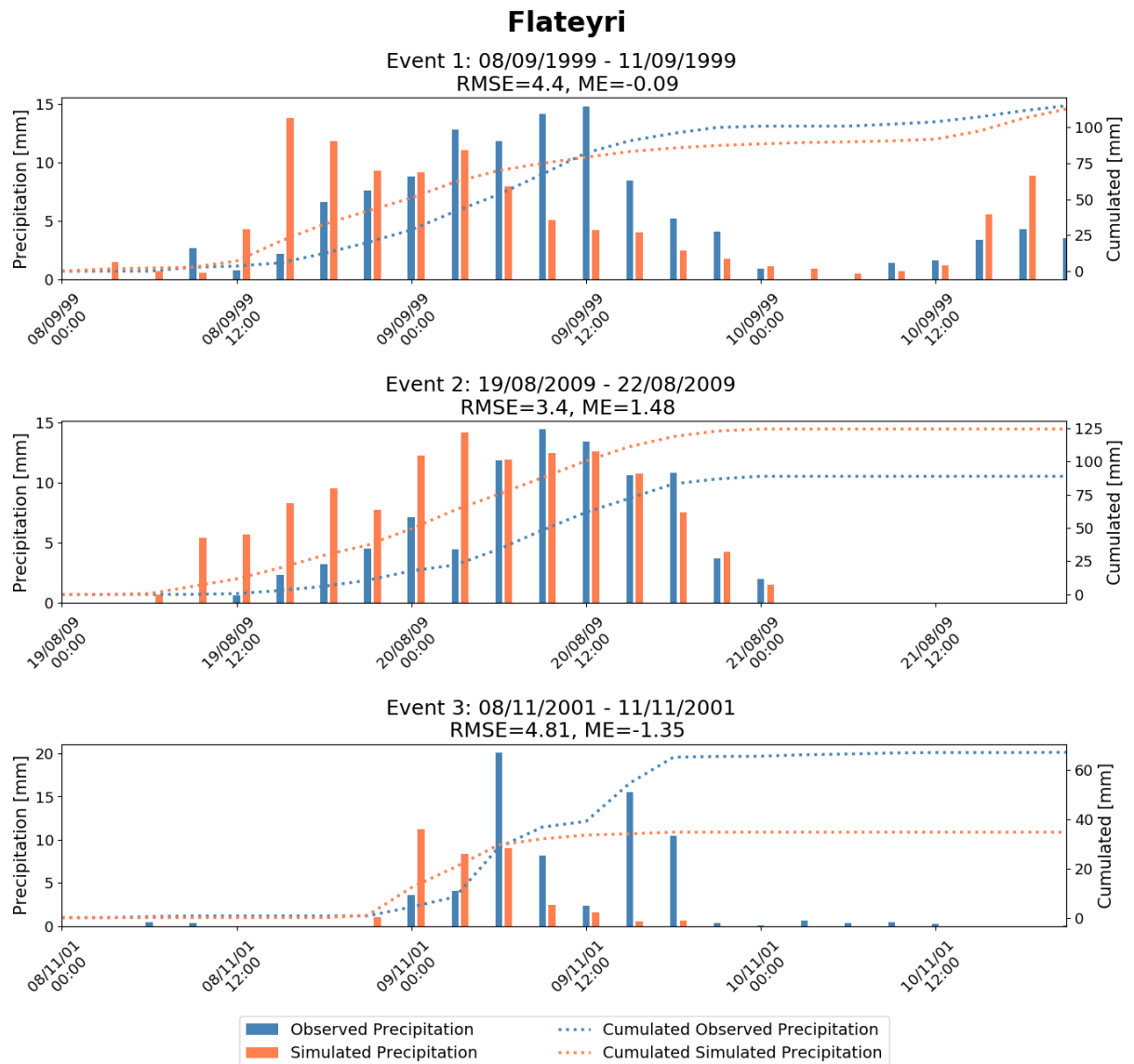


Figure I.2 – Histograms showing 3-hour accumulated observed (blue) and simulated (orange) precipitation (mm) over the course of 72 hours for the three largest precipitation events at Flateyri. Dashed lines show the corresponding accumulation over the 72-hours timespan.

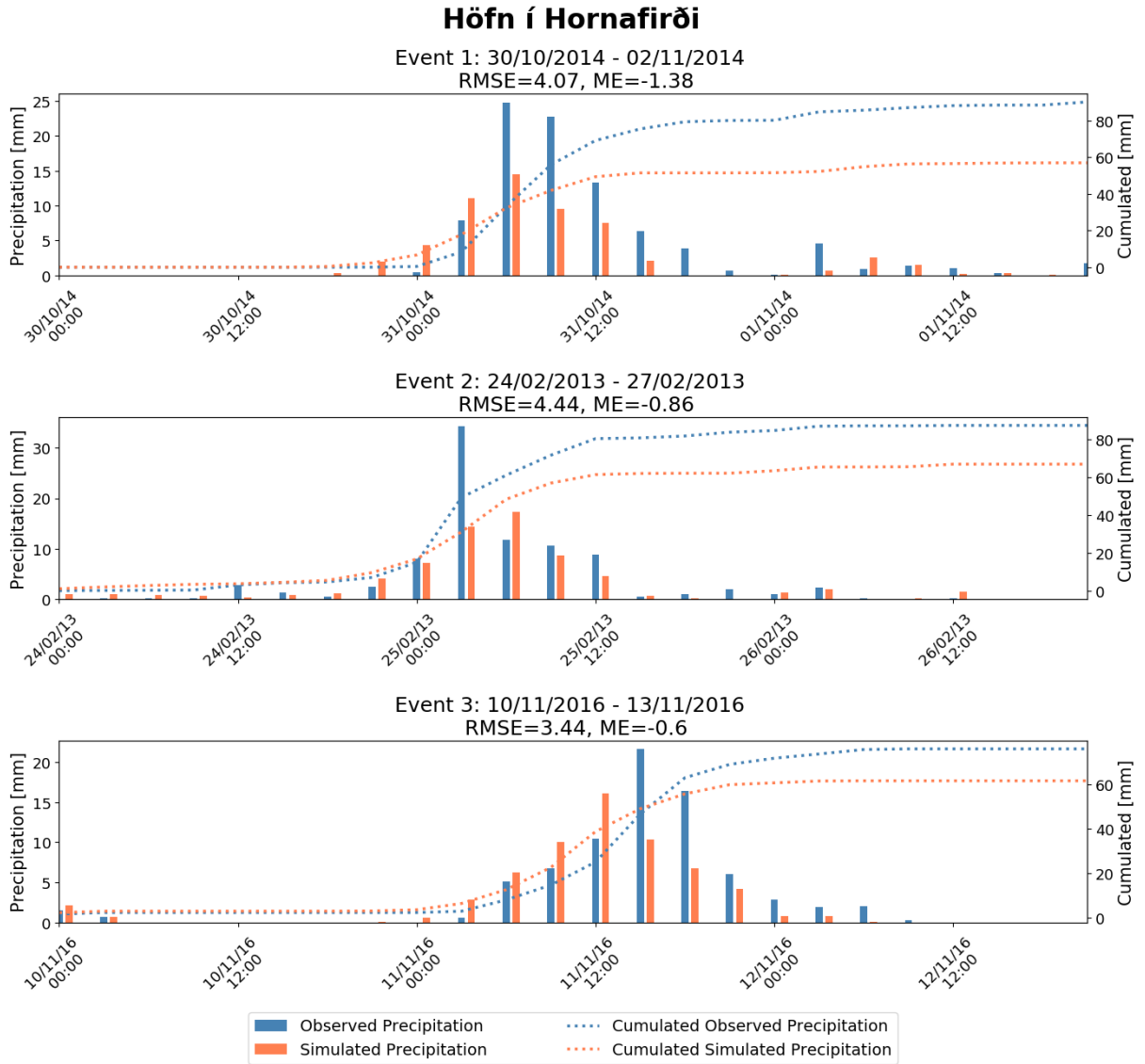


Figure 1.3 – Histograms showing 3-hour accumulated observed (blue) and simulated (orange) precipitation (mm) over the course of 72 hours for the three largest precipitation events at Höfn í Hornafirði. Dashed lines show the corresponding accumulation over the 72-hours timespan.

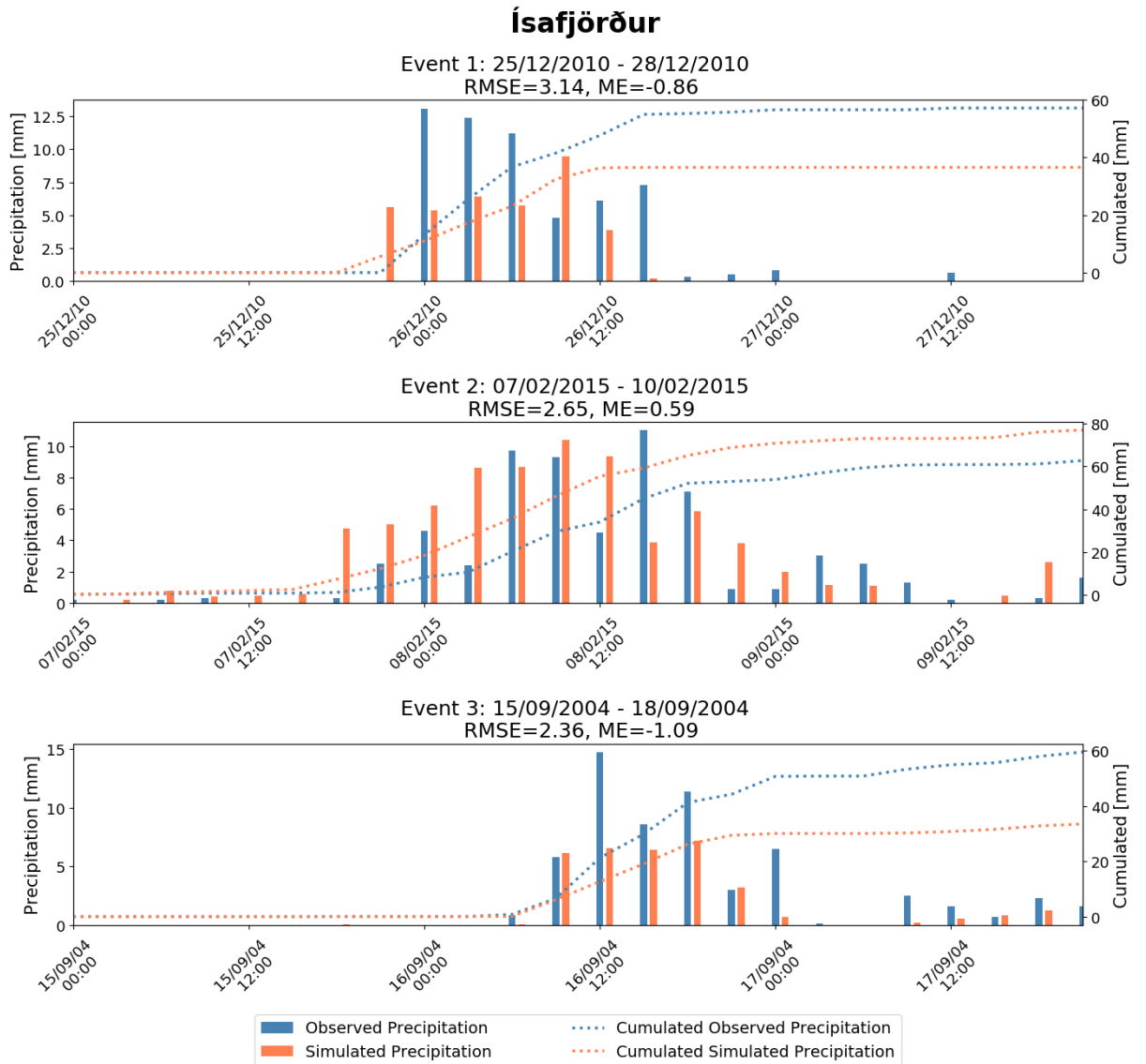


Figure 1.4 – Histograms showing 3-hour accumulated observed (blue) and simulated (orange) precipitation (mm) over the course of 72 hours for the three largest precipitation events at Ísafjörður. Dashed lines show the corresponding accumulation over the 72-hours timespan.

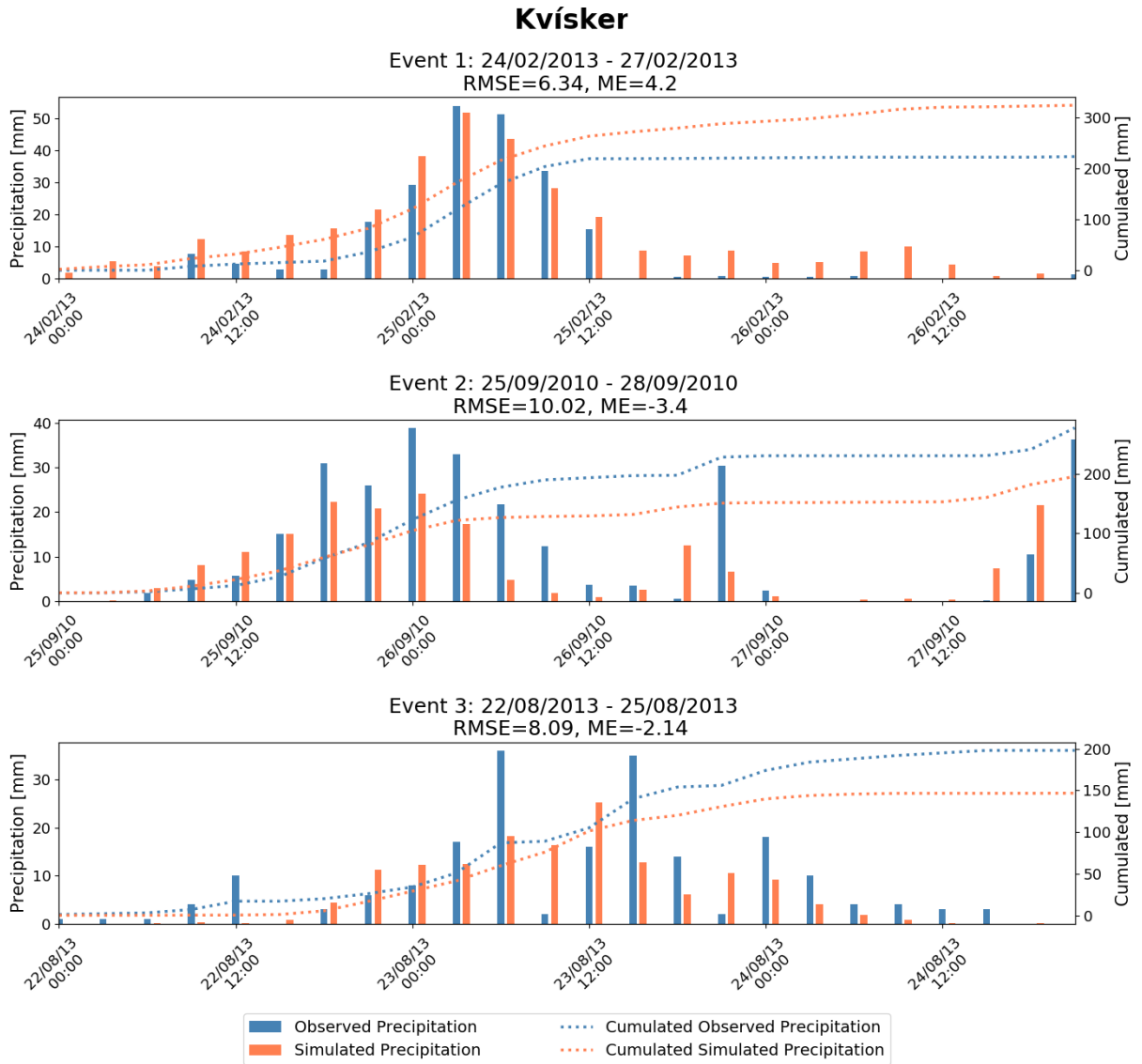


Figure 1.5 – Histograms showing 3-hour accumulated observed (blue) and simulated (orange) precipitation (mm) over the course of 72 hours for the three largest precipitation events at Kvísker. Dashed lines show the corresponding accumulation over the 72-hour timespan.

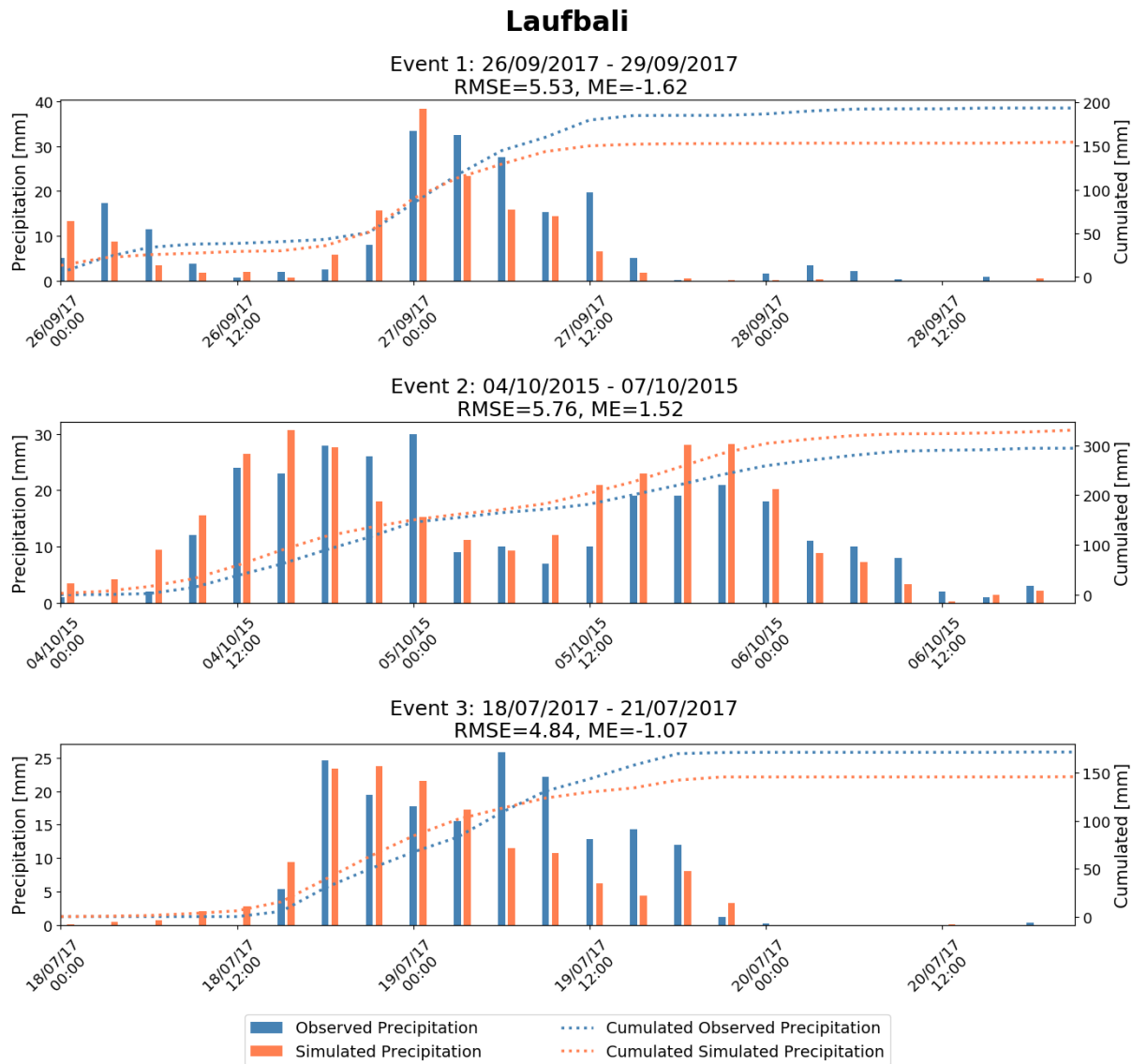


Figure I.6 – Histograms showing 3-hour accumulated observed (blue) and simulated (orange) precipitation (mm) over the course of 72 hours for the three largest precipitation events at Laufbali. Dashed lines show the corresponding accumulation over the 72-hours timespan.

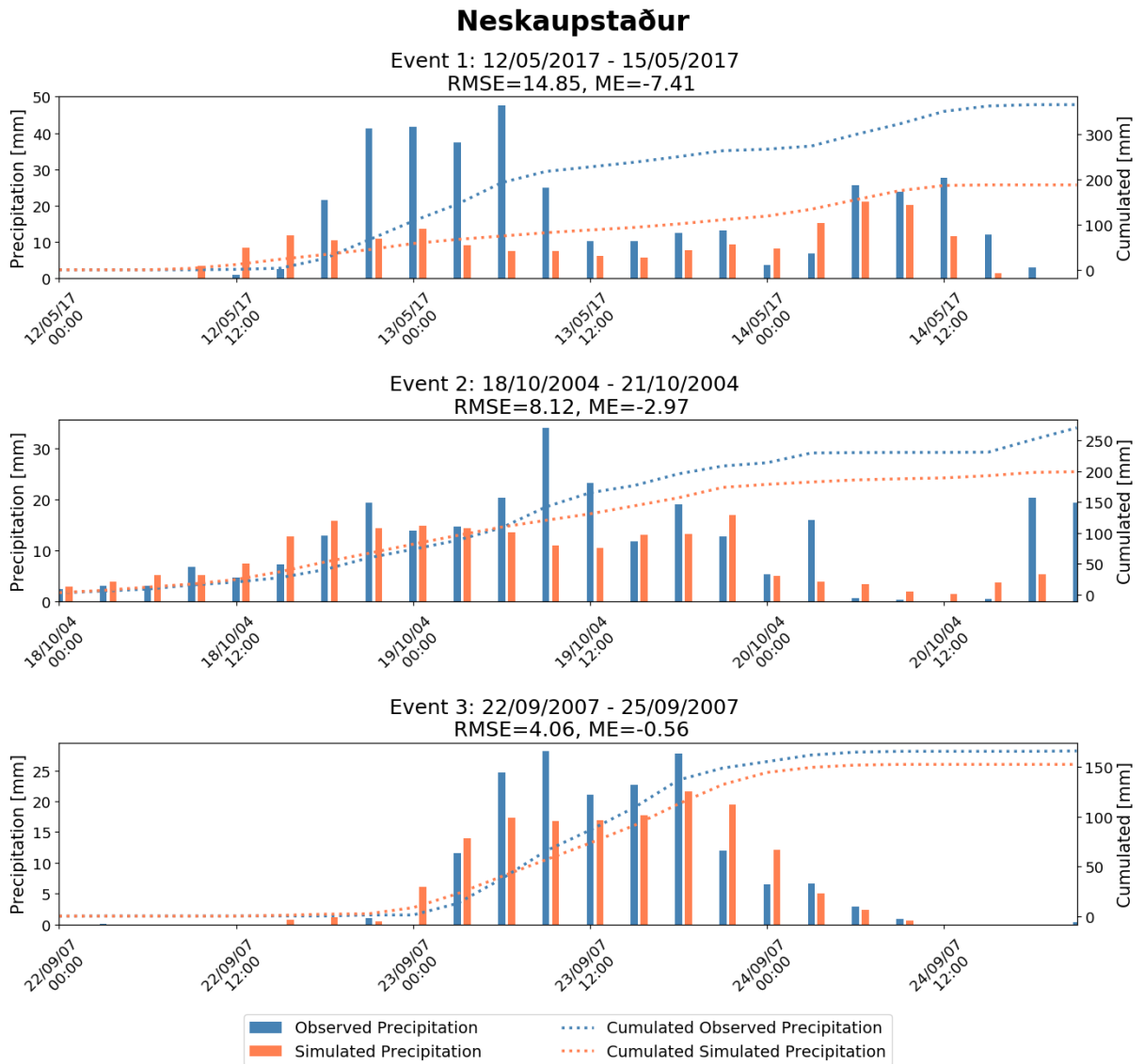


Figure 1.7 – Histograms showing 3-hour accumulated observed (blue) and simulated (orange) precipitation (mm) over the course of 72 hours for the three largest precipitation events at Neskaupstaður. Dashed lines show the corresponding accumulation over the 72-hours timespan.

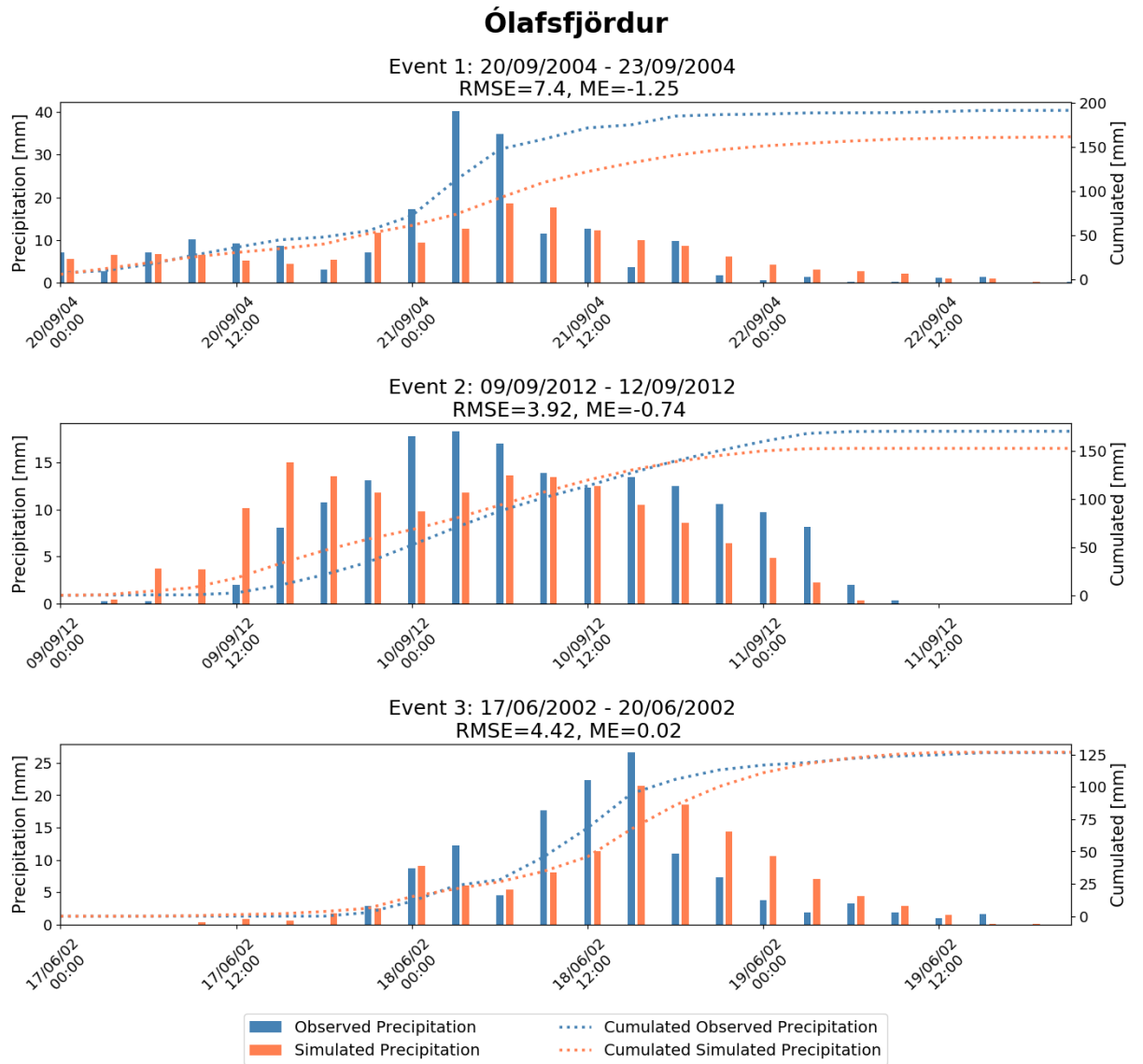


Figure 1.8 – Histograms showing 3-hour accumulated observed (blue) and simulated (orange) precipitation (mm) over the course of 72 hours for the three largest precipitation events at Ólafsfjörður. Dashed lines show the corresponding accumulation over the 72-hours timespan.

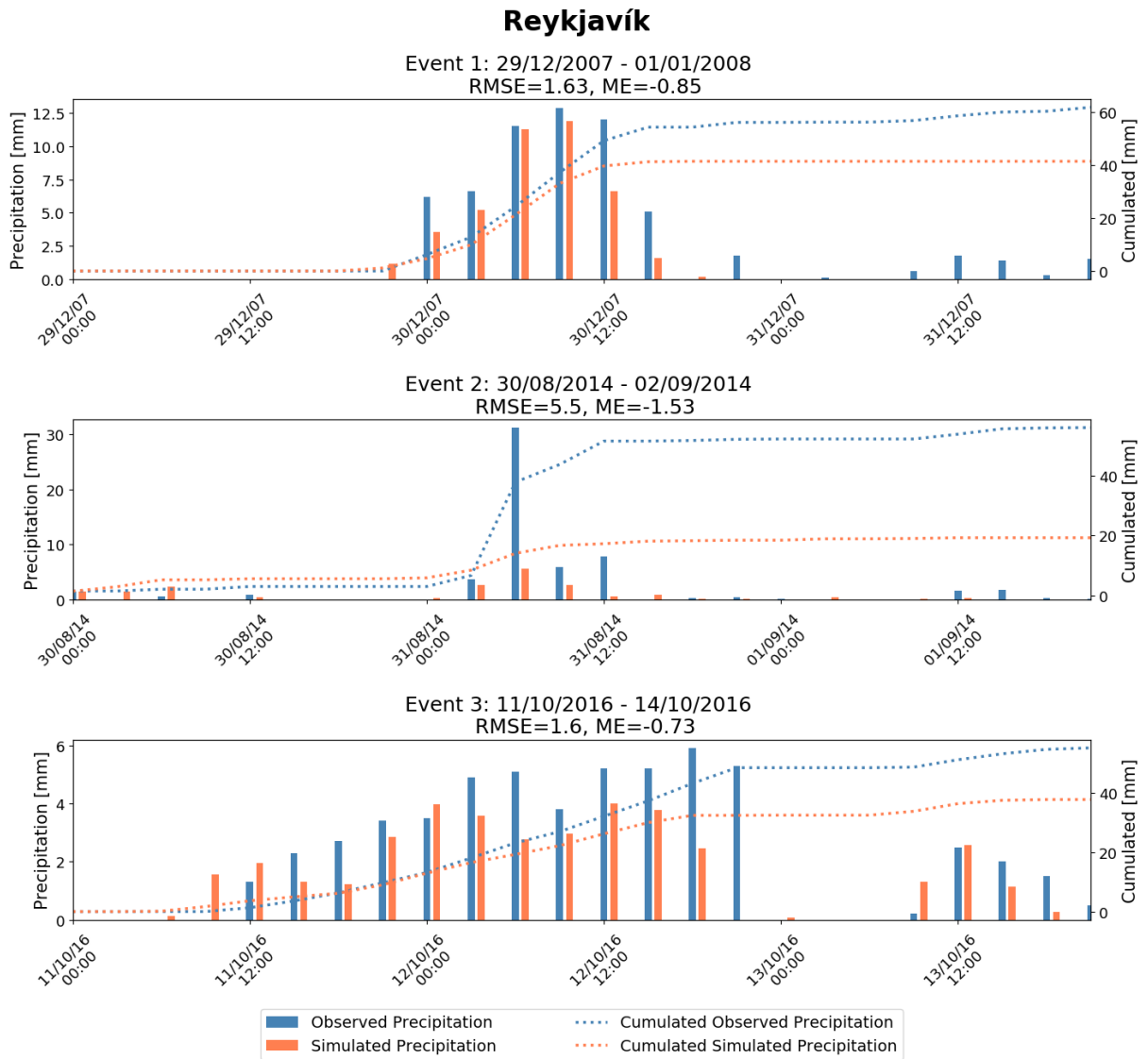


Figure 1.9 – Histograms showing 3-hour accumulated observed (blue) and simulated (orange) precipitation (mm) over the course of 72 hours for the three largest precipitation events at Reykjavik. Dashed lines show the corresponding accumulation over the 72-hours timespan.

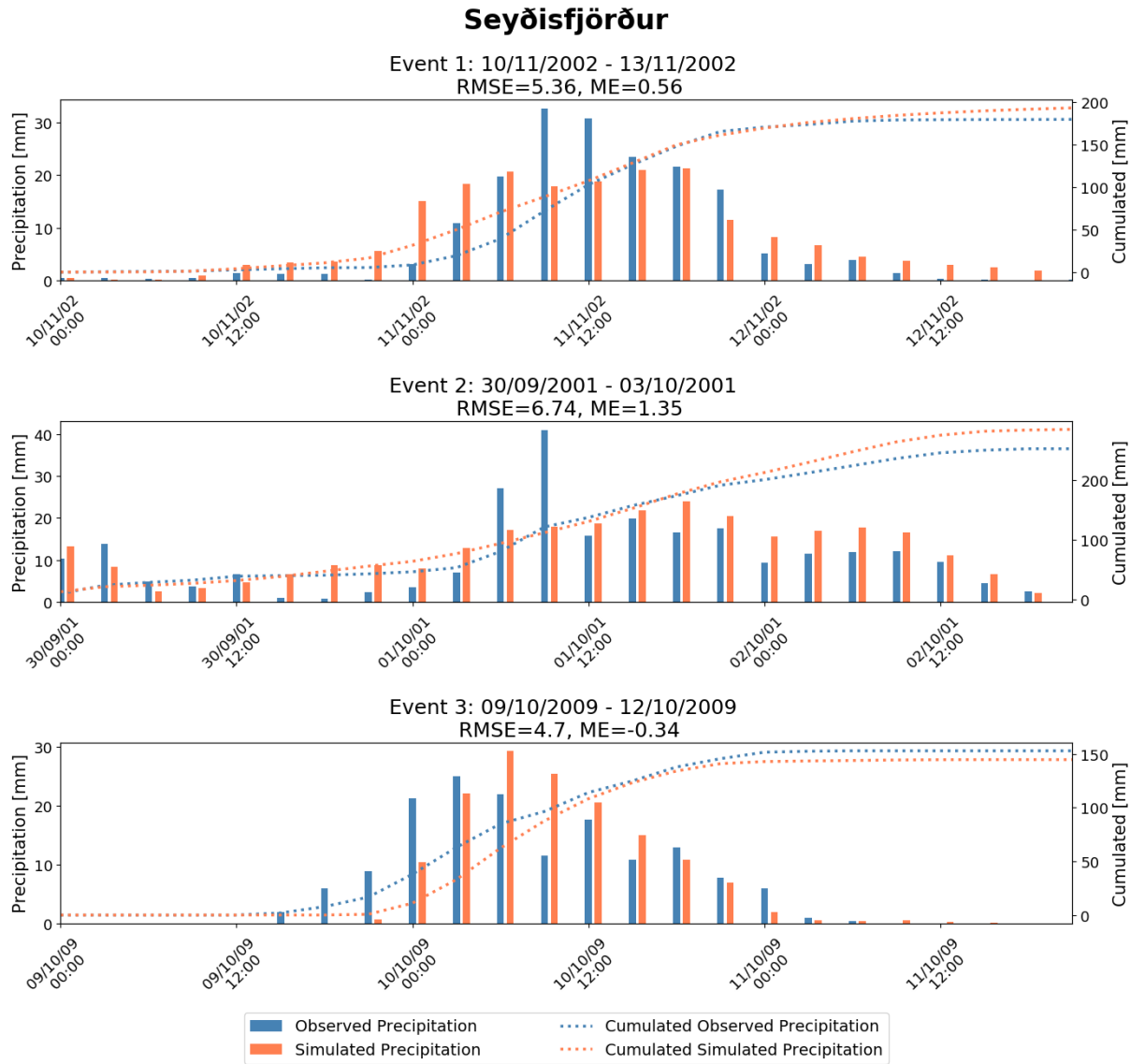


Figure I.10 – Histograms showing 3-hour accumulated observed (blue) and simulated (orange) precipitation (mm) over the course of 72 hours for the three largest precipitation events at Seyðisfjörður. Dashed lines show the corresponding accumulation over the 72-hours timespan.

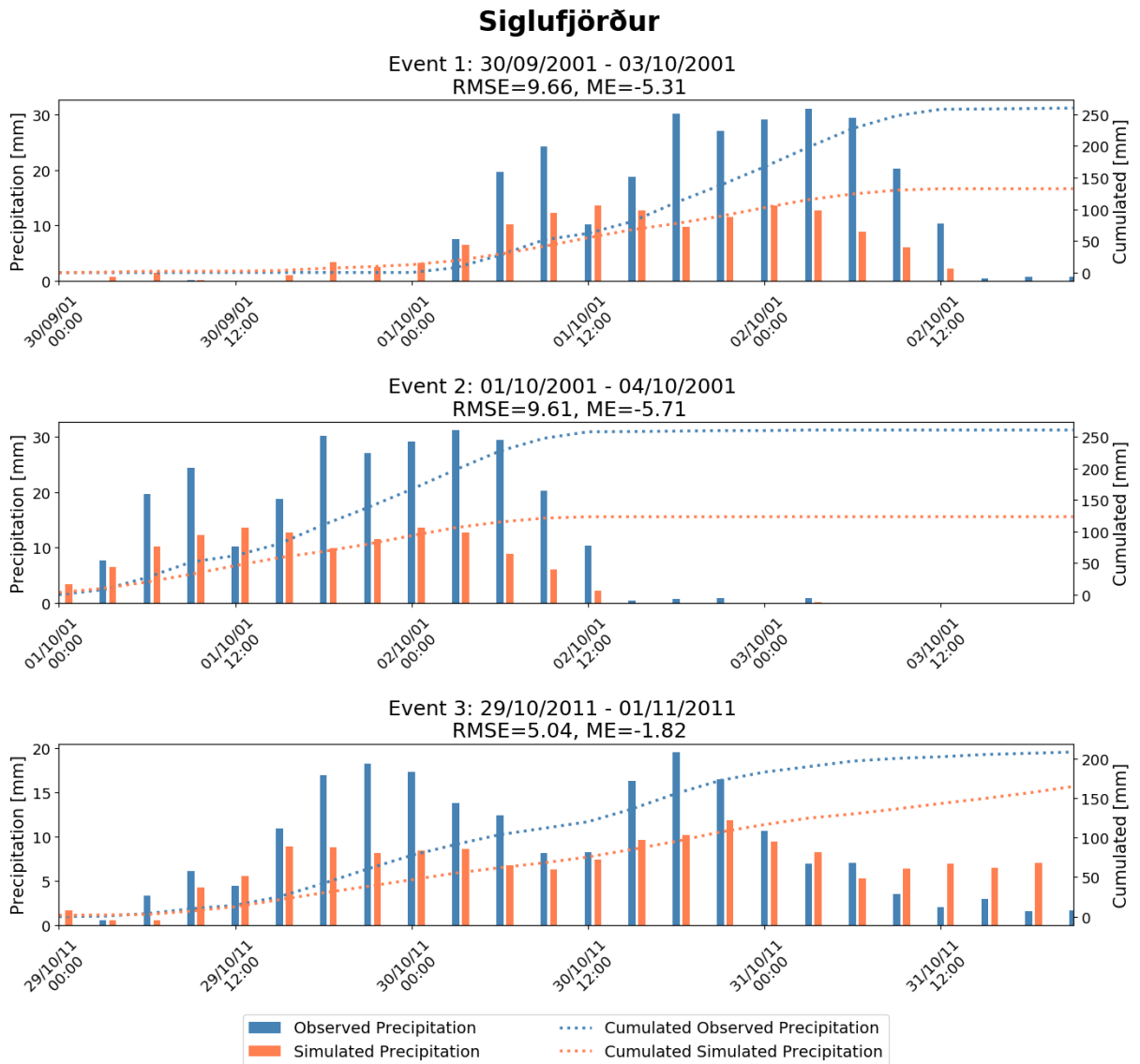


Figure I.11 – Histograms showing 3-hour accumulated observed (blue) and simulated (orange) precipitation (mm) over the course of 72 hours for the three largest precipitation events at Siglufjörður. Dashed lines show the corresponding accumulation over the 72-hours timespan.

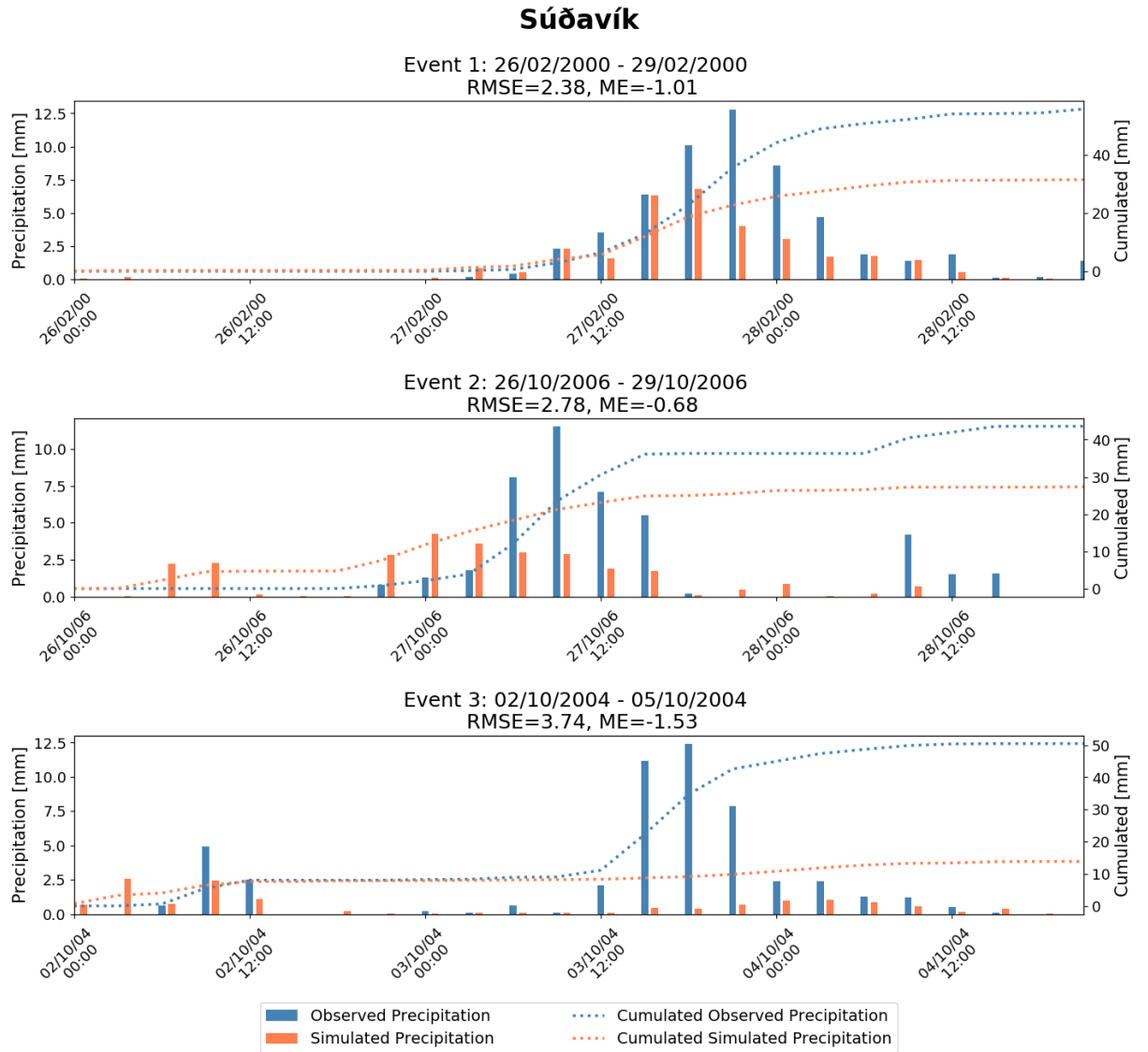


Figure 1.12 – Histograms showing 3-hour accumulated observed (blue) and simulated (orange) precipitation (mm) over the course of 72 hours for the three largest precipitation events at Súďavík. Dashed lines show the corresponding accumulation over the 72-hours timespan.

Appendix II. Heat maps

Heat maps are presented for each control station for the largest precipitation event over a 3-day timespan that includes the day before and the day after the event. Bar diagrams for each day are also shown with daily values of precipitation from measurements and the ICRA dataset.

Eskifjörður

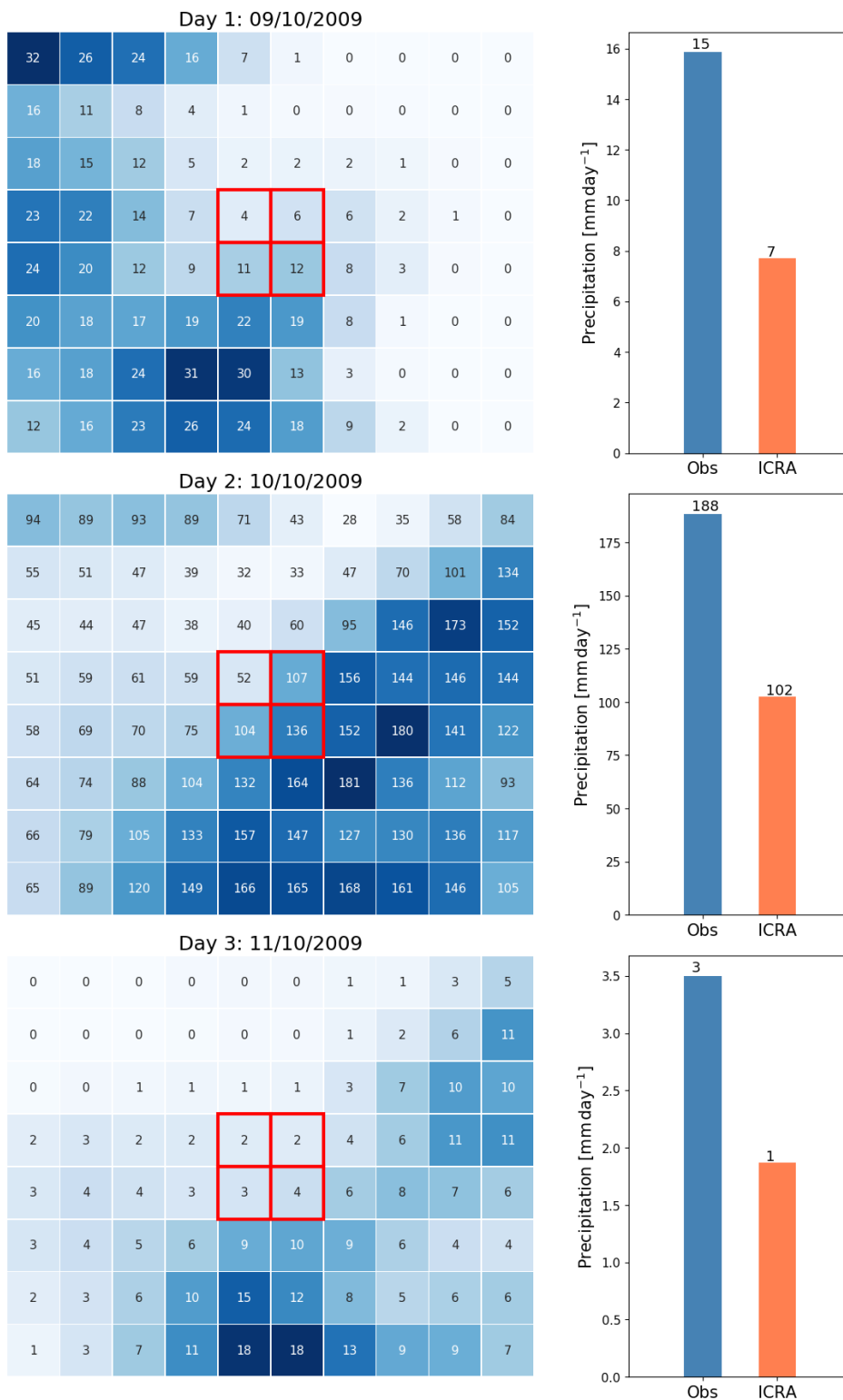


Figure II.1 – Heat maps showing daily precipitation from ICRA centred on the 4 nearest grid-points (red squares) to station Eskifjörður over a 3-day period with corresponding bar diagrams presenting the observed value at the station (blue) and the simulated value (orange). The station is located within the four nearest grid-points.

Flateyri

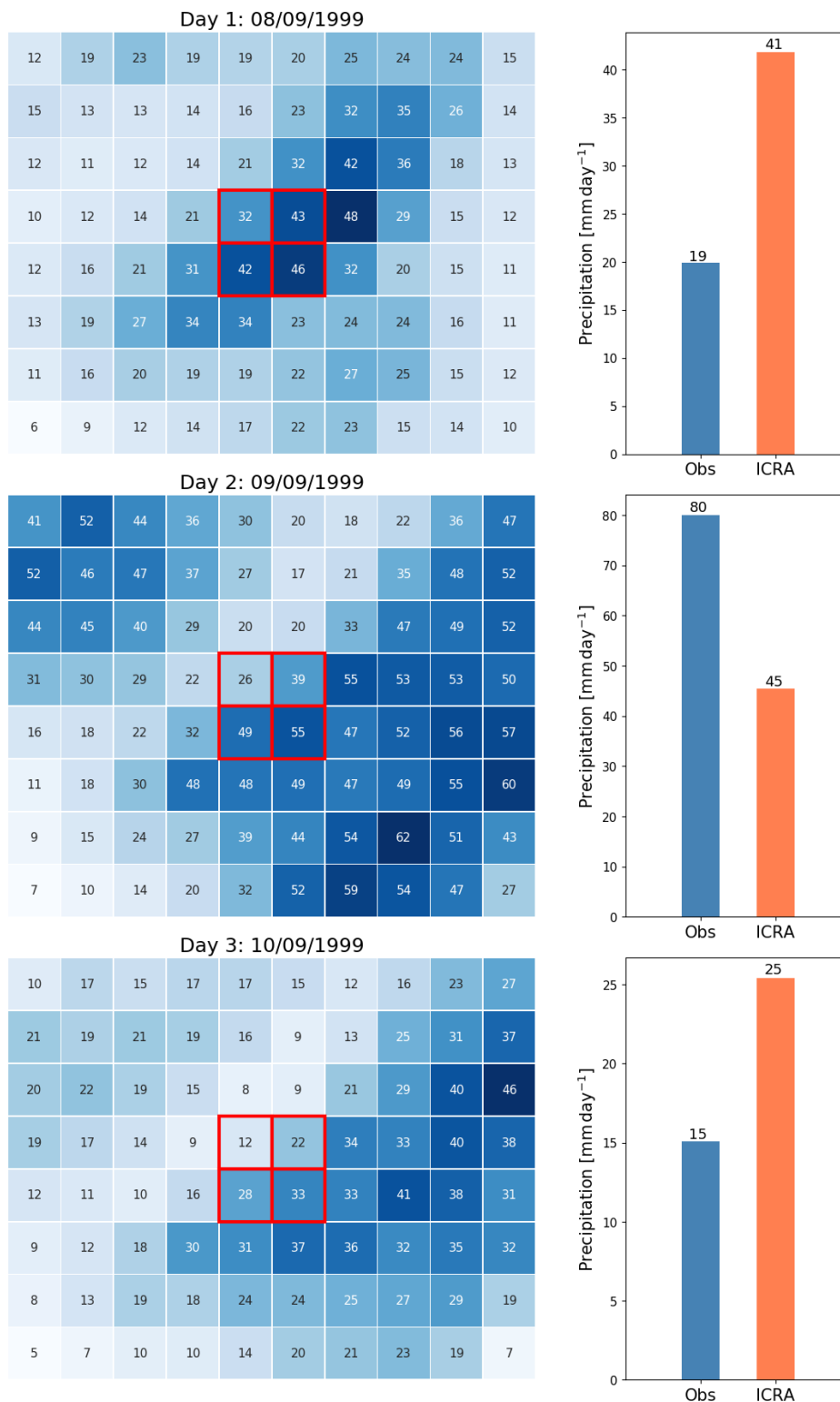


Figure II.2 – Heat maps showing daily precipitation from ICRA centred on the 4 nearest grid-points (red squares) to station Flateyri over a 3-day period with corresponding bar diagrams presenting the observed value at the station (blue) and the simulated value (orange). The station is located within the four nearest grid-points.

Höfn í Hornafirði

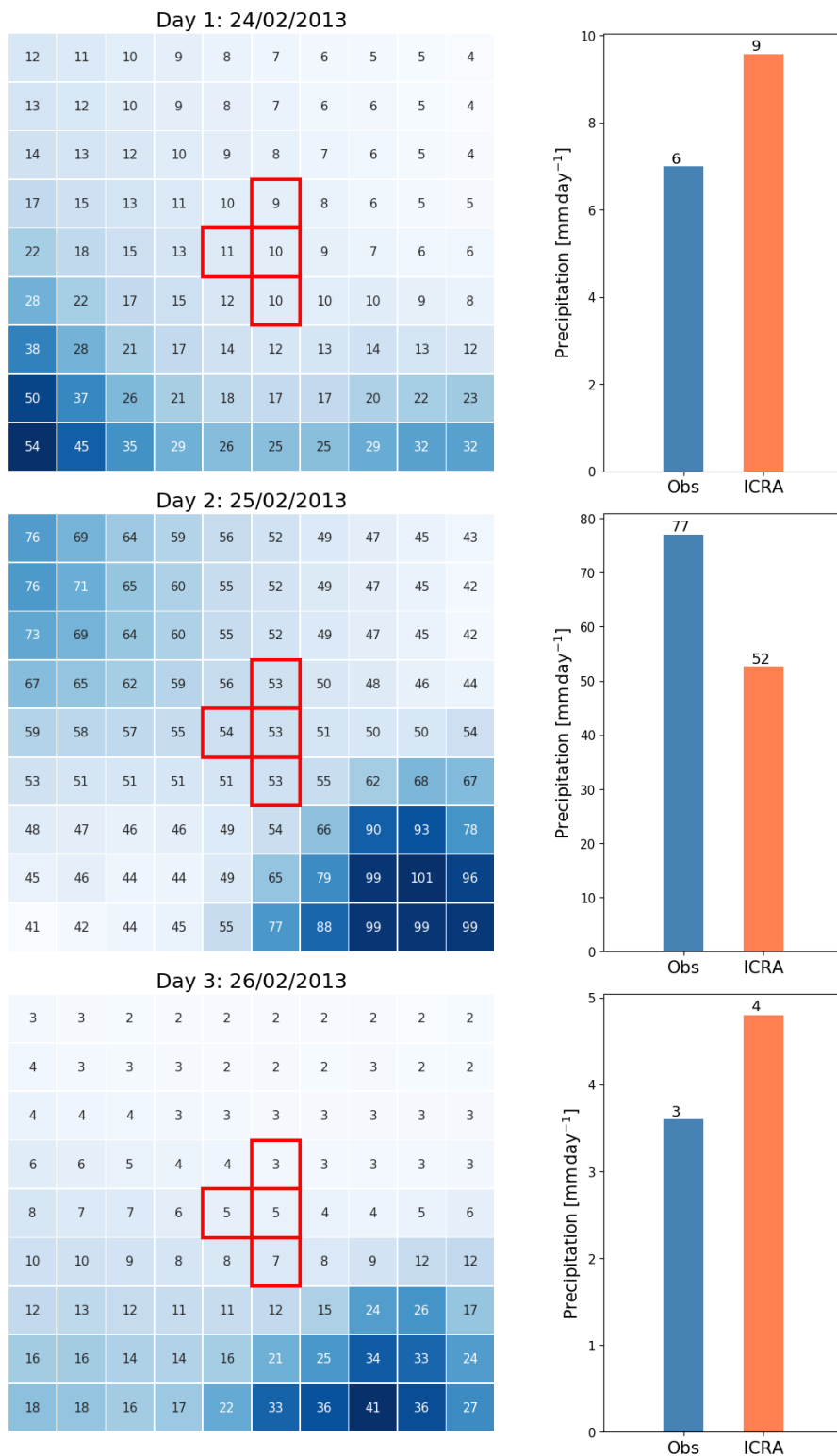


Figure II.3 – Heat maps showing daily precipitation from ICRA centred on the 4 nearest grid-points (red squares) to station Höfn í Hornafirði over a 3-day period with corresponding bar diagrams presenting the observed value at the station (blue) and the simulated value (orange). The station is located within the four nearest grid-points.

Ísafjörður

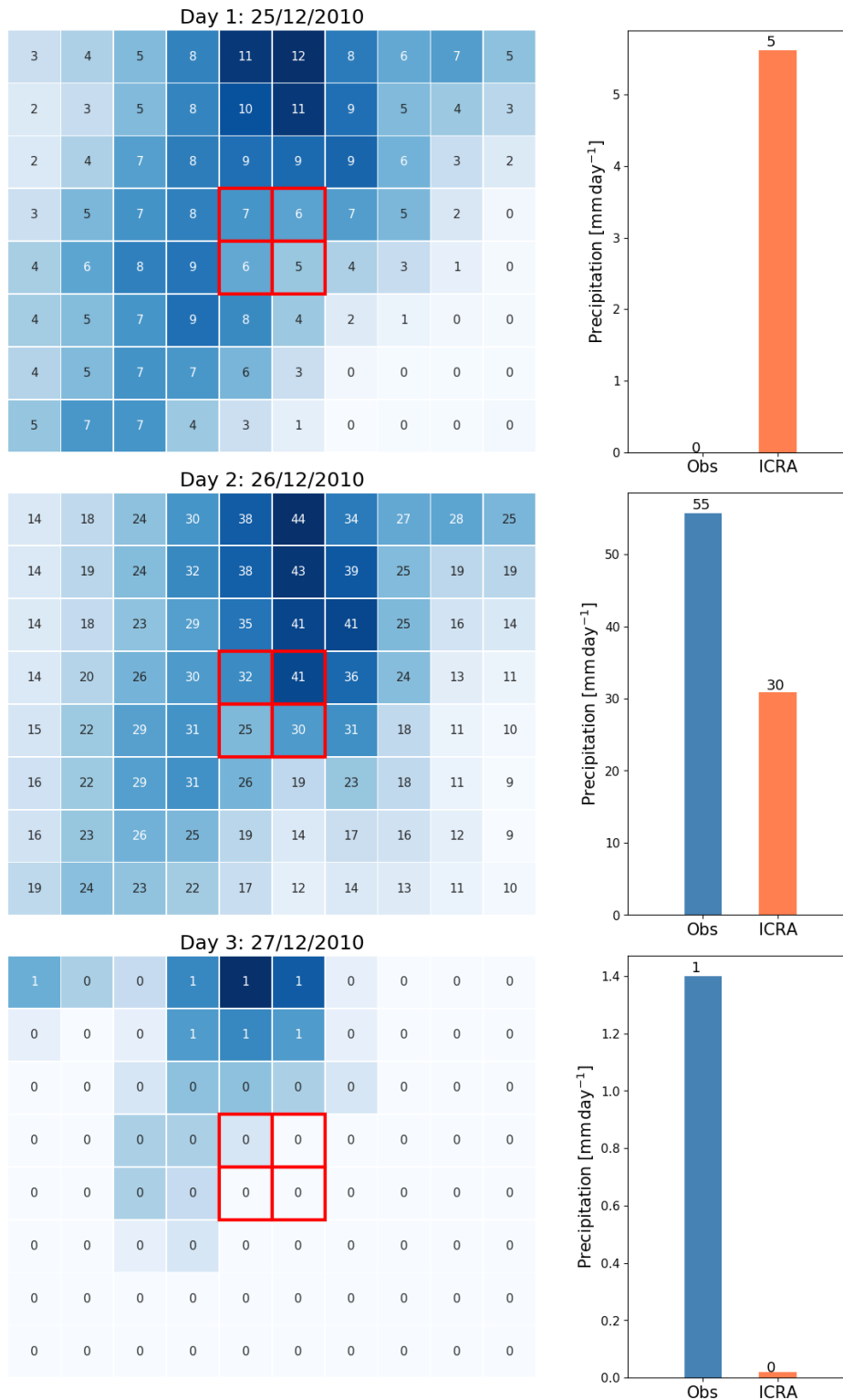


Figure II.4 – Heat maps showing daily precipitation from ICRA around the 4 nearest grid-points (red squares) to station Ísafjörður over a 3-day period with corresponding bar diagrams indicating the observed value at the station (orange) and the simulated value (blue). The station is located within the four nearest grid-points.

Kvísker

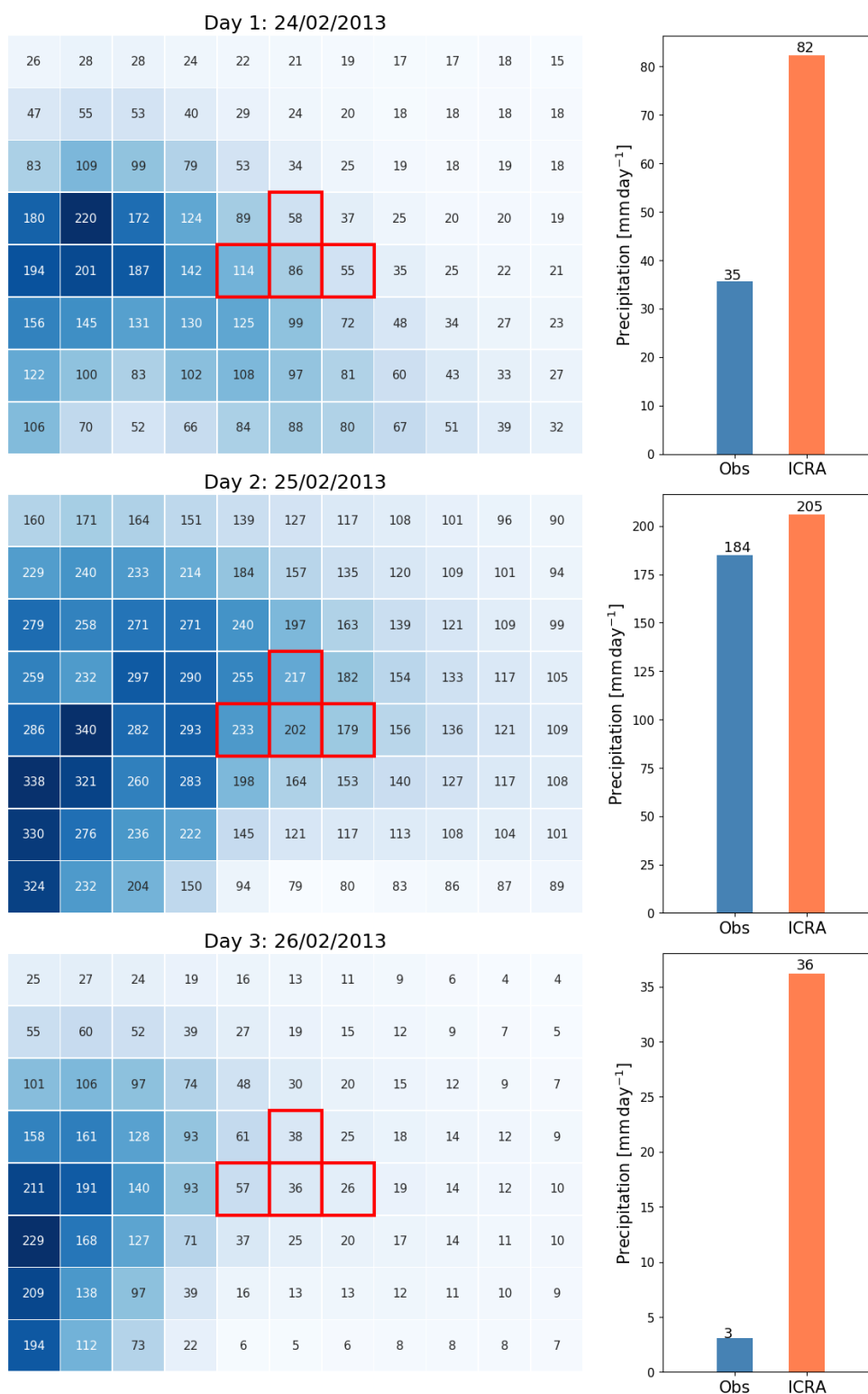


Figure II.5 – Heat maps showing daily precipitation from ICRA centred on the 4 nearest grid-points (red squares) to station Kvísker over a 3-day period with corresponding bar diagrams presenting the observed value at the station (blue) and the simulated value (orange). The station is located within the four nearest grid-points.

Laufbali

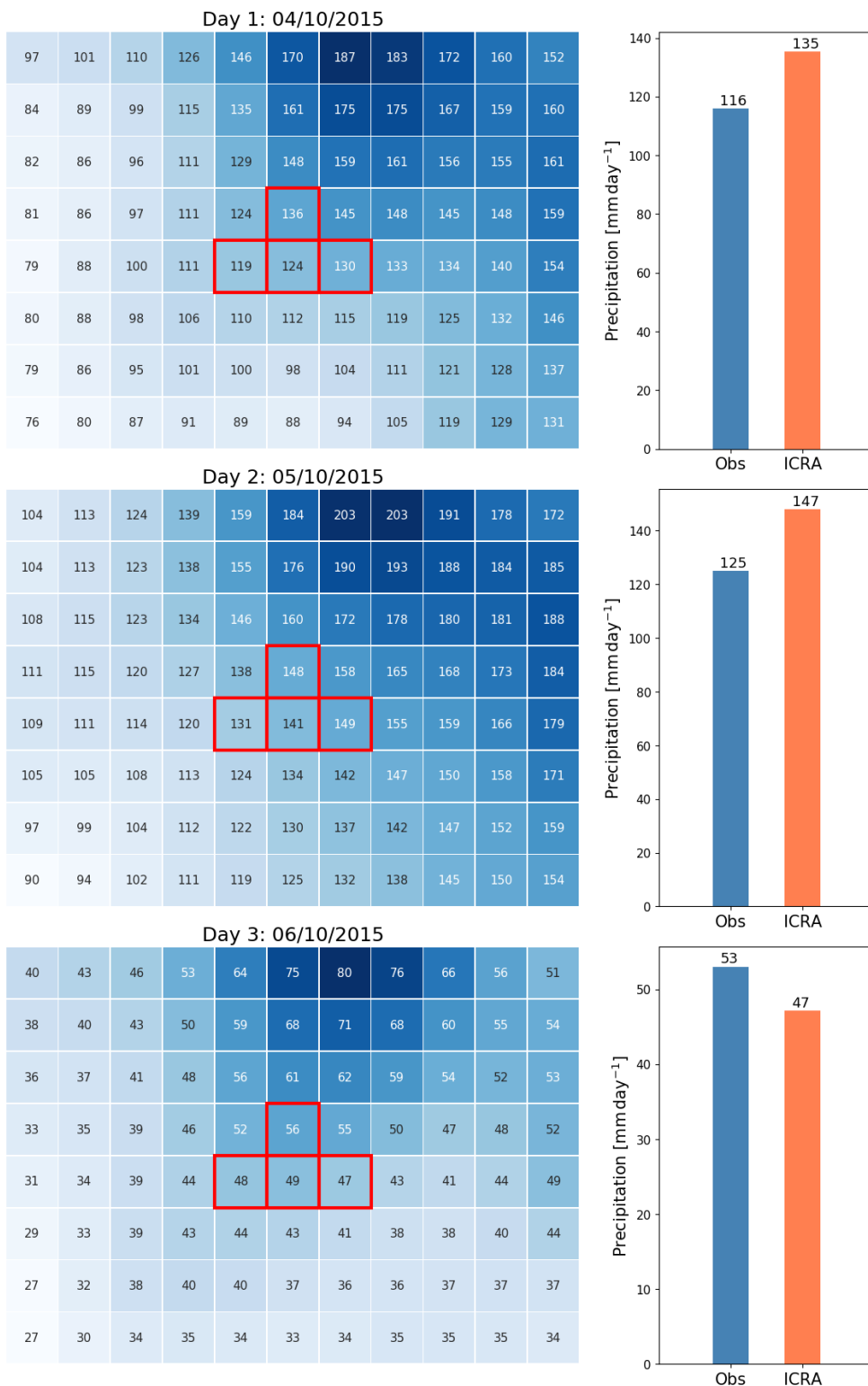


Figure II.6 – Heat maps showing daily precipitation from ICRA centred on the 4 nearest grid-points (red squares) to station Laufbali over a 3-day period with corresponding bar diagrams presenting the observed value at the station (blue) and the simulated value (orange). The station is located within the four nearest grid-points.

Neskaupstaður

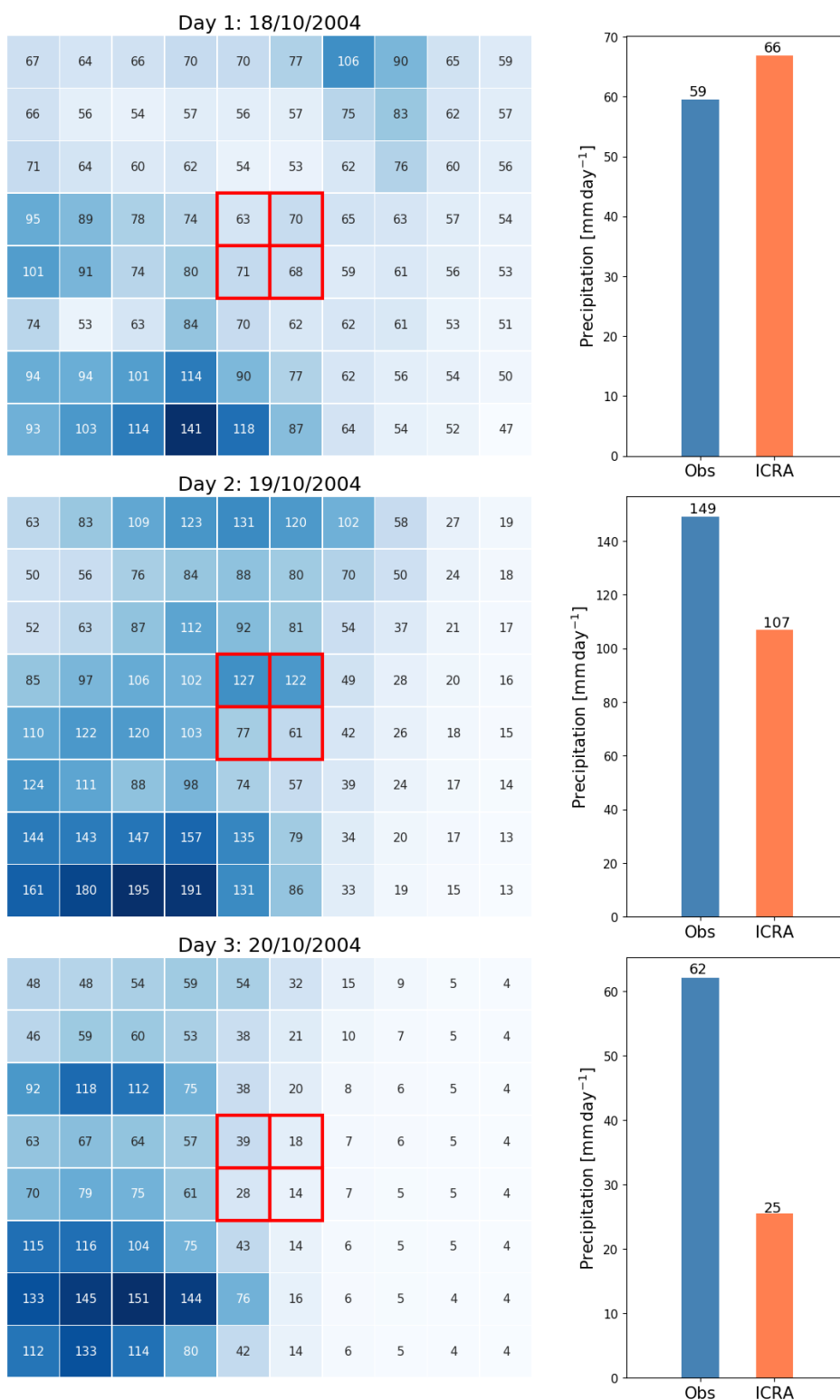


Figure II.7 – Heat maps showing daily precipitation from ICRA centred on the 4 nearest grid-points (red squares) to station Neskaupstaður over a 3-day period with corresponding bar diagrams presenting the observed value at the station (blue) and the simulated value (orange). The station is located within the four nearest grid-points.

Ólafsfjörður

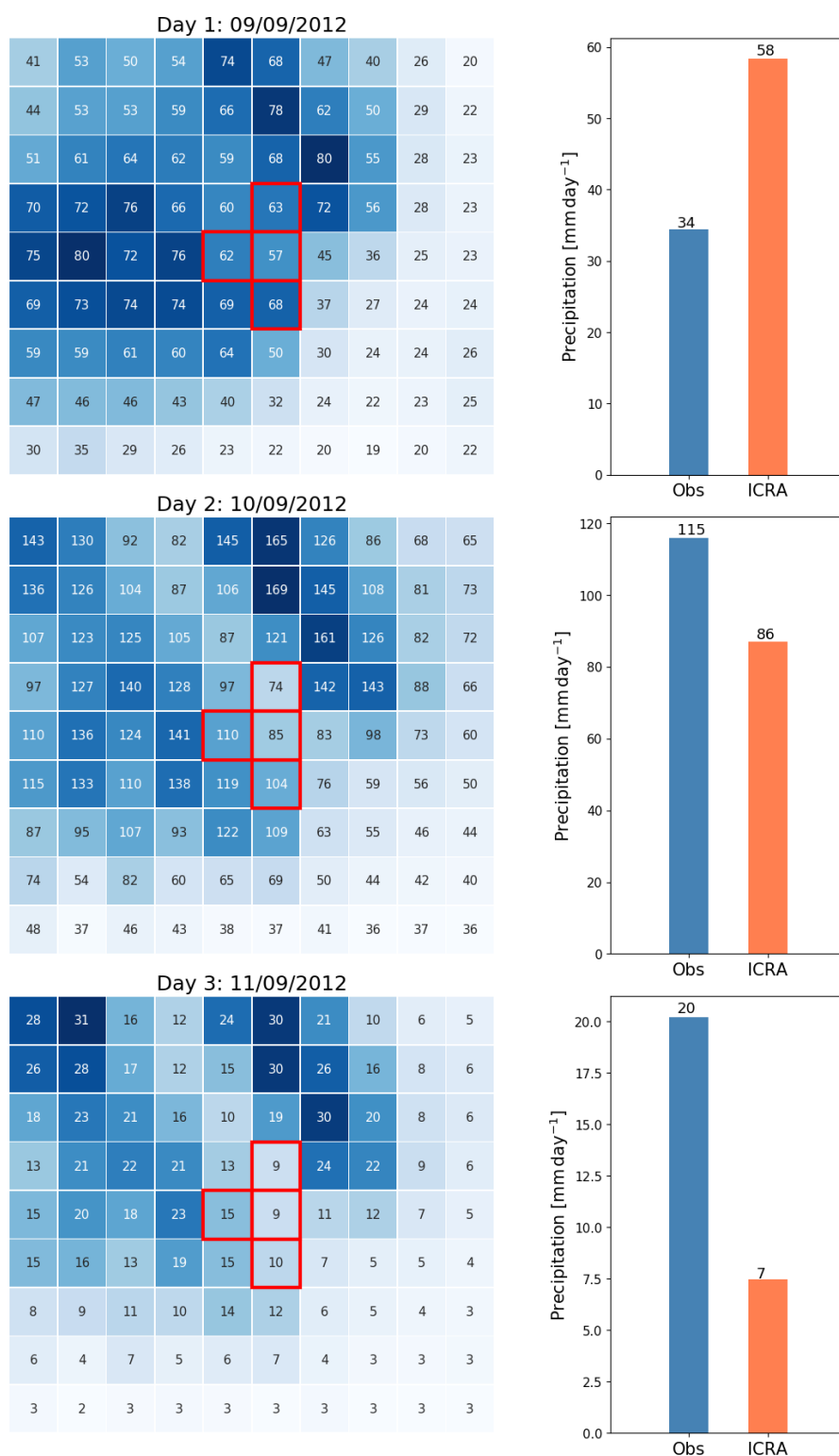


Figure II.8 – Heat maps showing daily precipitation from ICRA centred on the 4 nearest grid-points (red squares) to station Ólafsfjörður over a 3-day period with corresponding bar diagrams presenting the observed value at the station (blue) and the simulated value (orange). The station is located within the four nearest grid-points.

Reykjavík

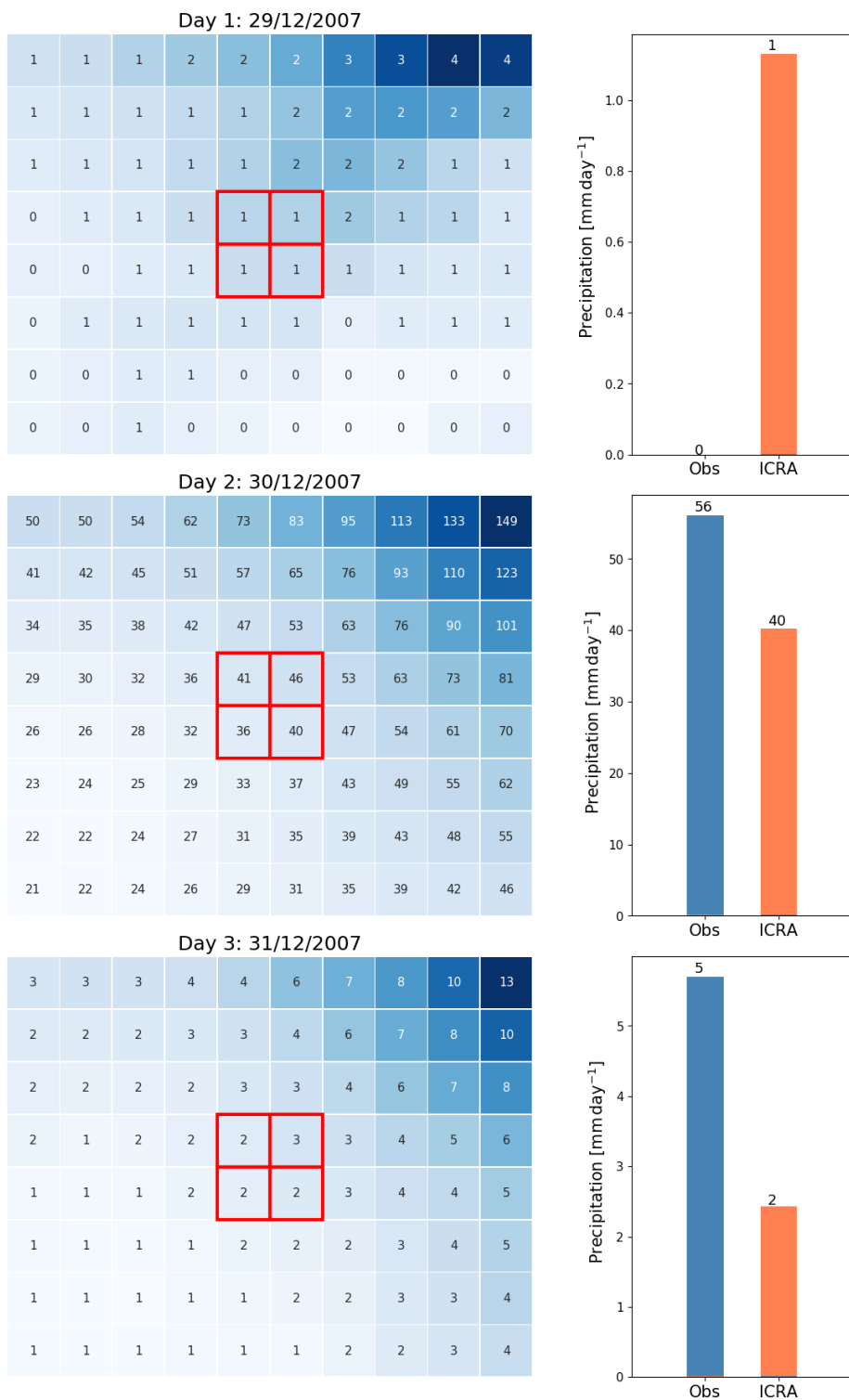


Figure II.9 – Heat maps showing daily precipitation from ICRA centred on the 4 nearest grid-points (red squares) to station Reykjavík over a 3-day period with corresponding bar diagrams presenting the observed value at the station (blue) and the simulated value (orange). The station is located within the four nearest grid-points.

Seyðisfjörður

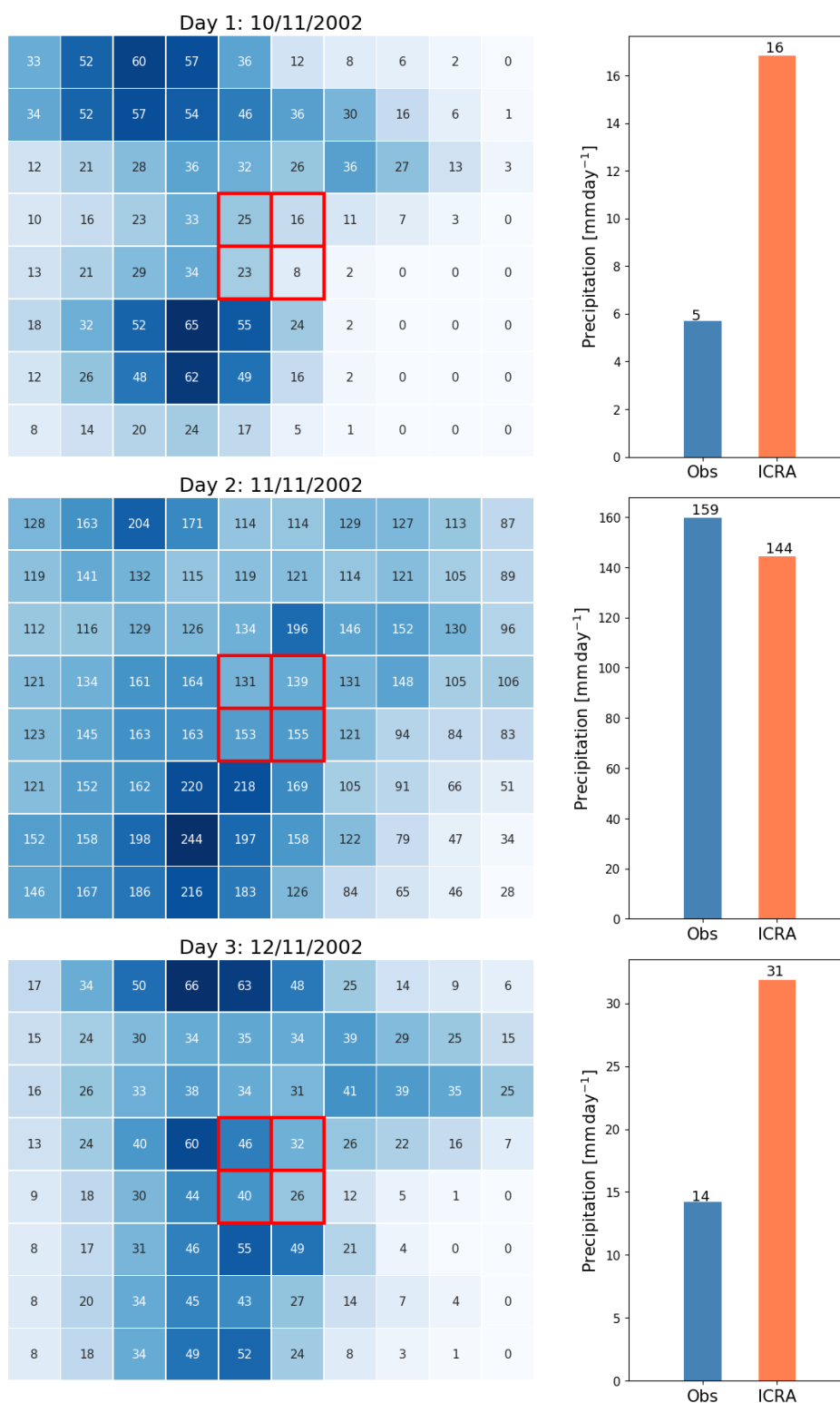


Figure II.10 – Heat maps showing daily precipitation from ICRA centred on the 4 nearest grid-points (red squares) to station Seyðisfjörður over a 3-day period with corresponding bar diagrams presenting the observed value at the station (blue) and the simulated value (orange). The station is located within the four nearest grid-points.

Siglufjörður

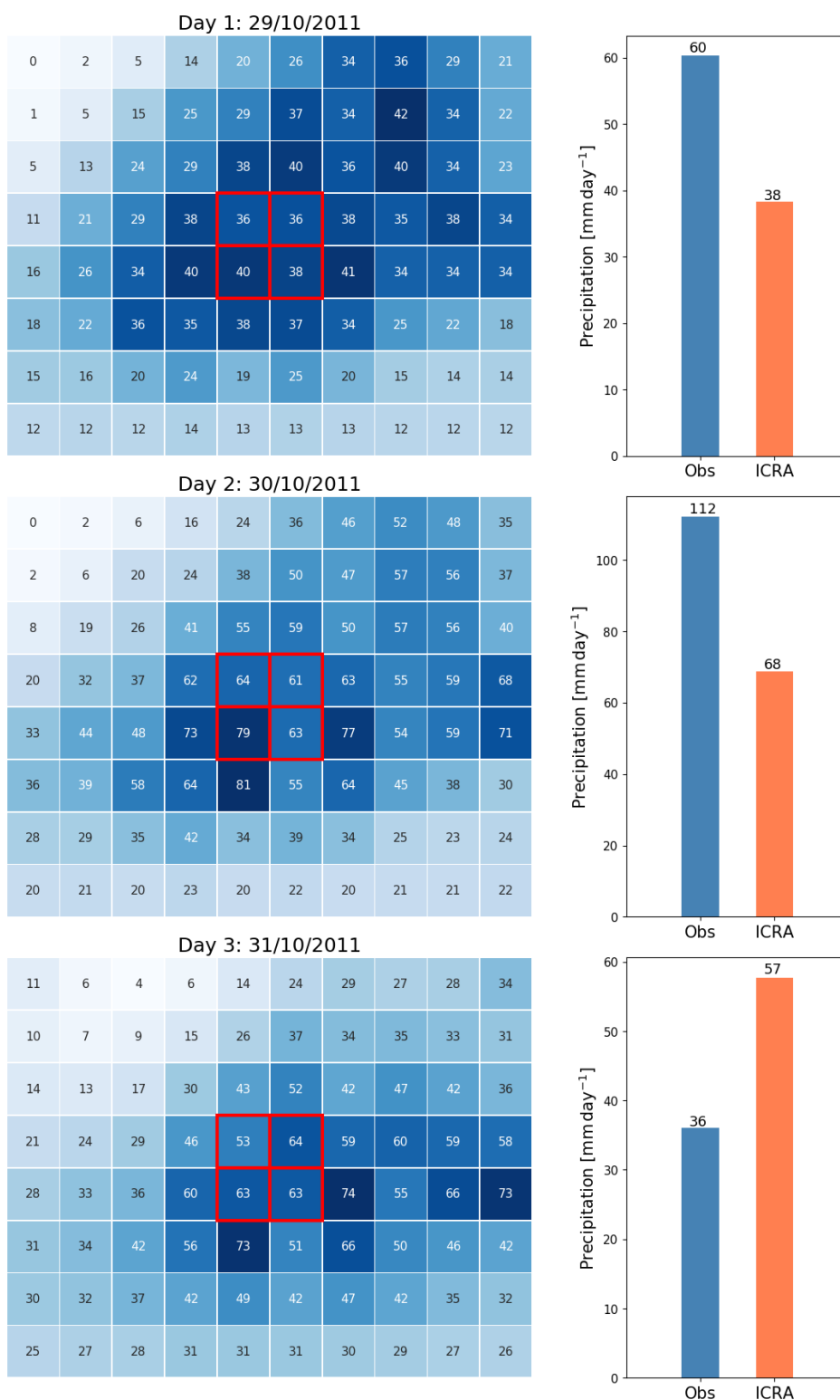


Figure II.11 – Heat maps showing daily precipitation from ICRA centred on the 4 nearest grid-points (red squares) to station Siglufjörður over a 3-day period with corresponding bar diagrams presenting the observed value at the station (blue) and the simulated value (orange). The station is located within the four nearest grid-points.

Súðavík

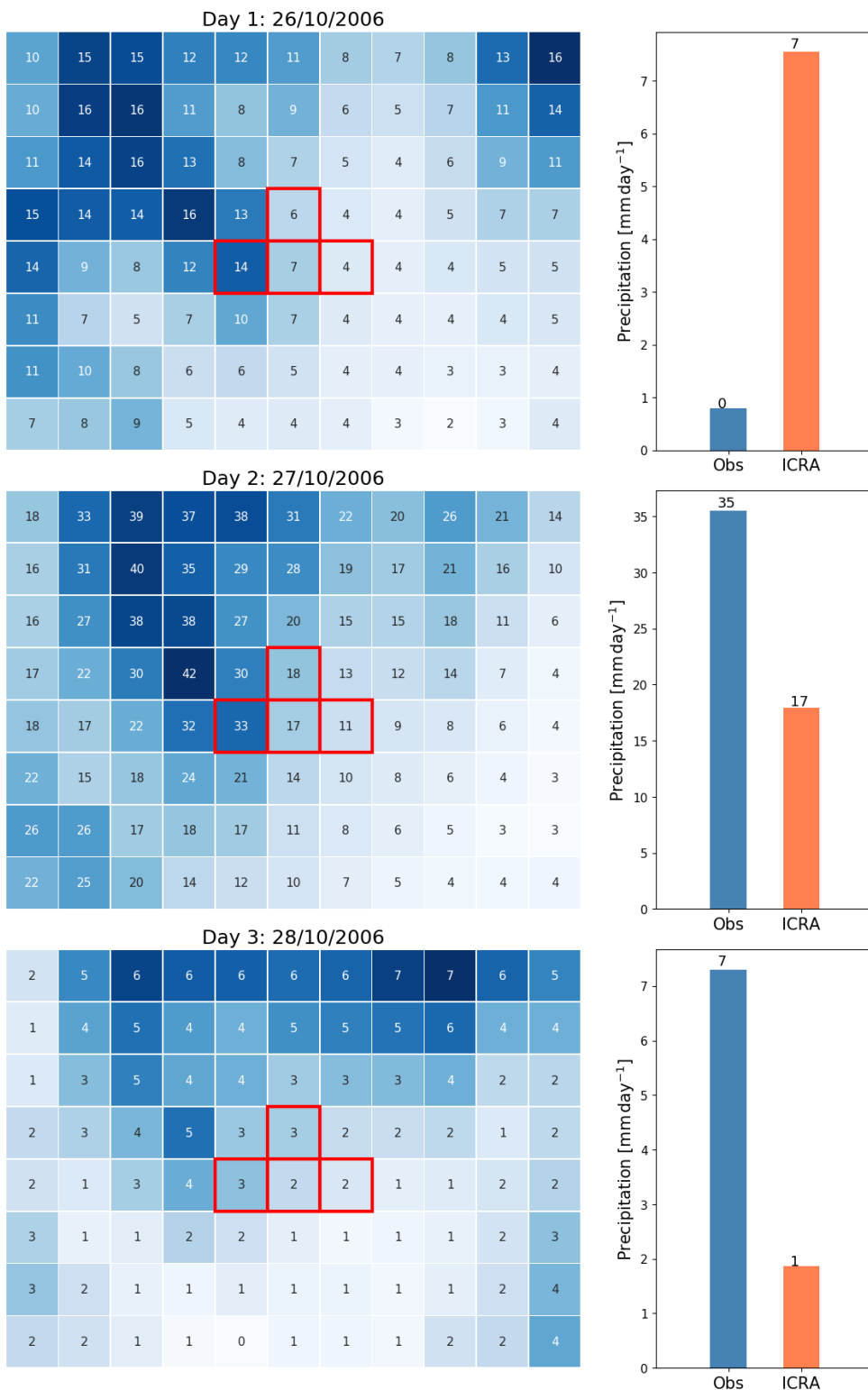


Figure II.12 – Heat maps showing daily precipitation from ICRA centred on the 4 nearest grid-points (red squares) to station Súðavík over a 3-day period with corresponding bar diagrams presenting the observed value at the station (blue) and the simulated value (orange). The station is located within the four nearest grid-points.

Appendix III. Intensity-Duration-Frequency curves and tables

In this appendix, Intensity-Duration-Frequency (IDF) results for the 43 selected stations are presented. Figure III.A shows location of the stations selected for this study. Figure III.B gives the closeness coefficient for all stations when the daily precipitation with 10-year return periods based on reanalysis are compared with the corresponding return levels based on measurements. The closest this coefficient is to 100, the more likely IDF curves derived from the ICRA are fitting the ones obtained from the observation. Figure III.1–III.43 show the IDF-curves, and Tables III.1–III.43 the same results in table form. The results are calculated from the entire reanalysis timeseries (1979–2017), using fixed clock-time intervals. For some stations, when converted to mm h^{-1} and shown as IDF curves, precipitation intensities increase with the duration, creating a bump in the usually decreasing IDF curves. Those values are attributed to the fact that the Peak-over-Threshold method was applied independently on timeseries for each duration.

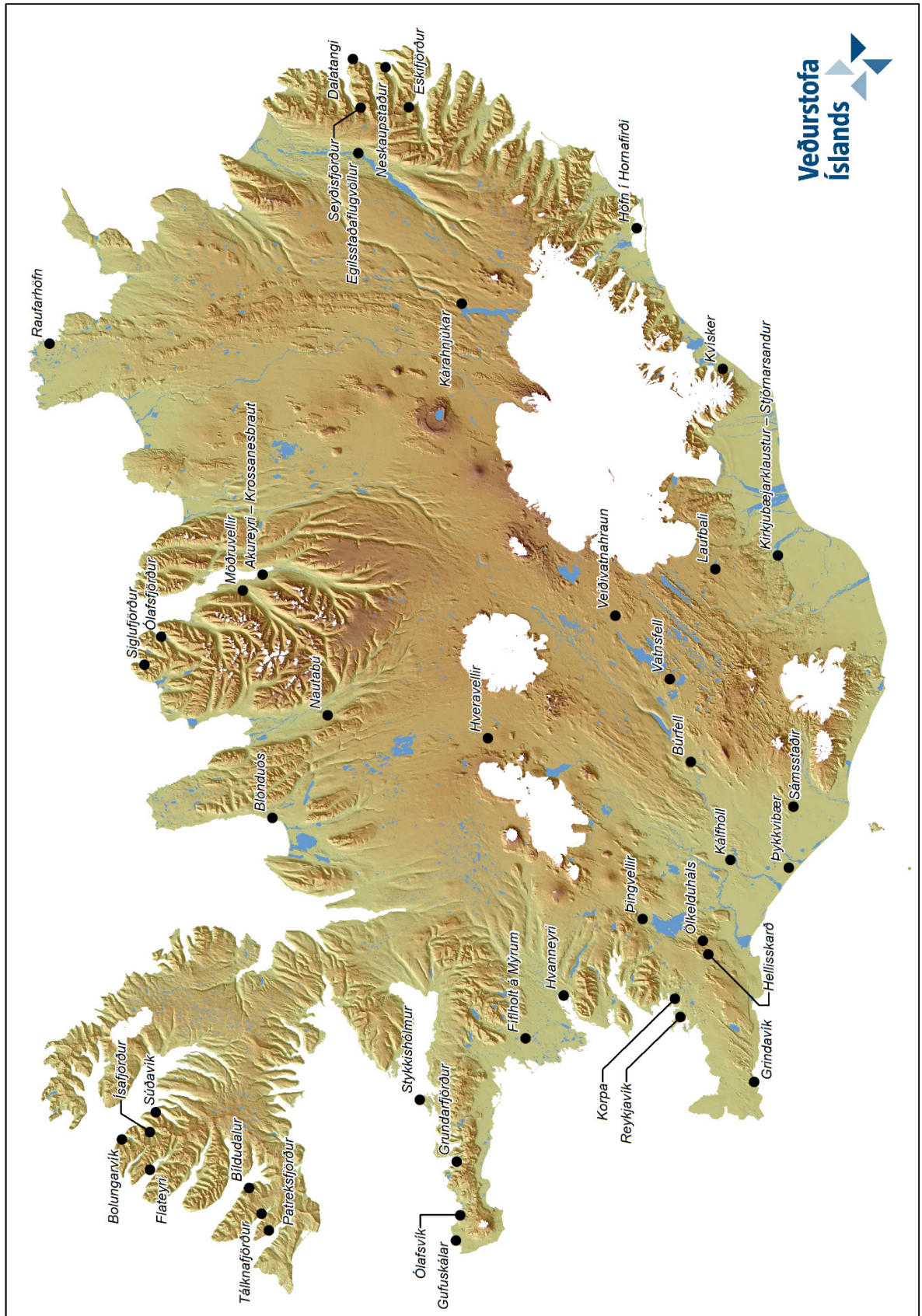


Figure III.A – Map of Iceland with all automatic gauging stations measuring precipitation as of January 2020

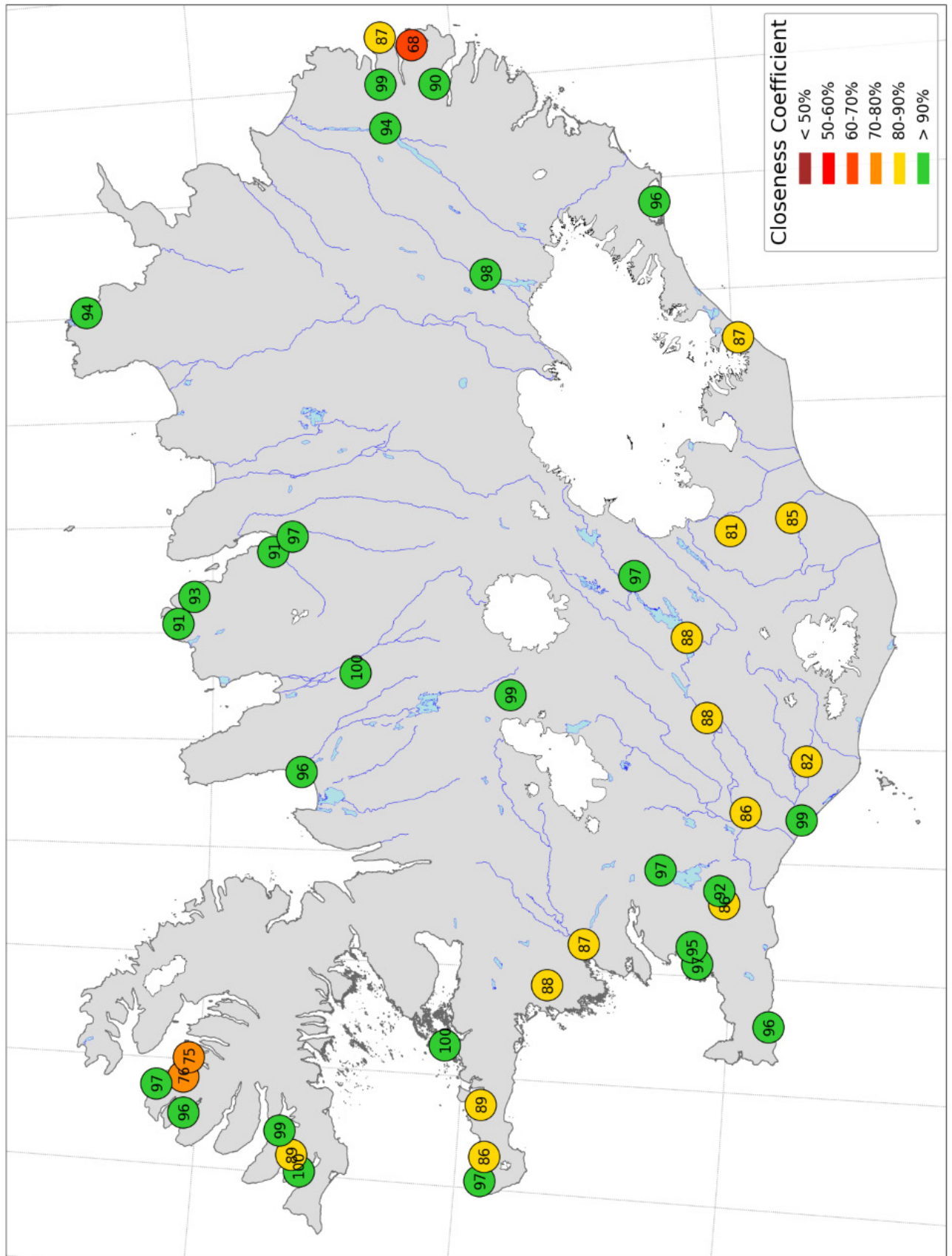


Figure III.B – Closeness Coefficients (%) comparing daily precipitation with a 10-year return period between observations and simulations at the 43 gauging stations selected for the study.

IDF CURVES: Akureyri

ICRA 1979 - 2017

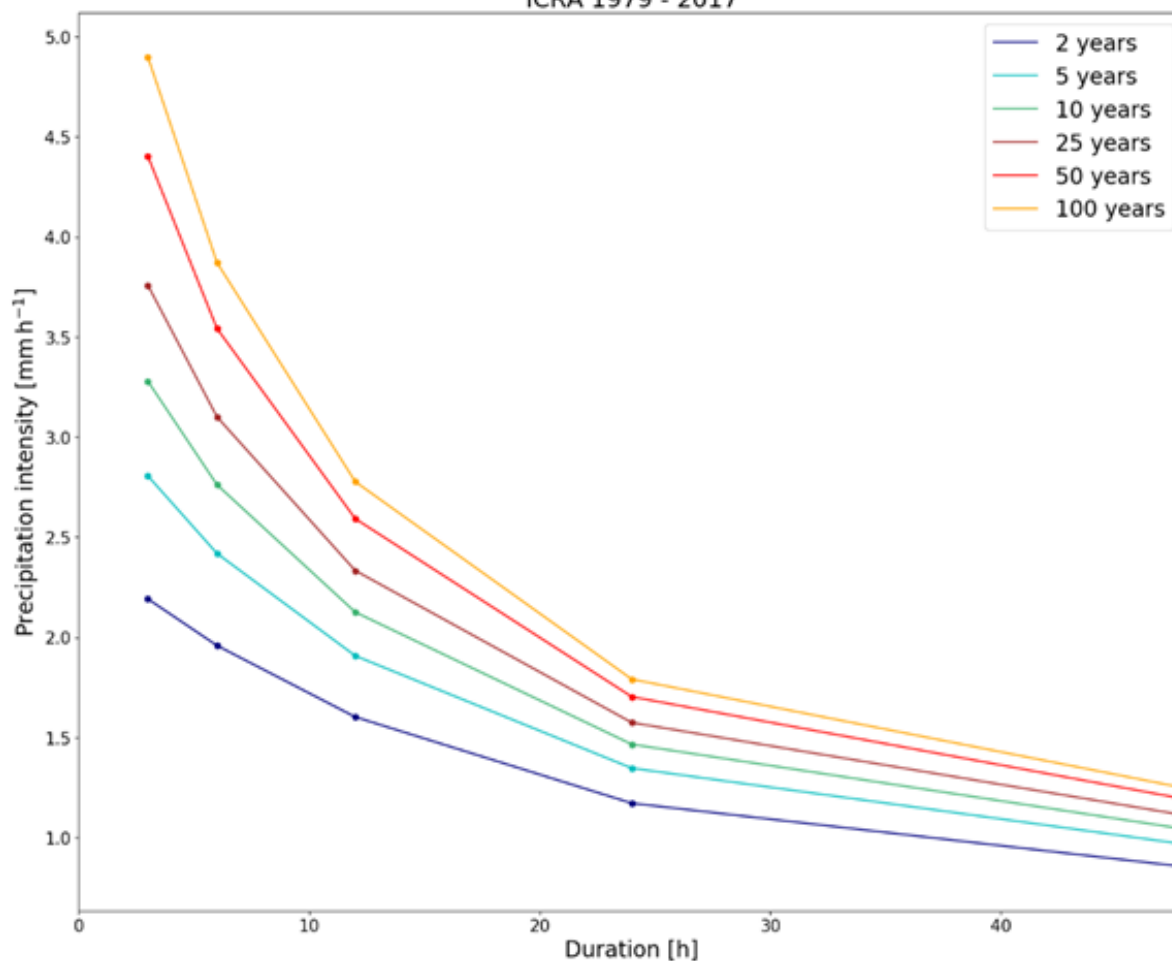


Figure III.1 – IDF curves for station Akureyri from entire ICRA. Solid points give return levels for 3, 6, 12, 24, 48 hours duration with a 2, 5, 10, 25, 50 and 100 return period. Each coloured line corresponds to a different return period as stated by the legend.

Table III.1 – Return levels (mm) for various durations and return periods based on the entire ICRA for station Akureyri. Values are given for 3-, 6-, 12-, 24-, 48-hour duration with a 2-, 5-, 10-, 25-, 50- and 100-year return period.

	2 years	5 years	10 years	25 years	50 years	100 years
3 hours	7	8	10	11	13	15
6 hours	12	15	17	19	21	23
12 hours	19	23	26	28	31	33
24 hours	28	32	25	28	41	43
48 hours	41	46	50	53	57	60

IDF CURVES: Bíldudalur

ICRA 1979 - 2017

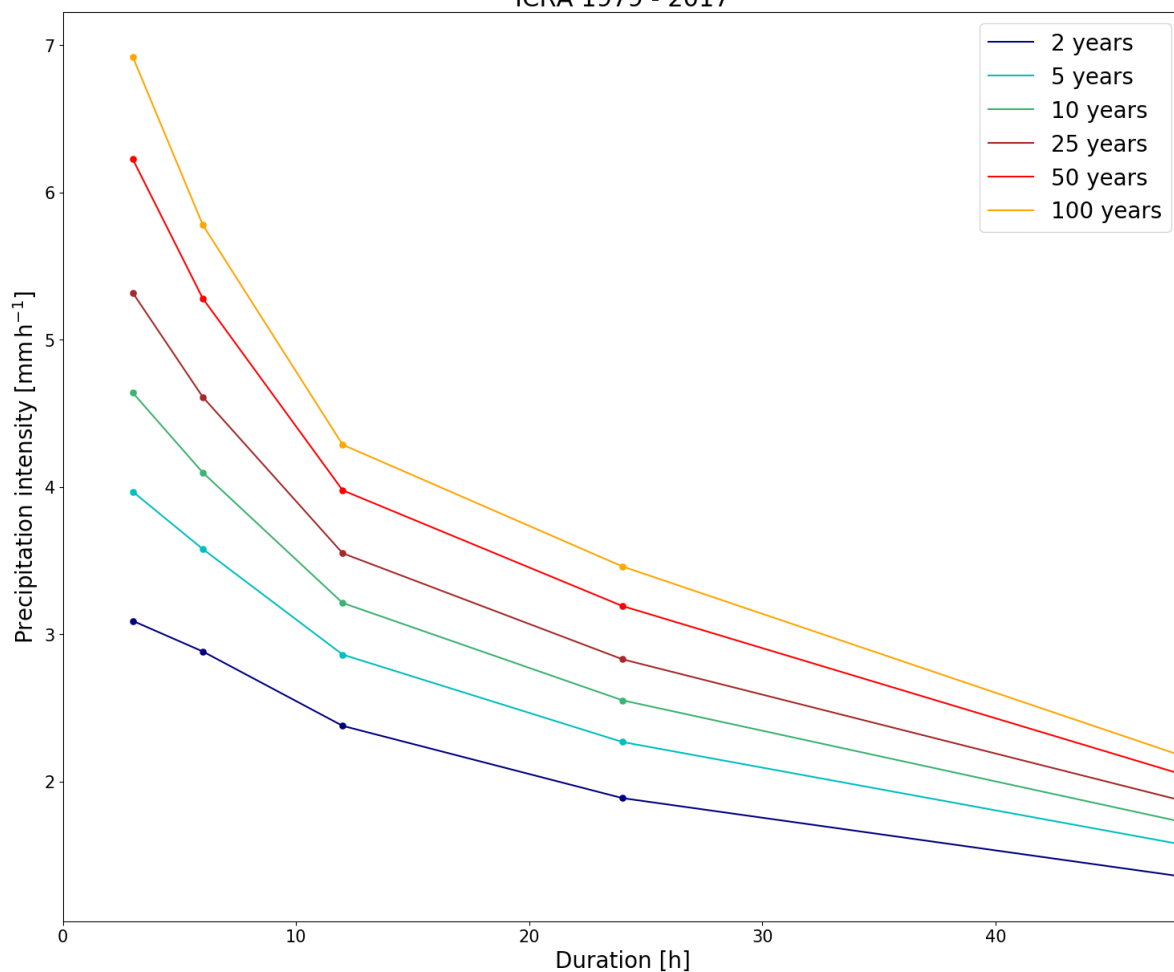


Figure III.2 – IDF curves for station Bíldudalur from entire ICRA. Solid points give return levels for 3-, 6-, 12-, 24-, 48-hour duration with a 2-, 5-, 10-, 25-, 50- and 100-year return period. Each coloured line corresponds to a different return period as stated by the legend.

Table III.2 – Return levels (mm) for various durations and return periods based on the entire ICRA for station Bíldudalur. Values are given for 3-, 6-, 12-, 24-, 48-hour duration with a 2-, 5-, 10-, 25-, 50- and 100-year return period.

	2 years	5 years	10 years	25 years	50 years	100 years
3 hours	9	12	14	16	19	21
6 hours	17	21	25	28	32	35
12 hours	29	34	39	43	48	51
24 hours	45	54	61	68	77	83
48 hours	65	75	83	90	98	104

IDF CURVES: Blönduós

ICRA 1979 - 2017

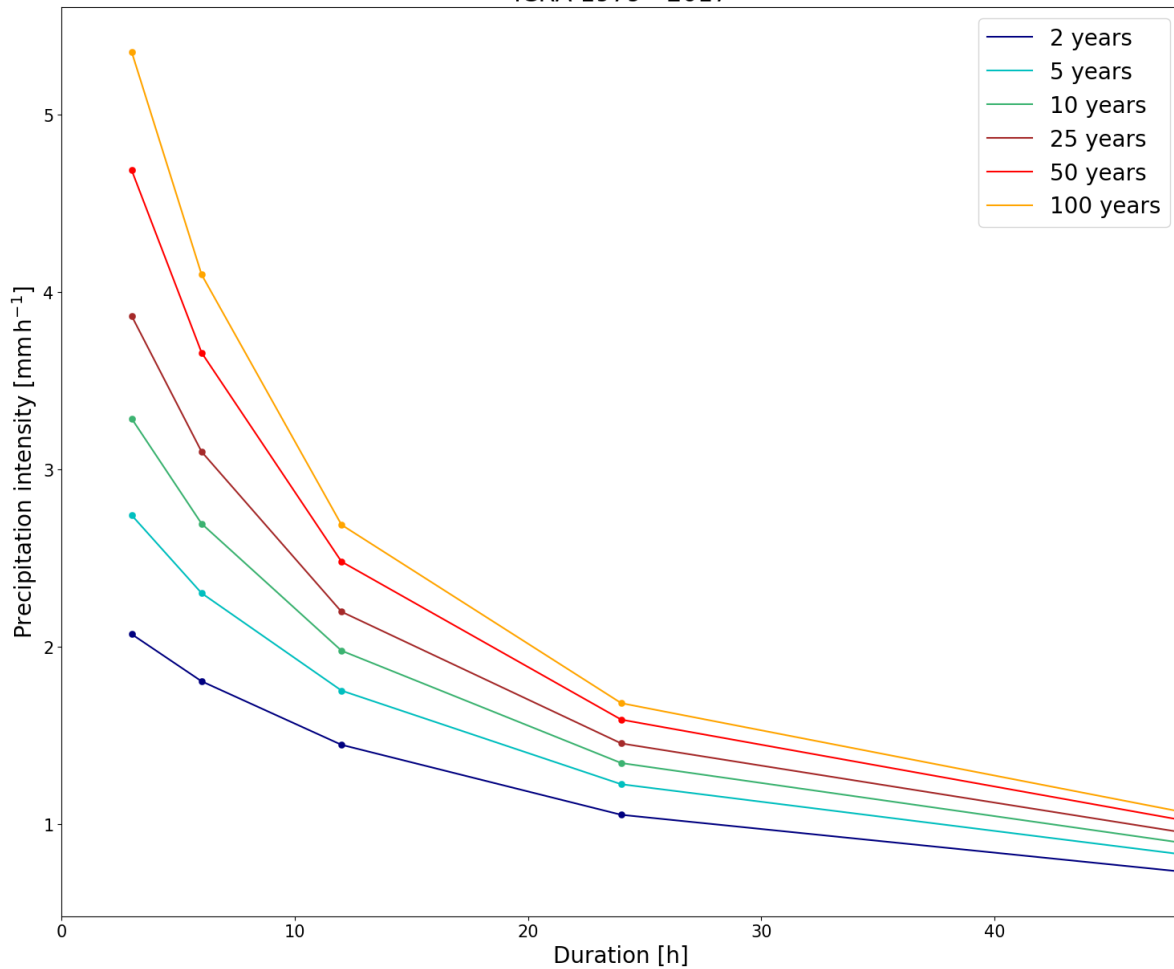


Figure III.3 – IDF curves for station Blönduós from entire ICRA. Solid points give return levels for 3-, 6-, 12-, 24-, 48-hour duration with a 2-, 5-, 10-, 25-, 50- and 100-year return period. Each coloured line corresponds to a different return period as stated by the legend.

Table III.3 – Return levels (mm) for various durations and return periods based on the entire ICRA for station Blönduós. Values are given for 3-, 6-, 12-, 24-, 48-hour duration with a 2-, 5-, 10-, 25-, 50- and 100-year return period.

	2 years	5 years	10 years	25 years	50 years	100 years
3 hours	6	8	10	12	14	16
6 hours	11	14	16	19	22	25
12 hours	17	21	24	26	30	32
24 hours	25	29	32	35	38	40
48 hours	35	40	43	46	49	51

IDF CURVES: Bolungarvík

ICRA 1979 - 2017

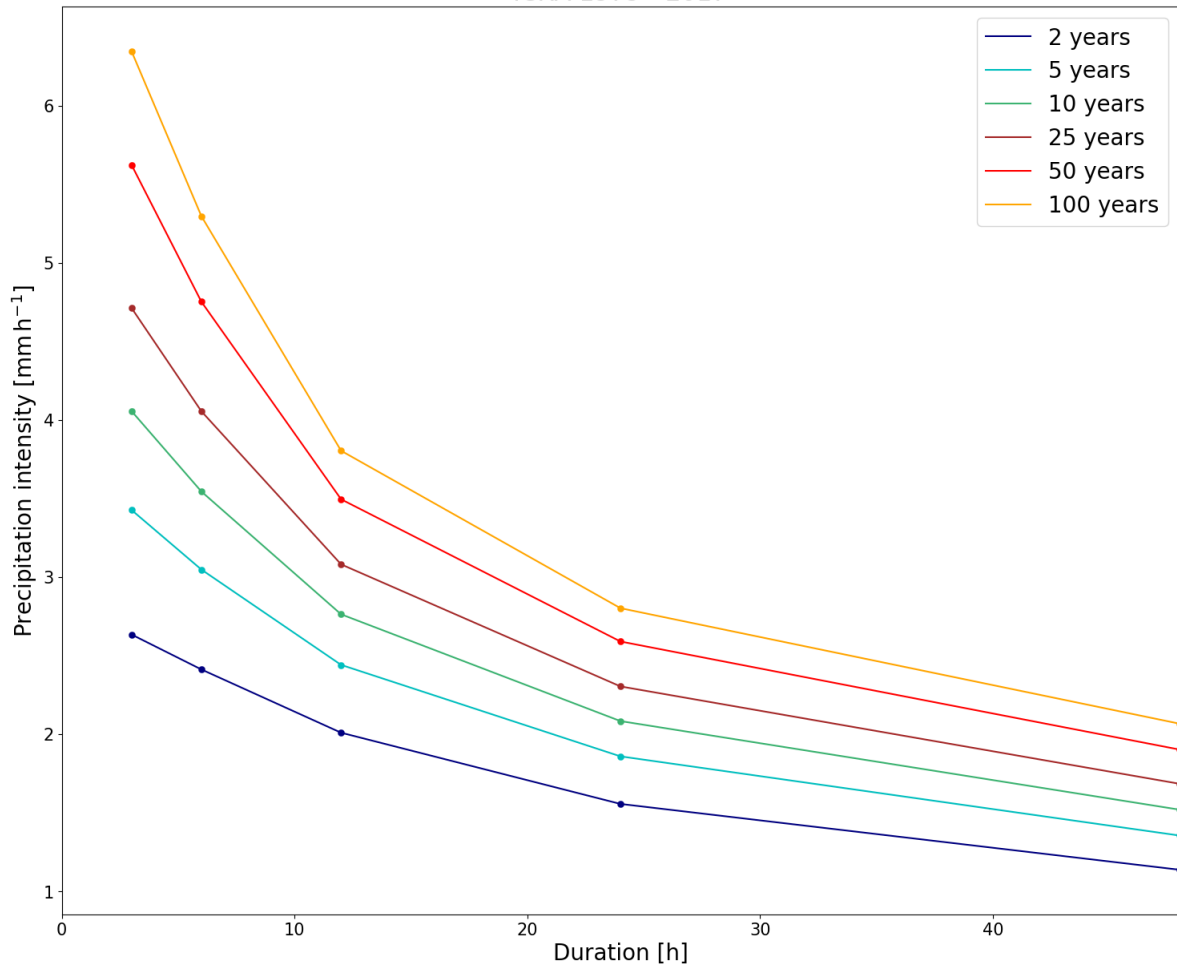


Figure III.4 – IDF curves for station Bolungarvík from entire ICRA. Solid points give return levels for 3-, 6-, 12-, 24-, 48-hour duration with a 2-, 5-, 10-, 25-, 50- and 100-year return period. Each coloured line corresponds to a different return period as stated by the legend.

Table III.4 – Return levels (mm) for various durations and return periods based on the entire ICRA for station Bolungarvík. Values are given for 3-, 6-, 12-, 24-, 48-hour duration with a 2-, 5-, 10-, 25-, 50- and 100-year return period.

	2 years	5 years	10 years	25 years	50 years	100 years
3 hours	8	10	12	14	17	19
6 hours	14	18	21	24	29	32
12 hours	24	29	33	37	42	46
24 hours	38	45	50	55	62	67
48 hours	55	65	73	81	91	99

IDF CURVES: Búrfell

ICRA 1979 - 2017

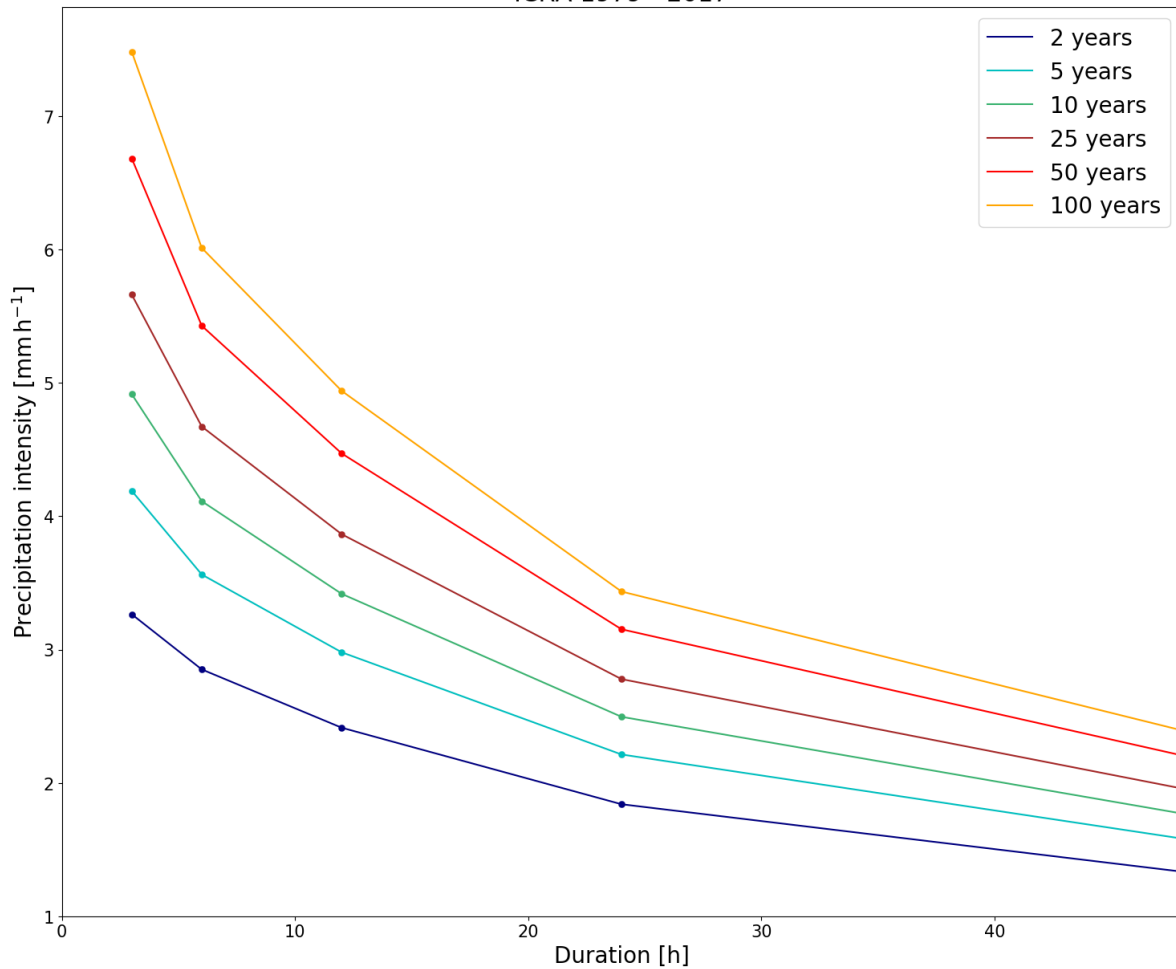


Figure III.5 – IDF curves for station Búrfell from entire ICRA. Solid points give return levels for 3-, 6-, 12-, 24-, 48-hour duration with a 2-, 5-, 10-, 25-, 50- and 100-year return period. Each coloured line corresponds to a different return period as stated by the legend.

Table III.5 – Return levels (mm) for various durations and return periods based on the entire ICRA for station Búrfell. Values are given for 3-, 6-, 12-, 24-, 48-hour duration with a 2-, 5-, 10-, 25-, 50- and 100-year return period.

	2 years	5 years	10 years	25 years	50 years	100 years
3 hours	10	13	15	17	20	22
6 hours	17	21	25	28	33	36
12 hours	29	36	41	46	54	59
24 hours	44	53	60	67	76	82
48 hours	64	76	85	94	106	115

IDF CURVES: Dalatangi

ICRA 1979 - 2017

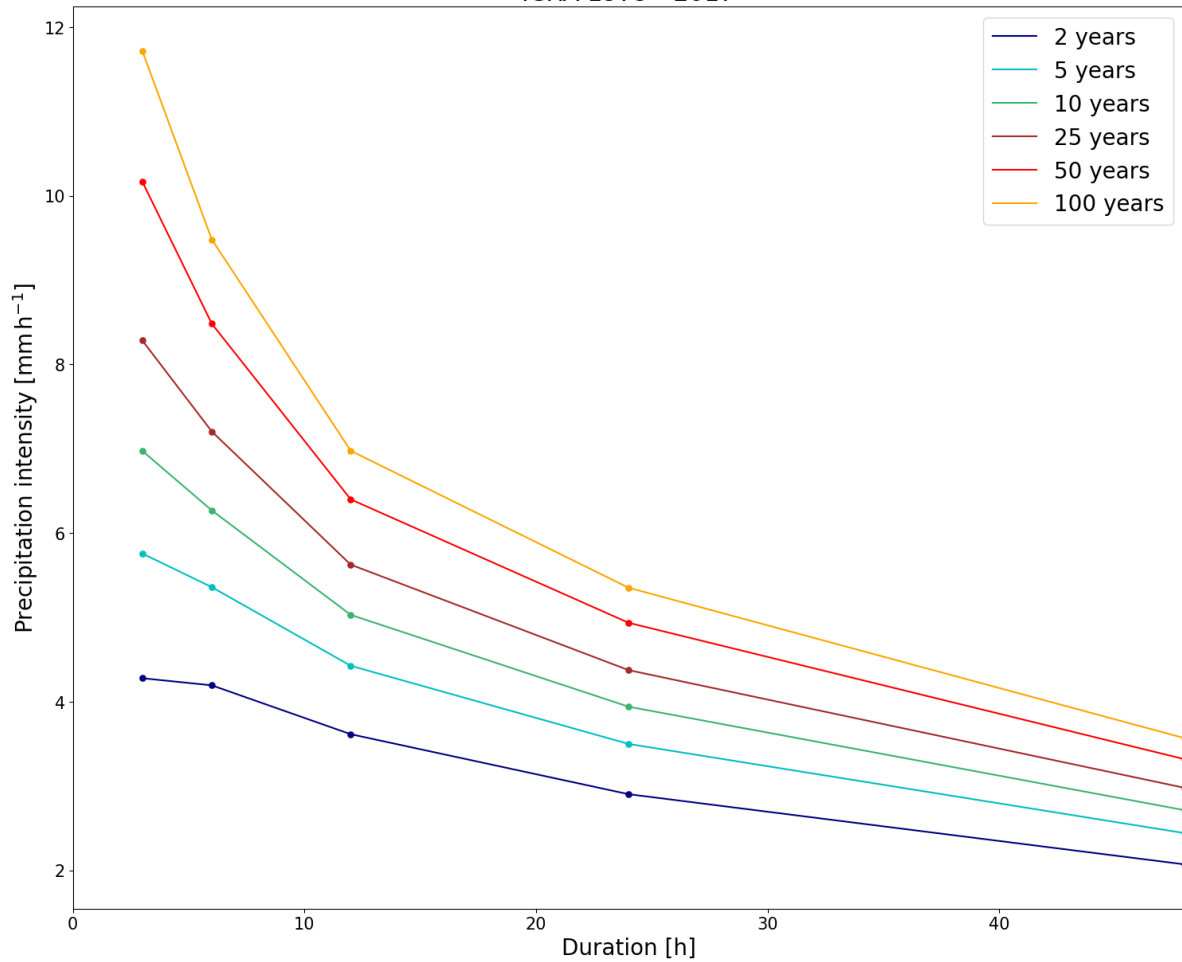


Figure III.6 – IDF curves for station Dalatangi from entire ICRA. Solid points give return levels for 3-, 6-, 12-, 24-, 48-hour duration with a 2-, 5-, 10-, 25-, 50- and 100-year return period. Each coloured line corresponds to a different return period as stated by the legend.

Table III.6 – Return levels (mm) for various durations and return periods based on the entire ICRA for station Dalatangi. Values are given for 3-, 6-, 12-, 24-, 48-hour duration with a 2-, 5-, 10-, 25-, 50- and 100-year return period.

	2 years	5 years	10 years	25 years	50 years	100 years
3 hours	13	17	21	25	31	35
6 hours	25	32	38	43	51	57
12 hours	43	53	60	67	77	84
24 hours	70	84	95	105	118	128
48 hours	99	117	130	143	159	171

IDF CURVES: Egilsstaðaflugvöllur

ICRA 1979 - 2017

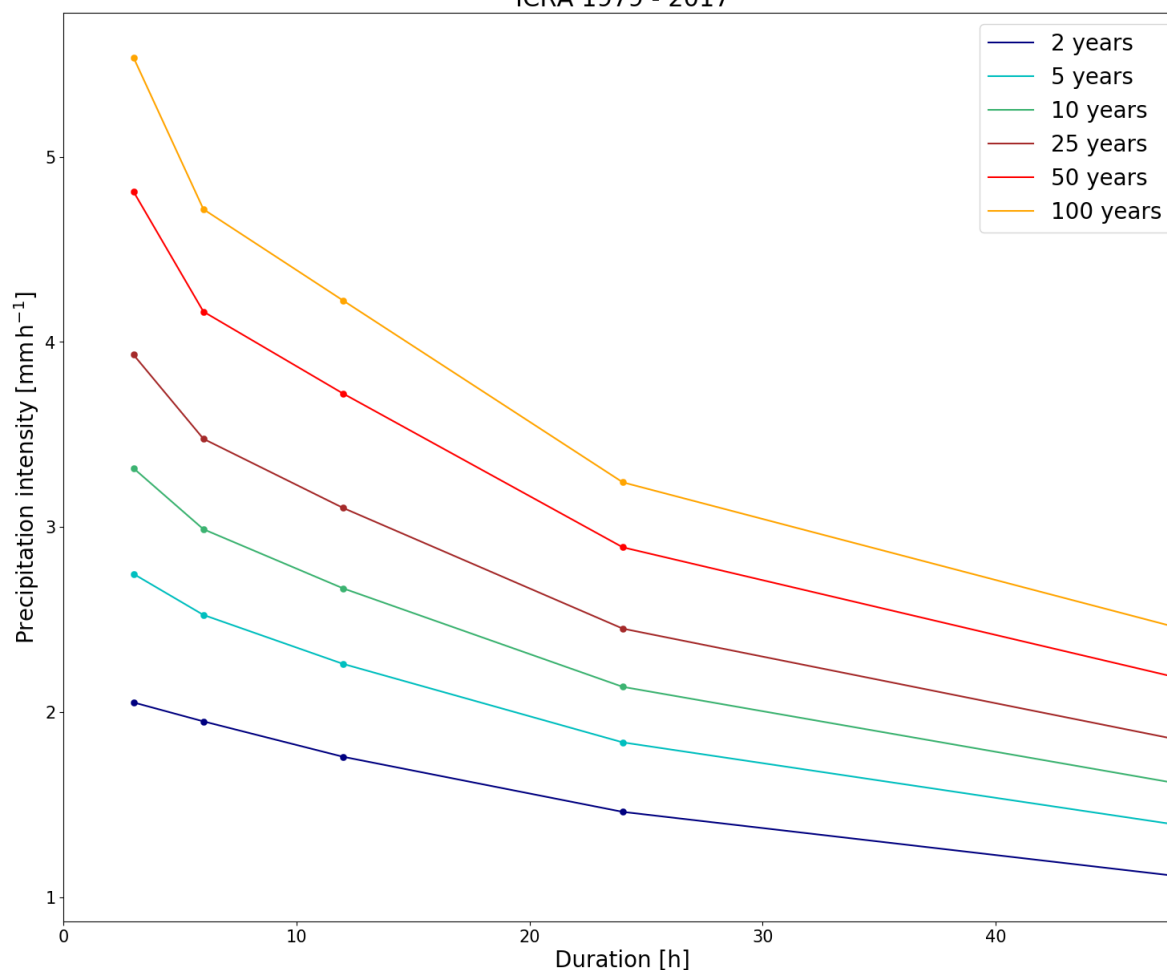


Figure III.7 – IDF curves for station Egilsstaðaflugvöllur from entire ICRA. Solid points give return levels for 3-, 6-, 12-, 24-, 48-hour duration with a 2-, 5-, 10-, 25-, 50- and 100-year return period. Each coloured line corresponds to a different return period as stated by the legend.

Table III.7 – Return levels (mm) for various durations and return periods based on the entire ICRA for station Egilsstaðaflugvöllur. Values are given for 3-, 6-, 12-, 24-, 48-hour duration with a 2-, 5-, 10-, 25-, 50- and 100-year return period.

	2 years	5 years	10 years	25 years	50 years	100 years
3 hours	6	8	10	12	14	17
6 hours	12	15	18	21	25	28
12 hours	21	27	32	37	45	51
24 hours	35	44	51	59	69	78
48 hours	53	67	77	88	105	118

IDF CURVES: Eskifjörður

ICRA 1979 - 2017

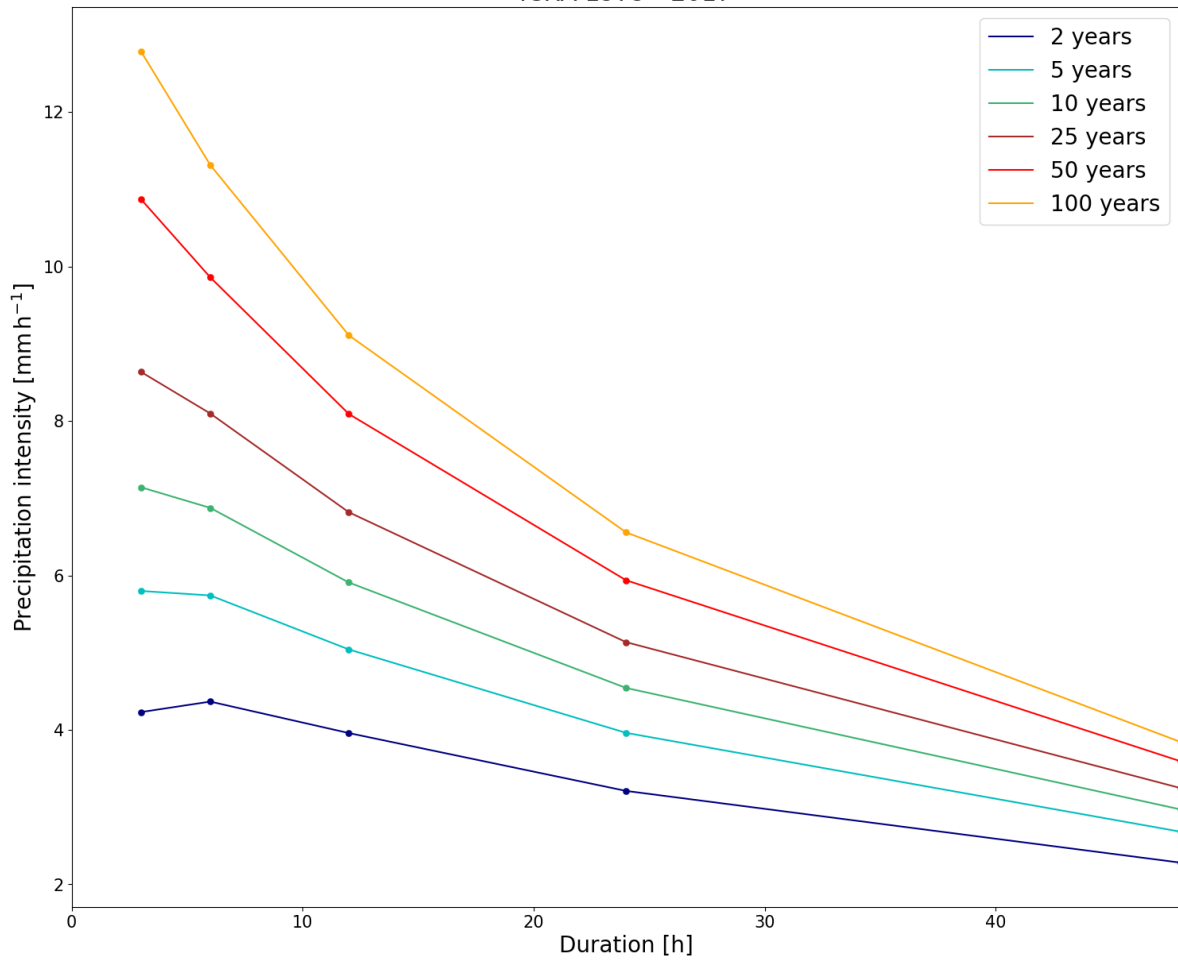


Figure III.8 – IDF curves for station Eskifjörður from entire ICRA. Solid points give return levels for 3-, 6-, 12-, 24-, 48-hour duration with a 2-, 5-, 10-, 25-, 50- and 100-year return period. Each coloured line corresponds to a different return period as stated by the legend.

Table III.8 – Return levels (mm) for various durations and return periods based on the entire ICRA for station Eskifjörður. Values are given for 3-, 6-, 12-, 24-, 48-hour duration with a 2-, 5-, 10-, 25-, 50- and 100-year return period.

	2 years	5 years	10 years	25 years	50 years	100 years
3 hours	13	17	21	26	33	38
6 hours	26	34	41	49	59	68
12 hours	48	60	71	82	97	109
24 hours	77	95	109	123	142	157
48 hours	110	129	143	156	173	185

IDF CURVES: Fíflholt á Mýrum

ICRA 1979 - 2017

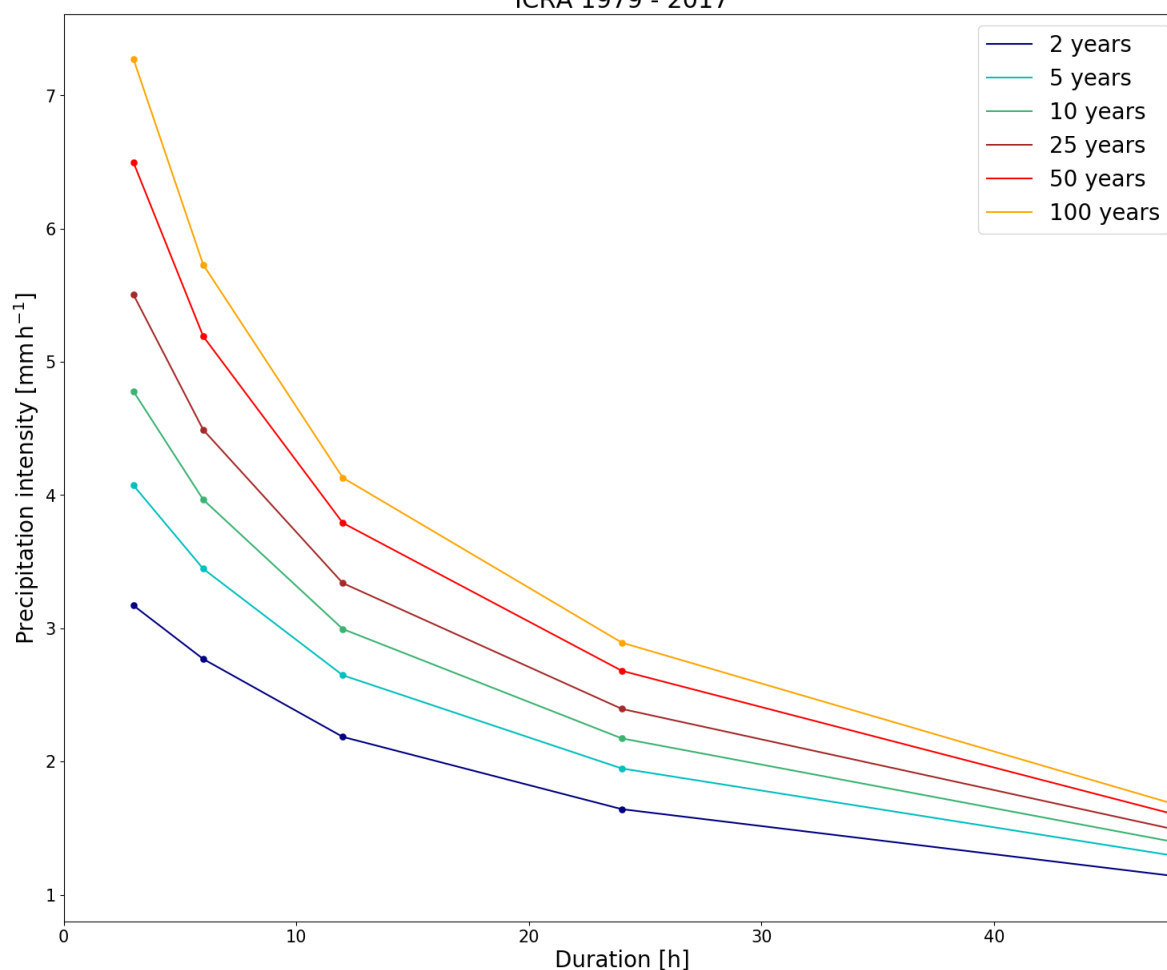


Figure III.9 – IDF curves for station Fíflholt á Mýrum from entire ICRA. Solid points give return levels for 3-, 6-, 12-, 24-, 48-hour duration with a 2-, 5-, 10-, 25-, 50- and 100-year return period. Each coloured line corresponds to a different return period as stated by the legend.

Table III.9 – Return levels (mm) for various durations and return periods based on the entire ICRA for station Fíflholt á Mýrum. Values are given for 3-, 6-, 12-, 24-, 48-hour duration with a 2-, 5-, 10-, 25-, 50- and 100-year return period.

	2 years	5 years	10 years	25 years	50 years	100 years
3 hours	10	12	14	17	19	22
6 hours	17	21	24	27	31	34
12 hours	26	32	36	40	45	50
24 hours	39	47	52	57	64	69
48 hours	54	62	67	71	76	80

IDF CURVES: Flateyri

ICRA 1979 - 2017

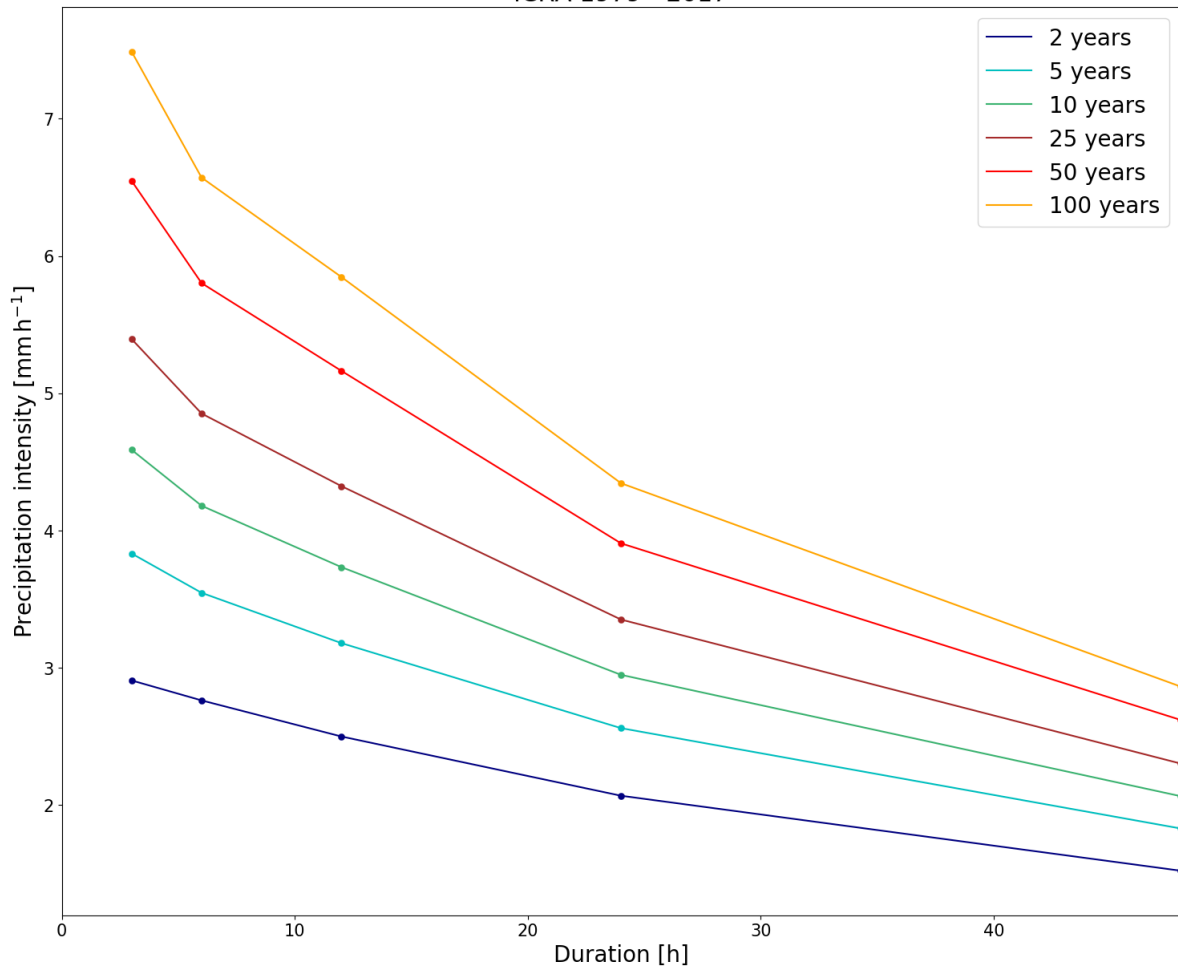


Figure III.10 – IDF curves for station Flateyri from entire ICRA. Solid points give return levels for 3-, 6-, 12-, 24-, 48-hour duration with a 2-, 5-, 10-, 25-, 50- and 100-year return period. Each coloured line corresponds to a different return period as stated by the legend.

Table III.10 – Return levels (mm) for various durations and return periods based on the entire ICRA for station Flateyri. Values are given for 3-, 6-, 12-, 24-, 48-hour duration with a 2-, 5-, 10-, 25-, 50- and 100-year return period.

	2 years	5 years	10 years	25 years	50 years	100 years
3 hours	9	11	14	16	20	22
6 hours	17	21	25	29	35	39
12 hours	30	38	45	52	62	70
24 hours	50	61	71	80	94	104
48 hours	73	88	99	110	126	137

IDF CURVES: Grindavik

ICRA 1979 - 2017

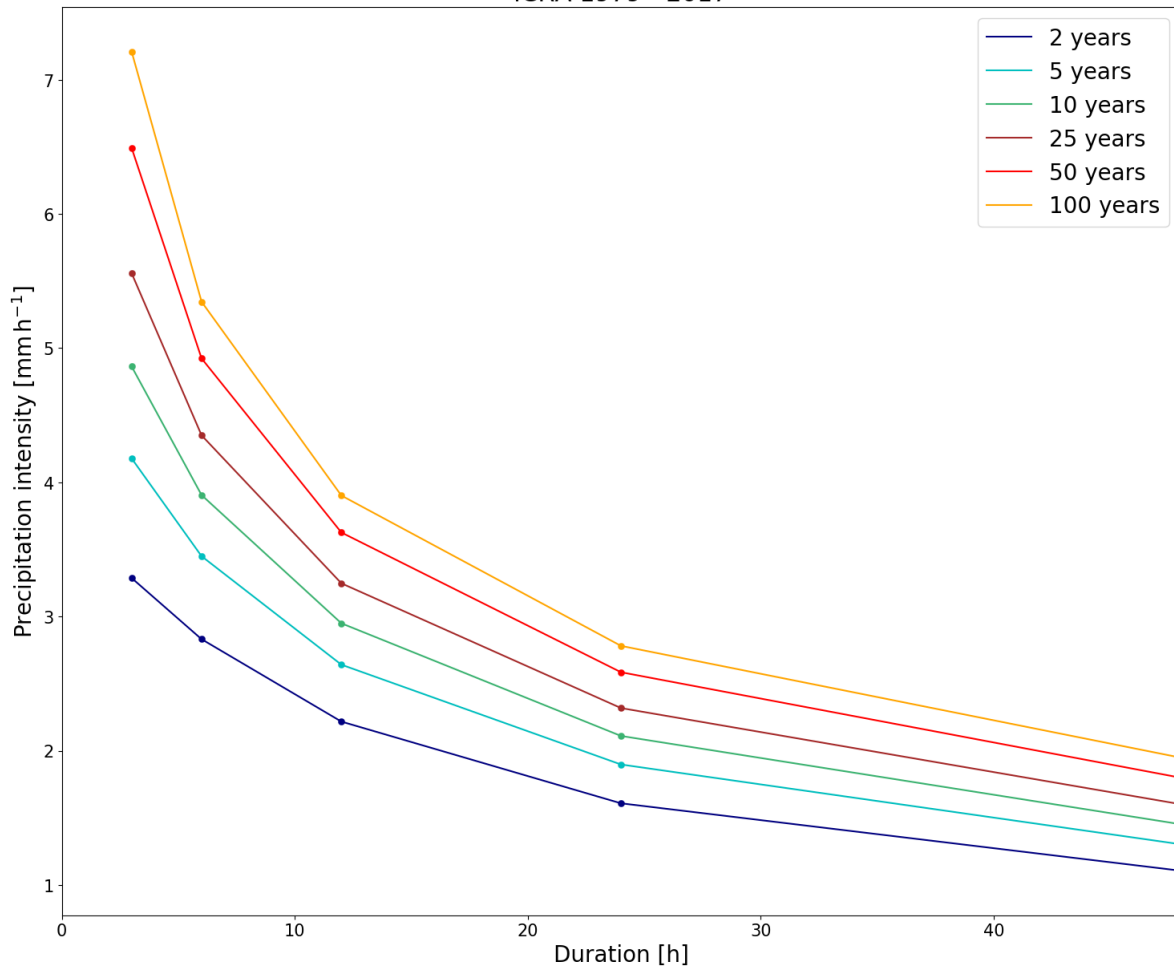


Figure III.11 – IDF curves for station Grindavik from entire ICRA. Solid points give return levels for 3-, 6-, 12-, 24-, 48-hour duration with a 2-, 5-, 10-, 25-, 50- and 100-year return period. Each coloured line corresponds to a different return period as stated by the legend.

Table III.11 – Return levels (mm) for various durations and return periods based on the entire ICRA for station Grindavik. Values are given for 3-, 6-, 12-, 24-, 48-hour duration with a 2-, 5-, 10-, 25-, 50- and 100-year return period.

	2 years	5 years	10 years	25 years	50 years	100 years
3 hours	10	13	15	17	19	22
6 hours	17	21	23	26	30	32
12 hours	27	32	35	39	44	47
24 hours	39	46	51	56	62	67
48 hours	53	63	70	77	86	94

IDF CURVES: Grundarfjörður

ICRA 1979 - 2017

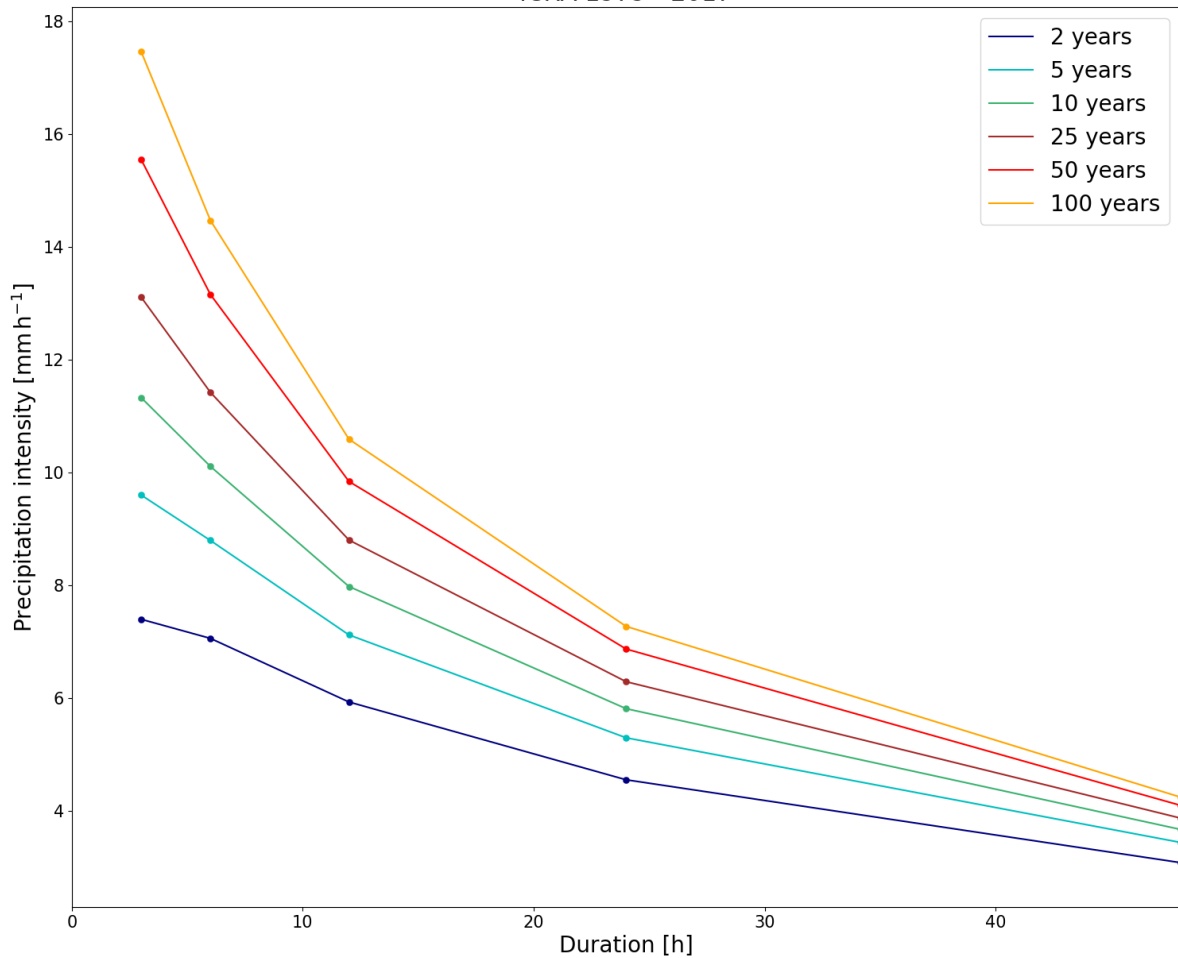


Figure III.12 – IDF curves for station Grundarfjörður from entire ICRA. Solid points give return levels for 3-, 6-, 12-, 24-, 48-hour duration with a 2-, 5-, 10-, 25-, 50- and 100-year return period. Each coloured line corresponds to a different return period as stated by the legend.

Table III.12 – Return levels (mm) for various durations and return periods based on the entire ICRA for station Grundarfjörður. Values are given for 3-, 6-, 12-, 24-, 48-hour duration with a 2-, 5-, 10-, 25-, 50- and 100-year return period.

	2 years	5 years	10 years	25 years	50 years	100 years
3 hours	22	29	34	39	47	52
6 hours	42	53	61	69	79	86
12 hours	71	85	96	106	118	127
24 hours	109	127	139	151	165	174
48 hours	148	165	176	186	196	203

IDF CURVES: Gufuskálar

ICRA 1979 - 2017

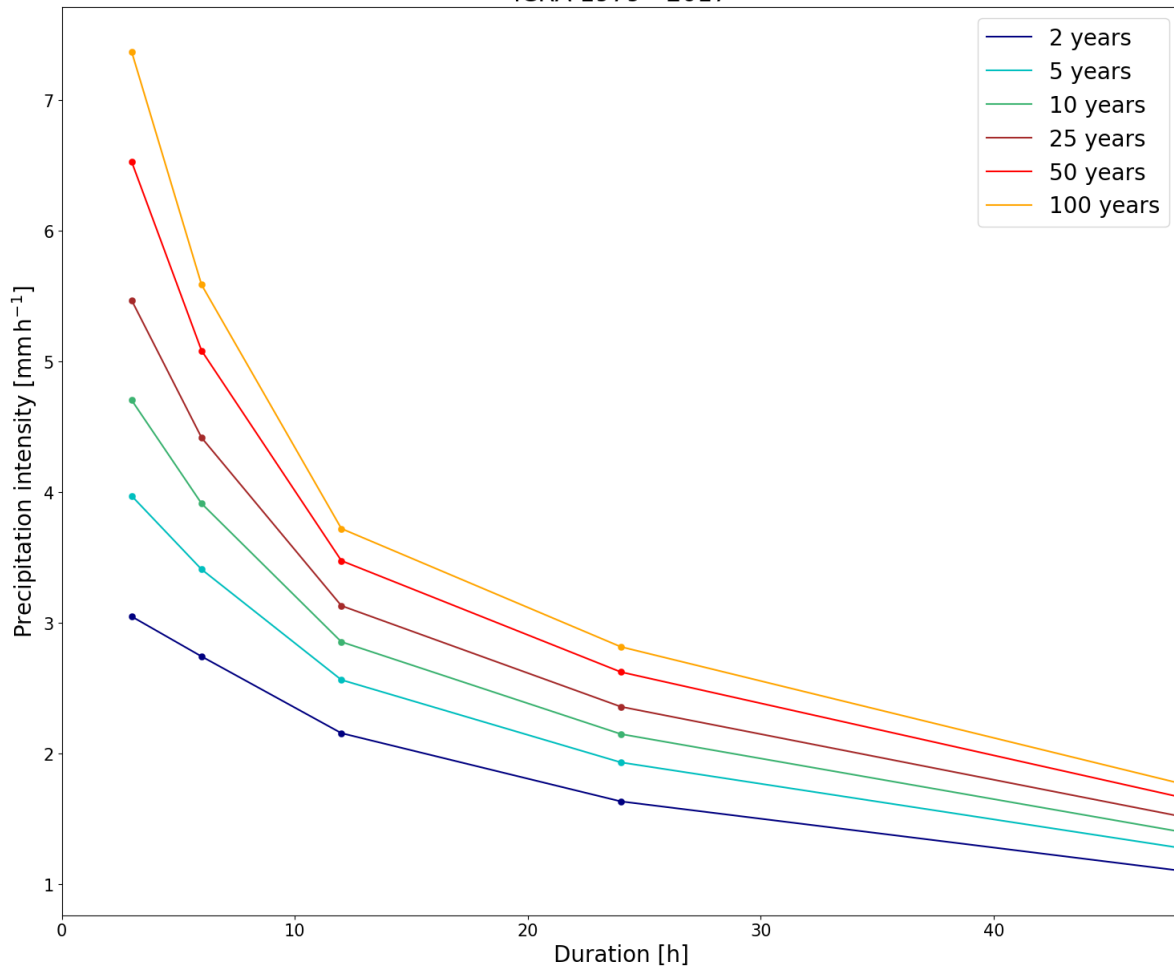


Figure III.13 – IDF curves for station Gufuskálar from entire ICRA. Solid points give return levels for 3-, 6-, 12-, 24-, 48-hour duration with a 2-, 5-, 10-, 25-, 50- and 100-year return period. Each coloured line corresponds to a different return period as stated by the legend.

Table III.13 – Return levels (mm) for various durations and return periods based on the entire ICRA for station Gufuskálar. Values are given for 3-, 6-, 12-, 24-, 48-hour duration with a 2-, 5-, 10-, 25-, 50- and 100-year return period.

	2 years	5 years	10 years	25 years	50 years	100 years
3 hours	9	12	14	16	20	22
6 hours	16	20	23	27	31	34
12 hours	26	31	34	38	42	45
24 hours	39	46	52	57	63	68
48 hours	53	61	67	73	80	85

IDF CURVES: Helliskarð

ICRA 1979 - 2017

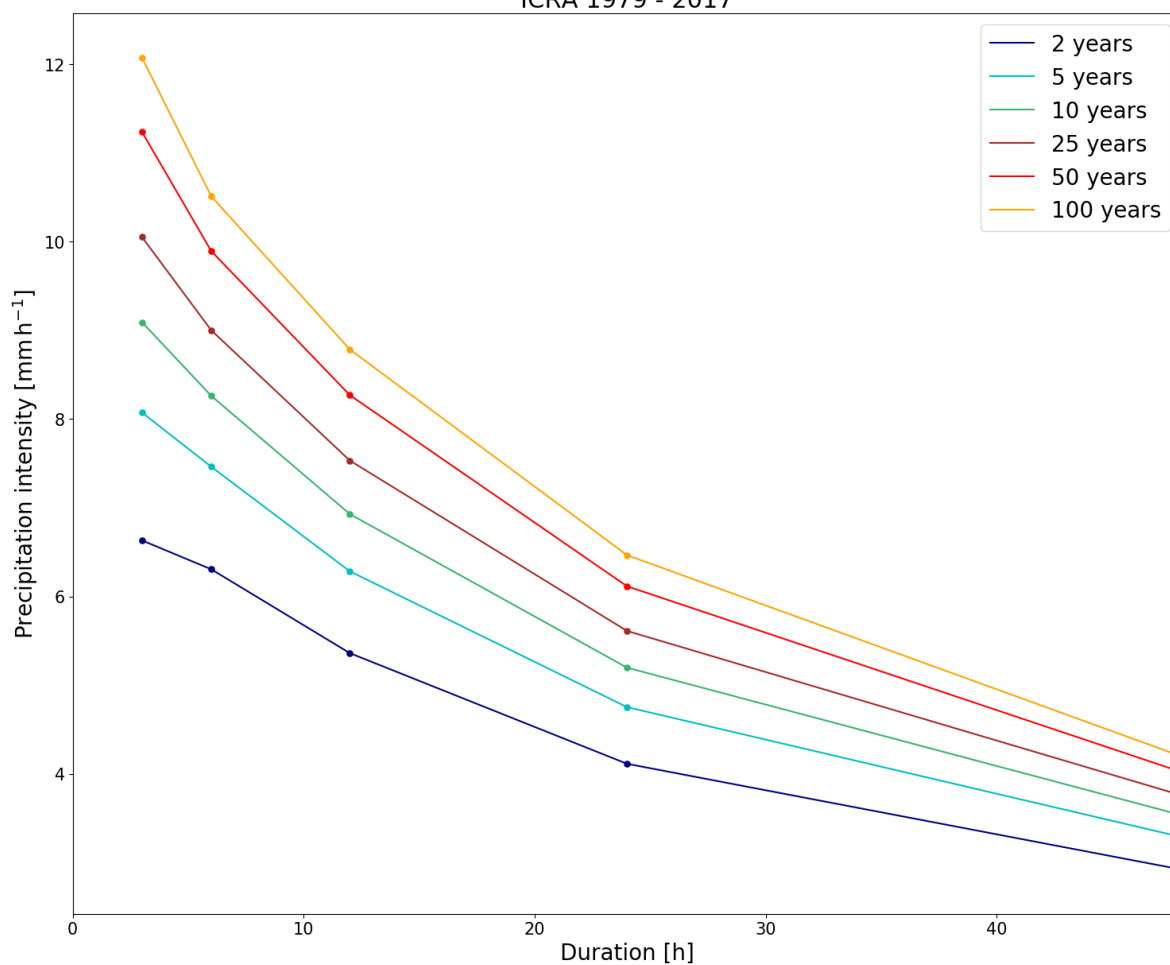


Figure III.14 – IDF curves for station Helliskarð from entire ICRA. Solid points give return levels for 3-, 6-, 12-, 24-, 48-hour duration with a 2-, 5-, 10-, 25-, 50- and 100-year return period. Each coloured line corresponds to a different return period as stated by the legend.

Table III.14 – Return levels (mm) for various durations and return periods based on the entire ICRA for station Helliskarð. Values are given for 3-, 6-, 12-, 24-, 48-hour duration with a 2-, 5-, 10-, 25-, 50- and 100-year return period.

	2 years	5 years	10 years	25 years	50 years	100 years
3 hours	20	24	27	30	34	36
6 hours	38	45	50	54	59	63
12 hours	64	75	83	90	99	105
24 hours	99	114	125	135	147	155
48 hours	140	158	170	180	193	201

IDF CURVES: Höfn í Hornafirði

ICRA 1979 - 2017

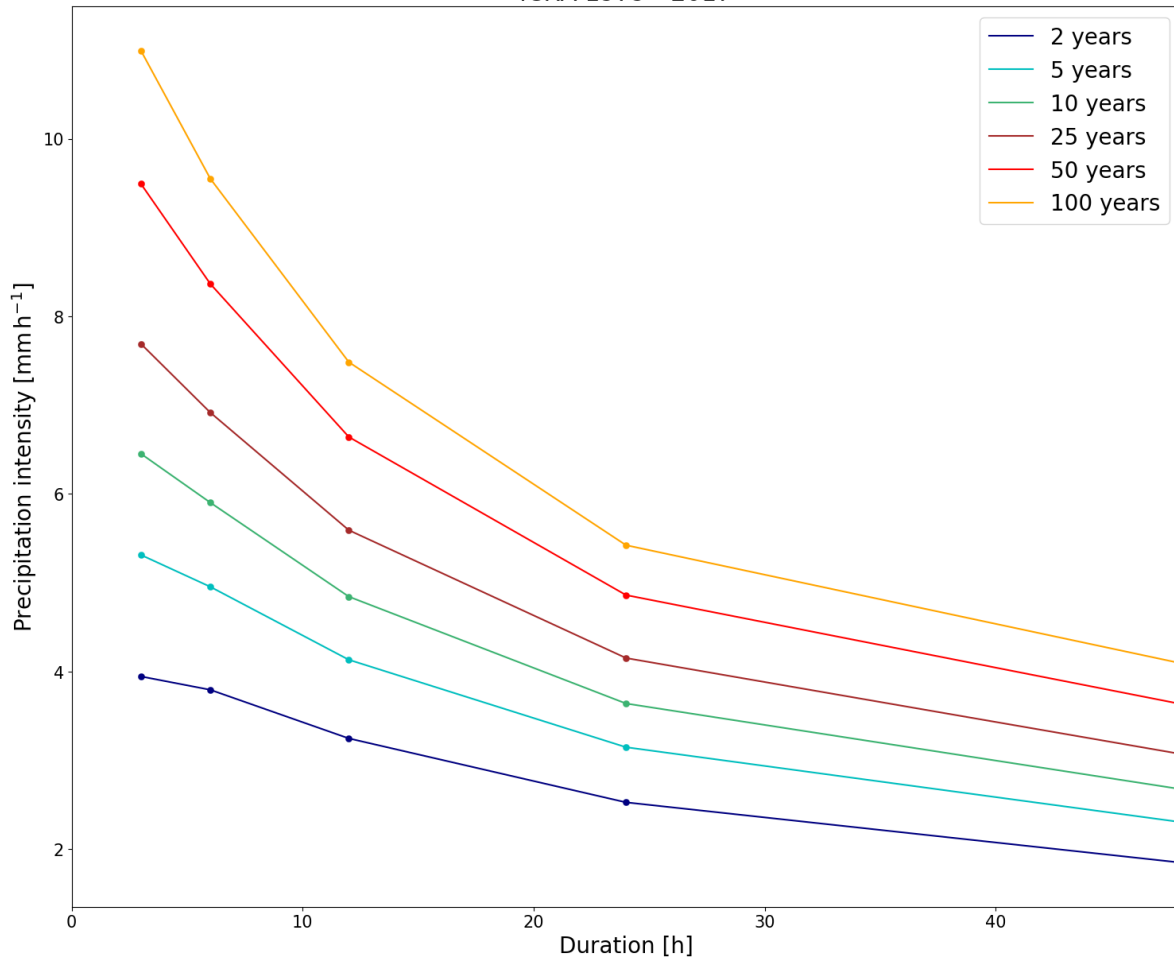


Figure III.15 – IDF curves for station Höfn í Hornafirði from entire ICRA. Solid points give return levels for 3-, 6-, 12-, 24-, 48-hour duration with a 2-, 5-, 10-, 25-, 50- and 100-year return period. Each coloured line corresponds to a different return period as stated by the legend.

Table III.15 – Return levels (mm) for various durations and return periods based on the entire ICRA for station Höfn í Hornafirði. Values are given for 3-, 6-, 12-, 24-, 48-hour duration with a 2-, 5-, 10-, 25-, 50- and 100-year return period.

	2 years	5 years	10 years	25 years	50 years	100 years
3 hours	12	16	19	23	28	33
6 hours	23	30	35	42	50	57
12 hours	39	50	58	67	80	90
24 hours	61	76	87	99	117	130
48 hours	89	111	128	147	174	196

IDF CURVES: Hvanneyri

ICRA 1979 - 2017

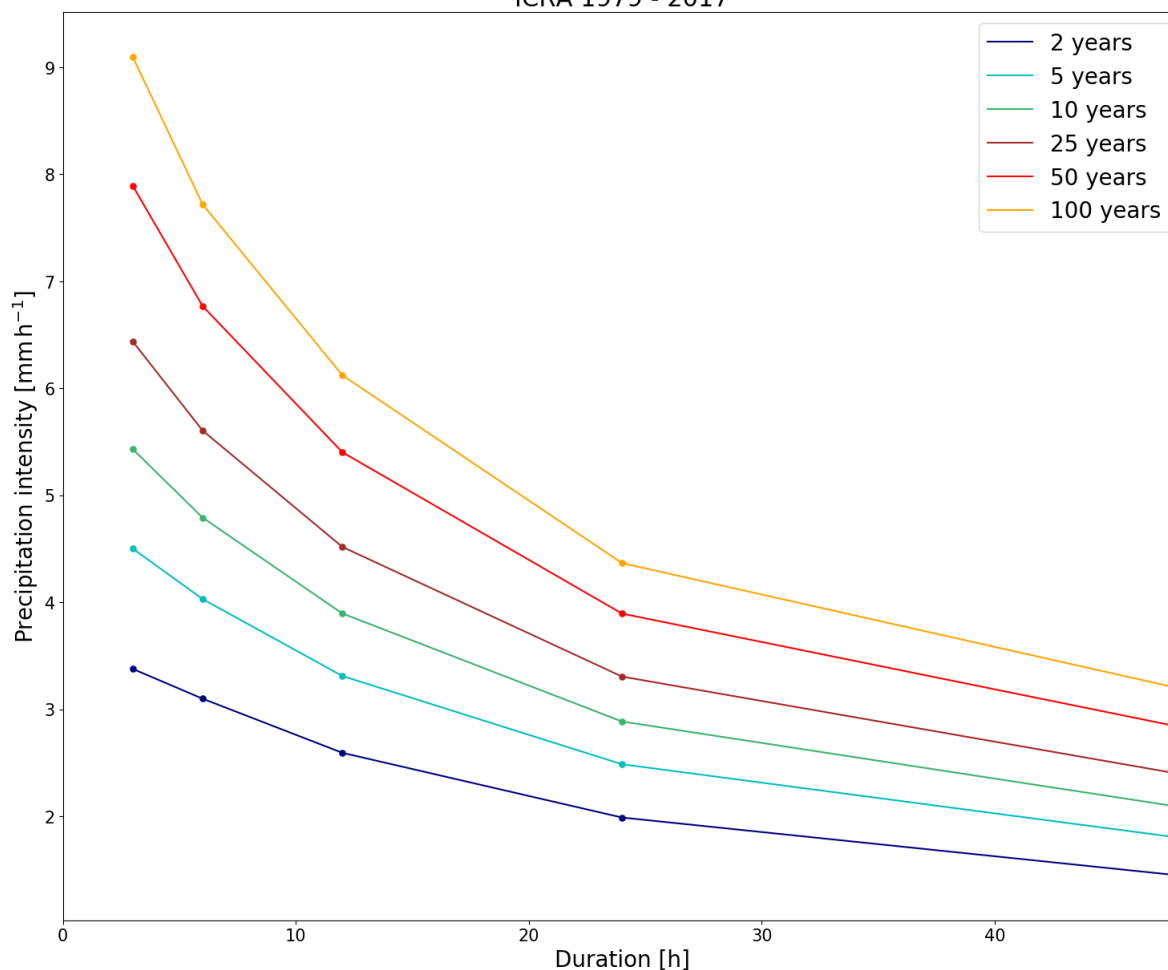


Figure III.16 – IDF curves for station Hvanneyri from entire ICRA. Solid points give return levels for 3-, 6-, 12-, 24-, 48-hour duration with a 2-, 5-, 10-, 25-, 50- and 100-year return period. Each coloured line corresponds to a different return period as stated by the legend.

Table III.16 – Return levels (mm) for various durations and return periods based on the entire ICRA for station Hvanneyri. Values are given for 3-, 6-, 12-, 24-, 48-hour duration with a 2-, 5-, 10-, 25-, 50- and 100-year return period.

	2 years	5 years	10 years	25 years	50 years	100 years
3 hours	10	14	16	19	24	27
6 hours	19	24	29	34	41	46
12 hours	31	40	47	54	65	73
24 hours	48	60	69	79	93	105
48 hours	69	86	100	115	136	153

IDF CURVES: Hveravellir

ICRA 1979 - 2017

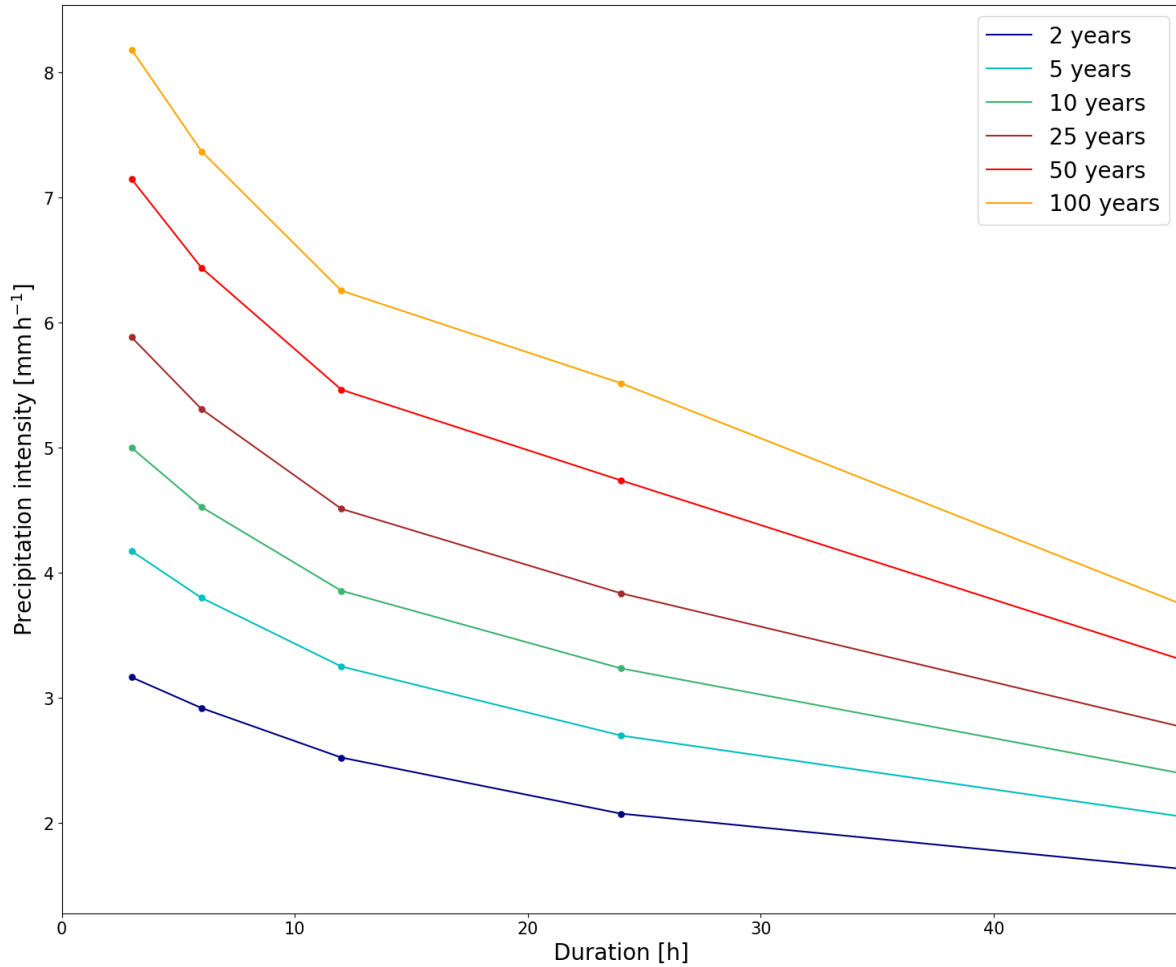


Figure III.17 – IDF curves for station Hveravellir from entire ICRA. Solid points give return levels for 3-, 6-, 12-, 24-, 48-hour duration with a 2-, 5-, 10-, 25-, 50- and 100-year return period. Each coloured line corresponds to a different return period as stated by the legend.

Table III.17 – Return levels (mm) for various durations and return periods based on the entire ICRA for station Hveravellir. Values are given for 3-, 6-, 12-, 24-, 48-hour duration with a 2-, 5-, 10-, 25-, 50- and 100-year return period.

	2 years	5 years	10 years	25 years	50 years	100 years
3 hours	9	13	15	18	21	25
6 hours	18	23	27	32	39	44
12 hours	30	39	46	54	66	75
24 hours	50	65	78	92	114	132
48 hours	78	99	115	133	159	180

IDF CURVES: Ísafjörður

ICRA 1979 - 2017

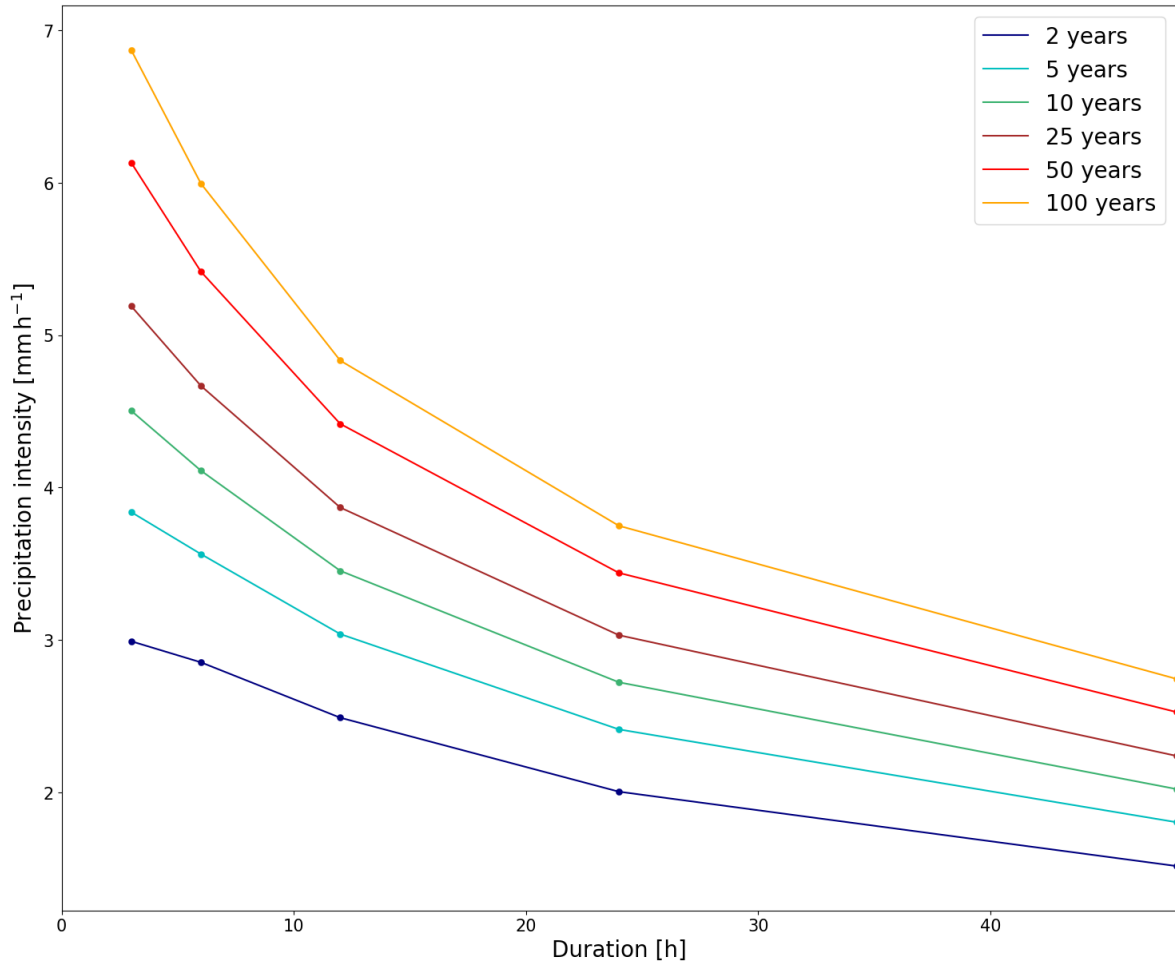


Figure III.18 – IDF curves for station Ísafjörður from entire ICRA. Solid points give return levels for 3-, 6-, 12-, 24-, 48-hour duration with a 2-, 5-, 10-, 25-, 50- and 100-year return period. Each coloured line corresponds to a different return period as stated by the legend.

Table III.18 – Return levels (mm) for various durations and return periods based on the entire ICRA for station Ísafjörður. Values are given for 3-, 6-, 12-, 24-, 48-hour duration with a 2-, 5-, 10-, 25-, 50- and 100-year return period.

	2 years	5 years	10 years	25 years	50 years	100 years
3 hours	9	12	14	16	18	21
6 hours	17	21	25	28	33	36
12 hours	30	36	41	46	53	58
24 hours	48	58	65	73	83	90
48 hours	73	87	97	108	121	134

IDF CURVES: Kálfhóll

ICRA 1979 - 2017

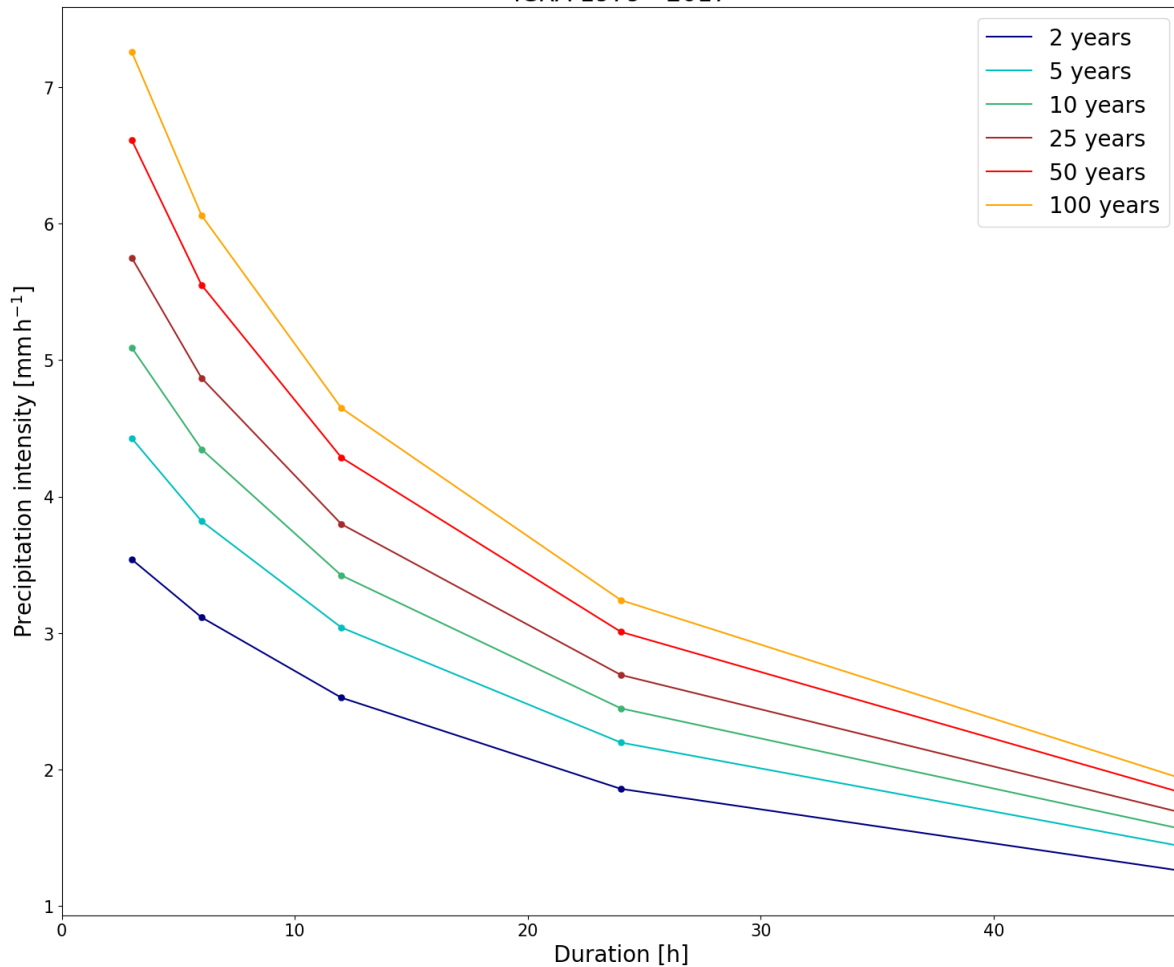


Figure III.19 – IDF curves for station Kálfhóll from entire ICRA. Solid points give return levels for 3-, 6-, 12-, 24-, 48-hour duration with a 2-, 5-, 10-, 25-, 50- and 100-year return period. Each coloured line corresponds to a different return period as stated by the legend.

Table III.19 – Return levels (mm) for various durations and return periods based on the entire ICRA for station Kálfhóll. Values are given for 3-, 6-, 12-, 24-, 48-hour duration with a 2-, 5-, 10-, 25-, 50- and 100-year return period.

	2 years	5 years	10 years	25 years	50 years	100 years
3 hours	11	13	15	17	20	22
6 hours	19	23	26	29	33	36
12 hours	30	36	41	46	51	56
24 hours	45	53	59	65	72	78
48 hours	60	69	75	81	88	93

IDF CURVES: Kárahnjúkar

ICRA 1979 - 2017

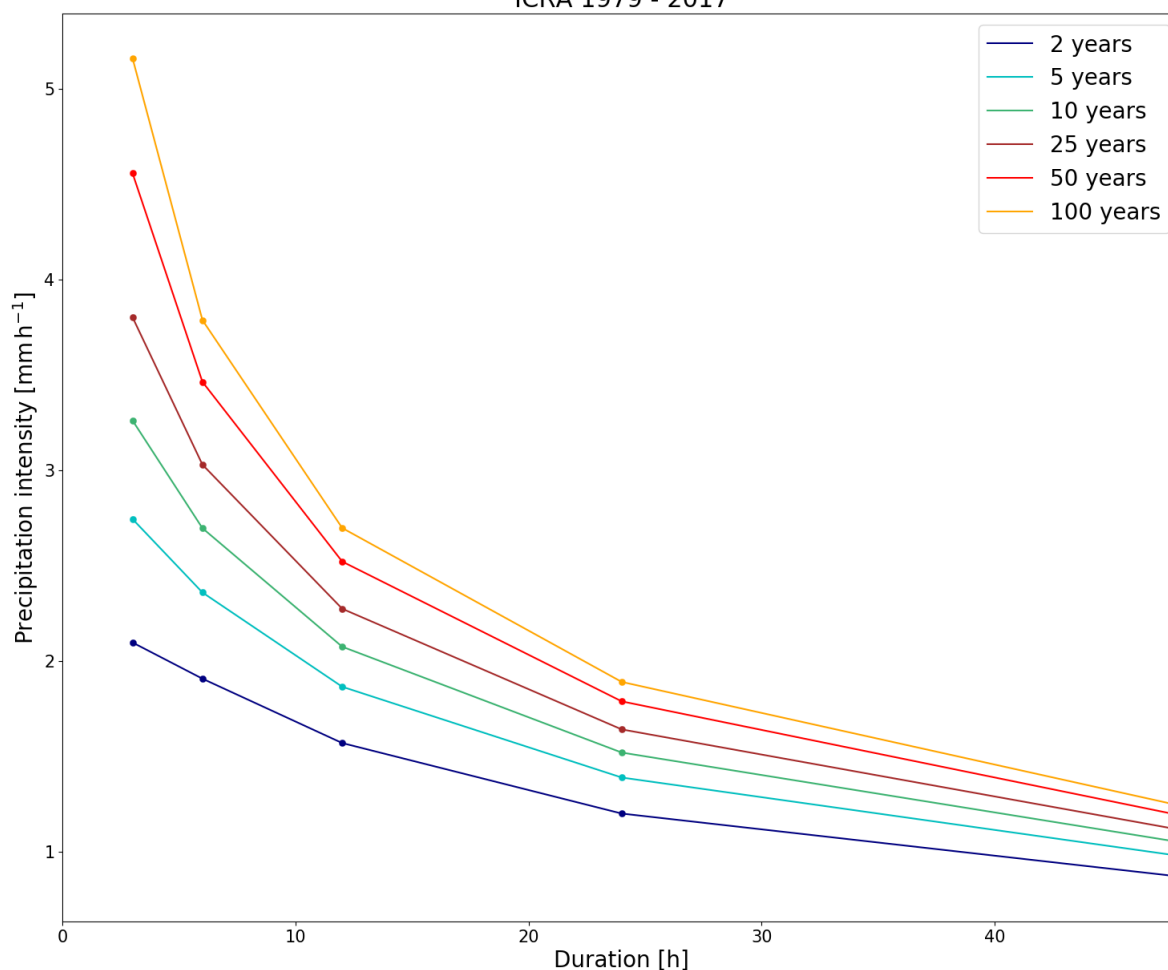


Figure III.20 – IDF curves for station Kárahnjúkar from entire ICRA. Solid points give return levels for 3-, 6-, 12-, 24-, 48-hour duration with a 2-, 5-, 10-, 25-, 50- and 100-year return period. Each coloured line corresponds to a different return period as stated by the legend.

Table III.20 – Return levels (mm) for various durations and return periods based on the entire ICRA for station Kárahnjúkar. Values are given for 3-, 6-, 12-, 24-, 48-hour duration with a 2-, 5-, 10-, 25-, 50- and 100-year return period.

	2 years	5 years	10 years	25 years	50 years	100 years
3 hours	6	8	10	11	14	15
6 hours	11	14	16	18	21	23
12 hours	19	22	25	27	30	32
24 hours	29	33	36	39	43	45
48 hours	42	47	50	53	57	59

IDF CURVES: Kirkjubæjarklaustur

ICRA 1979 - 2017

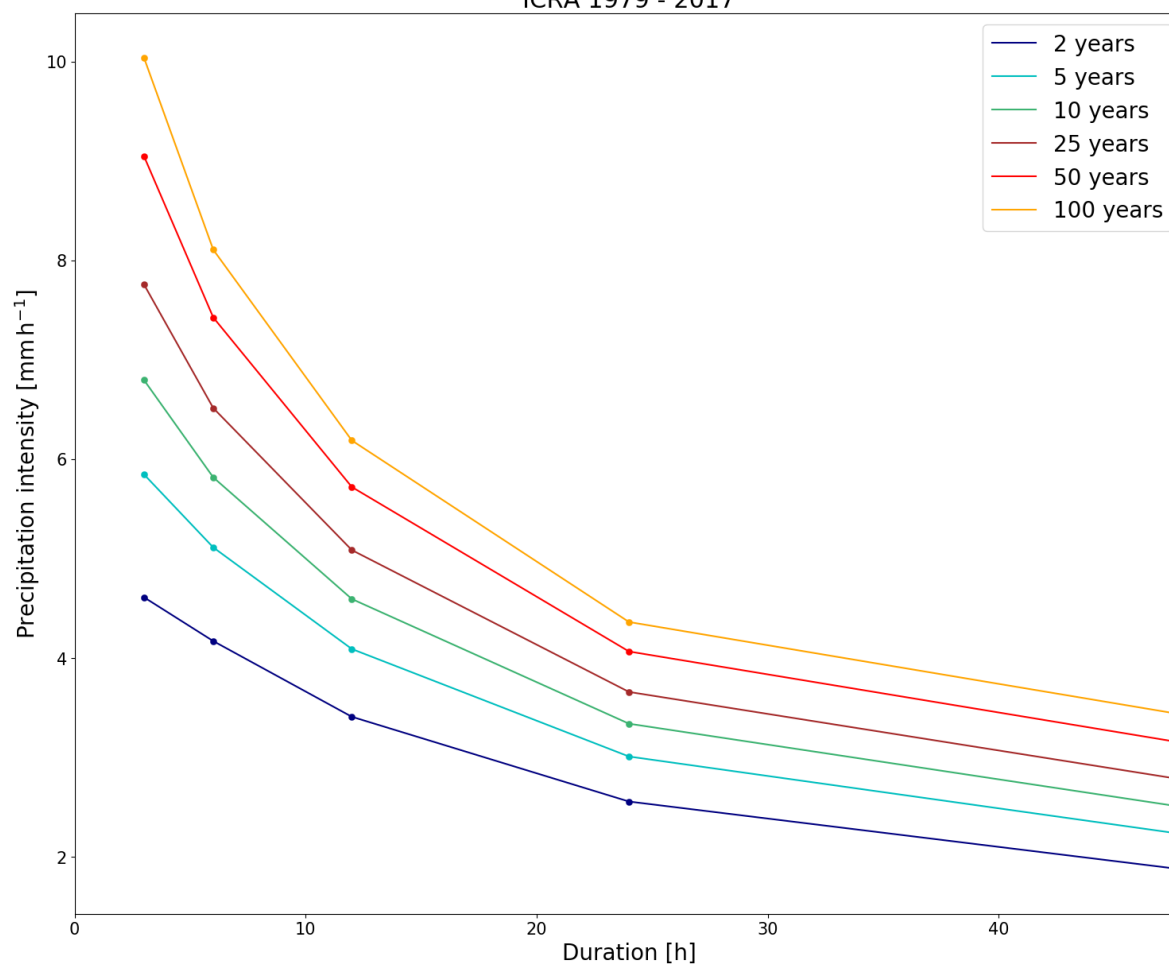


Figure III.21 – IDF curves for station Kirkjubæjarklaustur from entire ICRA. Solid points give return levels for 3-, 6-, 12-, 24-, 48-hour duration with a 2-, 5-, 10-, 25-, 50- and 100-year return period. Each coloured line corresponds to a different return period as stated by the legend.

Table III.21 – Return levels (mm) for various durations and return periods based on the entire ICRA for station Kirkjubæjarklaustur. Values are given for 3-, 6-, 12-, 24-, 48-hour duration with a 2-, 5-, 10-, 25-, 50- and 100-year return period.

	2 years	5 years	10 years	25 years	50 years	100 years
3 hours	14	18	20	23	27	30
6 hours	25	31	35	39	45	49
12 hours	41	49	55	61	69	74
24 hours	61	72	80	88	98	105
48 hours	90	107	120	133	151	164

IDF CURVES: Korpa

ICRA 1979 - 2017

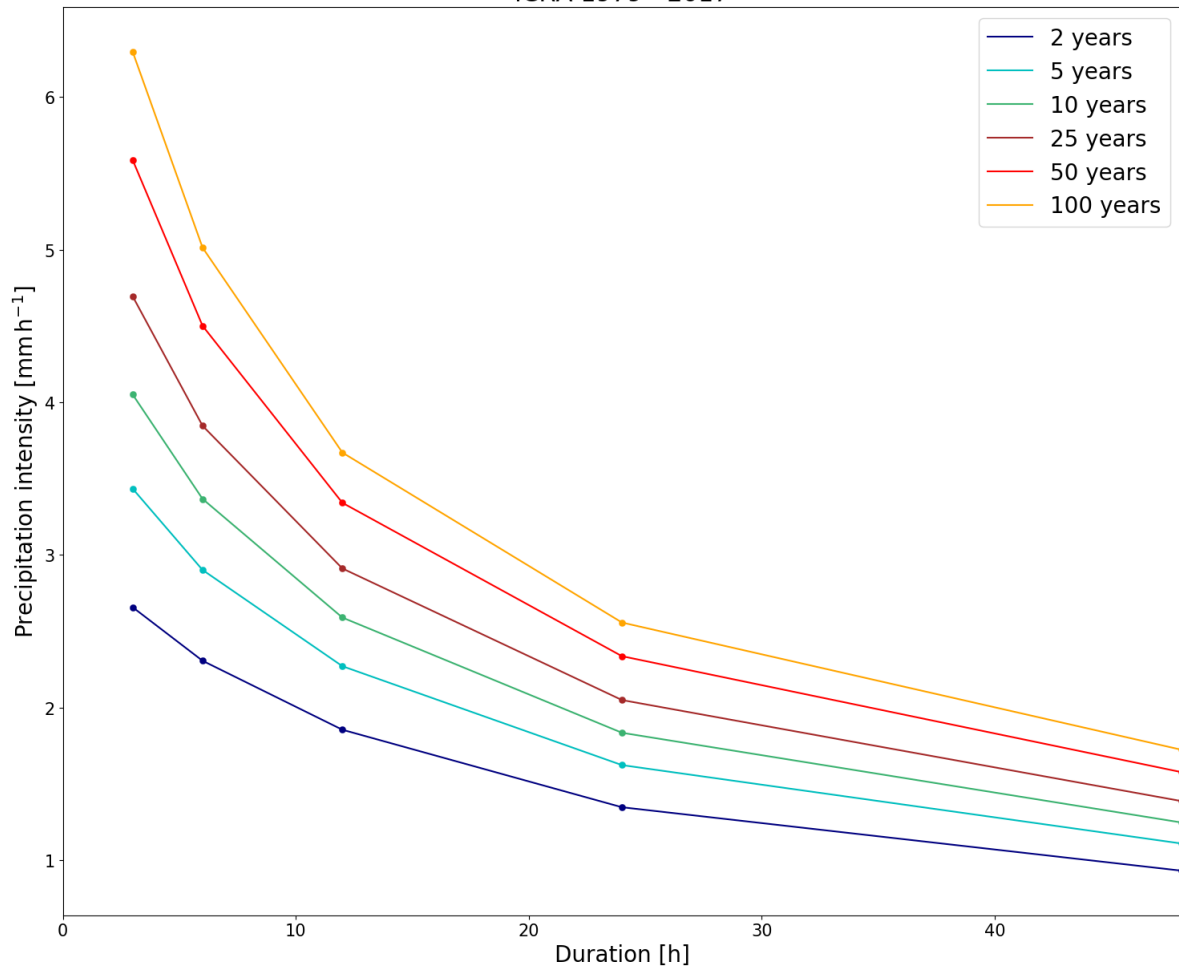


Figure III.22 – IDF curves for station Korpa from entire ICRA. Solid points give return levels for 3-, 6-, 12-, 24-, 48-hour duration with a 2-, 5-, 10-, 25-, 50- and 100-year return period. Each coloured line corresponds to a different return period as stated by the legend.

Table III.22 – Return levels (mm) for various durations and return periods based on the entire ICRA for station Korpa. Values are given for 3-, 6-, 12-, 24-, 48-hour duration with a 2-, 5-, 10-, 25-, 50- and 100-year return period.

	2 years	5 years	10 years	25 years	50 years	100 years
3 hours	8	10	12	14	17	19
6 hours	14	17	20	23	27	30
12 hours	22	27	31	25	40	44
24 hours	32	39	44	49	56	61
48 hours	45	53	60	67	76	83

IDF CURVES: Kvísker

ICRA 1979 - 2017

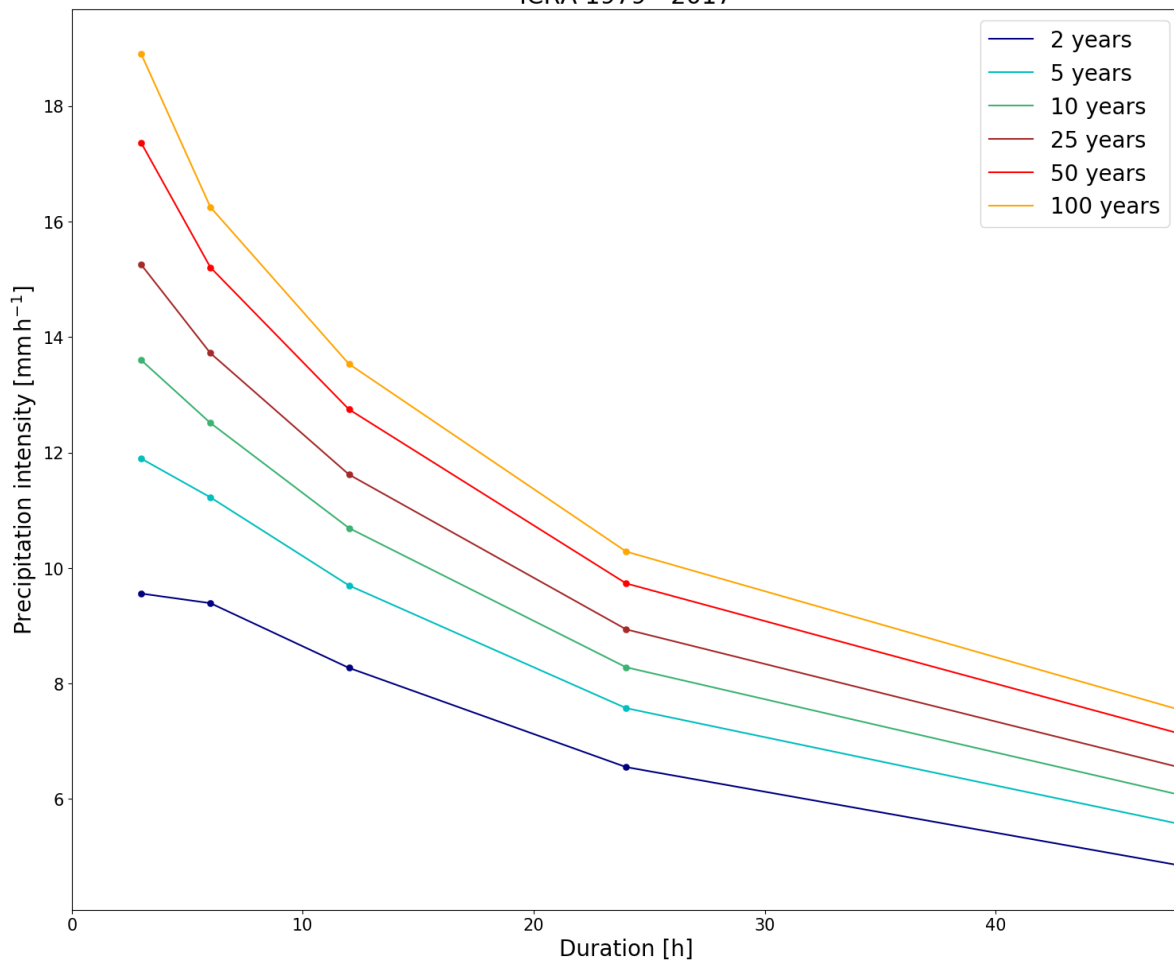


Figure III.23 – IDF curves for station Kvísker from entire ICRA. Solid points give return levels for 3-, 6-, 12-, 24-, 48-hour duration with a 2-, 5-, 10-, 25-, 50- and 100-year return period. Each coloured line corresponds to a different return period as stated by the legend.

Table III.23 – Return levels (mm) for various durations and return periods based on the entire ICRA for station Kvísker. Values are given for 3-, 6-, 12-, 24-, 48-hour duration with a 2-, 5-, 10-, 25-, 50- and 100-year return period.

	2 years	5 years	10 years	25 years	50 years	100 years
3 hours	29	36	41	46	52	57
6 hours	56	67	75	82	91	97
12 hours	99	116	128	139	153	162
24 hours	157	182	199	215	234	247
48 hours	233	267	291	314	342	362

IDF CURVES: Laufbali

ICRA 1979 - 2017

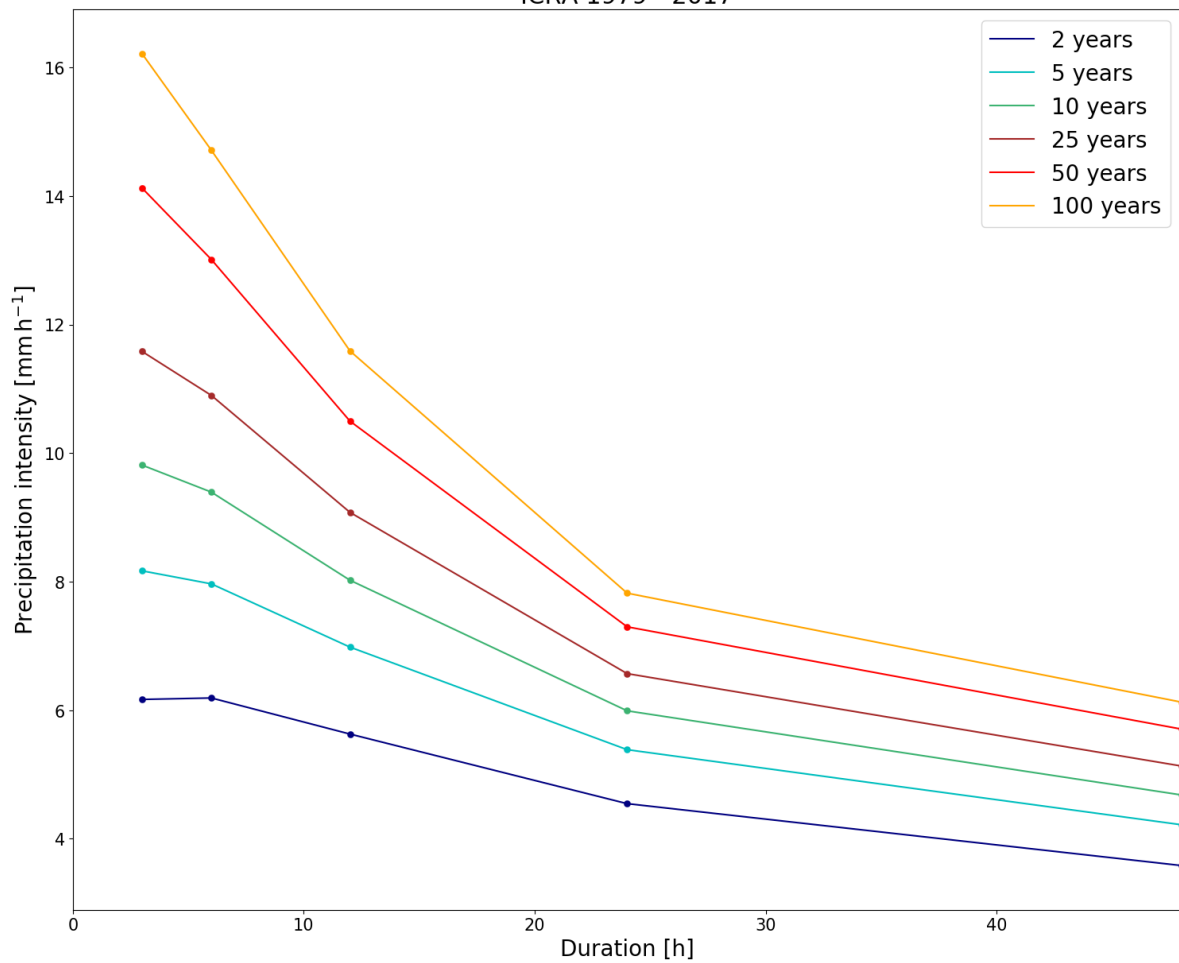


Figure III.24 – IDF curves for station Laufbali from entire ICRA. Solid points give return levels for 3-, 6-, 12-, 24-, 48-hour duration with a 2-, 5-, 10-, 25-, 50- and 100-year return period. Each coloured line corresponds to a different return period as stated by the legend.

Table III.24 – Return levels (mm) for various durations and return periods based on the entire ICRA for station Laufbali. Values are given for 3-, 6-, 12-, 24-, 48-hour duration with a 2-, 5-, 10-, 25-, 50- and 100-year return period.

	2 years	5 years	10 years	25 years	50 years	100 years
3 hours	19	25	29	35	42	49
6 hours	37	48	56	65	78	88
12 hours	68	84	96	109	126	139
24 hours	109	129	144	158	175	188
48 hours	172	202	225	246	274	294

IDF CURVES: Möðruvellir

ICRA 1979 - 2017

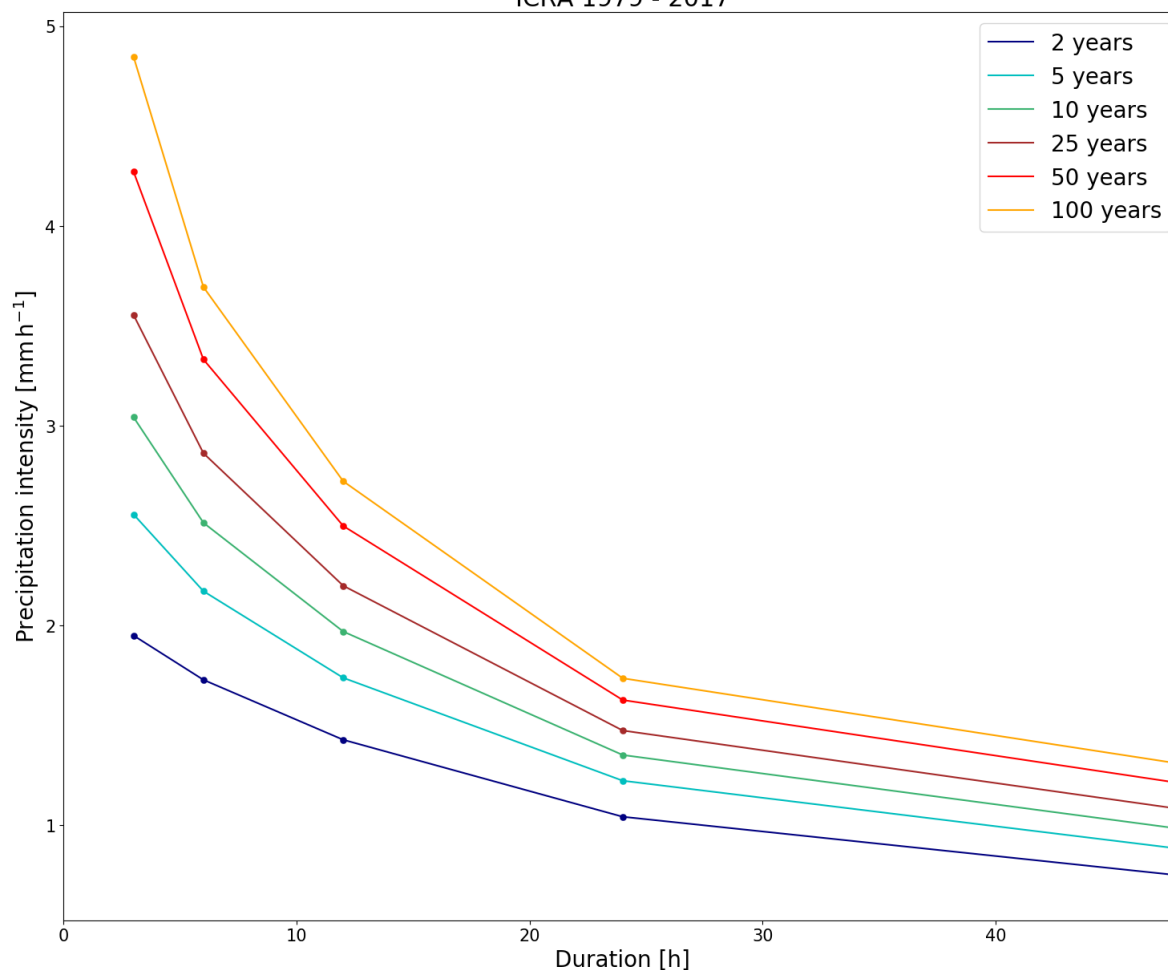


Figure III.25 – IDF curves for station Möðruvellir from entire ICRA. Solid points give return levels for 3-, 6-, 12-, 24-, 48-hour duration with a 2-, 5-, 10-, 25-, 50- and 100-year return period. Each coloured line corresponds to a different return period as stated by the legend.

Table III.25 – Return levels (mm) for various durations and return periods based on the entire ICRA for station Möðruvellir. Values are given for 3-, 6-, 12-, 24-, 48-hour duration with a 2-, 5-, 10-, 25-, 50- and 100-year return period.

	2 years	5 years	10 years	25 years	50 years	100 years
3 hours	6	8	9	11	13	15
6 hours	10	13	15	17	20	22
12 hours	17	21	24	26	30	33
24 hours	25	29	32	35	39	42
48 hours	36	42	47	52	58	63

IDF CURVES: Nautabú

ICRA 1979 - 2017

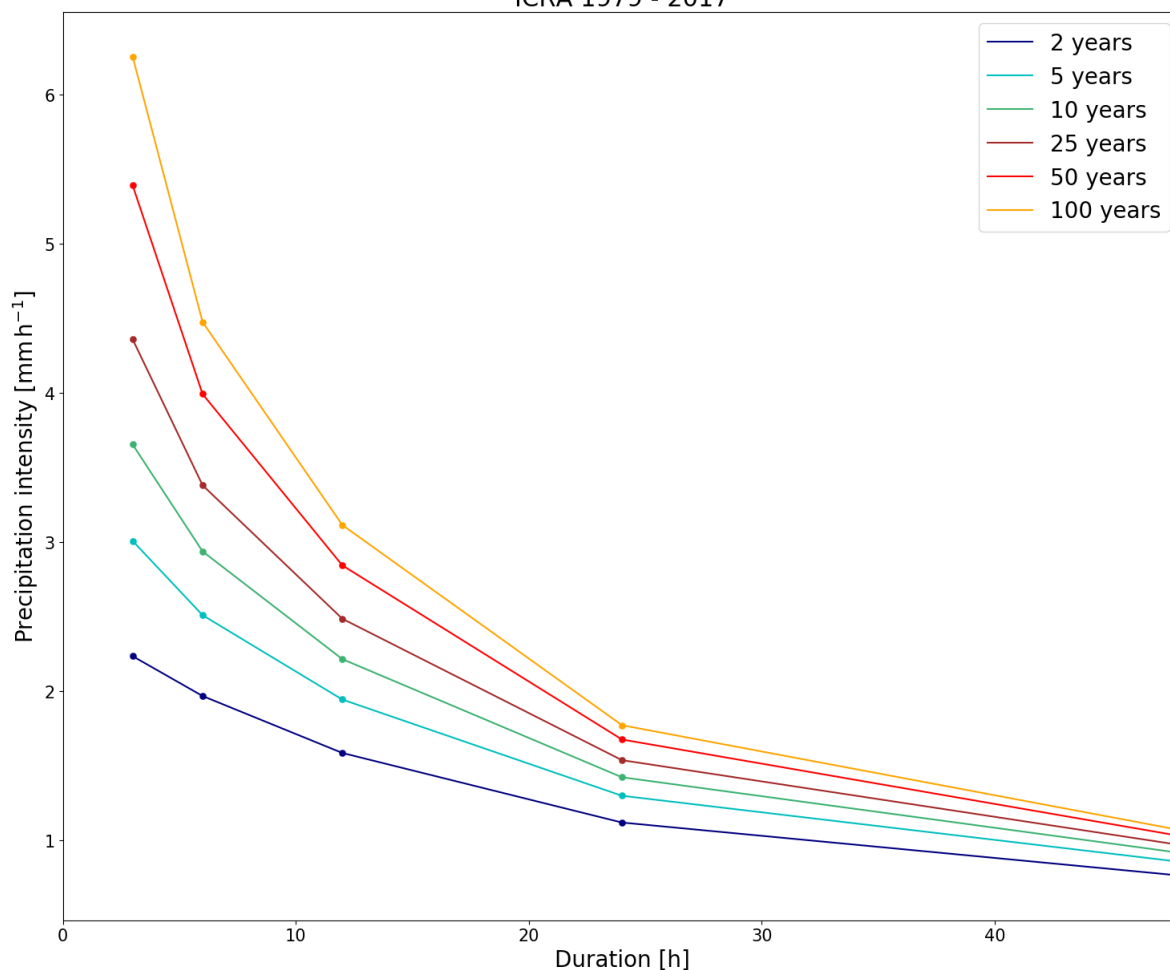


Figure III.26 – IDF curves for station Nautabú from entire ICRA. Solid points give return levels for 3-, 6-, 12-, 24-, 48-hour duration with a 2-, 5-, 10-, 25-, 50- and 100-year return period. Each coloured line corresponds to a different return period as stated by the legend.

Table III.26 – Return levels (mm) for various durations and return periods based on the entire ICRA for station Nautabú. Values are given for 3-, 6-, 12-, 24-, 48-hour duration with a 2-, 5-, 10-, 25-, 50- and 100-year return period.

	2 years	5 years	10 years	25 years	50 years	100 years
3 hours	7	9	11	13	16	19
6 hours	12	15	18	20	24	27
12 hours	19	23	27	30	34	37
24 hours	27	31	34	37	40	43
48 hours	37	41	44	46	49	51

IDF CURVES: Neskaupstaður

ICRA 1979 - 2017

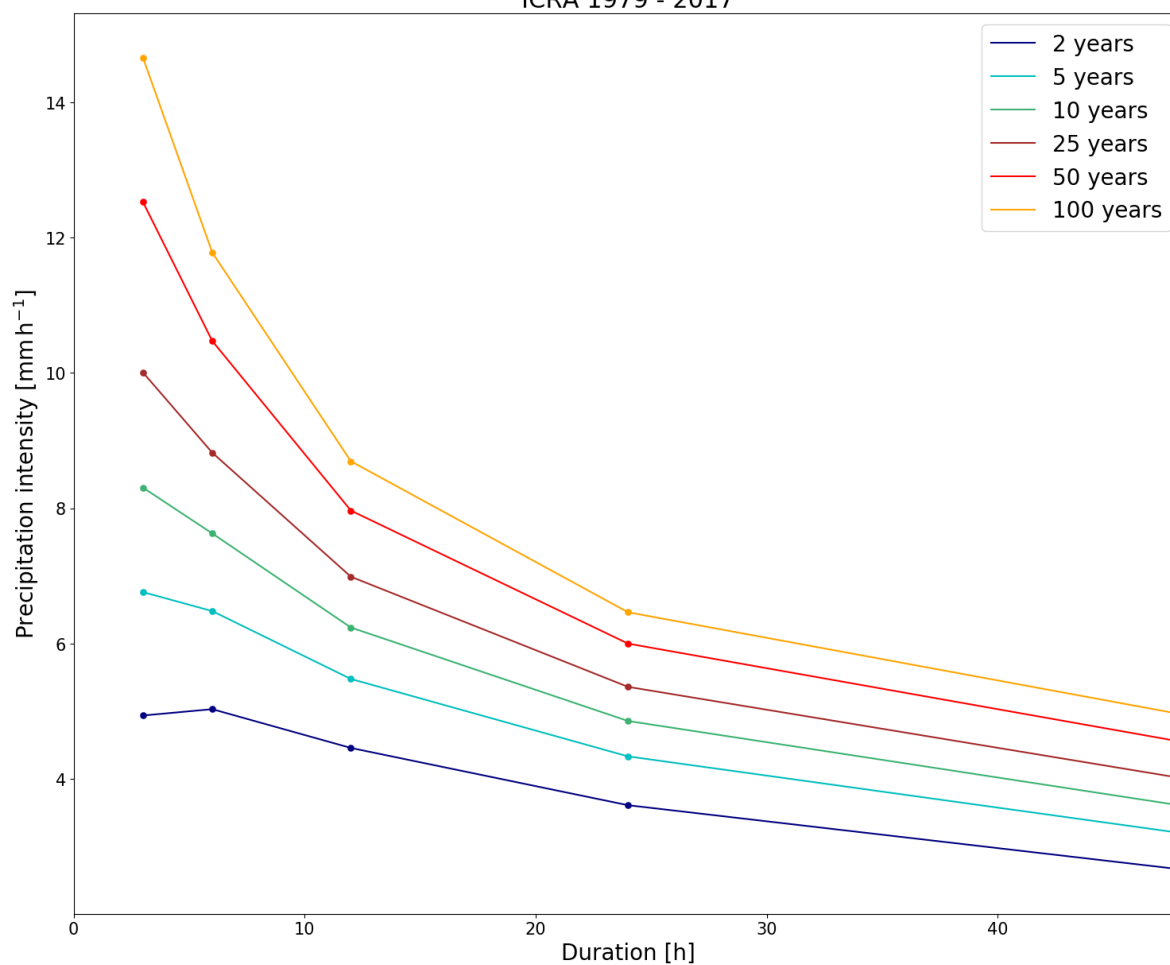


Figure III.27 – IDF curves for station Neskaupstaður from entire ICRA. Solid points give return levels for 3-, 6-, 12-, 24-, 48-hour duration with a 2-, 5-, 10-, 25-, 50- and 100-year return period. Each coloured line corresponds to a different return period as stated by the legend.

Table III.27 – Return levels (mm) for various durations and return periods based on the entire ICRA for station Neskaupstaður. Values are given for 3-, 6-, 12-, 24-, 48-hour duration with a 2-, 5-, 10-, 25-, 50- and 100-year return period.

	2 years	5 years	10 years	25 years	50 years	100 years
3 hours	15	20	25	30	38	44
6 hours	30	39	46	53	63	71
12 hours	53	66	75	84	96	104
24 hours	87	104	117	129	144	155
48 hours	128	153	173	192	218	238

IDF CURVES: Ólafsfjörður

ICRA 1979 - 2017

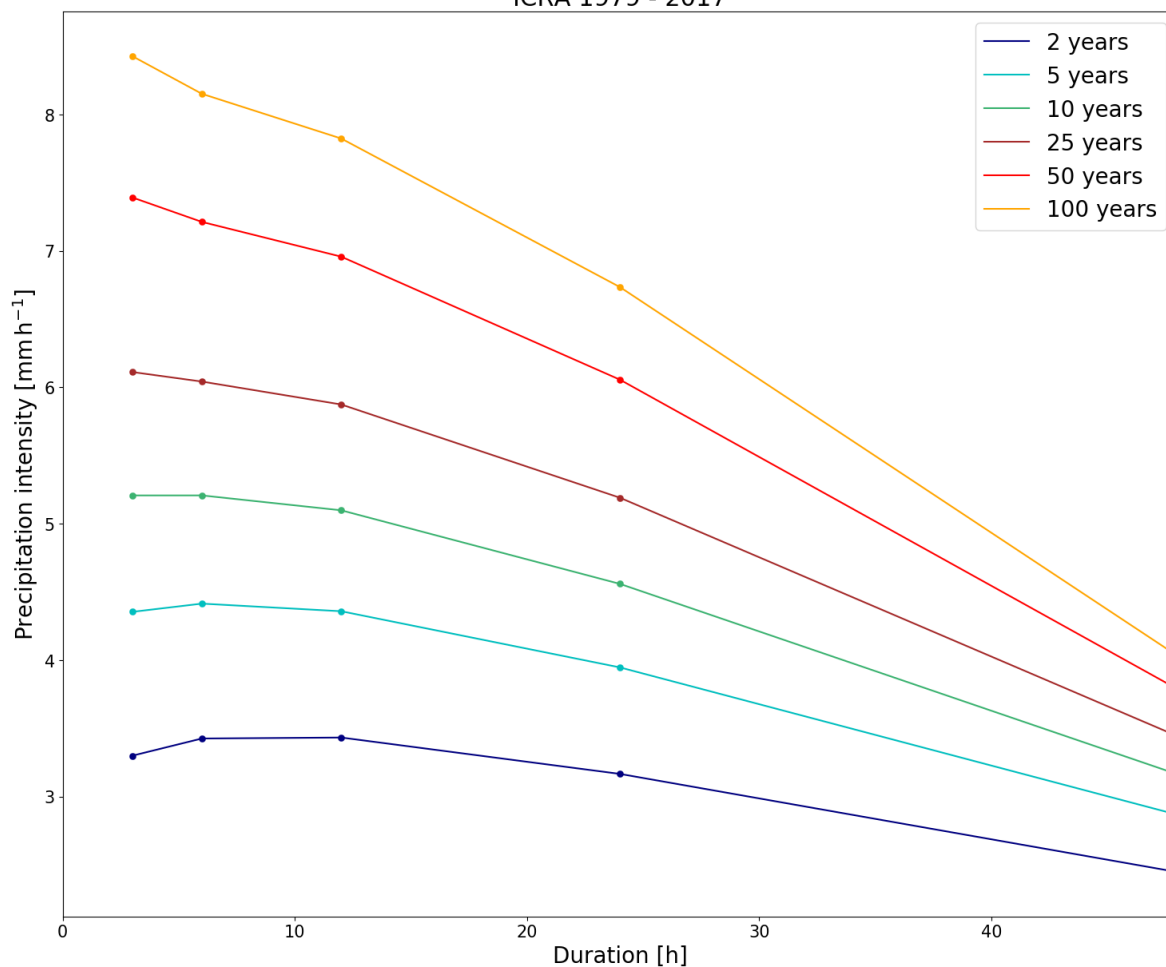


Figure III.28 – IDF curves for station Ólafsfjörður from entire ICRA. Solid points give return levels for 3-, 6-, 12-, 24-, 48-hour duration with a 2-, 5-, 10-, 25-, 50- and 100-year return period. Each coloured line corresponds to a different return period as stated by the legend.

Table III.28 – Return levels (mm) for various durations and return periods based on the entire ICRA for station Ólafsfjörður. Values are given for 3-, 6-, 12-, 24-, 48-hour duration with a 2-, 5-, 10-, 25-, 50- and 100-year return period.

	2 years	5 years	10 years	25 years	50 years	100 years
3 hours	10	13	16	18	22	25
6 hours	21	26	31	36	43	49
12 hours	41	52	61	70	83	94
24 hours	76	95	109	125	145	162
48 hours	117	138	152	165	182	194

IDF CURVES: Ólafsvík

ICRA 1979 - 2017

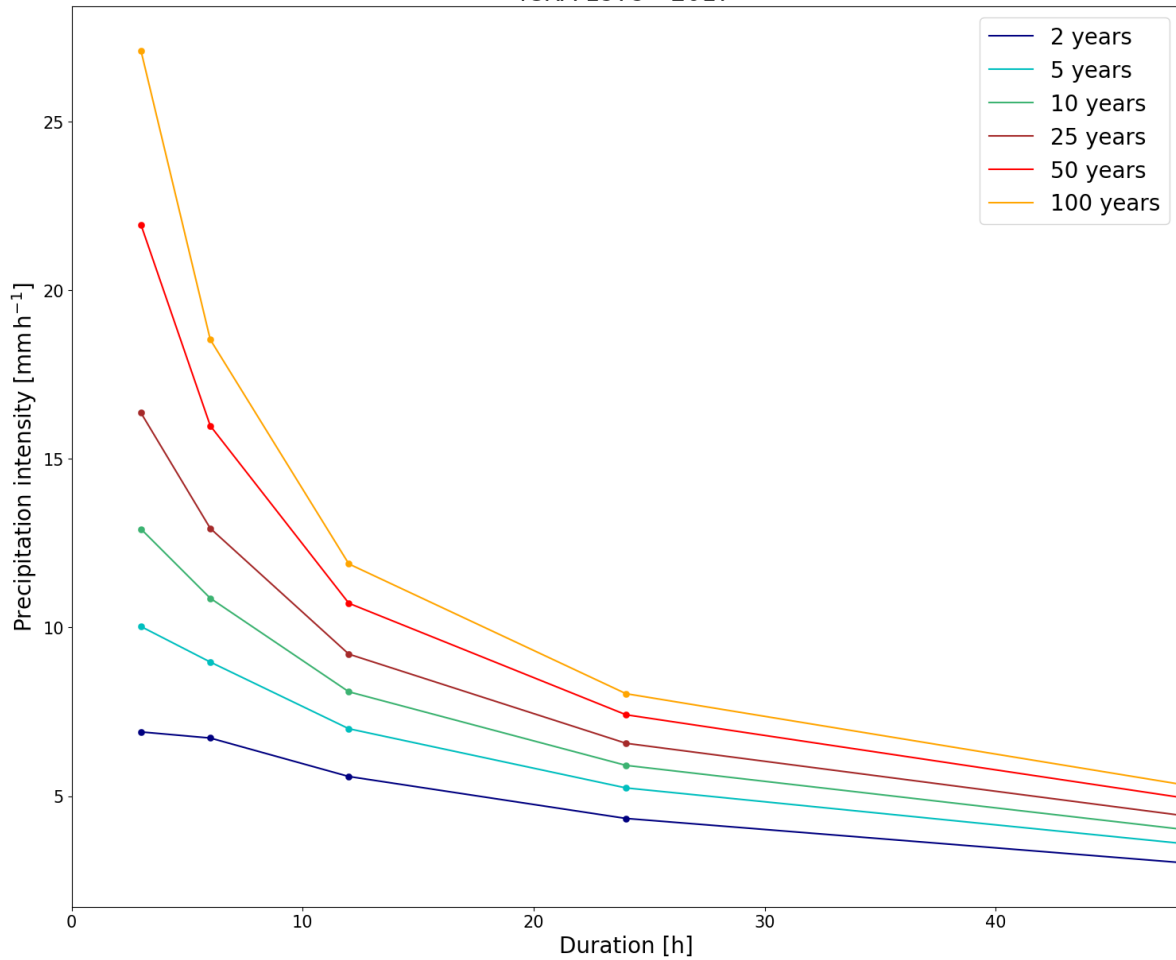


Figure III.29 – IDF curves for station Ólafsvík from entire ICRA. Solid points give return levels for 3-, 6-, 12-, 24-, 48-hour duration with a 2-, 5-, 10-, 25-, 50- and 100-year return period. Each coloured line corresponds to a different return period as stated by the legend.

Table III.29 – Return levels (mm) for various durations and return periods based on the entire ICRA for station Ólafsvík. Values are given for 3-, 6-, 12-, 24-, 48-hour duration with a 2-, 5-, 10-, 25-, 50- and 100-year return period.

	2 years	5 years	10 years	25 years	50 years	100 years
3 hours	21	30	39	49	66	81
6 hours	40	54	65	78	96	111
12 hours	67	84	97	111	129	143
24 hours	104	126	142	158	178	193
48 hours	146	173	193	213	239	257

IDF CURVES: Ölkelduháls

ICRA 1979 - 2017

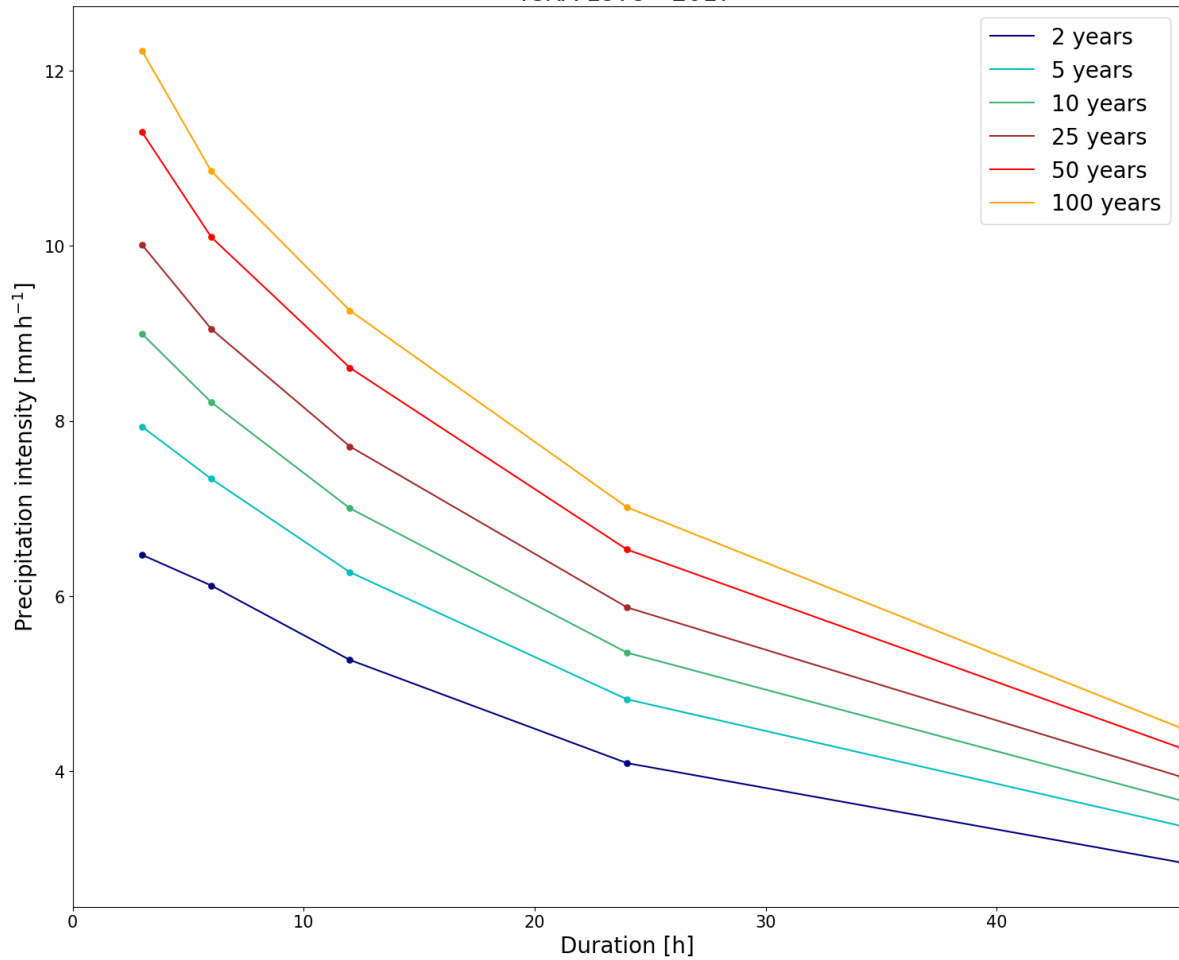


Figure III.30 – IDF curves for station Ölkelduháls from entire ICRA. Solid points give return levels for 3-, 6-, 12-, 24-, 48-hour duration with a 2-, 5-, 10-, 25-, 50- and 100-year return period. Each coloured line corresponds to a different return period as stated by the legend.

Table III.30 – Return levels (mm) for various durations and return periods based on the entire ICRA for station Ölkelduháls. Values are given for 3-, 6-, 12-, 24-, 48-hour duration with a 2-, 5-, 10-, 25-, 50- and 100-year return period.

	2 years	5 years	10 years	25 years	50 years	100 years
3 hours	19	24	27	30	34	37
6 hours	37	44	49	54	61	65
12 hours	63	75	84	93	103	111
24 hours	98	116	128	141	157	168
48 hours	142	162	176	189	206	216

IDF CURVES: Patreksfjörður

ICRA 1979 - 2017

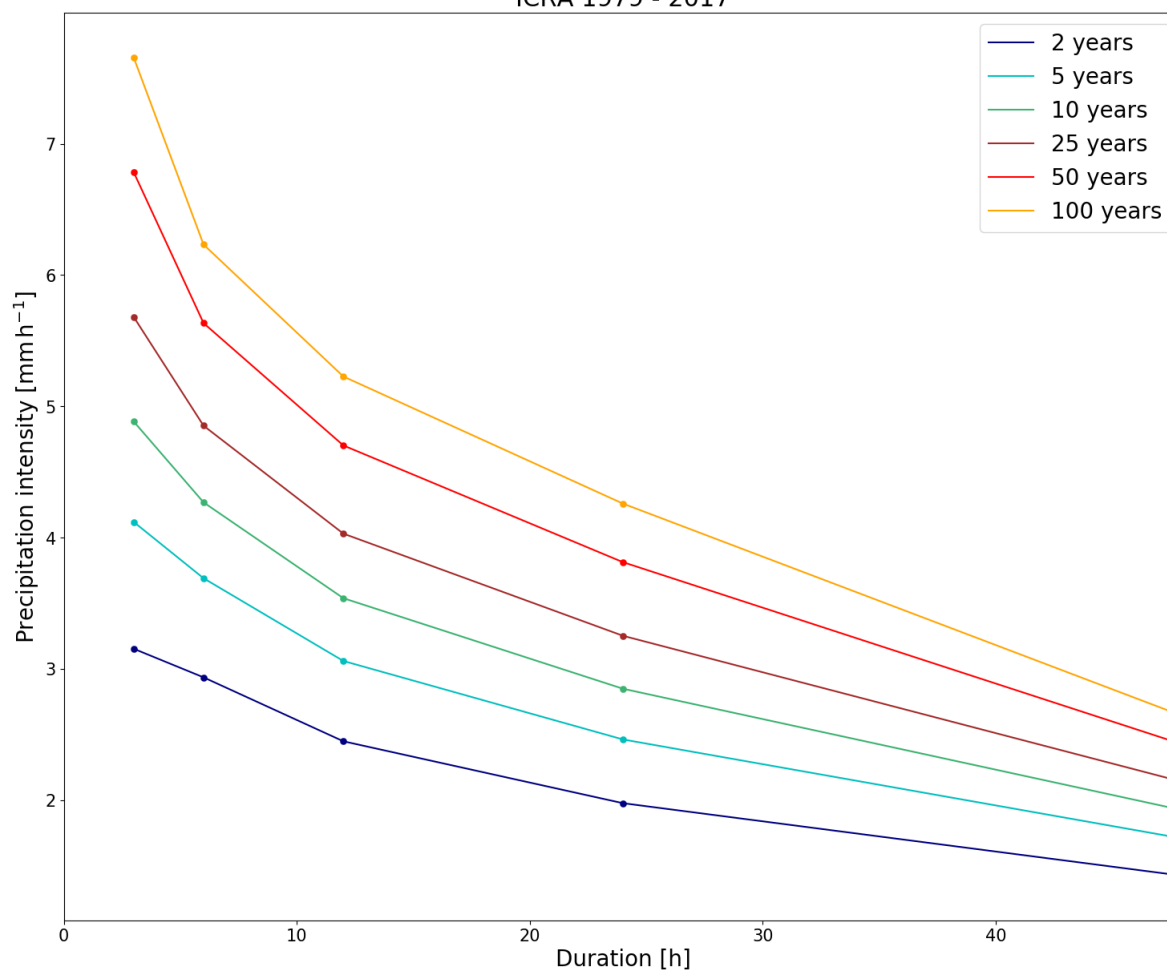


Figure III.31 – IDF curves for station Patreksfjörður from entire ICRA. Solid points give return levels for 3-, 6-, 12-, 24-, 48-hour duration with a 2-, 5-, 10-, 25-, 50- and 100-year return period. Each coloured line corresponds to a different return period as stated by the legend.

Table III.31 – Return levels (mm) for various durations and return periods based on the entire ICRA for station Patreksfjörður. Values are given for 3-, 6-, 12-, 24-, 48-hour duration with a 2-, 5-, 10-, 25-, 50- and 100-year return period.

	2 years	5 years	10 years	25 years	50 years	100 years
3 hours	9	12	15	17	20	23
6 hours	18	22	26	29	24	37
12 hours	29	37	42	48	56	63
24 hours	47	59	68	78	92	102
48 hours	68	82	92	103	117	127

IDF CURVES: Raufarhöfn

ICRA 1979 - 2017

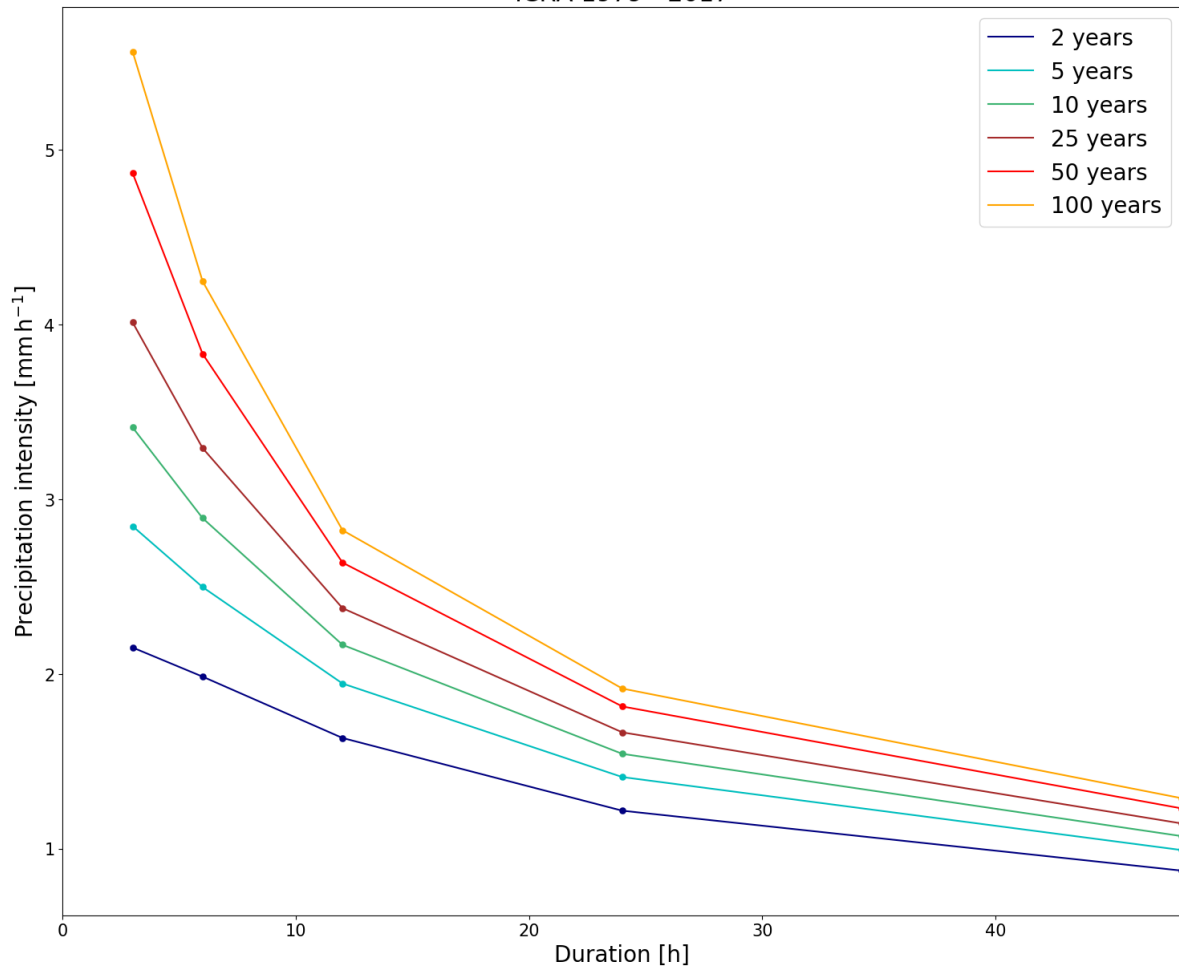


Figure III.32 – IDF curves for station Raufarhöfn from entire ICRA. Solid points give return levels for 3-, 6-, 12-, 24-, 48-hour duration with a 2-, 5-, 10-, 25-, 50- and 100-year return period. Each coloured line corresponds to a different return period as stated by the legend.

Table III.32 – Return levels (mm) for various durations and return periods based on the entire ICRA for station Raufarhöfn. Values are given for 3-, 6-, 12-, 24-, 48-hour duration with a 2-, 5-, 10-, 25-, 50- and 100-year return period.

	2 years	5 years	10 years	25 years	50 years	100 years
3 hours	6	9	10	12	15	17
6 hours	12	15	17	20	23	25
12 hours	20	23	26	29	32	34
24 hours	29	34	37	40	44	46
48 hours	42	48	51	55	59	62

IDF CURVES: Reykjavík

ICRA 1979 - 2017

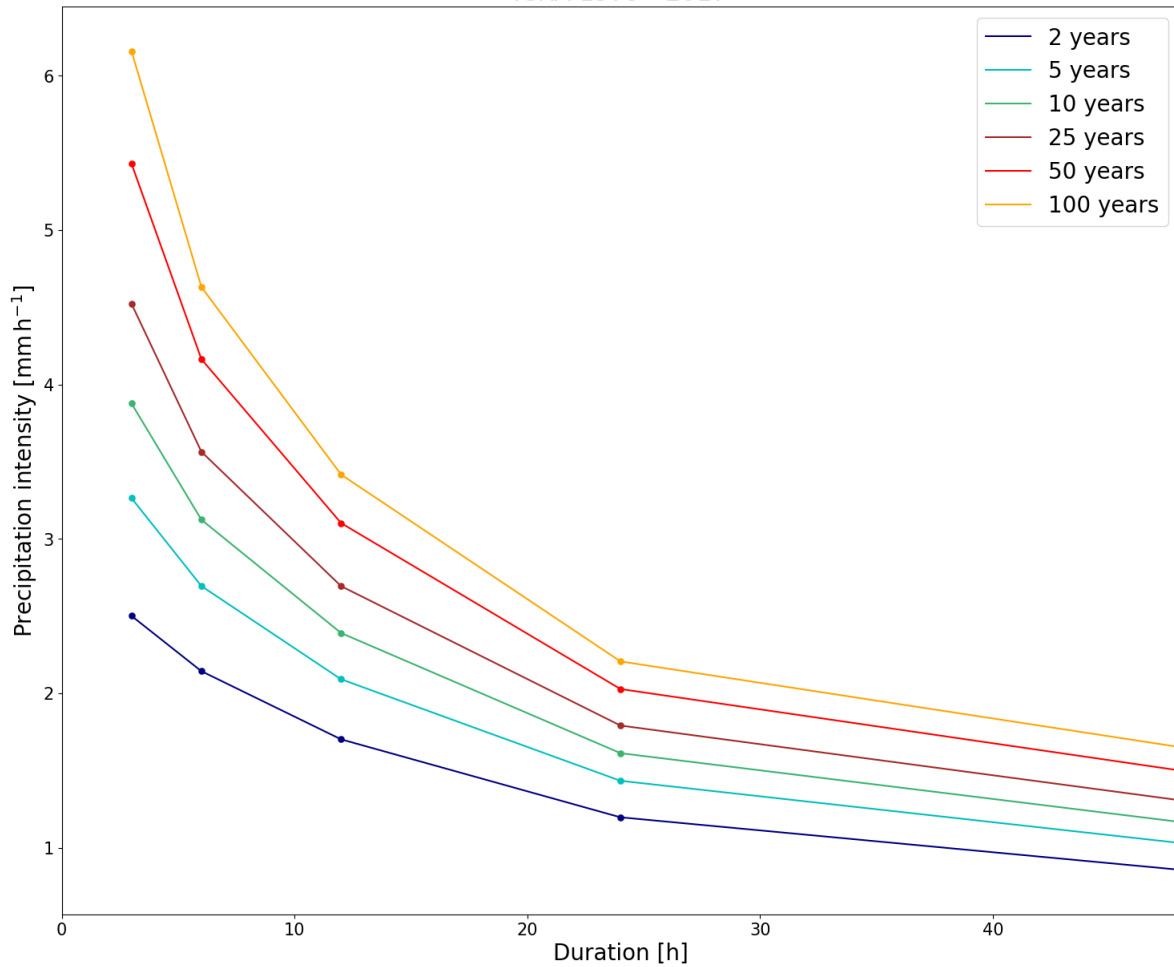


Figure III.33 – IDF curves for station Reykjavík from entire ICRA. Solid points give return levels for 3-, 6-, 12-, 24-, 48-hour duration with a 2-, 5-, 10-, 25-, 50- and 100-year return period. Each coloured line corresponds to a different return period as stated by the legend.

Table III.33 – Return levels (mm) for various durations and return periods based on the entire ICRA for station Reykjavík. Values are given for 3-, 6-, 12-, 24-, 48-hour duration with a 2-, 5-, 10-, 25-, 50- and 100-year return period.

	2 years	5 years	10 years	25 years	50 years	100 years
3 hours	8	10	12	14	16	18
6 hours	13	16	19	21	25	28
12 hours	20	25	29	32	37	41
24 hours	29	34	39	43	49	53
48 hours	41	50	56	63	72	79

IDF CURVES: Sámsstaðir

ICRA 1979 - 2017

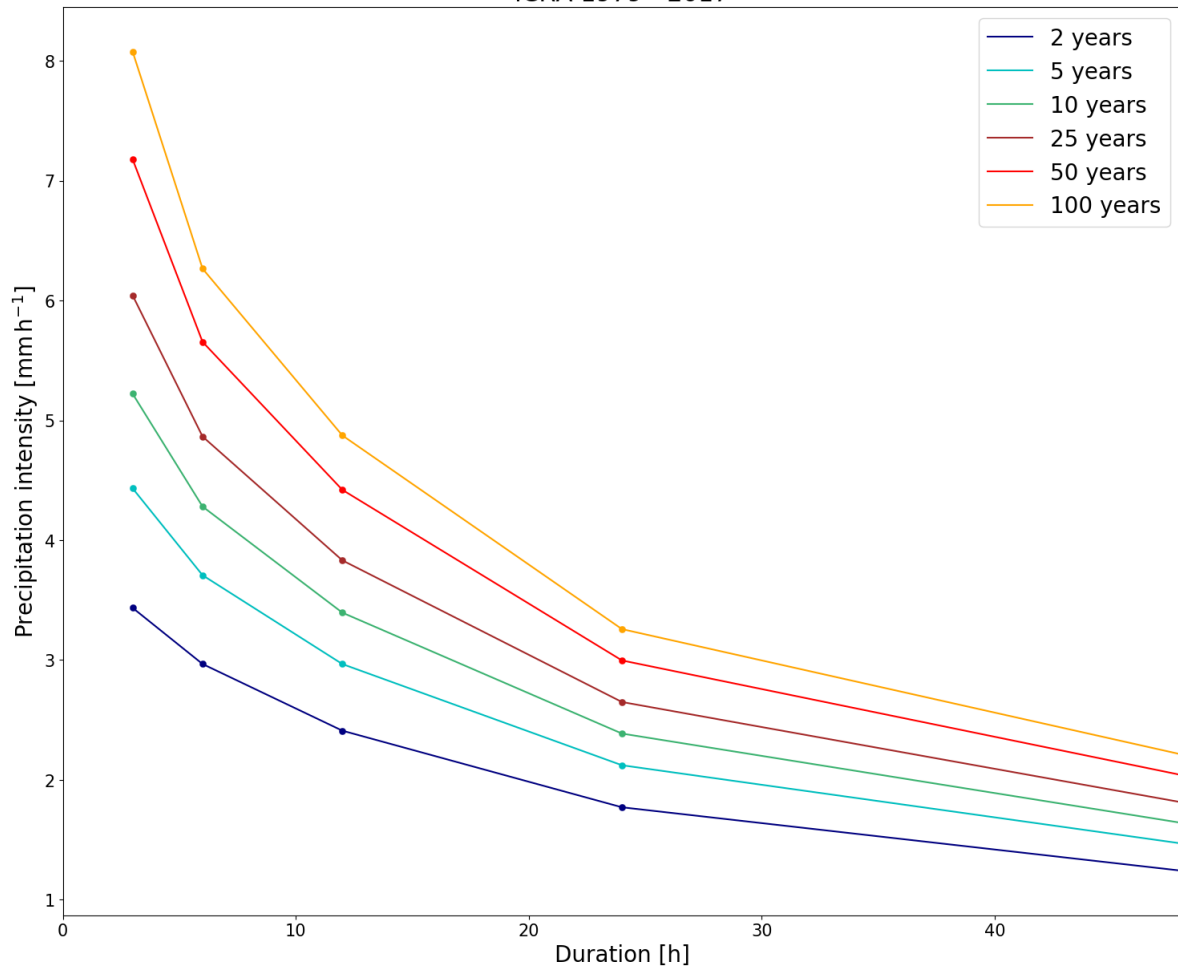


Figure III.34 – IDF curves for station Sámsstaðir from entire ICRA. Solid points give return levels for 3-, 6-, 12-, 24-, 48-hour duration with a 2-, 5-, 10-, 25-, 50- and 100-year return period. Each coloured line corresponds to a different return period as stated by the legend.

Table III.34 – Return levels (mm) for various durations and return periods based on the entire ICRA for station Sámsstaðir. Values are given for 3-, 6-, 12-, 24-, 48-hour duration with a 2-, 5-, 10-, 25-, 50- and 100-year return period.

	2 years	5 years	10 years	25 years	50 years	100 years
3 hours	10	13	16	18	22	24
6 hours	18	22	26	29	34	38
12 hours	30	36	41	46	53	58
24 hours	43	51	57	64	72	78
48 hours	60	71	79	87	98	106

IDF CURVES: Seyðisfjörður

ICRA 1979 - 2017

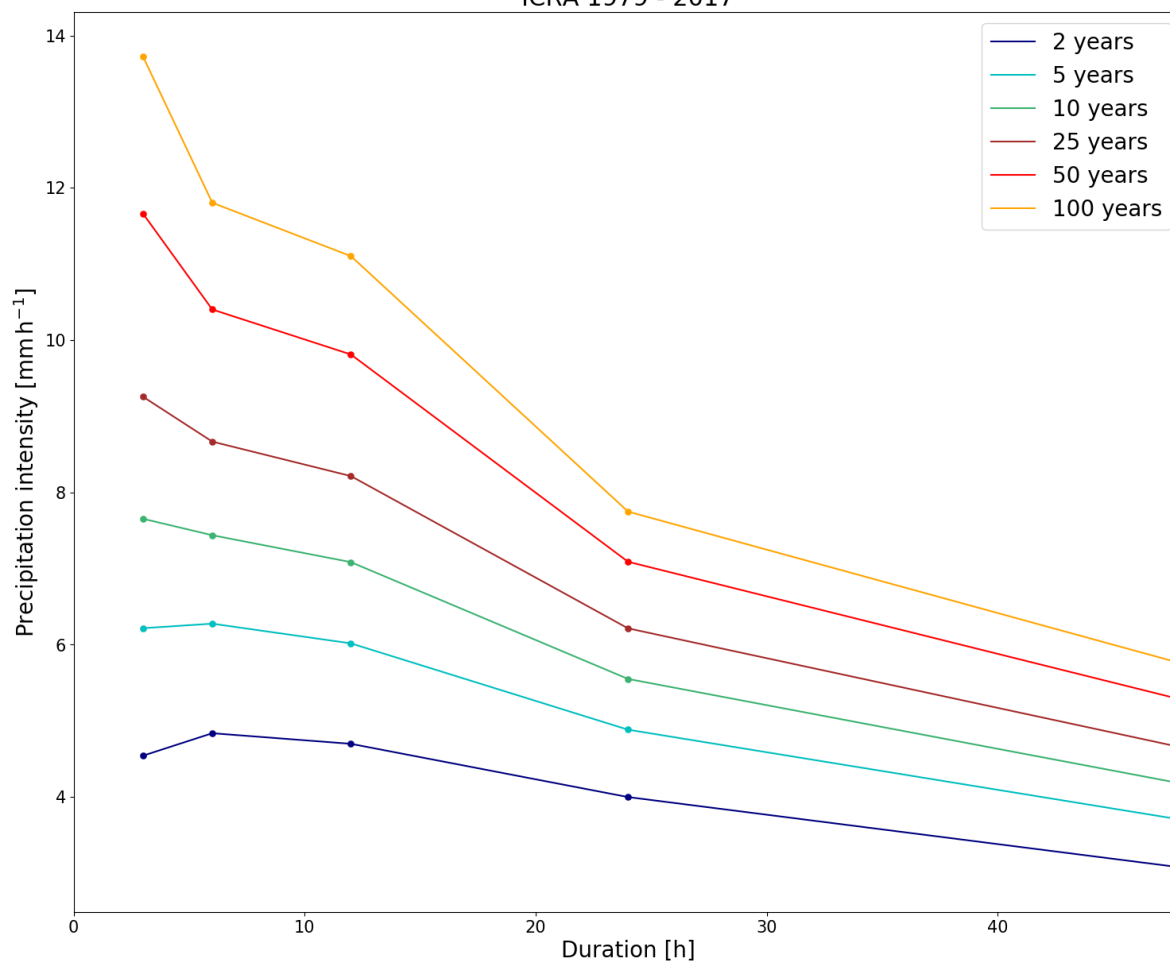


Figure III.35 – IDF curves for station Seyðisfjörður from entire ICRA. Solid points give return levels for 3-, 6-, 12-, 24-, 48-hour duration with a 2-, 5-, 10-, 25-, 50- and 100-year return period. Each coloured line corresponds to a different return period as stated by the legend.

Table III.35 – Return levels (mm) for various durations and return periods based on the entire ICRA for station Seyðisfjörður. Values are given for 3-, 6-, 12-, 24-, 48-hour duration with a 2-, 5-, 10-, 25-, 50- and 100-year return period.

	2 years	5 years	10 years	25 years	50 years	100 years
3 hours	14	19	23	28	35	41
6 hours	29	38	45	52	62	71
12 hours	56	72	85	99	118	133
24 hours	96	117	133	149	170	186
48 hours	147	177	200	223	253	276

IDF CURVES: Siglufjörður

ICRA 1979 - 2017

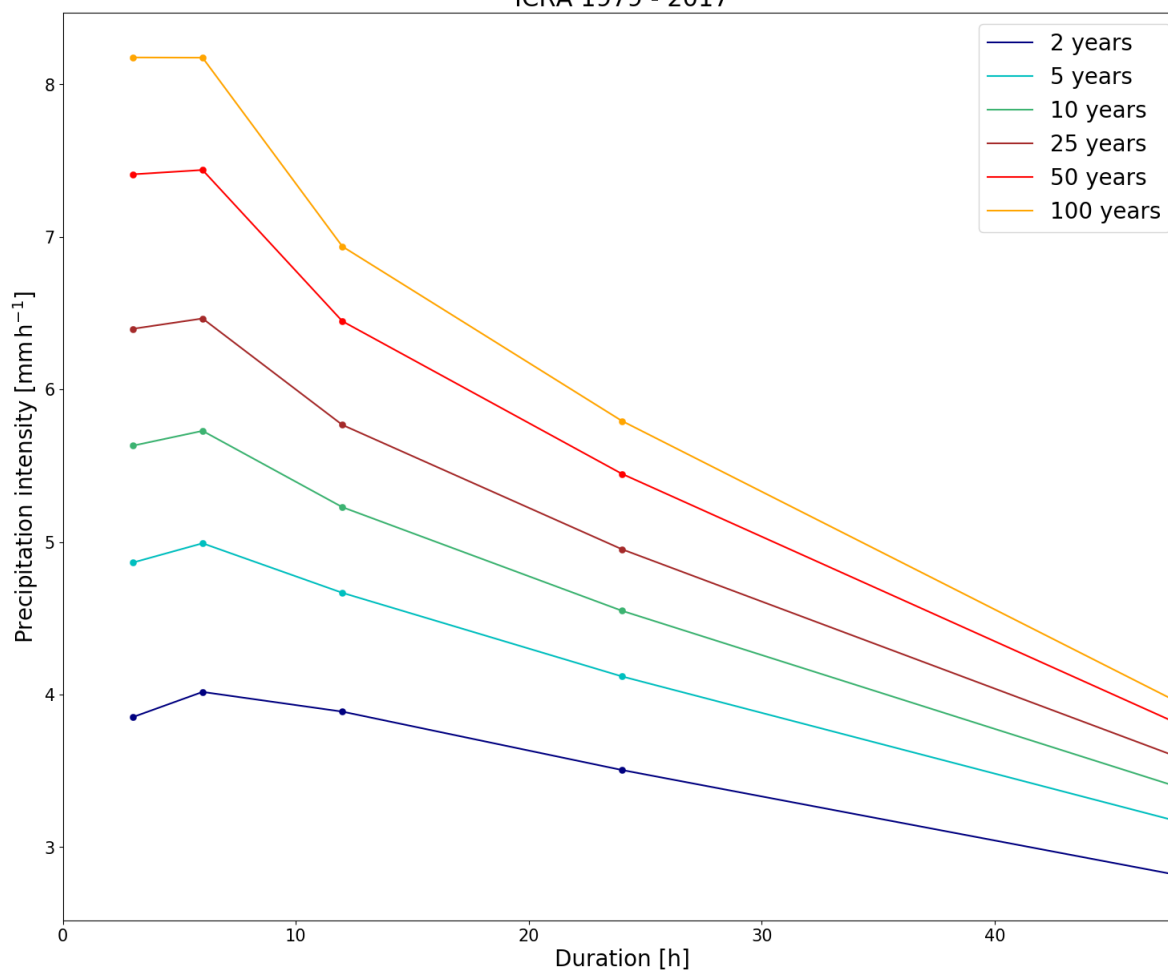


Figure III.36 – IDF curves for station Siglufjörður from entire ICRA. Solid points give return levels for 3-, 6-, 12-, 24-, 48-hour duration with a 2-, 5-, 10-, 25-, 50- and 100-year return period. Each coloured line corresponds to a different return period as stated by the legend.

Table III.36 – Return levels (mm) for various durations and return periods based on the entire ICRA for station Siglufjörður. Values are given for 3-, 6-, 12-, 24-, 48-hour duration with a 2-, 5-, 10-, 25-, 50- and 100-year return period.

	2 years	5 years	10 years	25 years	50 years	100 years
3 hours	12	15	17	19	22	25
6 hours	24	30	34	39	45	49
12 hours	47	56	63	69	77	83
24 hours	84	99	109	119	131	139
48 hours	135	152	163	172	182	189

IDF CURVES: Stykkishólmur

ICRA 1979 - 2017

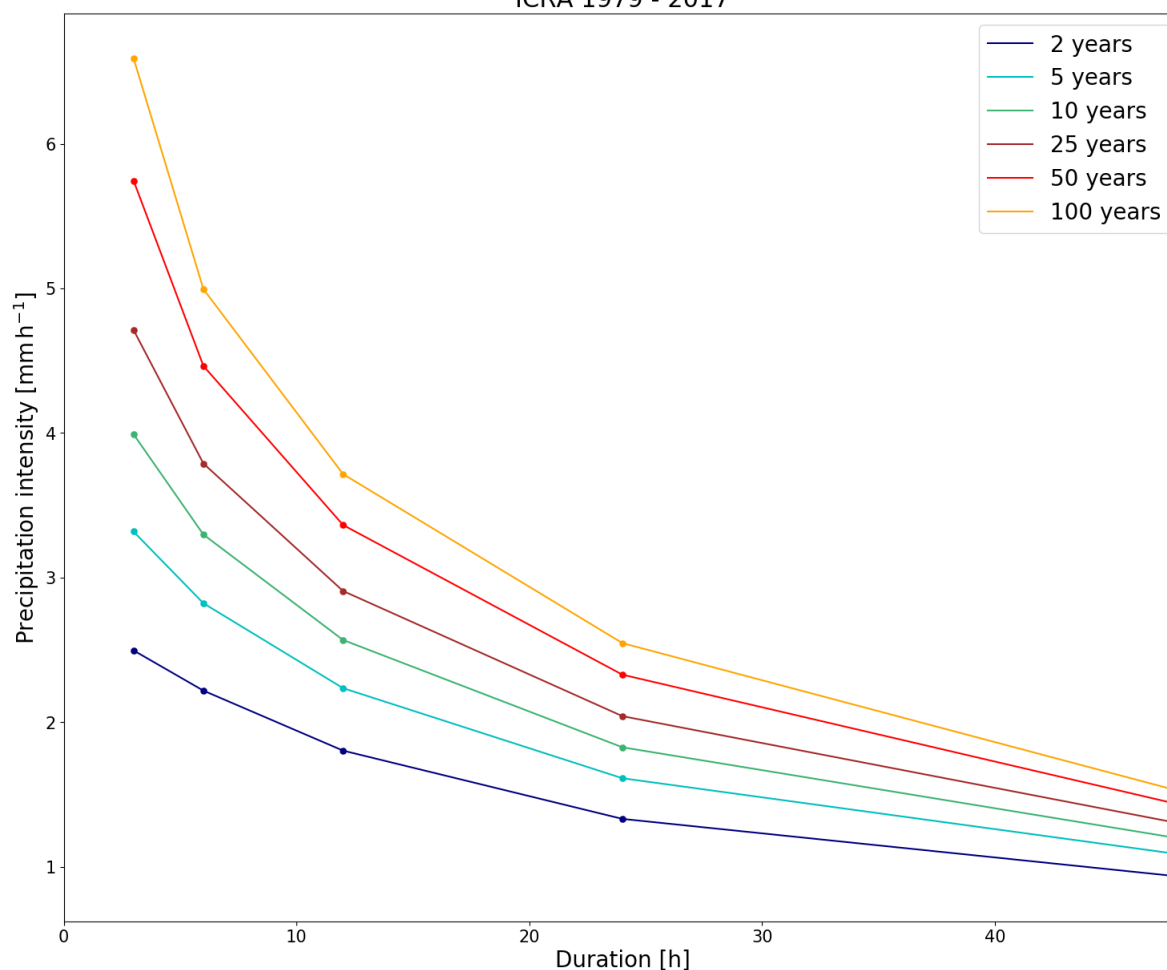


Figure III.37 – IDF curves for station Stykkishólmur from entire ICRA. Solid points give return levels for 3-, 6-, 12-, 24-, 48-hour duration with a 2-, 5-, 10-, 25-, 50- and 100-year return period. Each coloured line corresponds to a different return period as stated by the legend.

Table III.37 – Return levels (mm) for various durations and return periods based on the entire ICRA for station Stykkishólmur. Values are given for 3-, 6-, 12-, 24-, 48-hour duration with a 2-, 5-, 10-, 25-, 50- and 100-year return period.

	2 years	5 years	10 years	25 years	50 years	100 years
3 hours	7	10	12	17	20	20
6 hours	13	17	20	23	27	30
12 hours	22	27	31	35	40	45
24 hours	32	39	44	49	56	61
48 hours	45	52	57	62	69	73

IDF CURVES: Súđavík

ICRA 1979 - 2017

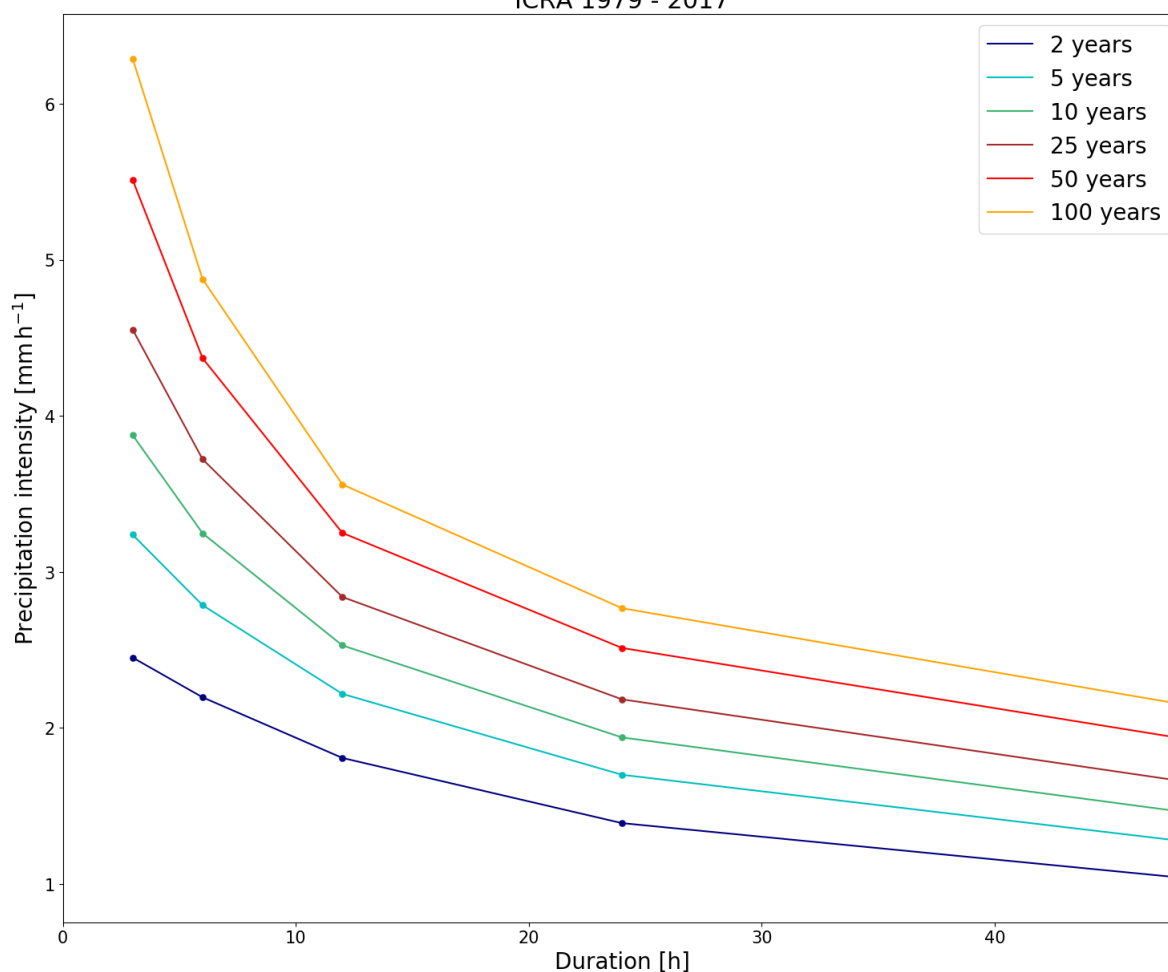


Figure III.38 – IDF curves for station Súđavík from entire ICRA. Solid points give return levels for 3-, 6-, 12-, 24-, 48-hour duration with a 2-, 5-, 10-, 25-, 50- and 100-year return period. Each coloured line corresponds to a different return period as stated by the legend.

Table III.38 – Return levels (mm) for various durations and return periods based on the entire ICRA for station Súđavík. Values are given for 3-, 6-, 12-, 24-, 48-hour duration with a 2-, 5-, 10-, 25-, 50- and 100-year return period.

	2 years	5 years	10 years	25 years	50 years	100 years
3 hours	7	10	12	14	17	19
6 hours	13	17	19	22	26	29
12 hours	22	27	30	34	39	43
24 hours	33	41	47	52	60	66
48 hours	50	61	70	80	93	103

IDF CURVES: Tálknafjörður

ICRA 1979 - 2017

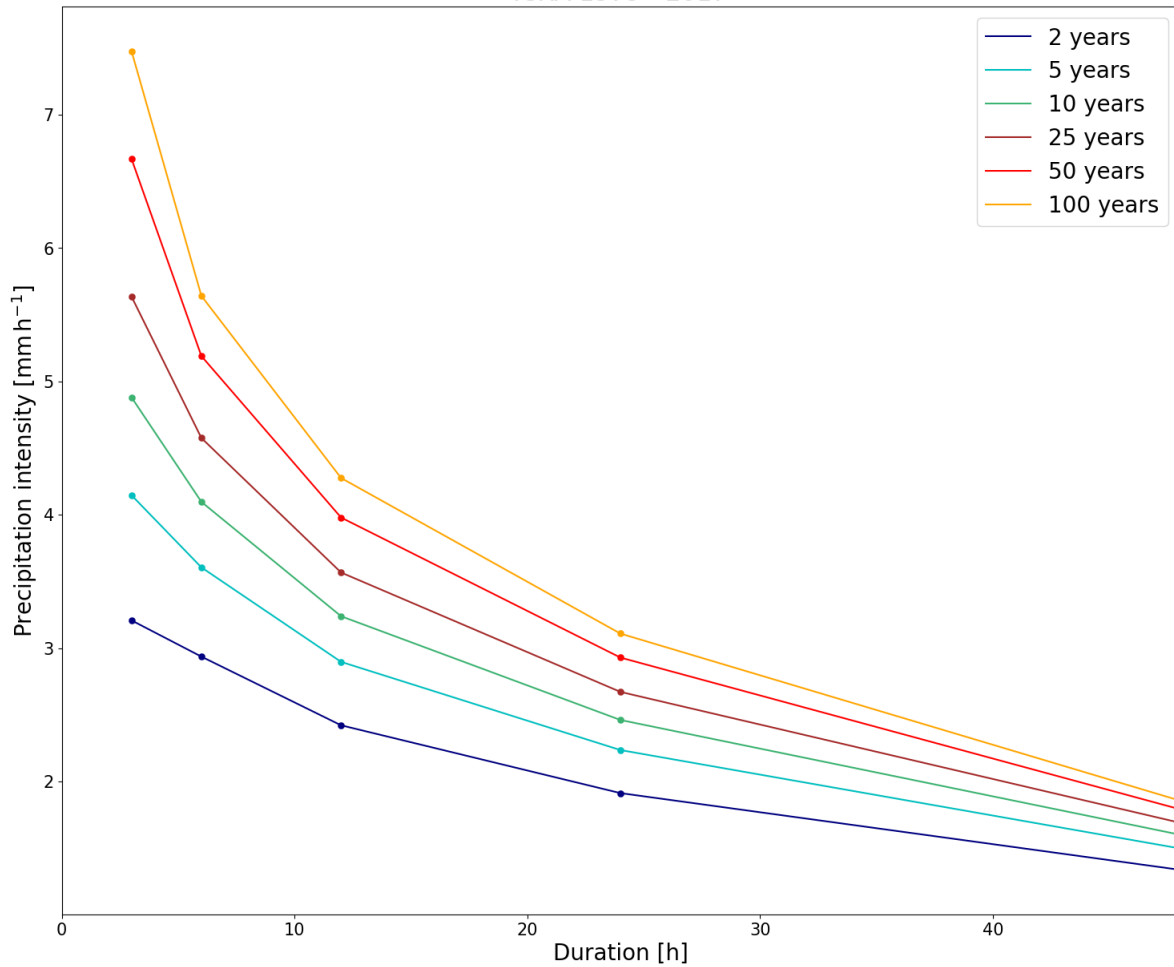


Figure III.39 – IDF curves for station Tálknafjörður from entire ICRA. Solid points give return levels for 3-, 6-, 12-, 24-, 48-hour duration with a 2-, 5-, 10-, 25-, 50- and 100-year return period. Each coloured line corresponds to a different return period as stated by the legend.

Table III.39 – Return levels (mm) for various durations and return periods based on the entire ICRA for station Tálknafjörður. Values are given for 3-, 6-, 12-, 24-, 48-hour duration with a 2-, 5-, 10-, 25-, 50- and 100-year return period.

	2 years	5 years	10 years	25 years	50 years	100 years
3 hours	10	12	15	17	20	22
6 hours	18	22	25	27	31	34
12 hours	29	35	39	43	48	51
24 hours	46	54	59	64	70	75
48 hours	64	72	77	81	86	89

IDF CURVES: Þingvellir

ICRA 1979 - 2017

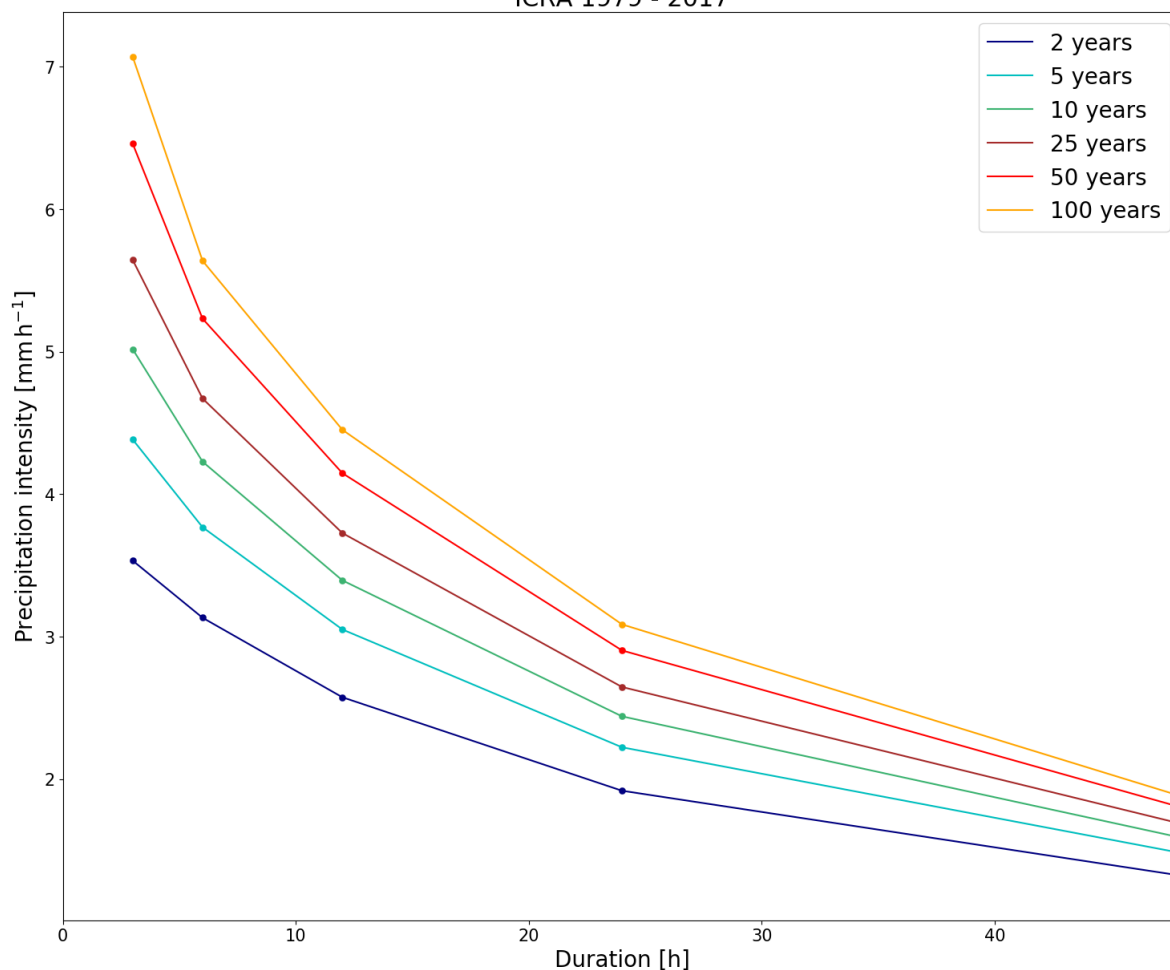


Figure III.40 – IDF curves for station Þingvellir from entire ICRA. Solid points give return levels for 3-, 6-, 12-, 24-, 48-hour duration with a 2-, 5-, 10-, 25-, 50- and 100-year return period. Each coloured line corresponds to a different return period as stated by the legend.

Table III.40 – Return levels (mm) for various durations and return periods based on the entire ICRA for station Þingvellir. Values are given for 3-, 6-, 12-, 24-, 48-hour duration with a 2-, 5-, 10-, 25-, 50- and 100-year return period.

	2 years	5 years	10 years	25 years	50 years	100 years
3 hours	11	13	15	17	19	21
6 hours	19	23	25	28	31	34
12 hours	31	37	41	45	50	53
24 hours	46	53	59	64	70	74
48 hours	63	71	76	81	86	90

IDF CURVES: Þykkvibær

ICRA 1979 - 2017

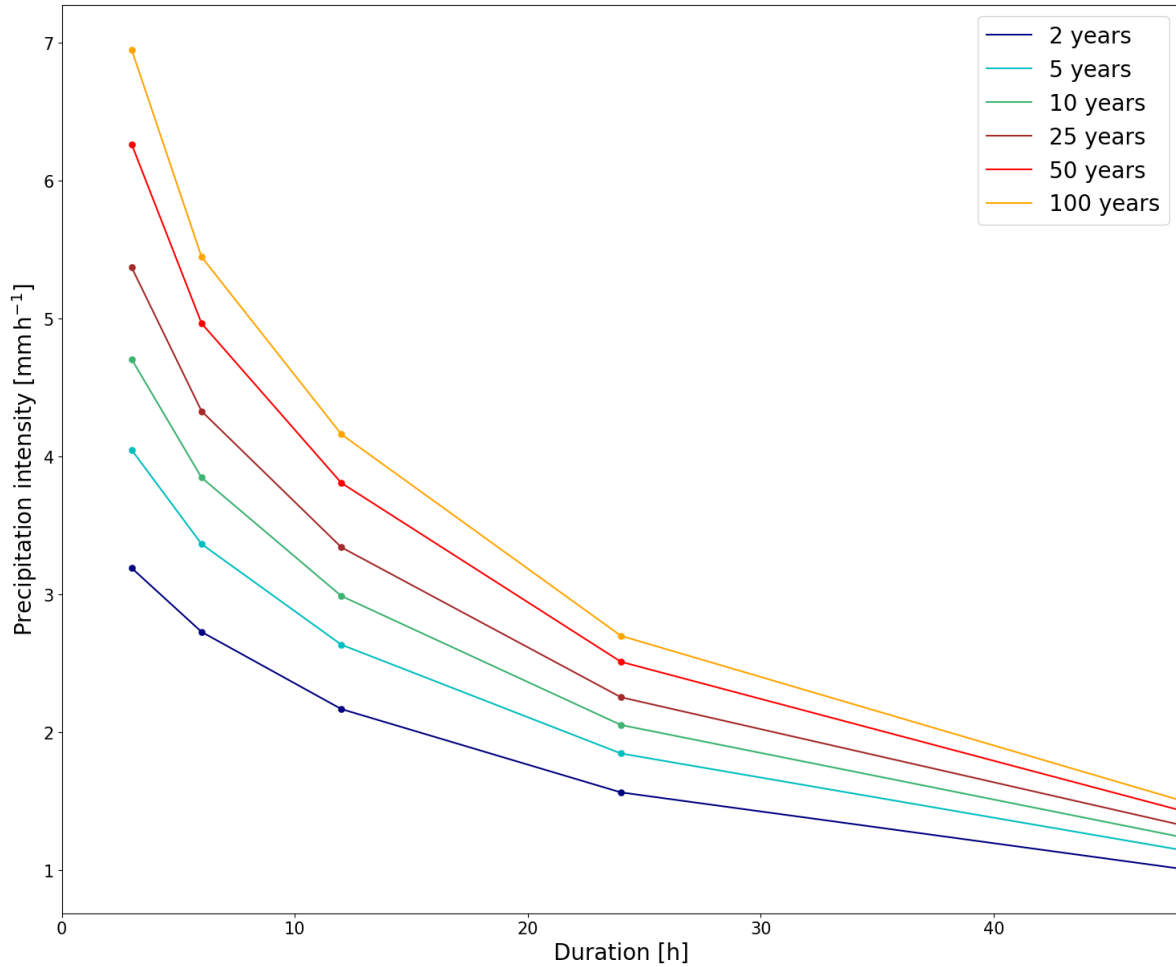


Figure III.41 – IDF curves for station Þykkvibær from entire ICRA. Solid points give return levels for 3-, 6-, 12-, 24-, 48-hour duration with a 2-, 5-, 10-, 25-, 50- and 100-year return period. Each coloured line corresponds to a different return period as stated by the legend.

Table III.41 – Return levels (mm) for various durations and return periods based on the entire ICRA for station Þykkvibær. Values are given for 3-, 6-, 12-, 24-, 48-hour duration with a 2-, 5-, 10-, 25-, 50- and 100-year return period.

	2 years	5 years	10 years	25 years	50 years	100 years
3 hours	10	12	14	16	19	21
6 hours	16	20	23	26	30	33
12 hours	26	32	36	40	46	50
24 hours	38	44	49	54	60	65
48 hours	49	55	60	64	69	72

IDF CURVES: Vatnsfell

ICRA 1979 - 2017

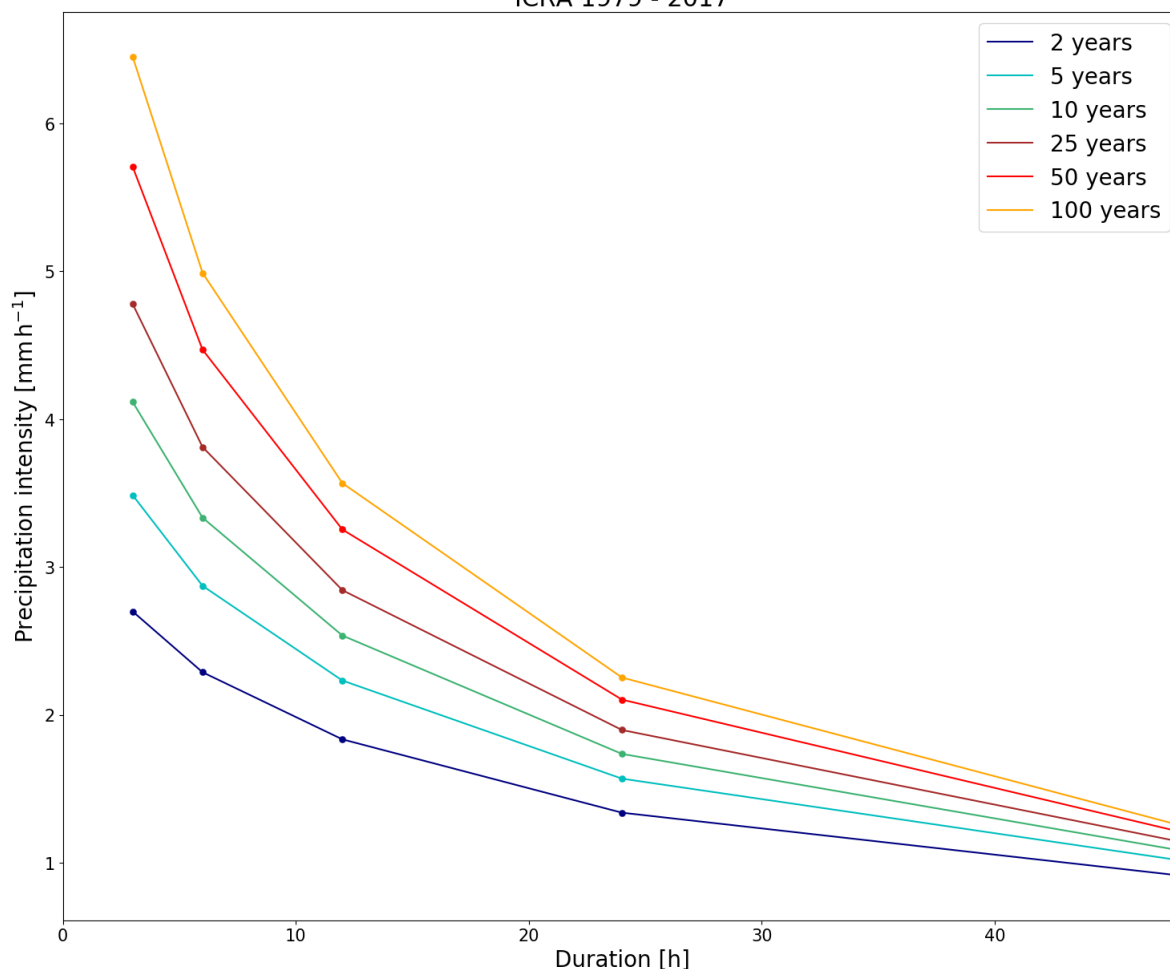


Figure III.42 – IDF curves for station Vatnsfell from entire ICRA. Solid points give return levels for 3-, 6-, 12-, 24-, 48-hour duration with a 2-, 5-, 10-, 25-, 50- and 100-year return period. Each coloured line corresponds to a different return period as stated by the legend.

Table III.42 – Return levels (mm) for various durations and return periods based on the entire ICRA for station Vatnsfell. Values are given for 3-, 6-, 12-, 24-, 48-hour duration with a 2-, 5-, 10-, 25-, 50- and 100-year return period.

	2 years	5 years	10 years	25 years	50 years	100 years
3 hours	8	10	12	14	17	19
6 hours	14	17	20	23	27	30
12 hours	22	27	30	34	39	43
24 hours	32	38	42	46	50	54
48 hours	44	49	52	55	58	60

IDF CURVES: Veiðivatnahraun

ICRA 1979 - 2017

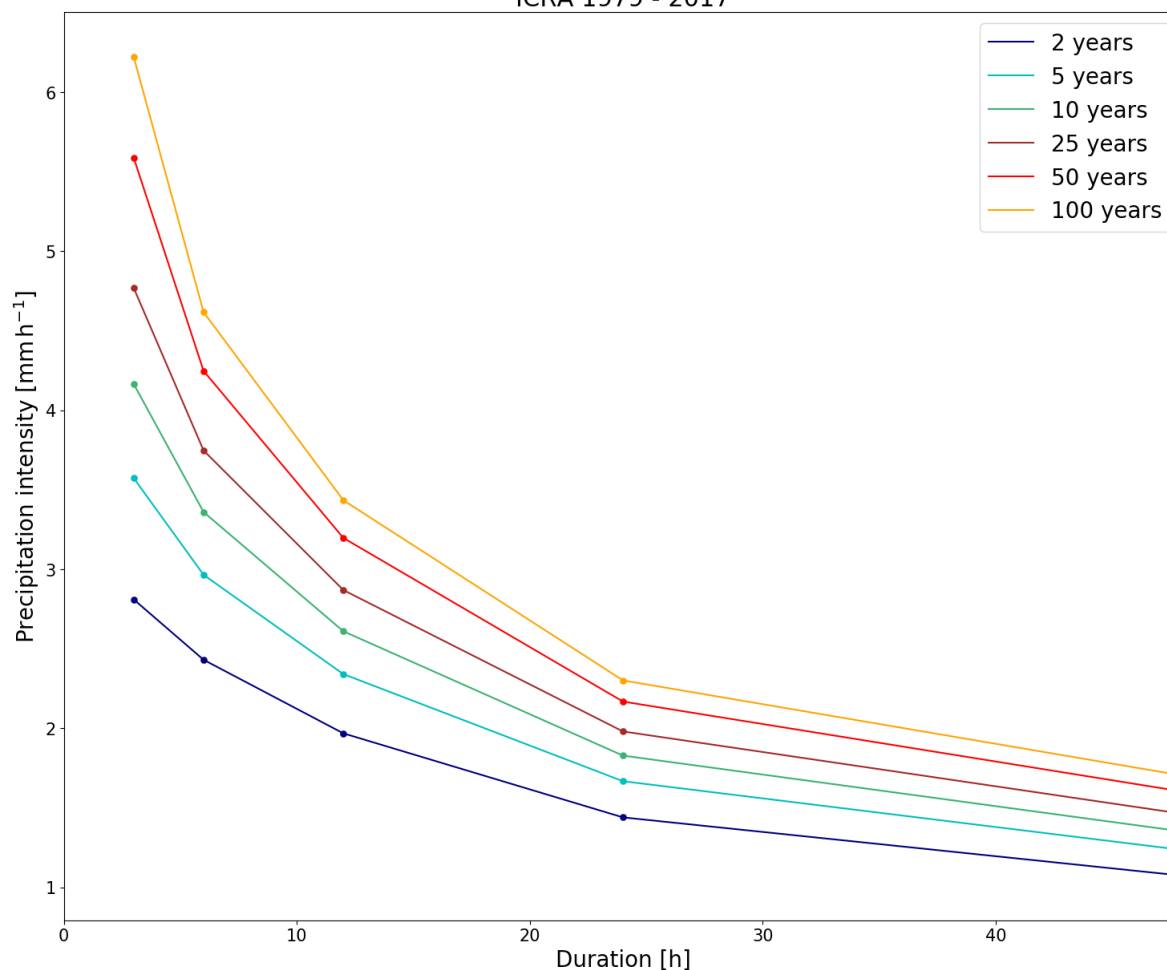


Figure III.43 – IDF curves for station Veiðivatnahraun from entire ICRA. Solid points give return levels for 3-, 6-, 12-, 24-, 48-hour duration with a 2-, 5-, 10-, 25-, 50- and 100-year return period. Each coloured line corresponds to a different return period as stated by the legend.

Table III.43 – Return levels for various durations and return periods based on the entire ICRA for station Veiðivatnahraun. Values are given for 3-, 6-, 12-, 24-, 48-hour duration with a 2-, 5-, 10-, 25-, 50- and 100-year return period.

	2 years	5 years	10 years	25 years	50 years	100 years
3 hours	8	11	12	14	17	19
6 hours	15	18	20	22	25	28
12 hours	24	28	31	34	38	41
24 hours	35	40	44	48	52	55
48 hours	52	59	65	70	77	82

Appendix IV. 1M5 values

1M5 precipitation values are given in Table IV for each station selected in the study, for several EVA methods and different datasets. Results in the first columns were directly taken from from the existing 1M5 map from Eliasson *et al.* (2009).

Table IV - 1M5 values are shown for each station as obtained by Eliasson et al. (2009) using the Block Maxima method, Block Maxima and Peak-over-Threshold methods with MLE based on daily precipitation from the entire ICRA dataset, and Peak-over-Threshold with MLE based on 24-hour precipitation from the entire ICRA dataset. The first 12 stations (bold) are the control stations.

Station	Block Maxima <i>Eliasson</i> <i>mm day⁻¹</i>	Block Maxima <i>mm day⁻¹</i>	Peak-over- Threshold <i>mm day⁻¹</i>	Peak-over- Threshold <i>mm 24-h⁻¹</i>
Eskifjörður	120	94	95	103
Flateyri	63	59	61	70
Höfn í Hornafirði	76	71	76	87
Ísafjörður	53	58	58	67
Kvísker	159	183	182	205
Laufbali	128	127	129	153
Neskaupstaður	105	103	104	117
Ólafsfjörður	79	89	95	130
Reykjavík	42	33	34	42
Seyðisfjörður	103	112	117	134
Siglufjörður	73	95	99	108
Súðavík	41	40	41	48
Grindavík	60	44	46	54
Korpa	48	38	39	46
Hellisskarð	84	114	114	131
Ölkelduháls	78	116	116	133
Þingvellir	72	54	53	61
Hvanneyri	72	60	60	71
Fíflholt	58	44	47	55
Gufuskálar	41	47	46	51
Ólafsvík	61	117	126	142
Grundarfjörður	67	125	127	141
Stykkishólmur	41	36	39	45

Patreksfjörður	69	55	59	66
Tálknafjörður	69	50	54	60
Bíldudalur	55	54	54	60
Bolungarvík	56	44	45	52
Nautabú	30	31	31	35
Blönduós	28	28	29	35
Möðruvellir	42	28	29	34
Akureyri	34	31	32	38
Dalatangi	99	82	84	93
Egilsstaðaflugvöllur	54	42	44	49
Raufarhöfn	36	32	34	39
Karahnjúkar	41	33	33	37
Þykkvibær	58	45	44	50
Sámsstaðir	58	51	51	60
Kirkjubæjarklaustur	66	71	72	84
Kálfhóll	65	53	53	61
Búrfell	60	53	53	62
Vatnsfell	51	37	38	42
Veiðivatnahraun	52	39	40	47
Hveravellir	65	61	65	78